UNIVERSITÉ DE LORRAINE | BIBLIOTHÈQUES UNIVERSITAIRES

AVERTISSEMENT

Ce document est le fruit d'un long travail approuvé par le jury de soutenance et mis à disposition de l'ensemble de la communauté universitaire élargie.

Il est soumis à la propriété intellectuelle de l'auteur. Ceci implique une obligation de citation et de référencement lors de l'utilisation de ce document.

D'autre part, toute contrefaçon, plagiat, reproduction illicite encourt une poursuite pénale.

Contact bibliothèque : ddoc-theses-contact@univ-lorraine.fr
(Cette adresse ne permet pas de contacter les auteurs)

LIENS

Code de la Propriété Intellectuelle. articles L 122. 4
Code de la Propriété Intellectuelle. articles L 335.2- L 335.10
http://www.cfcopies.com/V2/leg/leg_droi.php
http://www.culture.gouv.fr/culture/infos-pratiques/droits/protection.htm

École Doctorale :
Sciences et Ingénieries des Molécules, des Produits, des Procédés et de l'Énergie (SIMPPÉ)

Laboratoire Réactions et Génie des Procédés (LRGP-CNRS)

Thèse

Pour l'obtention du titre de
Docteur de l'Université de Lorraine
Mention: Génie des Procédés, des Produits et des Molécules

Sujet: Conception et synthèse catalytique d'élastomères haute performance à base de CO_2 par terpolymérisation: de l'ingénierie moléculaire aux nanocomposites fonctionnels

---

Par
Shuo ZENG

Présentée et soutenue publiquement le 19 septembre 2025

Membres du Jury:

Samuel DAGORNE	Directeur de recherche	Université de Strasbourg	Rapporteur
Aihua CHEN	Professeure	Université Beihang	Rapporteure
Isabelle ROYAUD	Professeure	Université de Lorraine	Présidente du jury
Jiajia XUE	Professeure	Université de Technologie Chimique de Pékin	Examinatrice
Guo-Hua HU	Professeur	Université de Lorraine	Directeur de thèse
Liqun ZHANG	Professeur	Université Jiaotong de Xi'an	Co-directeur de thèse

Acknowledgments

I would like to express my deepest gratitude to all those who have supported me throughout the journey of my Ph.D. study and the completion of this thesis.

First and foremost, I am profoundly indebted to my supervisors, Prof. Guo-hua HU and Prof. Liqun ZHANG. Their immense knowledge, insightful guidance, and unwavering support have been invaluable throughout my research. They taught me not only how to conduct rigorous scientific research but also how to think critically and independently. I would also give my sincere thanks to Prof. Zhao WANG, Prof. Runguo WANG, Dr. Qinghai ZHOU, and Prof. Xianhong WANG for their indispensable support, without which this work would not have progressed so smoothly.

I extend my sincere appreciation to my thesis committee members, Prof. Samuel DAGORNE, Prof. Aihua CHEN, Prof. Isabelle ROYAUD and Prof. Jiajia XUE, for their precious time, insightful comments, and constructive suggestions that have greatly improved this manuscript.

My heartfelt thanks go to all my colleagues and friends at the Center of Advanced Elastomer Materials (CAEM), Beijign University of Chemical Technology, Beijing, China, and the Laboratoire Réactions et Génie des Procédés (LRGP), Université de Lorraine, ENSIC, Nancy, France. I am grateful for their tremendous assistance in both my academic work and daily life, as well as for the rewarding experience of conducting research alongside them.

Special thanks must go to my family for their unconditional love, endless support, and for always believing in me. Words cannot express my full appreciation for their understanding and constant companionship throughout these challenging years.

30 June, 2025

Nancy, France

Abstract

With the accelerating depletion of fossil resources and the urgent need for climate change mitigation, converting carbon dioxide (CO_2) into high performance polymers has attracted growing attention in green chemistry and sustainable materials science. As a non-toxic, abundant, renewable C1 feedstock, CO_2 can be efficiently converted into polycarbonates via ring-opening copolymerization with epoxides. This thesis focuses on the terpolymerization of CO_2, allyl glycidyl ether (AGE), and long alkyl chain epoxides to synthesize elastomeric polycarbonates featuring low glass transition temperatures (T_g), pendant crosslinkable sites, and enhanced mechanical properties. We employed both a heterogeneous Zn-Co double metal cyanide (Zn-Co DMC) catalyst and a homogeneous aluminum porphyrin/PPNCl system to investigate catalyst type effects on polymer microstructure and performance, and developed a synergistic dual catalyst approach to achieve high molecular weight terpolymers. This work presents three main findings: (i) Zn-Co DMC catalyzed bulk polymerization yields poly(carbonate-co-ether)s with ≈ 55 % carbonate linkages and M_n ≈ 45 kg/mol; by varying AGE content and alkyl chain length of the epoxide, T_g can be tuned from –25 °C to +5 °C, crosslink density, tensile strength, and elongation at break are modulated; (ii) Al porphyrin/PPNCl catalysis produces fully carbonated terpolymers (100 % carbonate linkages) with M_n ≈ 30 kg/mol, with polar solvents (e.g., THF) favoring intramolecular backbiting, higher cyclic carbonate byproducts, and lower M_n compared to bulk or nonpolar systems; and (iii) a dual catalyst system combining DMC and Al porphyrin/PPNCl affords terpolymers with M_n up to 141 kg/mol and ≈ 80 % carbonate linkages. The AGE derived vinyl groups of the terpolymers are crosslinked via peroxide curing and reinforced with silica nanoparticles (optimal at 30 phr) to produce nanocomposites exhibiting markedly enhanced tensile strength and elongation at break. This thesis thus provides a strategy for designing CO_2-based elastomers with controllable thermal and mechanical properties, underpinned by detailed kinetic and mechanistic insights.

Résumé

Avec l'épuisement rapide des ressources fossiles et l'urgence croissante de lutter contre le changement climatique, la transformation du dioxyde de carbone (CO_2) en polymères haute performance suscite un intérêt majeur en chimie verte et science des matériaux durables. Cette thèse porte sur la terpolymérisation du CO_2, de l'allyl glycidyl éther (AGE) et d'époxydes à longue chaîne alkyle pour obtenir des polycarbonates élastomères à faible température de transition vitreuse (T_g), à sites fonctionnels réticulables et aux performances mécaniques optimisées. Nous avons étudié trois axes principaux: (i) la polymérisation en masse catalysée par Zn–Co DMC, aboutissant à des poly(carbonate-co-ether)s à ≈ 55% de liaisons carbonate et M_n ≈ 45 kg/mol, dont la T_g (–25 °C à +5 °C), la densité de réticulation, la résistance à la traction et l'allongement à la rupture sont modulés par la teneur en AGE et la longueur de chaîne alkyle; (ii) la catalyse homogène par porphyrine d'aluminium/PPNCl, produisant des terpolymères intégralement carbonatés (100 % de liaisons carbonate, M_n ≈ 30 kg/mol), avec un effet solvant prononcé THF favorise le backbiting, la formation de carbonates cycliques et réduit M_n comparé aux systèmes en masse ou en solvants non polaires; et (iii) un système double catalyseur combinant Zn–Co DMC et porphyrine d'aluminium/PPNCl, permettant d'atteindre M_n jusqu'à 141 kg/mol et ≈ 80 % de liaisons carbonate. Les groupes vinyl de l'AGE des terpolymères sont réticulés par peroxyde et renforcés par nanoparticules de silice (optimal à 30 phr), générant des nanocomposites à résistance et extensibilité significativement accrues. Cette thèse propose ainsi une stratégie complète pour la conception d'élastomères à base de CO_2 aux propriétés thermiques et mécaniques modulables, étayée par une analyse approfondie de la cinétique et des mécanismes réactionnels.

Contents

Acknowledgments ..... **I**

Abstract ..... **III**

Résumé ..... **V**

Contents ..... **VII**

Résumé étendu en français ..... **IX**

I. Introduction IX

II. Objectifs XI

III. Contenu de la recherche et résultats principaux XIII

IV. Conclusions et perspectives XX

Chapter 1 General introduction **1**

1.1 Overview 1

1.2 Objectives 3

1.3 Thesis outline 4

Chapter 2 Research background and state of the art **7**

2.1 Chemical utilization of carbon dioxide 7

2.2 Reaction between CO_2 and epoxides 8

2.3 Catalytic system for copolymerization of CO_2 and epoxides 13

2.3.1 Heterogeneous catalytic systems 17

2.3.1.1 Zinc glutarate 18

2.3.1.2 Rare earth metal complexes 19

2.3.1.3 Double metal cyanide complexes 21

2.3.2 Homogeneous catalytic systems 24

2.3.2.1 β-diimine complexes 24

2.3.2.2 Metal-porphyrin complexes 27

2.3.2.3 Metal-salen complexes 32
2.3.2.4 Metal-free organocatalysts 38
2.4 Development of CO_2-based polymers 43
2.4.1 CO_2-based plastic 43
2.4.2 CO_2-based polyurethane 46
2.4.3 CO_2-based elastomer 48
Chapter 3 Materials and characterization 51
3.1 Materials 51
3.2 Characterizations 51
3.2.1 Product characterization and conversion/selectivity calculations 51
3.2.2 Characterization of molecular weights 59
3.2.3 Glass transition temperature of polymers 59
3.2.4 Characterization of microstructure 59
3.2.5 Characterization of rheological and viscoelastic properties 59
3.2.6 Characterization of the dynamic viscoelastic properties and filler-rubber interactions 59
3.2.7 Characterization of mechanical properties 60
Chapter 4 DMC catalyzed terpolymerization for CO_2-based elastomers 61
Chapter 5 Solution vs. Bulk terpolymerization via Al porphyrin/PPNCl catalysis 83
Chapter 6 Dual catalyst strategy and composite reinforcement 101
Chapter 7 General conclusions and perspectives 123
7.1 General conclusions 123
7.2 Innovations 124
7.3 Perspectives 125
Nomenclature 127
Publications 131
References 133

Résumé étendu en français

I. Introduction

Ces dernières années, sous l'effet conjugué de l'épuisement des ressources fossiles et de l'aggravation du changement climatique, la valorisation à haute valeur ajoutée du dioxyde de carbone (CO_2) est devenue un sujet central en chimie verte et dans le développement de matériaux durables. En tant que molécule C1 abondante, non toxique et peu coûteuse, le CO_2 peut être transformé catalytiquement en une large gamme de produits chimiques tels que le méthane, le méthanol, l'urée, les carbonates cycliques ou encore les polycarbonates. Toutefois, en raison de sa son inertie thermodynamique élevée, sa conversion efficace nécessite généralement des co-réactifs à fort contenu énergétique, comme l'hydrogène, les composés cycliques contraints (par exemple, les époxydes) ou les amines. Parmi les différentes approches explorées, la copolymérisation du CO_2 avec des époxydes pour former des polycarbonates apparaît comme l'une des plus prometteuses, en raison de son économie d'atomes assez elevee, parfois proche de (100 %) et de sa faisabilité à grande échelle. Les polymères ainsi obtenus présentent des propriétés modulables et une bonne processabilité, ce qui est intéressant pour diverses applications telles que les plastiques, les élastomères thermoplastiques, ou encore les polyols polyéthers destinés aux polyuréthanes.

Malgré ces avancées, la recherche reste largement centrée sur des époxydes conventionnels tels que l'oxyde de propylène (PO) et l'oxyde de cyclohexène (CHO), en raison de leur réactivité, leur sélectivité et leur disponibilité industrielle. Par exemple, le poly(carbonate de cyclohexène) (PCHC) présente une température de transition vitreuse (T_g) élevée, d'environ 115 °C, ainsi qu'une excellente stabilité thermique (~300 °C), ce qui le rend adapté aux plastiques techniques. À l'inverse, le poly(carbonate de propylène) (PPC), avec une T_g plus faible (30−50 °C), est plutôt utilisé dans les emballages ou les films biodégradables. Toutefois, la rigidité intrinsèque et la Tg relativement élevée de ces matériaux restreignent leur aptitude aux applications élastomériques, qui exigent souplesse et déformation réversible à

température ambiante. Pour surmonter cette limitation, l'utilisation d'époxydes fonctionnalisés contenant des groupes vinyles permet d'introduire des sites réactifs pour des réactions de réticulation post-polymérisation (comme les réactions thiol–ène), tandis que l'incorporation de longues chaînes alkyles augmente la flexibilité en abaissant la T_g, ouvrant ainsi la voie à leur emploi en tant que matériaux souples et flexibles.

Pour concevoir des élastomères à base de CO_2 présentant un comportement caoutchouteux à température ambiante, plusieurs critères moléculaires doivent être satisfaits: (1) Une basse température de transition vitreuse (T_g < 0 °C): elle garantit la flexibilité du matériau à température ambiante. (2) La présence d'unités susceptibles d'être réticulés : l'introduction de groupes fonctionnels (par exemple, vinyles) permet la formation de réseaux tridimensionnels après polymérisation, améliorant ainsi l'élasticité et la résistance aux solvants. (3) Une structure amorphe : elle favorise la mobilité des chaînes polymères et une flexibilité homogène. (4) Une masse molaire élevée: il est essentiel pour assurer la formation de réseaux robustes et maintenir l'intégrité mécanique du matériau. Pour répondre à ces exigences, nous avons introduit des époxydes portant de longues chaînes alkyles afin d'abaisser la T_g, ainsi que l'allyl glycidyl éther (AGE) en tant que monomère fonctionnel pour conférer une capacité de réticulation. La terpolymérisation du CO_2 avec l'AGE et des époxydes flexibles constitue ainsi une voie prometteuse pour élaborer des élastomères à base de CO_2 alliant souplesse et résistance mécanique.

Les catalyseurs utilisés pour la copolymérisation du CO_2 avec des époxydes se classent généralement en deux catégories: les complexes métalliques hétérogènes et homogènes. Les catalyseurs hétérogènes, tels que les complexes cyanurés à double métal zinc–cobalt(III) (Zn–Co DMC), largement utilisés dans l'industrie, présentent une grande stabilité, un coût réduit, mais souffrent souvent d'une large distribution des masses molaires et d'une sélectivité limitée vis-à-vis du polymère formé. En comparaison, les catalyseurs homogènes, comme le complexe porphyrine d'aluminium associé au chlorure de bis(triphénylphosphine)iminium (PPNCl), permettent un meilleur contrôle de la polymérisation et conduisent à des architectures macromoléculaires bien définies, ce qui est tres interessant pour les études mécanistiques. Néanmoins, ces catalyseurs montrent généralement une activité plus faible et nécessitent des

temps de réaction plus longs.

Malgré les progrès réalisés, des défis importants subsistent dans la mise en œuvre de la terpolymérisation. La plupart des catalyseurs existants sont conçus pour des monomères standards tels que PO ou CHO, et montrent une efficacité limitée lorsqu'ils sont appliqués à des époxydes fonctionnalisés comme AGE ou à ceux portant de longues chaînes alkyles. Il demeure difficile de concilier simultanément une masse molaire élevée, une formation minimale de carbonates cycliques en tant que sous-produits, et un contrôle précis de la structure macromoléculaire. Par ailleurs, l'influence de la polarité du solvant sur les propriétés des polymères n'est pas encore entièrement élucidée. Enfin, de nombreuses études abordent séparément la performance catalytique et les propriétés des matériaux obtenus, sans adopter une approche intégrée reliant la conception moléculaire, l'activité catalytique et les performances à l'usage. Répondre à ces enjeux nécessite une stratégie interdisciplinaire combinant l'innovation en catalyse, la compréhension mécanistique des réactions, et la conception rationnelle de matériaux afin d'exploiter pleinement le potentiel des élastomères à base de CO_2.

II. Objectifs

Cette thèse porte sur la conception et la synthèse d'élastomères à base de CO_2 par terpolymérisation catalytique, ainsi que sur le développement de nanocomposites à haute performance présentant des propriétés mécaniques et thermiques modulables. L'approche adoptée repose sur une intégration de l'ingénierie des monomères, de l'optimisation des catalyseurs et des conditions de réaction, du contrôle de la polymérisation, ainsi que de stratégies de post-fonctionnalisation (comme illustré dans le **Schéma I**). En s'appuyant sur une démarche fondée sur la relation procédé de polymérisation-structure–propriétés, ce travail vise à établir une voie de synthèse durable et industrialisable pour la production d'élastomères à base de CO_2. Il apporte à la fois des éclairages mécanistiques sur la terpolymérisation contrôlée par catalyse, et des orientations pratiques pour le développement d'alternatives écologiques aux matériaux élastomères issus du pétrole.

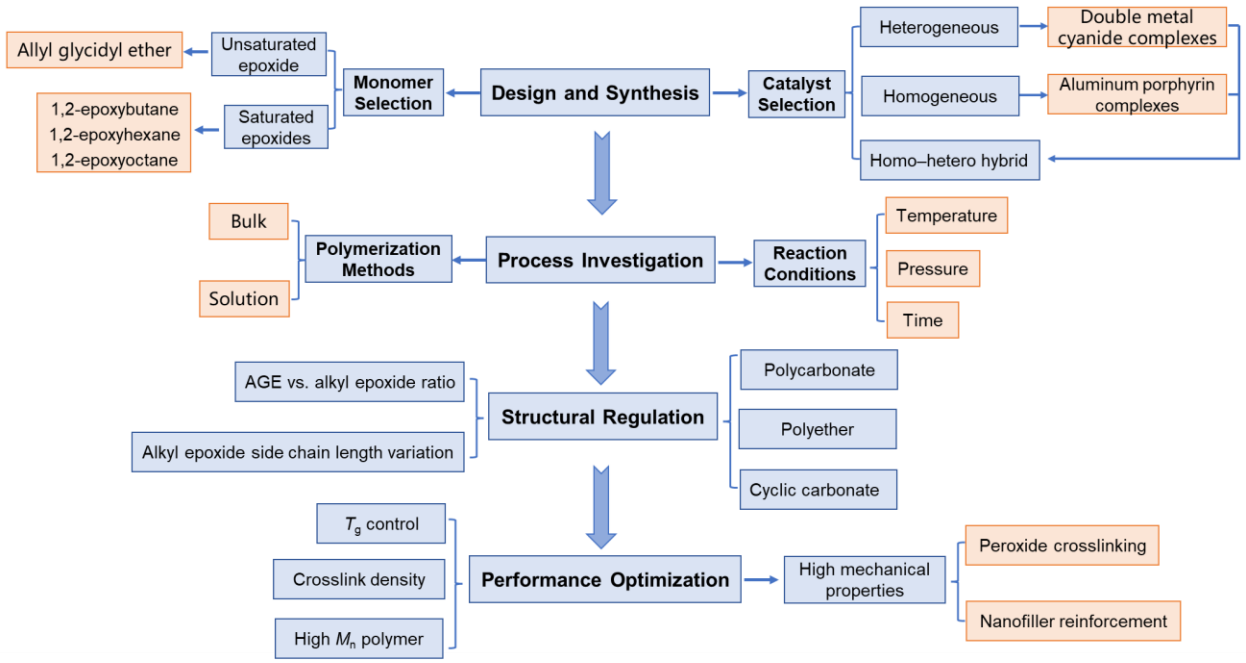

Schéma I. Cadre de recherche pour la synthèse d'élastomères à base de CO_2 par terpolymérisation du CO_2, d'un époxyde insaturé et d'un époxyde saturé.

Les objectifs spécifiques de cette recherche sont les suivants :

(1) Concevoir et synthétiser des élastomères à base de CO_2 par terpolymérisation de CO_2, AGE et d'époxydes alkyles à longue chaîne, en utilisant des systèmes catalytiques simples et doubles, dans le but d'introduire des segments flexibles ainsi que des sites réactifs pour une réticulation ultérieure.

(2) Étudier de manière systématique les effets du type de catalyseur (DMC hétérogène vs porphyrine d'aluminium/chlorure de bis(triphénylphosphine)iminium (PPNCl) homogène), de la polarité du solvant et d'autres paramètres de réaction sur la cinétique de polymérisation, la sélectivité des monomères et les masses molaires obtenues, afin d'éclairer la relation entre le procédé de polymérisation, la structure des polymères et leurs propriétés.

(3) Développer un système catalytique double synergique capable de surmonter les limites des catalyseurs individuels, permettant ainsi la production de poly(carbonate-co-éther)s de masse molaire élevée avec de meilleures performances mécaniques adaptées aux applications élastomériques.

(4) Améliorer les propriétés finales des matériaux en introduisant une réticulation covalente et en renforçant la matrice avec des nanoparticules de silice, dans le but de construire

des nanocomposites élastomères à base de CO_2 robustes, présentant une résistance mécanique, une élasticité et une résistance aux solvants accrues.

III. Contenu de la recherche et résultats principaux

Dans cette thèse, une stratégie globale a été développée pour concevoir des élastomères à base de CO_2 par terpolymérisation catalytique de CO_2, AGE et d'époxydes à longue chaîne alkyle. Les objectifs incluaient l'introduction de liaisons flexibles et de groupes allyles réactifs pour permettre la réticulation, le contrôle du comportement de polymérisation via le choix du catalyseur et l'optimisation des conditions de réaction, ainsi que la production finale d'élastomères réticulés et de nanocomposites présentant des propriétés mécaniques et thermiques améliorées. La recherche a été divisée en trois volets principaux correspondant aux systèmes catalytiques hétérogène, homogène et bicatalytique.

1. Ajustement des relations structure–propriétés par terpolymérisation en masse catalysée par le Zn–Co DMC

En utilisant un catalyseur Zn–Co DMC, une série de terpolymères poly(carbonate-co-éther) a été synthétisée par terpolymérisation en une seule étape de CO_2, AGE et d'époxydes saturés à différentes longueurs de chaîne alkyle (BO, HO, OO) (**Fig. III-1**). La composition et la structure des terpolymères obtenus ont pu être modulées efficacement en ajustant la température, la pression de CO_2 et les ratios d'alimentation en monomères. Les températures plus basses (50–60 °C) favorisent la formation de liaisons carbonates et permettent la synthèse de polymères de masse molaire élevée (jusqu'à 61 kg/mol), tandis que les températures plus élevées favorisent les réactions secondaires telles que le réaction d'auto-cyclisation (backbiting) et le transfert de chaîne, ce qui entraîne une sélectivité réduite et une augmentation de la formation de liaisons éther et de carbonates cycliques. L'augmentation de la pression de CO_2 de 3 à 5 MPa contribue également à une incorporation accrue de liaisons carbonates dans le poly(carbonate-co-éther) ainsi qu'à une masse molaire plus élevée.

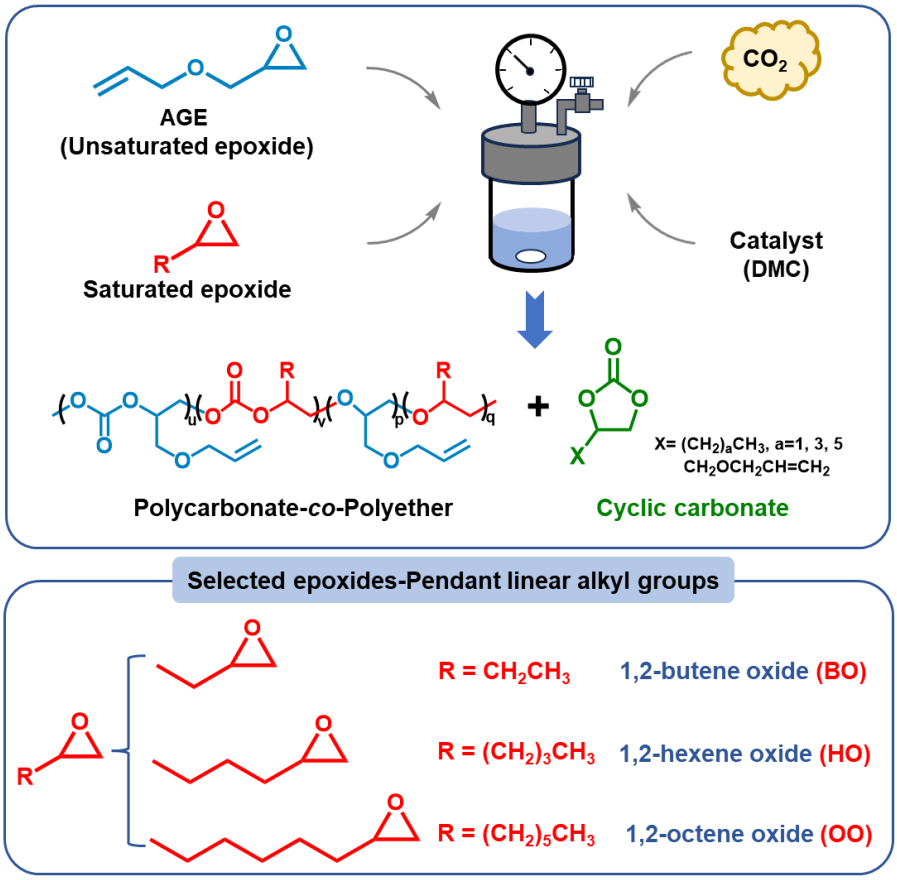

Fig. III-1. Schéma de la terpolymérisation du CO_2, de l'AGE et des époxydes à longues chaînes alkyles utilisant un catalyseur DMC.

L'étude de la cinétique de polymérisation a révélé une période d'induction distincte d'environ 120 minutes avant le début de la réaction (**Fig. III-2**). Ce délai est attribué à l'activation lente du catalyseur DMC, probablement en raison de la coordination compétitive de ligands polaires résiduels tels que l'eau et le tert-butanol (issus de la synthèse du DMC). Après cette période d'induction, une augmentation rapide de la conversion des monomères a été observée: l'AGE et le HO ont atteint environ 80 % de conversion en 40 minutes. Parallèlement, la sélectivité du polymère est restée élevée (97–100 %), bien que la sélectivité des liaisons carbonates ait d'abord légèrement augmenté (jusqu'à 76 %) avant de chuter (à 54 %) en raison de l'accumulation de chaleur dans le système en masse, ce qui a accéléré la réaction tout en réduisant la sélectivité. La masse molaire moyenne (M_n) a augmenté de manière continue avec le temps de réaction, tandis que l'indice de polymolécularité (PDI) est resté stable (~2,76).

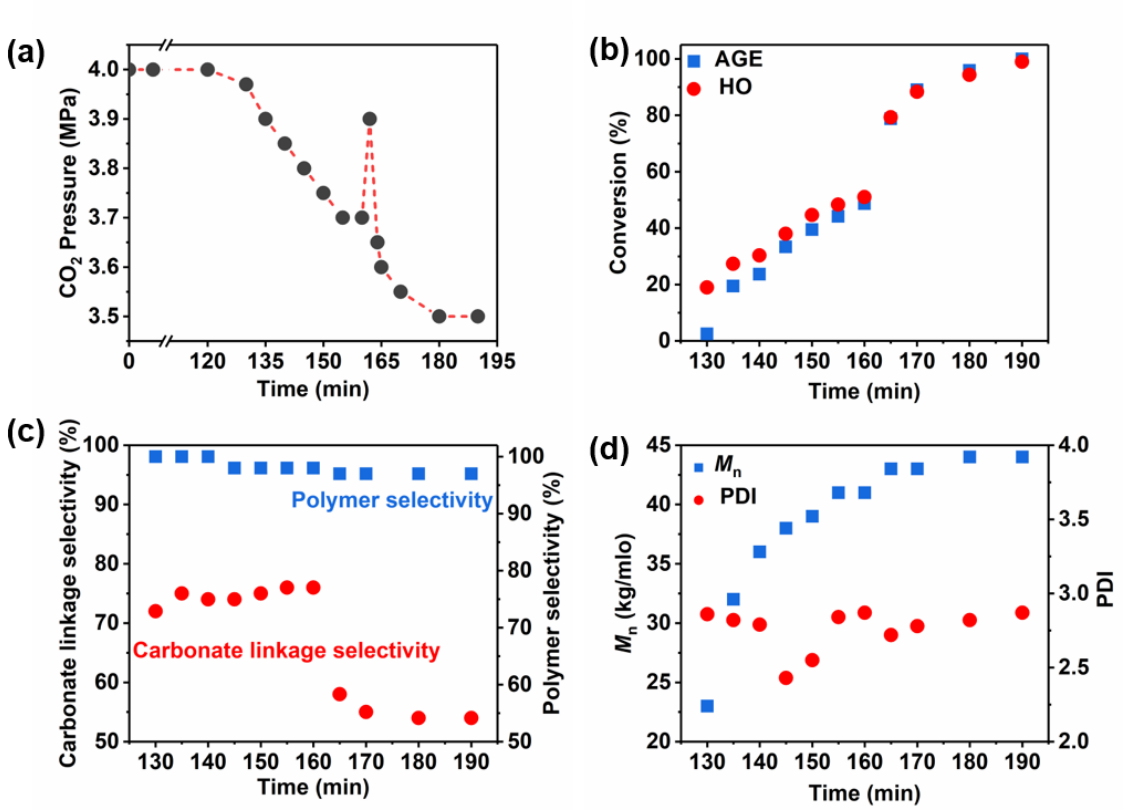

Fig. III-2. Cinétique de la terpolymérisation du CO_2, de l'AGE et du HO en fonction du temps de polymérisation, illustrant l'évolution de la pression de CO_2 (a), des conversions des monomères (b), de la sélectivité du polymère et de la sélectivité des liaisons carbonates (c), ainsi que de la masse molaire du polymère (d).

La T_g et les propriétés mécaniques des terpolymères pouvaient être modulées en ajustant la teneur en AGE ainsi que la longueur de la chaîne alkyle des époxydes saturés. En augmentant la teneur en AGE et en allongeant les chaînes alkyles, la T_g a été systématiquement réduite de +5 °C à −25 °C. À teneur constante en AGE (5 mol %), les polymères synthétisés avec BO, HO et OO ont présenté des T_g respectives de +5 °C, −11 °C et −22 °C, ce qui met en évidence l'effet plastifiant interne des chaînes latérales plus longues. Lorsque la longueur de chaîne de l'époxyde saturé était maintenue constante, comme dans la série terpolymère CO_2–AGE–HO, la T_g a diminué de −11 °C à −14 °C avec une augmentation de l'AGE de 5 à 15 mol %, en raison de la flexibilité introduite par les liaisons éther de l'AGE.

Le comportement mécanique de ces terpolymères est illustré par les courbes contrainte–déformation présentées dans la **Fig. III-3 (a–c)**, mettant en évidence l'influence de la longueur

de la chaîne alkyle à teneur en AGE constante. Pour une même teneur en AGE, la résistance à la traction et l'allongement à la rupture diminuent selon l'ordre BO > HO > OO. Par ailleurs, lorsque la teneur en AGE augmente (**Fig. III-3d–f**), la densité de réticulation s'accroît, ce qui conduit à une augmentation de la résistance à la traction mais à une diminution de l'allongement à la rupture.

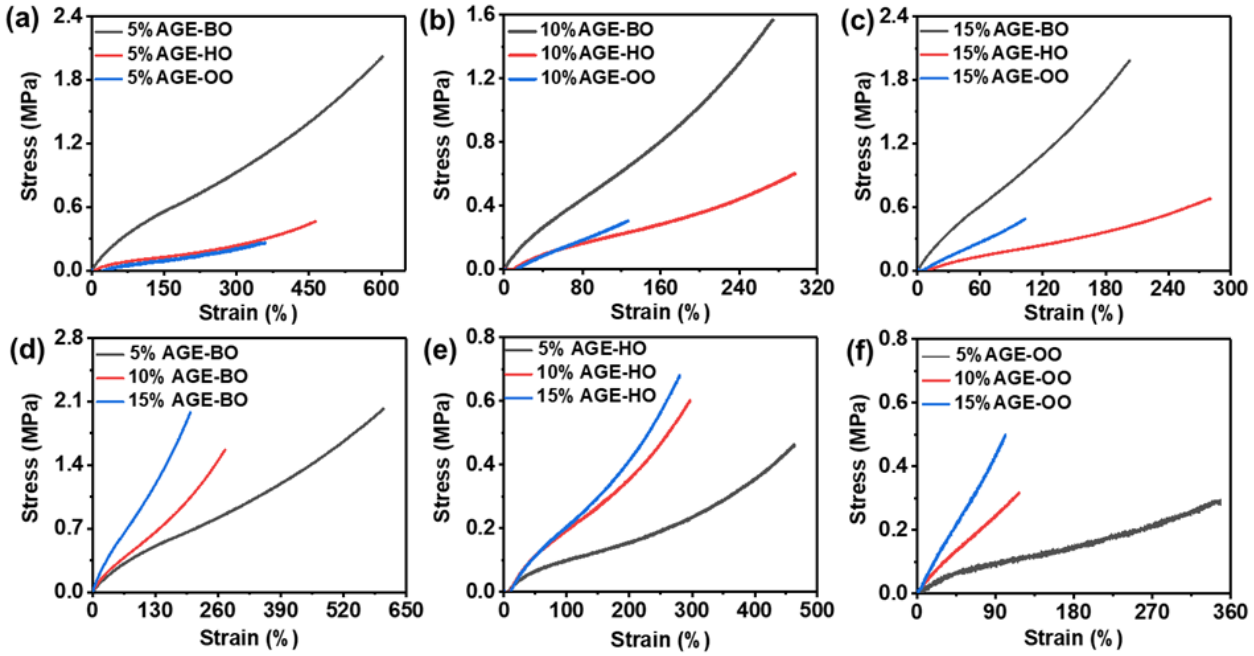

Fig. III-3. Effet de la longueur de la chaîne alkyle de l'époxyde saturé sur la courbe contrainte–déformation en traction du terpolymère CO_2–AGE–époxyde saturé. (a), (b) et (c): rapports molaires AGE/époxyde saturé constants avec différentes longueurs de chaîne alkyle de l'époxyde saturé; (d), (e) et (f): différents rapports molaires AGE/époxyde saturé pour une longueur de chaîne alkyle donnée de l'époxyde saturé.

2. Régulation de la cinétique et de la sélectivité par catalyse à base de porphyrine d'aluminium/chlorure de bis(triphénylphosphine)iminium (PPNCl)

Afin de mieux comprendre le mécanisme de la terpolymérisation, un système catalytique homogène à base de porphyrine d'aluminium/chlorure de bis(triphénylphosphine)iminium (PPNCl) a été étudié en solution et en masse. Les effets de la polarité du solvant et de la température de réaction sur la cinétique de polymérisation, la composition du produit et la masse molaire ont été examinés en comparant plusieurs solvants (THF, toluène et cyclohexane). L'analyse cinétique a révélé que la réaction suit une cinétique de premier ordre par rapport à la

concentration en époxyde. Bien que la polarité du solvant ait peu d'effet sur les constantes de vitesse, elle influence fortement la sélectivité du polymère et sa qualité. Parmi les solvants testés, le cyclohexane, non polaire, a permis d'obtenir la meilleure sélectivité en polycarbonate (>75 %) ainsi qu'une masse molaire élevée (~34 kg/mol), tandis que le THF, solvant polaire, a favorisé des réactions secondaires de type réaction d'auto-cyclisation (backbiting), entraînant une formation accrue de carbonates cycliques (~40–60 %) et une masse molaire plus faible (~16 kg/mol). Ces effets sont attribués à la capacité de coordination des solvants envers le centre Al^{3+}: la forte coordination du THF affaiblit la liaison Al–O, favorisant la dissociation des chaînes et les réactions de réaction d'auto-cyclisation (backbiting), tandis que le cyclohexane offre un environnement plus inerte stabilisant les espèces catalytiques actives (**Fig. III-4**).

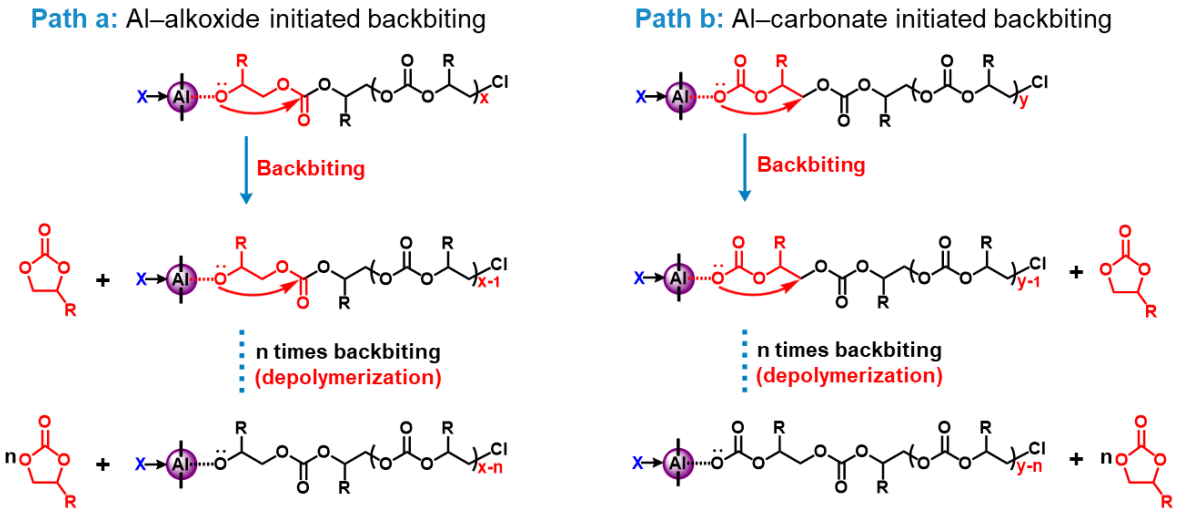

Fig. III-4. Mécanismes de dépolymérisation des chaînes polymères par réaction d'auto-cyclisation (backbiting). La voie (a) s'effectue par réaction d'auto-cyclisation (backbiting) à partir de l'extrémité de chaîne Al–alcoxyde, tandis que la voie (b) implique un réaction d'auto-cyclisation (backbiting) à partir de l'extrémité Al–carbonate. Chaque événement de réaction d'auto-cyclisation (backbiting) libère une unité monomère et une molécule de CO_2, contribuant progressivement à une dépolymérisation par étapes. X désigne une espèce coordinante liée à l'Al^{3+}, incluant les solvants (THF, toluène) et les espèces anioniques (Cl^- provenant du co-catalyseur PPNCl).

Pour la polymérisation en masse, sans solvant, la réaction a présenté des constantes de vitesse apparentes plus élevées (0.09 h^{-1}) que dans les systèmes en solution (0.06 h^{-1}),

permettant d'obtenir une M_n plus élevée et une meilleure sélectivité en polycarbonate (environ 85 % au début). Cependant, l'augmentation de la viscosité à des taux de conversion élevés a limité la diffusion des monomères et ralenti la réaction. L'analyse de la composition des produits a montré que la formation de carbonates cycliques augmentait avec le temps, en raison de réactions de réaction d'auto-cyclisation (backbiting) des chaînes, ce qui a été confirmé par une analyse mécanistique identifiant deux voies principales de dépolymérisation impliquant des intermédiaires de type Al–alcoxyde et Al–carbonate. De plus, la température joue un rôle déterminant: une augmentation de la température de 60 °C à 70 °C a permis d'améliorer la conversion des monomères et la masse molaire (M_n = 36 kg/mol, PDI = 1.23), tandis qu'une temperature de 80 °C a entraîné une diminution de M_n (~22 kg/mol) et de la sélectivité en polycarbonate (~45 %), en raison de l'accélération des réactions secondaires. Ces résultats montrent que le choix judicieux du solvant ainsi qu'une température modérée sont essentiels pour obtenir une bonne sélectivité en polycarbonate et une masse molaire élevée lors des terpolymérisations CO_2/époxyde catalysées par le système porphyrine d'aluminium/PPNCl.

3. Système bicatalytique synergique et amélioration des performances des nanocomposites

Afin de combiner les avantages des deux approches systèmes catalytiques, un système bicatalytique (porphyrine d'aluminium/PPNCl + DMC) a été développé testé en vue d'une pour permettre la terpolymérisation efficace du CO_2, du HO et de l'AGE. En associant la haute activité de la catalyse hétérogène au contrôle moléculaire précis de la catalyse homogène, ce système hybride a permis d'obtenir des conversions de monomères élevées ainsi qu'une augmentation marquée du M_n (~141 kg/mol). Les études cinétiques ont montré que la polymérisation évolue selon une transition temporelle de la catalyse homogène vers une catalyse coopérative. Aux premiers stades, la croissance des chaînes était dominée par le système porphyrine d'aluminium/PPNCl, produisant des polymères de faible M_n avec 100 % de liaisons carbonates. Lorsque le DMC est activé, un mécanisme synergique se met en place, caractérisé par un transfert de chaîne dynamique entre les centres catalytiques Zn et Al (**Fig. III-5**). Ce mécanisme de propagation double a permis de supprimer efficacement les réactions de réaction d'auto-cyclisation (backbiting) et de terminaison de chaîne, conduisant à une

sélectivité polymère améliorée (~92 %) et à une augmentation progressive du M_n au cours du temps. La T_g est restée inférieure à la température ambiante (jusqu'à –14 °C), ce qui favorise un comportement élastomère.

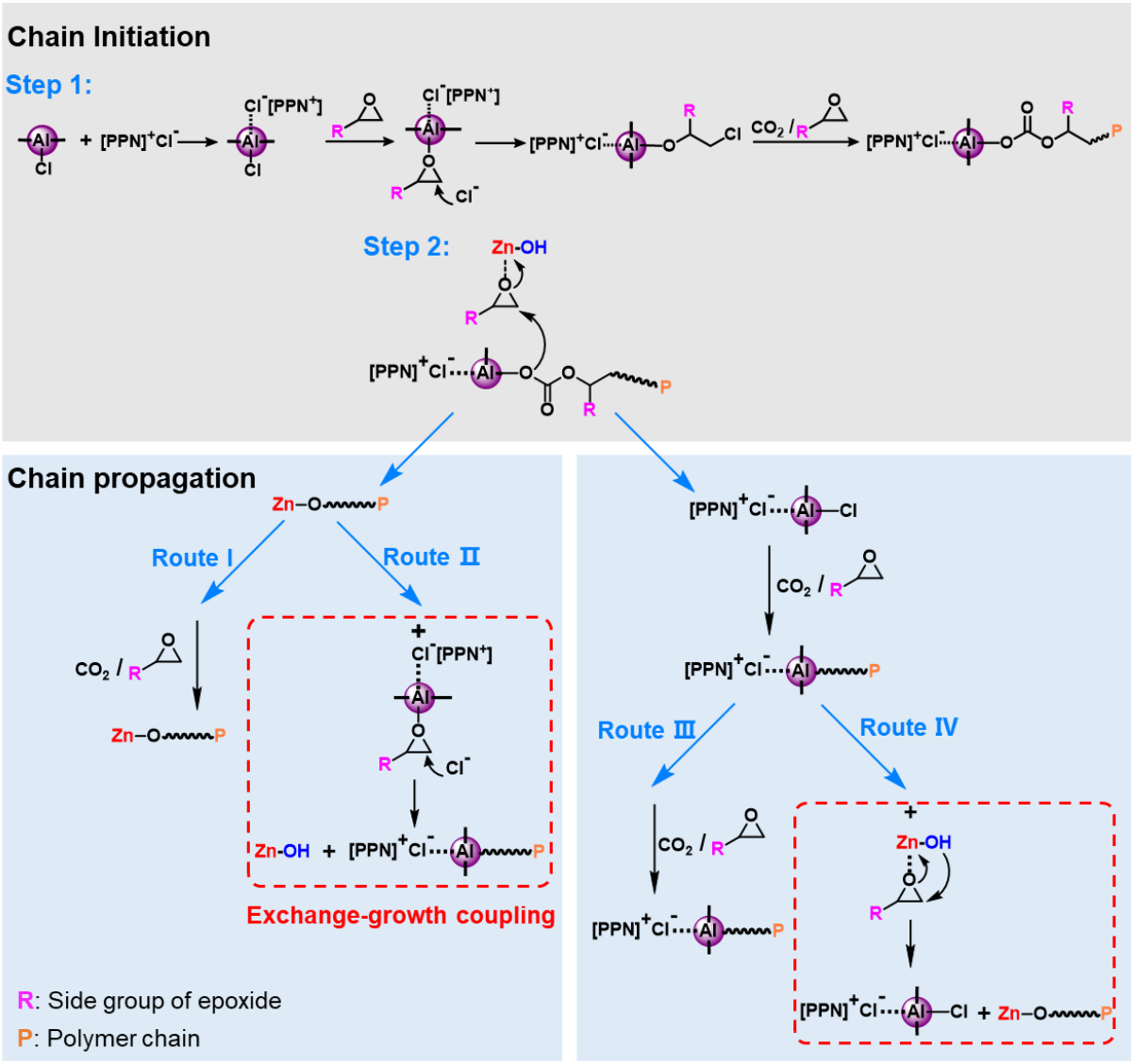

Fig. III-5. Voies mécanistiques proposées pour la terpolymérisation du CO_2 et des époxydes catalysée de manière coopérative par la porphyrine d'aluminium/PPNCl et le DMC.

Des mesures viscoélastiques en fonction de la température ont montré que l'augmentation de la teneur en SiO_2 dans la matrice réticulée CO_2–AGE–HO entraînait une élévation du module élastique et une diminution du tan δ, traduisant un renforcement des interactions entre le caoutchouc et la charge. Pour des teneurs en silice inférieures à 30 phr, une meilleure interaction interfaciale a conduit à une augmentation de la T_g, tandis qu'à des teneurs plus élevées,

l'agrégation excessive de la charge a atténué cet effet. Les essais mécaniques réalisés sur les nanocomposites réticulés au peroxyde ont révélé une relation non monotone entre la teneur en charge et les propriétés mécaniques, avec des performances optimales obtenues pour 30 phr de silice et 10 mol % d'AGE. Comme illustré dans la **Fig. III-6**, le terpolymère CO_2–AGE–HO constitue la matrice élastomère, tandis que les nanoparticules de silice jouent le rôle d'agents renforçants. Le dicumylperoxyde (DCP) permet la réticulation des chaînes polymères pendant la vulcanisation, formant un réseau robuste. Ce réseau est probablement renforcé par des interactions de type liaison hydrogène entre les segments polaires du polymère et les groupes silanol en surface de la silice. Le nanocomposite obtenu présente une résistance à la traction de 5.5 MPa et un allongement à la rupture de 748 %, soit une amélioration de 7.9 fois par rapport à l'élastomère non chargé. Ces résultats démontrent l'efficacité de la catalyse bicomposant dans la production d'élastomères à base de CO_2 performants, aux propriétés ajustables grâce à un contrôle à la fois moléculaire et morphologique.

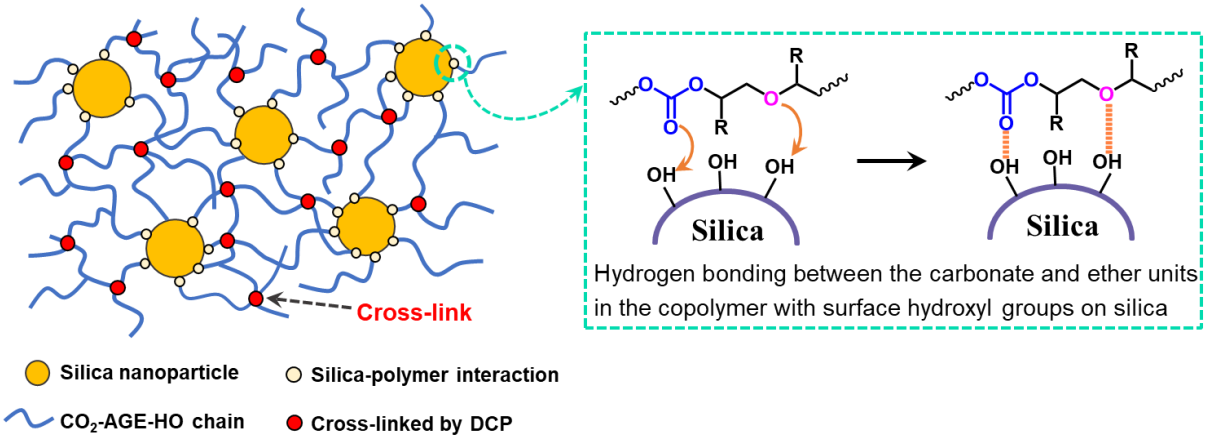

Fig. III-6. Microstructure de l'élastomère poly(carbonate-co-éther) réticulé et renforcé par la silice.

IV. Conclusions et perspectives

Ce travail présente une approche globale de la conception et de la synthèse d'élastomères à base de CO_2 aux propriétés modulables, rendue possible grâce à une sélection rationnelle des monomères, à l'optimisation des stratégies catalytiques et à l'analyse des corrélations structure–propriétés. En utilisant trois systèmes catalytiques distincts, un complexe à base de DMC, une

porphyrine d'aluminium en présence de PPNCl, ainsi qu'un système de catalyse bicomposant, cette étude a permis de mettre en place des voies efficaces pour la production de poly(carbonate-co-éther)s de haute masse molaire, présentant des températures de transition vitreuse ajustables et une diversité de comportements mécaniques. L'introduction d'époxydes fonctionnalisés par des groupes allyles a permis une réticulation post-polymérisation, tandis que les époxydes saturés à longue chaîne ont conféré de la flexibilité, rendant ces matériaux adaptés aux applications élastomères. Par ailleurs, les analyses cinétiques ont apporté un éclairage sur les performances des catalyseurs, les effets du solvant et les mécanismes réactionnels, en soulignant le rôle de la coordination dynamique et des mécanismes de transfert de chaîne dans l'ajustement de la sélectivité et de l'efficacité de propagation.

Le système bicatalytique combinant le DMC et la porphyrine d'aluminium/PPNCl a permis d'atteindre une M_n allant jusqu'à 141 kg/mol, avec une excellente sélectivité et une bonne processabilite. L'intégration de nanorenforts tels que la silice a en outre démontré le potentiel de ces matériaux en tant que composites élastomères fonctionnels. Les nanocomposites optimisés ont présenté une amélioration significative de la résistance à la traction et de l'allongement à la rupture, confirmant les avantages liés à la catalyse bicomposant et à l'ingénierie des composites. Dans l'ensemble, ce travail pose les bases du développement d'élastomères à base de CO_2 évolutifs, durables et aux propriétés modulables, présentant un fort potentiel d'application dans les matériaux souples, les revêtements et les dispositifs flexibles.

Les recherches futures pourraient se concentrer sur le développement de catalyseurs innovants, en particulier la conception de systèmes commutables ou synergiques présentant une activité renforcée et un meilleur contrôle de la séquence de polymérisation. L'élargissement de la gamme de monomères pour inclure des époxydes renouvelables et fonctionnalisés pourrait ouvrir la voie à des élastomères dérivés du CO_2 dotés de propriétés avancées telles que la résistance chimique, la capacité d'auto-réparation et la stabilité thermique. Des études mécanistiques approfondies, appuyées par des techniques de caractérisation in situ et la modélisation computationnelle, seront essentielles pour élucider les mécanismes de propagation et de désactivation des chaînes. Parallèlement, l'optimisation des réseaux

polymères par une réticulation de précision, des liaisons dynamiques et une conception ciblée des charges nanométriques pourrait conduire à une nouvelle génération de matériaux offrant une meilleure ténacité, une reprocessabilité accrue et des fonctionnalités multiples. L'ensemble de ces axes contribuera à accélérer le développement de polymères performants et respectueux du climat à base de dioxyde de carbone.

Chapter 1 General introduction

1.1 Overview

In recent years, with the depletion of fossil resources and the accelerating impact of global climate change, the efficient utilization of carbon dioxide (CO_2) has emerged as a key focus in the fields of green chemistry and sustainable materials. As an abundant, non-toxic, and inexpensive C1 feedstock, CO_2 can be catalytically converted into diverse chemicals such as methane, methanol, urea, cyclic carbonates, and polycarbonates. However, due to its thermodynamic stability, effective transformation typically requires high energy reactants like hydrogen, strained cyclic compounds (e.g., epoxides), or amines. Among various strategies, the copolymerization of CO_2 with epoxides to form polycarbonates is particularly attractive because it offers near 100% atom economy and is highly scalable. These polymers exhibit tunable properties and good processability, making them suitable for applications such as plastics, thermoplastic elastomers, and polyether polyols for polyurethanes.

Despite this progress, research remains largely focused on conventional epoxides like propylene oxide (PO) and cyclohexene oxide (CHO), valued for their reactivity, selectivity, and industrial availability. For example, poly(cyclohexene carbonate) (PCHC) has a high T_g (~115 °C) and excellent thermal stability (~300 °C), making it suitable for engineering plastics. In contrast, poly(propylene carbonate) (PPC) with a lower T_g (30–50 °C), making it attractive for packaging and biodegradable films. However, the intrinsic stiffness and relatively high T_g of these materials limit their suitability for elastomeric applications that require flexibility and reversible deformation at room temperature. To overcome this limitation, the introduction of epoxides bearing long alkyl side chains enhances chain mobility, thereby lowering the T_g and broadening their application in soft and flexible materials. At the same time, the use of functionalized epoxides bearing vinyl groups provides reactive sites for post-polymerization crosslinking reactions (e.g., thiol–ene reactions), ensuring sufficient mechanical strength.

To develop CO_2-based elastomers, several criteria must be met: (1) Low glass transition temperature ($T_g < 0$ °C): ensures flexibility and softness at room temperature. (2) Cross-linkable

units: the introduction of functional groups (e.g., vinyls) allows the formation of three-dimensional networks after polymerization, thus improving elasticity and solvent resistance. (3) Low crystallinity or amorphous morphology: facilitates free chain mobility and prevents phase separation, which are essential for uniform cross-linking and mechanical flexibility in elastomeric materials. (4) High molecular weight: critical for forming robust networks with minimal sol fraction, thereby enhancing mechanical strength and elasticity. To meet these requirements, we introduced epoxides bearing long alkyl chains to lower the T_g, as well as allyl glycidyl ether (AGE) as a functional monomer to confer crosslinking capacity. The terpolymerization of CO_2, AGE, and long alkyl chain epoxides represents a promising strategy for the design of CO_2-based elastomers that combine flexibility with mechanical robustness.

Catalyst design plays a pivotal role in determining catalytic efficiency, polymer architecture and molecular weight. Currently, catalytic systems for CO_2/epoxide copolymerization can be broadly classified into heterogeneous and homogeneous types. Heterogeneous catalysts, such as zinc–cobalt(III) double metal cyanide complexes (Zn-Co DMC), are widely used in industry due to their low cost, high stability, and good activity. However, they often suffer from poorly defined active sites, broad molecular weight distributions, and limited control over polymer microstructure. Homogeneous catalysts like aluminum porphyrin combined with bis(triphenylphosphoranylidene)ammonium chloride (PPNCl) provide better control and defined architectures, making them suitable for mechanistic studies, though they typically exhibit lower activity and longer reaction times.

Despite significant progress in both catalyst development and monomer design, several challenges remain in the field of CO_2/epoxide terpolymerization. Most existing catalytic systems are designed for standard monomers such as PO or CHO, and show limited efficiency when applied to functionalized epoxides such as AGE or those bearing long alkyl chains. It remains difficult to simultaneously reconcile high molecular weight, minimal formation of cyclic carbonates as by-products, and precise control of the molecular structure. Furthermore, the influence of polymerization techniques (bulk vs. solution polymerization) on polymer properties is not fully understood, especially in relation to solvent polarity. Finally, many studies treat catalytic performance and material properties separately and lack a unified

framework that connects catalyst design, polymer microstructure, and final material properties. Addressing these challenges requires an interdisciplinary strategy that unifies catalyst innovation, mechanistic understanding, and materials design to realize the full potential of CO_2-based elastomers.

1.2 Objectives

This thesis focuses on the design and synthesis of CO_2-based elastomers by catalytic terpolymerization, as well as the development of high performance nanocomposites with tunable mechanical and thermal properties. The study integrates monomer engineering, catalyst and process optimization, polymerization control, and post-functionalization strategies (as illustrated in **Scheme I**). Through a structure and property driven approach, this work aims to develop a robust, scalable, and environmentally sustainable strategy for the controlled synthesis of high molecular weight, high-performance CO_2-based elastomers. The study not only investigates the mechanistic aspects of catalyst controlled terpolymerization but also provides practical guidance for utilizing CO_2 as a renewable carbon feedstock in the production of sustainable polymeric materials.

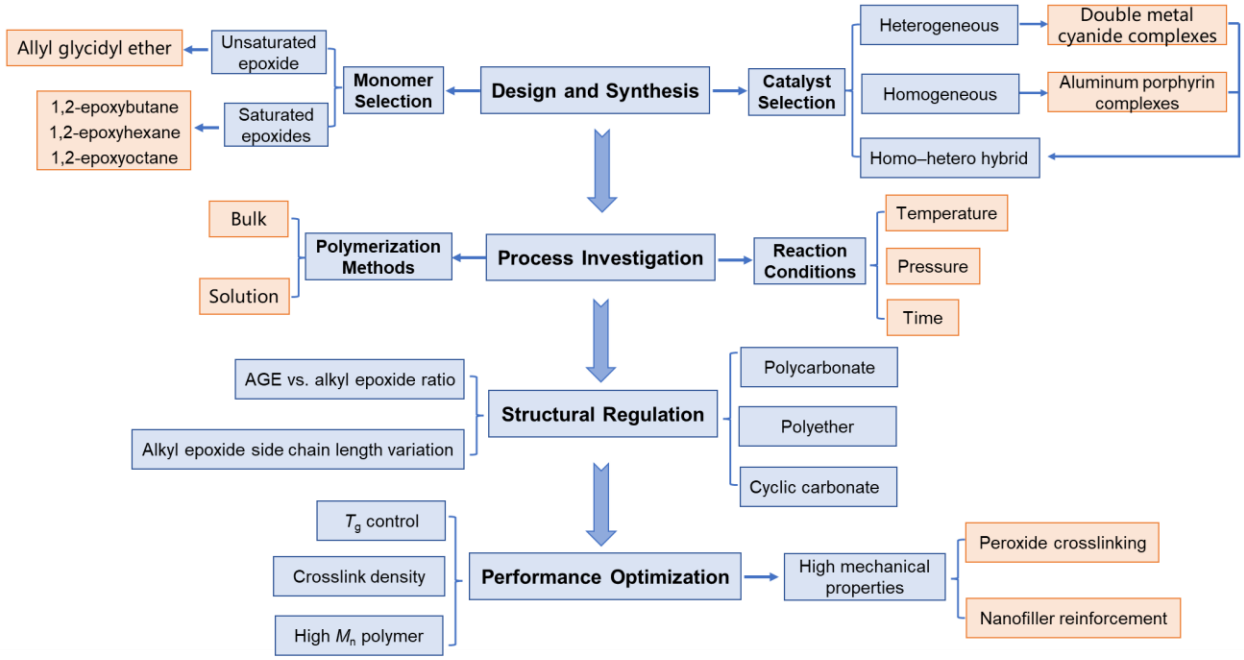

Scheme 1. Research framework for CO_2-based elastomer synthesis via terpolymerization of CO_2, unsaturated epoxide, and saturated epoxide.

The main objectives of this thesis are as follows:

(1) Designing and synthesizing CO_2-based elastomers via the terpolymerization of CO_2, AGE (for reactive crosslinking sites), and long-chain alkyl epoxides (for flexible segments) using both single and dual catalyst systems.

(2) Systematically studying the influence of catalyst type (heterogeneous Zn-Co DMC vs. homogeneous Al porphyrin/PPNCl), solvent polarity, and reaction conditions on polymerization kinetics, selectivity, and molecular weight.

(3) Developing a synergistic dual catalyst system to overcome the limitations of single catalysts, enabling the synthesis of high molecular weight poly(carbonate-co-ether)s with improved mechanical properties.

(4) Enhancing the functionality of the resulting polymers through peroxide crosslinking and silica nanoparticle reinforcement to develop robust elastomeric nanocomposites.

1.3 Thesis outline

This thesis is organized into seven chapters:

Chapter 1 includes general introduction, objectives of this thesis, and thesis outline.

Chapter 2 summarizes recent advances in CO_2/epoxide copolymerization, covering carbon dioxide utilization, reaction mechanisms, catalytic systems, and the development of CO_2-based polymers including plastics, polyurethanes, and elastomers.

Chapter 3 describes the materials and characterization techniques employed throughout this work.

Chapter 4 presents the synthesis and thermal mechanical tuning of CO_2-based elastomers via Zn-Co DMC catalyzed terpolymerization, emphasizing the influence of monomer composition on T_g and mechanical properties.

Chapter 5 investigates the kinetics and mechanism of CO_2/AGE/HO terpolymerization under various solvent and temperature conditions using the Al porphyrin/PPNCl catalyst system, offering insights into process optimization.

Chapter 6 introduces a dual catalytic approach combining Zn-Co DMC and Al porphyrin/PPNCl to synthesize high molecular weight terpolymers. The resulting elastomers are crosslinked and reinforced with silica nanoparticles to yield high performance nanocomposites.

Chapter 7 summarizes the main findings and discusses future research directions in sustainable CO_2-based polymer development.

Chapter 2 Research background and state of the art

2.1 Chemical utilization of carbon dioxide

Over the past few decades, fossil fuels have served as a primary energy source for various industrial processes. However, the extensive consumption of petroleum and its derivatives, driven by ongoing industrialization and urbanization, has led to a marked increase in atmospheric CO_2, which is a major driver of global warming.[1, 2] As a result, widespread environmental consequences have emerged, including sea level rise, more frequent extreme weather events, biodiversity loss, and disruption of ecosystem stability.[3, 4] Meanwhile, the elevated atmospheric CO_2 concentration has placed increasing pressure on natural carbon sinks such as oceans and forests, thereby disturbing the global carbon cycle.[5-7] Therefore, the effective utilization of anthropogenic CO_2 emissions has become a crucial strategy not only for mitigating greenhouse gas concentrations but also for enabling the sustainable development of carbon-based chemical feedstocks.

CO_2 can be utilized through various physical means and chemically transformed into value added products.[8-10] In physical utilization, liquid CO_2 is commonly employed as a cryogenic fluid, while solid CO_2 is used to maintain frozen environments. Additionally, owing to its natural antimicrobial properties, CO_2 is widely used to extend the shelf life of food and drinks.[11, 12] Its non-flammable nature also makes it suitable for use in fire extinguishers, where it displaces oxygen to suppress combustion.

With growing emphasis on economic and environmental sustainability, the chemical transformation of CO_2 into valuable compounds has gained significant attention.[4, 13, 14] However, its high thermodynamic stability, often requiring energy input or catalytic assistance for effective conversion. Currently, CO_2 is used as a carbon feedstock in the synthesis of various industrial chemicals such as methanol, dimethyl ether, dimethyl carbonate, urea, styrene, and salicylic acid.[15, 16] These compounds have broad applications across energy, agriculture, materials science, and pharmaceuticals.

Beyond small molecule synthesis, CO_2 can be chemically incorporated into polymers through copolymerization with substrates such as diamines, diols, olefins, alkynes, epoxides, episulfides, and aziridines.[17-19] These reactions yield diverse polymers including polyureas, polyesters, polycarbonates, poly(ether-co-carbonate)s, and polythiocarbonates. Among these, the copolymerization of CO_2 with epoxides has emerged as one of the most promising approaches due to its mild reaction conditions, relatively high reactivity, and tunable product structures.[20] Therefore, this thesis focuses on the CO_2/epoxide copolymerization route, aiming to develop high performance, sustainable polycarbonates and poly(carbonate-co-ether)s.

2.2 Reaction between CO_2 and epoxides

As shown in **Fig. 2.1**, although the copolymerization system of CO_2 and epoxides involves only two simple reactants, the underlying chemical reaction mechanisms and issues related to microscopic control are extremely complex and diverse.

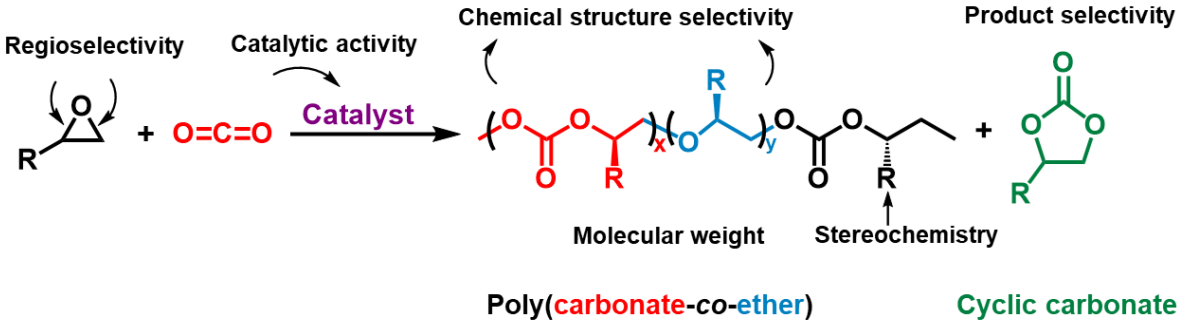

Fig. 2.1. Copolymerization of CO_2 and epoxide.

(1) Product selectivity (polymer vs. cyclic carbonate):

The copolymerization of CO_2 and epoxides is often accompanied by the formation of cyclic carbonates, which are small molecule byproducts generated alongside the desired polymer. Product selectivity is typically defined as the proportion of polymer relative to the total product. This selectivity is significantly influenced by the epoxide structure, catalyst system, and reaction conditions.

In general, terminal epoxides bearing electron withdrawing groups (e.g., epichlorohydrin (ECH), styrene oxide (SO)) exhibit a stronger tendency to form cyclic carbonates. Terminal

epoxides with electron donating groups (e.g., propylene oxide (PO)) show moderate selectivity toward polymer formation, while alicyclic epoxides (e.g., cyclohexene oxide (CHO), limonene oxide (LO)) display the lowest propensity for generating cyclic byproducts due to the significant steric hindrance, which limits the intramolecular backbiting required for cyclic carbonate formation.[21, 22]

From a catalyst design perspective, bifunctional or multi site catalysts with cooperative catalytic effects have been shown to effectively suppress side reactions and enhance polymer selectivity.[23, 24] Regarding reaction conditions, elevated temperatures or reduced CO_2 pressure tend to favor the formation of cyclic carbonates, thereby decreasing polymer selectivity.[25-27] Therefore, rational design of catalytic systems and optimization of reaction parameters are crucial for achieving high selectivity in CO_2/epoxide copolymerization.

(2) Chemical structure selectivity of the polymer (carbonate linkage vs. ether linkage):

The alternating copolymerization of CO_2 with epoxides results in the formation of polycarbonates, whereas the successive insertion of epoxide monomers leads to the generation of ether linkages. The formation of carbonate vs. ether linkages is competitive and directly determines the chemical structure of the resulting polymer chains. Structural selectivity is typically evaluated by the proportion of carbonate units in the polymer, which is commonly referred to as carbonate linkage selectivity.

Similar to product selectivity, the carbonate linkage selectivity is governed by a combination of factors, including the nature of the catalyst, the type of epoxide used, and the reaction conditions.[21, 28] This structural selectivity has a direct impact on the material properties and potential applications of the resulting polymers. For instance, in CO_2-based polycarbonates such as polypropylene carbonate intended for biodegradable plastics, the presence of ether linkages generally reduces the degradation rate of the material. In contrast, for elastomeric applications, a controlled incorporation of ether linkages can lower the T_g, thereby enhancing the flexibility of the polymer. Thus, the tunable coexistence of carbonate and ether linkages provides a structural and design advantage for tailoring the performance of these materials.

(3) Regioselectivity (α-ring opening vs. β- ring opening):

Regioselectivity refers to the preference for the nucleophilic attack site during the ring opening of epoxides. In the copolymerization of CO_2 with epoxides, the nucleophilic attack can occur at either the secondary carbon (α-position) or the methylene carbon (β-position) of the epoxide ring.[29, 30] When the ring-opening consistently occurs at either the α- or β-position, the resulting polymer chains adopt a head-to-tail configuration. In contrast, alternating α- and β-ring openings give rise to head-to-head and tail-to-tail linkages (**Fig. 2.2**).

Epoxides typically undergo nucleophilic ring-opening at the β-position, which is favored due to lower steric hindrance. However, under practical catalytic conditions, the limited regioselectivity of most catalysts results in polymers with regiorandom structures, where both α- and β-opening pathways occur simultaneously. In addition, the electronic properties of ring substituents significantly influence regioselectivity. Epoxides bearing electron withdrawing groups (e.g., SO, ECH) are more susceptible to nucleophilic attack at the α-position, whereas epoxides substituted with electron donating groups (e.g., PO) predominantly undergo β-ring opening.[30, 31]

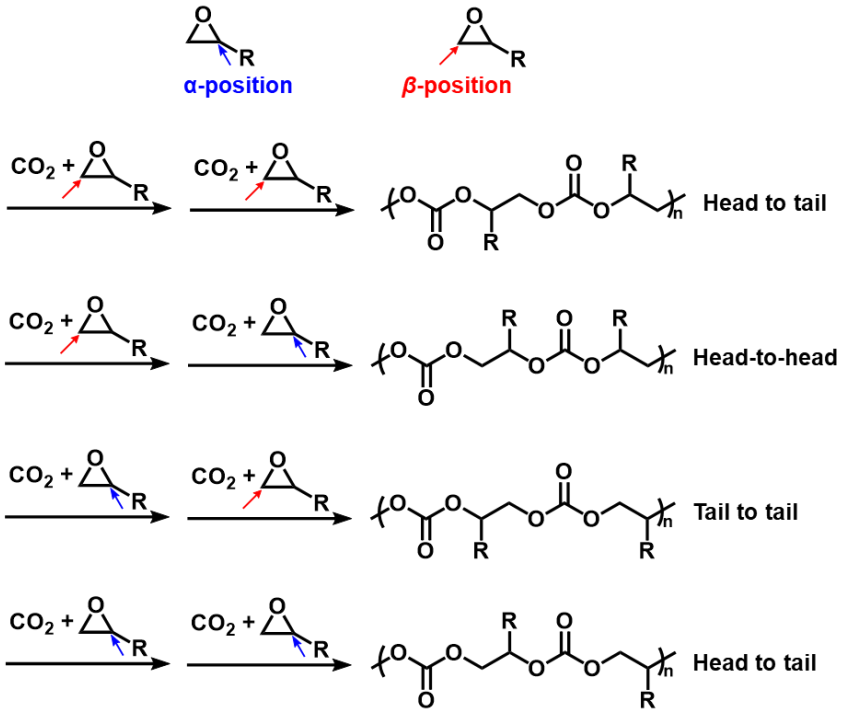

Fig. 2.2. Regiochemistry of polycarbonates from terminal epoxides and CO_2.[30]

(4) Stereoselectivity (isotactic, syndiotactic, atactic):

Stereoselectivity refers to the differential reactivity of chiral epoxides under chiral catalysts, leading to the formation of stereoregular polymer chains composed of tactic isomers. Depending on the configuration of the chiral centers in adjacent carbonate units, the resulting polymer can be classified as isotactic, syndiotactic, or atactic (**Fig. 2.3**).[32] In an isotactic structure, the chiral centers of neighboring carbonate units possess the same absolute configuration; in a syndiotactic structure, the configurations alternate in a regular fashion; and in an atactic structure, the configurations are randomly distributed. High stereoregularity (i.e., a high degree of isotacticity or syndiotacticity) facilitates the ordered packing of polymer chains, which enhances thermal stability and gas barrier properties. In contrast, polymers with low stereoregularity tend to be amorphous and are well suited for applications requiring flexibility or biodegradability.[33]

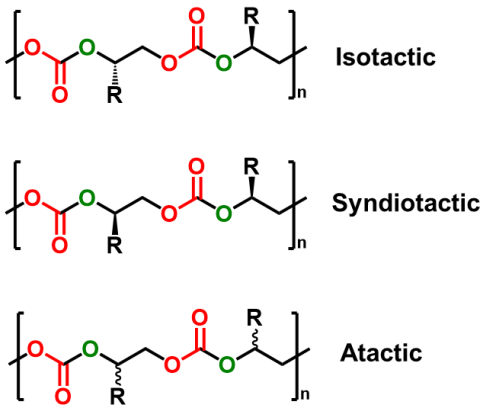

Fig. 2.3. Stereoselectivity in the copolymerization of epoxide and CO_2.[32]

(5) Molecular Weight:

In the ring opening alternating copolymerization of CO_2 and epoxides, the number average molecular weight (M_n) of the resulting polymer is a key metric reflecting both polymerization efficiency and the degree of control. The regulation of M_n is governed by a combination of factors.

Foremost among the factors affecting polymer molecular weight is the catalyst system, particularly the structure of the active site. Bimetallic catalysts with flexible bridging ligands often exhibit cooperative effects that enhance catalytic activity and facilitate the formation of high M_n polymers.[21, 34] The electronic and steric properties of the ligand framework also

play a critical role in monomer activation and chain propagation, ultimately influencing M_n.[22, 27, 35] The use of chain transfer agents (e.g., diols) enables precise control over polymer chain length and polydispersity index (PDI) via chain transfer reactions. In addition, reaction parameters such as temperature and CO_2 pressure significantly impact on M_n. While elevated temperatures may accelerate polymerization rates, they also promote side reactions that reduce M_n.[36] In contrast, higher CO_2 pressure tends to suppress side reactions and enhance polymer M_n.[37, 38]

(6) Types of epoxides:

From a structural standpoint, the most widely studied epoxide in CO_2 copolymerization are terminal epoxides (e.g., PO) and alicyclic epoxides (e.g., CHO). More recently, a broad range of functionalized epoxides has been investigated (**Fig. 2.4**) to access polycarbonates with tailored structures and properties.[31] As epoxide side chains shift from short alkyl groups to longer or ether containing substituents, catalytic activity typically declines and side reactions such as the formation of cyclic carbonates become more prevalent. This trend is primarily attributed to increased steric hindrance and electronic effects introduced by bulky or electron-donating substituents, which can interfere with epoxide coordination and activation at the catalytic site, thereby reducing the selectivity of CO_2 insertion.[39, 40]

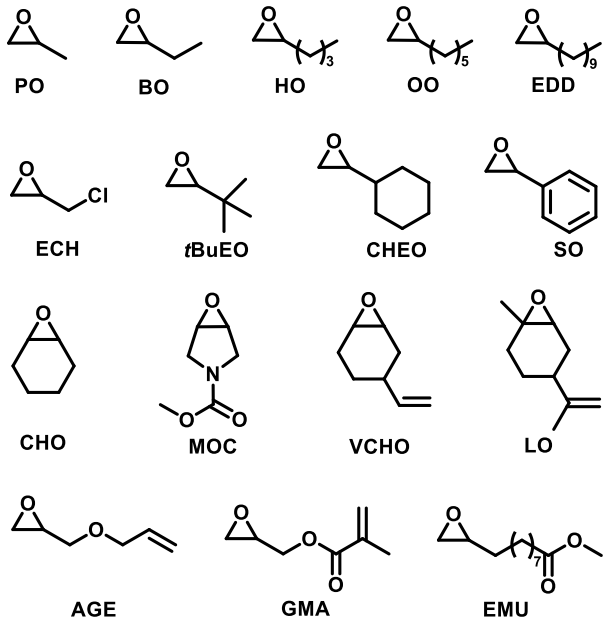

Fig. 2.4. Epoxides reported to be used in the copolymerization of CO_2 and epoxides.

The growing diversity of epoxide structures presents new challenges for catalyst performance in terms of activity and selectivity. Many conventional catalysts are not well-suited to accommodate such variations in steric and electronic environments. These effects highlight the critical role of catalyst design in determining polymerization efficiency, product selectivity, and polymer architecture, particularly in systems involving structurally diverse epoxides. Consequently, the development of new, high performance catalysts capable of accommodating a broad range of epoxide structures has become a central focus in recent CO_2/epoxide copolymerization research. The following sections review representative catalyst architectures, their mechanisms of action, and recent advances in the field.

2.3 Catalytic system for copolymerization of CO_2 and epoxides

In 1969, Inoue and his colleagues discovered that a mixture of diethylzinc ($ZnEt_2$) and water was catalytically active for the alternating copolymerization of propylene oxide (PO) and CO_2.[41] Since then, significant progress has been made in the development of both heterogeneous and homogeneous catalytic systems. However, a comprehensive understanding of the reaction mechanism is still lacking. As a result, this area continues to attract active considerable research interest. Although the full reaction pathway has not been conclusively established, the “coordination–insertion” mechanism is widely accepted as the fundamental model of CO_2/epoxide copolymerization.[34, 42]

(1) Chain initiation

As illustrated in **Fig. 2.5**, the general copolymerization typically begins when a nucleophilic species (X) attacks a metal-activated epoxide, resulting in ring-opening and the generation of a metal alkoxide intermediate. CO_2 subsequently inerts rapidly into the metal–alkoxide bond, without requiring external activation,[43-45] forming a metal carbonate species. The mode of initiation differs depending on the nature of the catalytic system. Broadly, these systems can be classified by the number of active components involved, giving rise to two principal initiation mechanisms: single component initiation and two component initiation.

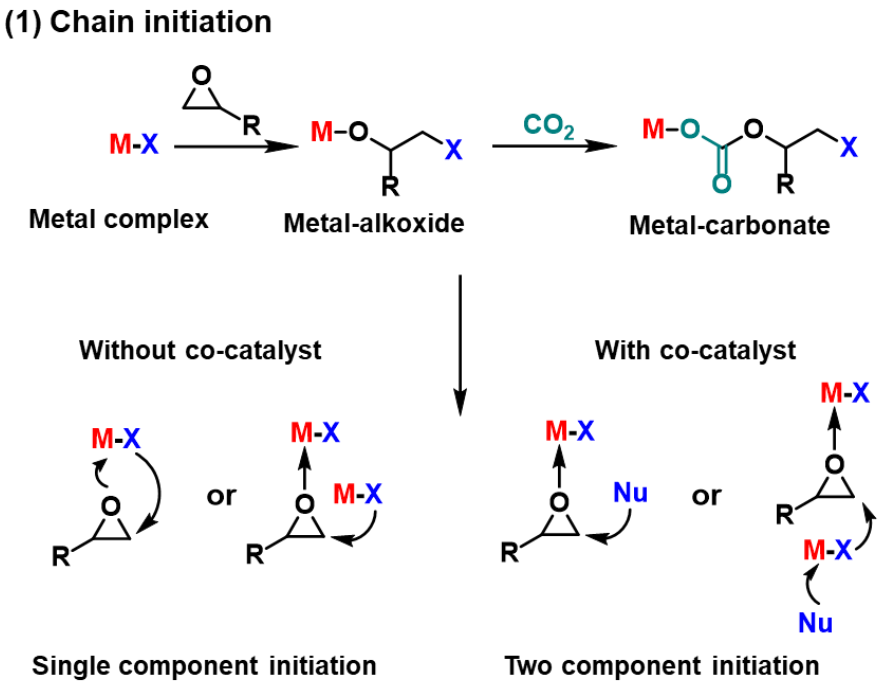

Fig. 2.5. Proposed initiation mechanism for CO_2/epoxide copolymerization. M = metal center of catalyst; X = nucleophilic group; Nu = externally added nucleophile.

Single component initiation refers to a process in which only the metal complex participates in chain initiation, without requiring an external nucleophile. In this mechanism, the epoxide first coordinates to the metal center. Then followed by heterolytic cleavage of the M–X bond, and the dissociated X group intramolecularly attacks the activated epoxide, resulting in ring-opening and insertion into the M–X bond. Alternatively, in systems involving multinuclear or bimetallic complexes, one metal center may coordinate to and activate the epoxide, while a nucleophilic ligand (X) from a second metal complex attacks the activated epoxide, thereby achieving ring-opening and insertion.

In contrast, two component initiation involves an intermolecular cooperative effect between a catalyst and an external co-catalyst. The co-catalyst typically plays one or two principal roles: (i) as a promoter, it coordinates to the metal center and weakens the M–X bond, thereby facilitating the release of X, which subsequently acts as a nucleophile to attack the epoxide; (ii) as an initiator, it directly participates in the ring-opening of the epoxide through nucleophilic attack.

In homogeneous catalytic systems, such co-catalysts are often essential for enhancing catalytic activity. These co-catalysts typically fall into two categories (**Fig. 2.6**): neutral organic bases, such as 4-(dimethylamino)pyridine (DMAP) and N-methylimidazole (NMeIm); and ionic quaternary salts, such as bis(triphenylphosphine)iminium chloride (PPNCl) and bis(triphenylphosphine)iminium azide ($PPNN_3$).[42]

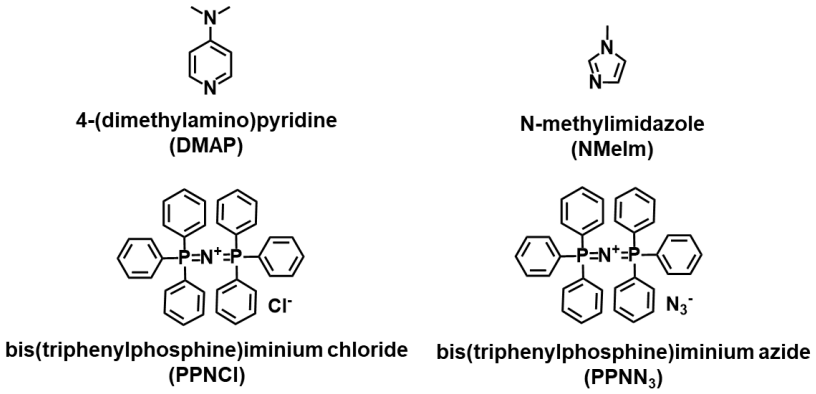

Fig. 2.6. Typical co-catalyst structures involved in CO_2/epoxide copolymerization systems.[42]

(2) Chain propagation

The chain propagation process proceeds via nucleophilic attack by the metal–carbonate species, formed during initiation, on a newly coordinated epoxide. Subsequent CO_2 insertion regenerates the metal–carbonate species and extends the polycarbonate chain, thereby continuing the catalytic cycle (**Fig. 2.7**). A key feature of this process is the coordination–dissociation equilibrium between the metal center of catalyst and the growing anionic polymer chain.[22, 46] Maintaining this equilibrium is critical for effective propagation. When the anionic chain end is insufficiently stabilized by coordination to the metal center, a back-biting reaction may occur, where the uncoordinated chain end undergoes intramolecular attack on the polymer backbone, leading to the formation of cyclic carbonate byproducts and compromising high molecular weight polymer formation.[47] This process is more favorable in the uncoordinated state due to a lower energy barrier compared to the coordinated form.[48] Additionally, in some catalytic systems, the metal–alkoxide intermediate can promote consecutive epoxide ring-opening events without CO_2 insertion, resulting in the incorporation of ether linkages into the polymer backbone.[21, 49] This reaction reduces carbonate linkage

selectivity and thus influences both polymer structure and properties. Therefore, the polymer selectivity and carbonate linkage selectivity are assessed and reported in this thesis.

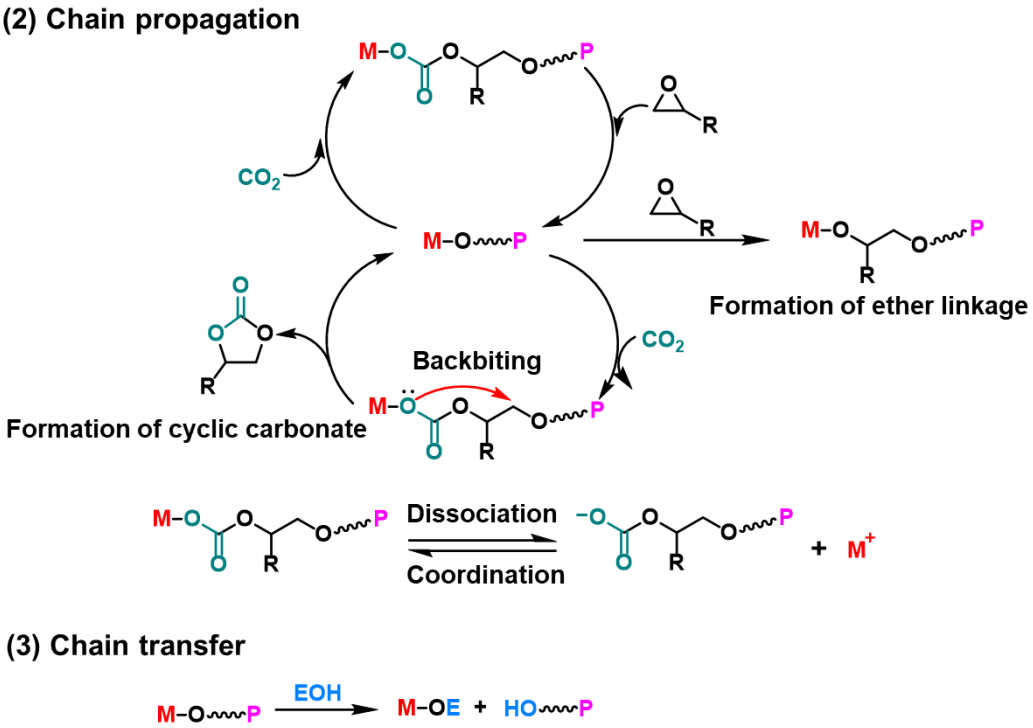

Fig. 2.7. Proposed chain propagation mechanism in CO_2/epoxide copolymerization, highlighting the coordination–dissociation equilibrium between the metal center (M) and the growing polymer chain (P).

(3) Chain transfer

Chain transfer reactions typically occur through the interaction of the growing anionic chain end with proton compounds (EOH) such as water or ethanol.[31, 34] This terminates the active species and results in the formation of hydroxyl-terminated polymer chains, thereby limiting molecular weight and compromising structural uniformity. As such, uncontrolled chain transfer is generally undesirable and requires rigorous purification of monomers and solvents. Nevertheless, chain transfer can also be strategically harnessed to control polymer architecture. For instance, the use of multifunctional chain transfer agents enables the synthesis of block copolymers, star-shaped polymers, or branched polycarbonates through controlled termination and re-initiation mechanisms.[50] Therefore, maintaining a favorable balance among initiation, propagation, and chain transfer processes is critical. Such control not only ensures the formation

of well-defined polycarbonates with high molecular weights but also enables the rational design of more complex and functional polymer architectures.

These mechanistic features directly influence the control over polymerization outcomes, including molecular weight, dispersity, and polymer architecture. Therefore, understanding the relationship between initiation, propagation, and potential side reactions is essential for evaluating and optimizing catalytic performance. In a well-controlled copolymerization system, initiation typically occurs at a faster rate than chain propagation. This kinetic characteristic ensures that most polymer chains begin growing simultaneously, leading to a degree of polymerization (DP) that is primarily governed by the catalyst concentration and directly correlated with the number average molecular weight (M_n). To evaluate the degree of control in such systems, several key criteria are widely recognized: (i) a linear relationship between M_n and monomer conversion, (ii) a narrow molecular weight distribution (i.e., low polydispersity index, PDI), (iii) the ability to sequentially incorporate different monomers for block copolymer synthesis, (iv) a high ratio of initiation to propagation rates (k_i/k_p), and (v) a high propagation to chain transfer rate ratio (k_p/k_{tr}).

2.3.1 Heterogeneous catalytic systems

The development of catalyst systems for the alternating copolymerization of CO_2 and epoxides began with the study of heterogeneous catalysts. Compared to homogeneous systems, heterogeneous catalysts typically tend to produce polymers with broader molecular weight distributions and more ether linkages. Moreover, their structural non-uniformity limits control over active sites, making it difficult to investigate the reaction mechanism. Despite these drawbacks, heterogeneous catalysts offer high catalytic activity and are made from inexpensive raw materials, making them more suitable for the industrial production of CO_2-based polycarbonates. As a result, most commercially produced CO_2-based polycarbonates still rely on heterogeneous catalysts. The most widely used types include zinc carboxylates, rare-earth ternary complexes, and double metal cyanide catalysts, which are discussed in detail in the following sections.

2.3.1.1 Zinc glutarate

Zinc glutarate (ZnGA), a widely studied heterogeneous metal carboxylate catalyst, has drawn extensive attention in the field of CO_2/epoxide copolymerization due to its low toxicity, thermal stability, and catalytic efficiency. Its ease of synthesis and scalability have further facilitated its transition from laboratory research to industrial application.[30] ZnGA is typically synthesized by reacting zinc oxide with glutaric acid in toluene, followed by azeotropic removal water and vacuum drying.[51] Due to its extremely low solubility, ZnGA remains heterogeneous in nature, which historically hindered the elucidation of its crystalline structure and limited understanding of its molecular architecture. This limitation was overcome in 2004, when Kim et al. successfully determined its crystal structure via single-crystal X-ray diffraction. The study revealed that ZnGA comprises a layered coordination polymer, in which Zn^{2+} ions are tetrahedrally coordinated by oxygen atoms from four distinct glutarate ligands (**Fig. 2.8**).[52]

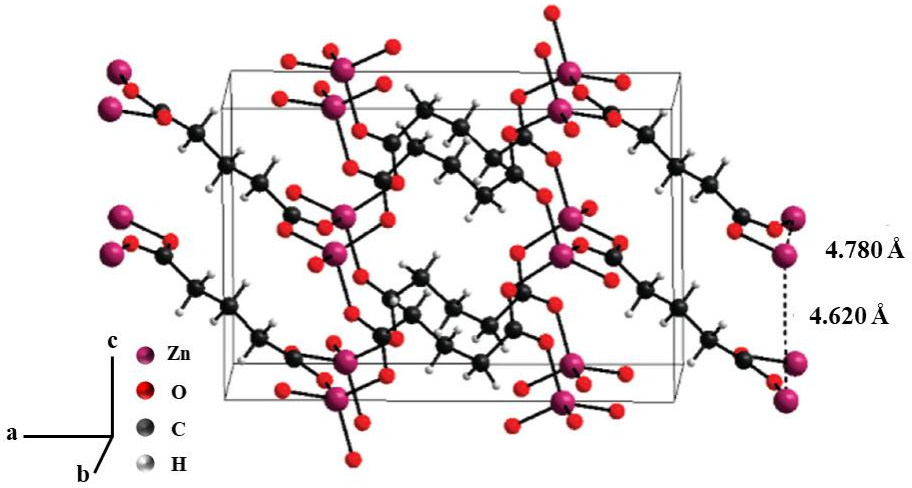

Fig. 2.8. Schematic representation of the crystal structure of ZnGA.[52]

Although ZnGA is structurally stable and easy to prepare, its catalytic performance remains limited, with turnover frequencies (TOFs) below 5 h^{-1}.[47] To enhance activity, considerable research efforts have focused on reducing particle size and increasing surface area.[53] Mechanical treatments such as ball milling or ultrasonication have been shown to decrease ZnGA particle size to the submicron level (0.2–0.3 μm), leading to a notable increase in TOF from 3.4 h^{-1} to 7.8 h^{-1}.[54] Post-synthetic activation in humid atmospheres has also

shown considerable performance improvement, attributed to the generation of surface Zn–OH groups that likely serve as active initiation sites.[55]

In addition to physical methods, structural modifications of ZnGA have also been explored to improve catalytic activity. Efforts to alter the coordination environment by varying zinc precursors or dicarboxylate ligands have yielded mixed outcomes. For example, ZnGA synthesized using diethyl zinc ($ZnEt_2$) and subsequently activated with SO_2 to form surface-bound ethylsulfinate species exhibits significantly enhanced productivity, reaching up to 300 g polymer/g Zn,[56] which is higher than that of conventionally prepared ZnGA (< 100 g polymer/g Zn).[53, 57] Further modifications involved substituting glutaric acid with homologous dicarboxylic acids to investigate the effect of alkylene chain length on catalytic performance. Although it was previously assumed that only glutarate (C_5) exhibited catalytic activity, later studies demonstrated that zinc adipate (ZnAA, C_6) and zinc pimelate (ZnPA, C_7) could achieve comparable TOFs of 5.4 and 5.2 h^{-1}, respectively.[58, 59] In contrast, zinc succinate (ZnSA, C_4) remains essentially inactive. This limitation is attributed to the crystal structure of ZnGA, which lacks the critical Zn–Zn separation distance of 3 to 5 Å, a geometric requirement believed to enable cooperative catalysis by facilitating simultaneous activation of CO_2 and epoxide on adjacent zinc centers.[44, 60]

Overall, ZnGA remains a cornerstone in heterogeneous CO_2-epoxide copolymerization catalysis, especially due to its low cost, safe and scalable synthesis, and proven suitability for industrial applications. Nevertheless, its catalytic activity is fundamentally constrained by surface limited reactivity and diffusion barriers. Future research should prioritize efforts to elucidate the nature of surface active species, potentially through a combination of in situ spectroscopic techniques and complementary computational modeling.

2.3.1.2 Rare earth metal complexes

Rare earth metal (REM) complexes were initially explored for their remarkable catalytic activity in the ring opening polymerization of epoxides and alkylene sulfides. These catalysts typically involve the in situ formation of heterometallic complexes from a rare earth metal salt, an organometallic co-catalyst (e.g., $Al(i\text{-}Bu)_3$ or $ZnEt_2$), and a multidentate alcohol such as

glycerol. Early examples, such as $Y(P204)_3$–$Al(i\text{-}Bu)_3$–glycerol, demonstrated moderate catalytic activity for CO_2/PO copolymerization, producing polymers with relatively low carbonate linkage content (~30–40%) despite achieving high M_n about 476 kg/mol and TOF around 2500 g polymer/mol catalyst.[61] These results were promising but insufficient for practical applications due to the low incorporation of CO_2.

To improve carbonate incorporation, Tan et al. replaced the aluminum alkyls with zinc-based cocatalysts ($ZnEt_2$) and used more reactive rare earth salts such as $Y(CF_3COO)_3$. In the presence of glycerol, this ternary system produced poly(propylene carbonate) (PPC) with over 95% carbonate linkages, M_n exceeding 100 kg/mol, and TOF around 4200 g polymer/mol cat.[62] This strategy was also applicable to other epoxides. When cyclohexene oxide (CHO) was used as monomer, the system produced fully alternating poly(cyclohexene carbonate) (PCHC) with 100% carbonate linkages and M_ns between 100–300 kg/mol.[63] Mechanistic studies revealed that $ZnEt_2$ primarily generated the active sites, while the rare earth salt facilitated epoxide activation and stabilized the reaction environment.

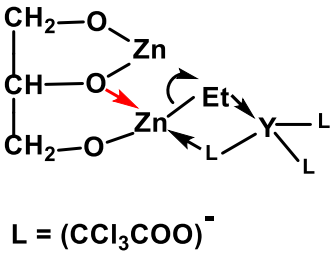

Fig. 2.9. Possible structure of $Y(CCl_3COO)_3$–$ZnEt_2$–glycerol ternary catalytic system.[64]

Due to the high synthesis cost and complexity of $Y(CF_3COO)_3$, $Y(CCl_3COO)_3$ was introduced as a cost-effective substitute,[65] exhibiting comparable catalytic performance.[66] However, the overall efficiency of the $Y(CCl_3COO)_3$–$ZnEt_2$–glycerol system was hampered by limited active site accessibility, only about 11.7% of the theoretical active centers were effectively involved in catalysis. This inefficiency was attributed to agglomeration caused by coordination between unsaturated Zn centers and nucleophilic oxygen atoms, potentially leading to partial embedding of active centers.[67] To address this, Lu and co-workers immobilized the $Y(CCl_3COO)_3$–glycerol–$ZnEt_2$ catalyst on inorganic supports, particularly γ-Al_2O_3 (**Fig. 2.9**).[64] This strategy significantly mitigated aggregation and enhanced site

accessibility, resulting in a 36% improvement in catalytic activity. The supported catalyst enabled PPC synthesis with M_n up to 143 kg/mol and carbonate linkages reaching 99%.

Building upon this support-based approach, Cheng et al. further enhanced catalyst performance by modifying silica supports with ZnO and introducing quaternary ammonium salts as co-catalysts.[68] The ZnO modification imparted amphoteric surface properties, promoting both active site dispersion and CO_2 adsorption. Meanwhile, tetramethylammonium fluoride (TMAF, Me_4NF) served to stabilize the anionic polymer chain end (**Fig. 2.10**), thereby suppressing back-biting side reactions. This dual modification significantly increased catalytic activity, achieving TOFs exceeding 5000 g polymer/mol Zn, maintaining high carbonate incorporation (up to 96%) and enabling the production of polymers with M_n exceeding 200 kg/mol.

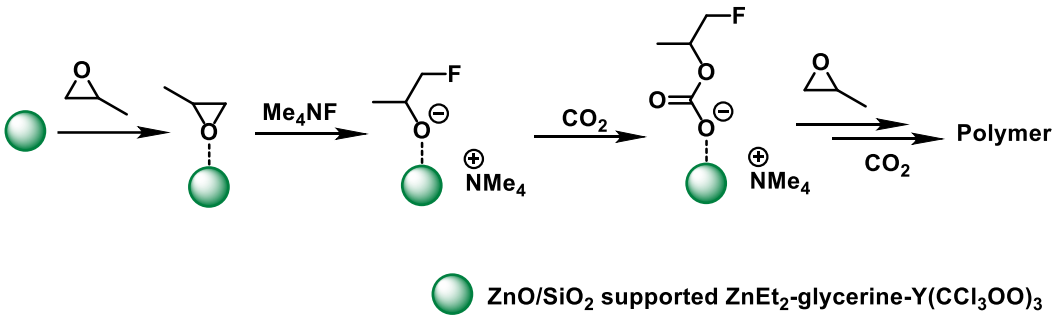

Fig. 2.10. Possible CO_2/PO copolymerization mechanism using the ZnO/SiO_2-supported $ZnEt_2$–glycerine–$Y(CCl_3OO)_3$/Me_4NF catalyst system.[68]

2.3.1.3 Double metal cyanide complexes

Double metal cyanide (DMC) catalysts were first reported in 1966 for the ring-opening polymerization of propylene oxide.[69] These heterometallic complexes typically composed of metal–cyanide and metal–ligand fragments, with a general molecular formula of $M_a[M'(CN)_b]_c \cdot xMX_d \cdot yL \cdot zH_2O$. M represents Zn, Fe(II), Ni(II), etc.; M' denotes Co(III), Fe(II), Fe(III), etc.; MX_d refers to a salt of metal M used for synthesizing the DMC complex; and L stands for an organic ligand. [70] A representative example is the Zn–Co DMC catalyst, which adopts the formula $Zn_3[Co(CN)_6]_2 \cdot xZnCl_2 \cdot yH_2O \cdot zCA$, where CA is an organic complexing agent such as tert-butanol, amides, or carboxylic acids.[71, 72] This catalyst features a 3D open-framework structure formed by bridging cyanide ligands that link $[Co(CN)_6]^{3-}$ units with Zn^{2+}

centers (**Fig. 2.11**).[73] The stoichiometric factors x, y, and z in the general formula of Zn–Co DMC are determined by the preparation method, as well as the type and ratio of the reagents used.

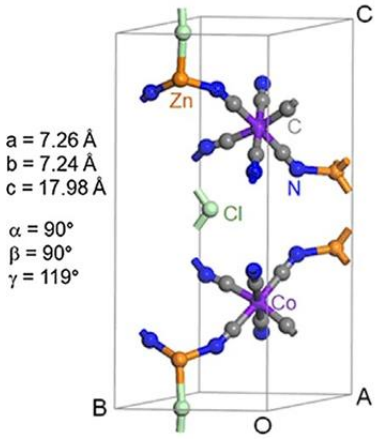

Fig. 2.11. Schematic representation of the unit cell of Zn–Co DMC.[73]

The potential of DMC catalysts for CO_2/epoxide copolymerization was first demonstrated by Kruper in 1985 using Zn–Fe DMC.[74] Subsequent work by Qi and co-workers showed that replacing Fe^{3+} with Co^{3+} in the DMC structure significantly enhanced catalytic activity, reaching approximately 2 kg polymer/g catalyst.[75] However, the resulting polycarbonates generally had low M_ns (< 4000 g/mol), due to the use of polyether polyols as initiators, which act as chain transfer agents and compete with epoxides at the active sites.[76] To address this, Wang et. al conducted the reaction without polyether polyols, resulting in a Zn–Co DMC catalyst that achieved much higher performance, yielding 60 kg polymer/g catalyst, and high M_n of 130 kg/mol.[77] Nevertheless, the resulting polymers contained more than 50% ether linkages, which compromised their thermal stability and biodegradability.

Mechanistic understanding of heterogeneous DMC catalysts has been challenging due to their structural complexity and undefined active sites. Early studies in the 2000s proposed that Lewis acid Zn^{2+} centers playing a critical role in activating epoxides during CO_2 copolymerization.[78] Later investigations introduced model systems that suggested bimetallic cooperation between Zn and transition metals such as Co.[25, 76] More recently, spectroscopic studies provided direct evidence that the active site in Zn–Co DMC is a tetrahedrally

coordinated Zn^{2+} species carrying a terminal OH group (**Fig. 2.12**), supporting a mononuclear Lewis acid based activation mechanism.[79]

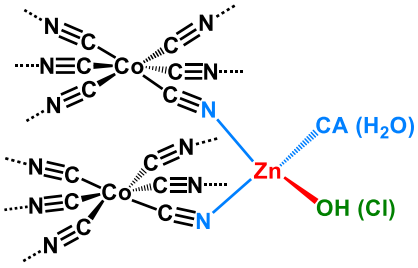

Fig. 2.12. Possible active site structure for the Zn–Co DMC catalyzed copolymerization of CO_2 and epoxides.[79]

Building upon this understanding, Wei et al. designed nanolamellar Zn–Co DMC catalysts with significantly enhanced surface areas (561–653 m^2/g) (**Fig. 2.13**), aiming to increase the exposure of active Zn–OH sites.[80] Compared to conventional aggregated Zn–Co DMC catalysts (~230 m^2/g), these nanostructured Zn–Co DMC exhibit markedly higher catalytic activity and better control over polymer microstructure, yielding copolymers with carbonate linkages exceeding 90%. However, due to the presence of multiple active sites, the resulting polymers exhibit broad molecular weight distributions (PDI ≈ 3).

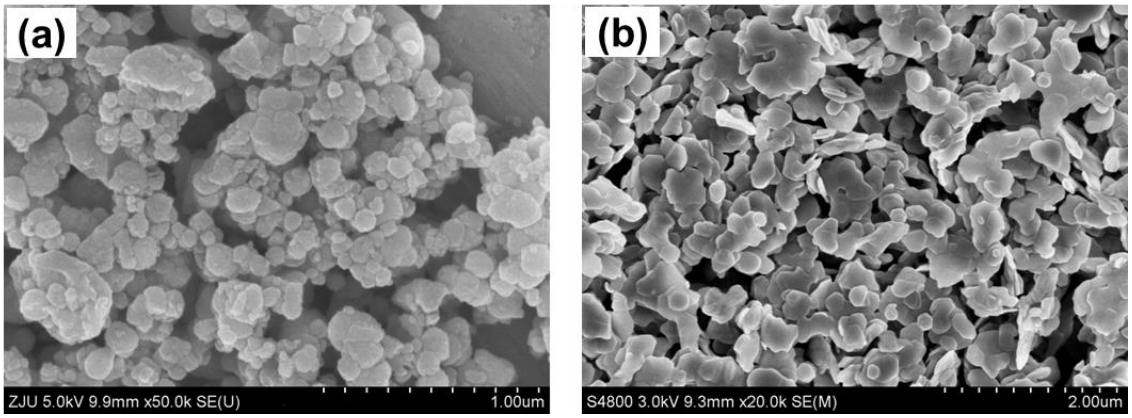

Fig. 2.13. SEM images comparing (a) conventional and (b) nanostructured Zn–Co DMC catalysts.[80]

Despite advancements in catalyst design, the induction period remains an intrinsic challenge in Zn–Co DMC catalyzed systems.[81-83] This phenomenon is often attributed to the gradual formation of active sites and the presence of trace moisture in the reaction medium.[73, 84] A key strategy to mitigate this issue involves the rational selection of

complexing agents (CAs). For instance, catalysts employing tert-butanol as the CA exhibit high activity but suffer from prolonged induction periods and significant exothermicity, which complicates thermal control.[72, 85] In contrast, alkoxy alcohol based CAs can significantly shorten or eliminate the induction period and stabilize the reaction process, though usually at the expense of catalytic efficiency.[84] Apart from catalyst structure optimization through ligand modulation, physical methods have also been investigated to enhance catalyst performance. One effective strategy is the application of microwave irradiation during CO_2/CHO copolymerization, which facilitates rapid initiation.[86] Unlike conventional heating, microwave energy selectively activates polar monomers such as cyclohexene oxide, thereby accelerating catalyst activation and effectively eliminating the induction period.

2.3.2 Homogeneous catalytic systems

Compared to heterogeneous systems, homogeneous catalysts for the copolymerization of CO_2 and epoxides offer more well-defined molecular structures and catalytic mechanisms, enabling precise control over the polymerization process. Although they generally exhibit lower catalytic activity, they afford polymers with highly uniform alternating structures and narrow molecular weight distributions. In recent years, significant progress has been made in developing homogeneous systems with improved activity and selectivity. Representative examples include β-diimine zinc complexes, metal porphyrin complexs, metal salen complexes, and metal-free organocatalysts.

2.3.2.1 β-diimine complexes

In 1995, Brookhart and co-workers developed a diimine based catalytic system in which bulky diimine ligands coordinated with transition metals such as palladium and nickel, initially applied to olefin polymerization.[87] Building on this foundation, Coates et al. introduced zinc β-diimine complexes for the copolymerization of CO_2 and epoxides, initiating extensive interest in this catalyst class.[88-91] Catalytic performance is strongly influenced by both the initiating group and the steric and electronic properties of the β-diimine ligands.[30]

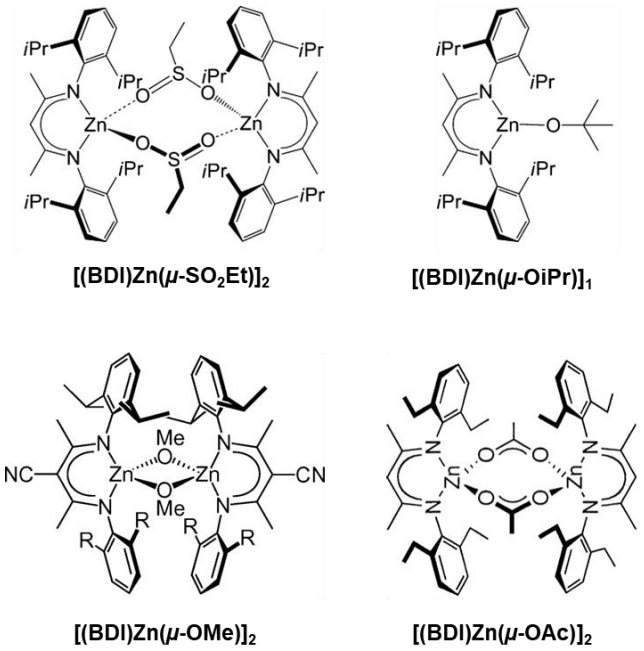

Fig. 2.14. Structure of β-diiminato zinc complexes featuring diverse initiating groups.

These complexes typically adopt the formula LnZnX, where X represents the initiating group responsible for epoxide ring-opening. Acetate is commonly used as the initiating group, and mechanistic investigations have demonstrated that the metal–acetate bond is directly involved in the initiation step.[91] In addition to acetate, other initiating groups have been examined for their influence on activity. Complexes incorporating alkoxide[88] and ethylsulfinato[92] exhibit comparable and slightly enhanced catalytic performances, respectively (**Fig. 2.14**). The catalytic efficiency following the trend: X = SO_2Et > OiPr > OMe > OAc. Notably, this order is inversely related to the leaving group ability of the initiators.[92, 93].

Ligand sterics also play a critical role. Complexes bearing small substituents are generally inactive, whereas moderate steric bulk enhances catalytic performance, particularly in CO_2/CHO copolymerization (**Fig. 2.15**).[91] Further improvement was achieved by incorporating asymmetric backbones bearing ethyl and isopropyl groups on the N-aryl rings along with electron-withdrawing substituents, resulting in a TOF of up to 729 h^{-1}.

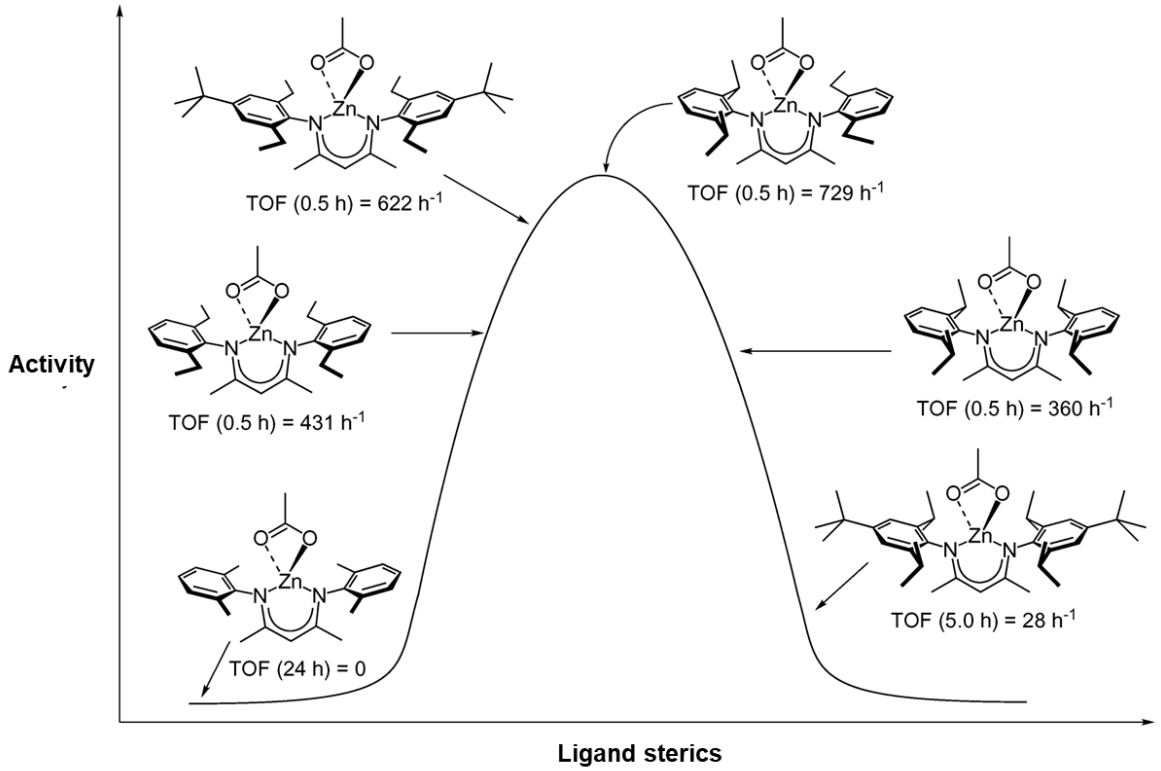

Fig. 2.15. Dependence of catalytic efficiency on qualitative ligand steric effects for (BDI)ZnOAc complexes in the copolymerization of CO_2 and CHO.[91]

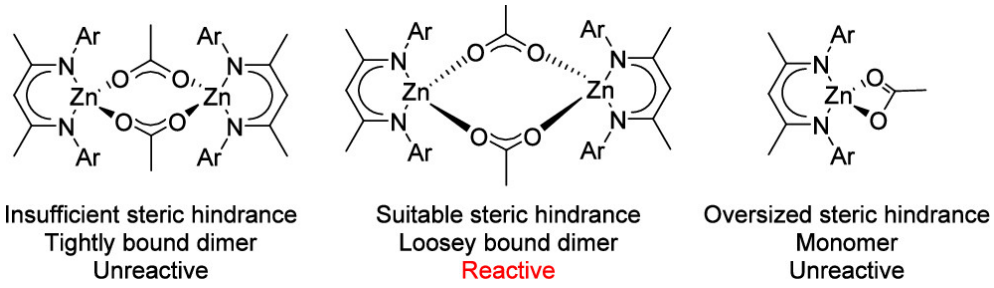

Fig. 2.16. Tightly bound dimers and monomers show low activity, while loosely bound dimers are highly effective in CO_2/CHO copolymerization (Ar = 2,6-diisopropylphenyl (Dipp)).[31]

X-ray single-crystal diffraction analysis revealed that the zinc centers in β-diimine complexes adopt tetrahedral coordination geometry and assemble into dimeric bimetallic structures, serving as the catalytically active species during chain propagation.[91] The catalytic activity depends sensitively on both the rigidity of the complex and the distance between the two zinc centers. When the Zn–Zn distance are too close or too far apart, the activity is significantly reduced. (**Fig. 2.16**).[31] These observations support a bimetallic cooperative

mechanism in which both zinc centers act synergistically facilitate polymerization (**Fig. 2.17**). The steric hindrance of ortho-substituents modulates the Zn–Zn distance and significantly influences catalytic performance. When the distance is too short, inactive dimers are formed, whereas bulky substituents hinder metal–metal cooperation.

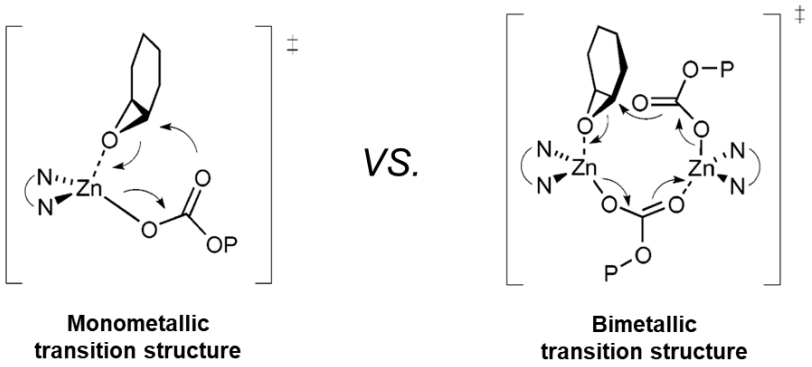

Fig. 2.17. Potential structures for ground and transition states during CHO ring opening.

Building upon this structural and mechanistic foundation, Lehenmeier and co-workers reported a Lewis acidic β-diiminato zinc complex that acts as a highly versatile catalyst for the copolymerization and terpolymerization of various epoxides with CO_2 under mild, additive-free conditions.[94] The active catalyst precursor, bearing a $N(SiMe_3)_2$ ligand, undergoes in situ CO_2 insertion to form a dinuclear zinc carbonate complex, which was confirmed by single-crystal X-ray diffraction. Importantly, mechanistic studies revealed that the catalytically active species is not the original amido complex, but this in situ formed bimetallic intermediate. Its structure supports the previously proposed dual site activation model involving cooperative catalysis by two zinc centers. The catalyst demonstrated high activity and selectivity across a broad range of epoxides, including CHO, PO, LO, and ECH. Moreover, it enabled the first successful terpolymerizations of CHO/PO/CO_2 and LO/PO/CO_2, producing polymers with tunable glass transition temperatures and excellent optical transparency.

2.3.2.2 Metal-porphyrin complexes

Inspired by the photosynthetic function of chlorophyll, Inoue first reported in 1978 that tetraphenylporphyrin aluminum (TPPAl) could catalyze the copolymerization of CO_2 with propylene oxide to form polycarbonates.[95] Under mild conditions (20 °C, 0.8 MPa), the

reaction over 19 days produced a copolymer containing 40% carbonate linkages, with a M_n of 3.9 kg/mol and a narrow PDI of 1.15. Later, he found that introducing an equimolar amount of $EtPh_3PBr$ as a co-catalyst significantly improved catalytic activity and raised the carbonate linkages up to 99%.[96] This advancement led to numerous investigations into binary catalytic systems comprising a metal–porphyrin complex as the primary catalyst and an organic base or quaternary ammonium salt as the co-catalyst (**Fig. 2.18**).

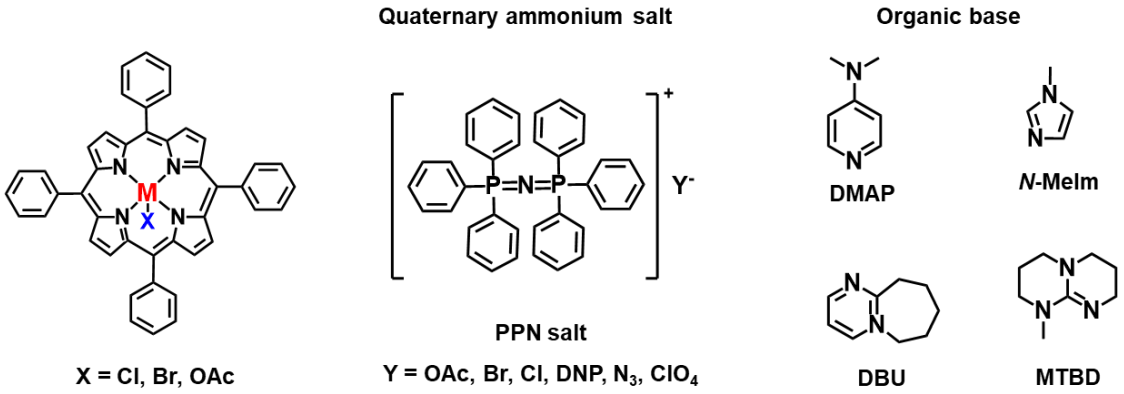

Fig. 2.18. Typical architecture of porphyrin complexes and frequently applied co-catalysts.

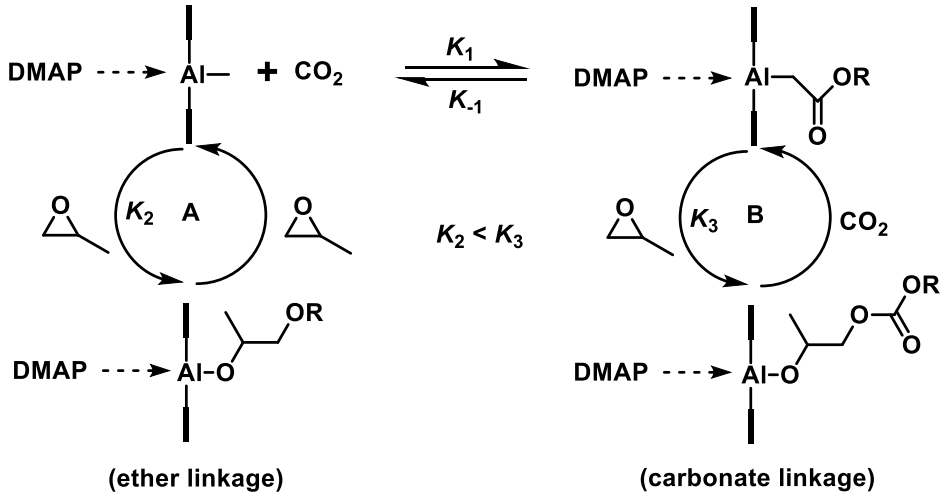

Fig. 2.19. Proposed mechanism for the copolymerization of CO_2 and propylene oxide catalyzed by (TPP)Al in the presence of DMAP.[97]

In 2004, Chisholm and co-workers investigated the effect of various X substituents (Cl, OR, O_2CR, etc.) in the (TPP)AlX system on the copolymerization of PO with CO_2.[97] The catalytic activity was strongly dependent on the X group, following the trend Cl > OR > O_2CR. Interestingly, the addition of 4-dimethylaminopyridine (DMAP) reversed this order to O_2CR >

OR, suggesting that DMAP significantly alters the electronic environment of the catalytic center. Mechanistic studies revealed that CO_2 reversibly inserts into the Al–OR bond to form a carbonate intermediate (**Fig. 2.19**). DMAP promotes this step by stabilizing the transition state or intermediate, thereby shifting the equilibrium toward carbonate formation ($K_1 > K_{-1}$). As a result, polycarbonate formation is favored over polyether production.

Following the achievements of Al (III) porphyrin catalysts, researchers extended their efforts to other metalloporphyrins. Mang and co-workers reported that a chromium porphyrin complex (CrTFPPCl), combined with DMAP and supercritical CO_2 as both solvent and reactant, efficiently catalyzed the copolymerization of CHO with CO_2.[98] At 222 atm and 110 °C, the system achieved a TOF exceeding 150 h^{-1}, producing a polymer more than 90% carbonate linkages, with a M_n of approximately 3500 g/mol and a PDI below 1.4. Under milder conditions (50 atm, 80 °C), a manganese porphyrin catalyst (MnTPPOAc) also promoted CHO/CO_2 copolymerization, yielding PCHC with 99% carbonate incorporation.[99] The polymer exhibited a relatively low M_n of 6700 and a PDI of 1.3. Notably, the same catalyst remained active even under low pressure conditions (1 atm CO_2, 80 °C), delivering a TOF of 3 h^{-1}. The resulting polymer contained 95% carbonate linkages, with M_n = 3000 and PDI = 1.6. This represents the first report of efficient CHO/CO_2 copolymerization under atmospheric CO_2 pressure. Similarly, a cobalt porphyrin complex (CoTPPCl) demonstrated catalytic activity at 1 atm CO_2 and room temperature, achieving a TOF of 3 h^{-1}. The resulting polycarbonate contained over 99% carbonate linkages, with a M_n of 1500, and a narrow PDI of 1.11.[100]

During the copolymerization of CO_2 and epoxides, poly(propylene carbonate) (PPC) and cyclic carbonate (cPC) compete as possible products. The selectivity of metal-porphyrin catalysts between PPC and cPC is strongly influenced by the type and amount of co-catalyst. At low cocatalyst loadings (0.5–1 equiv.), PPC formation is favored,[101] whereas higher loadings promote cPC formation. For example, Wang et al. reported a porphyrin aluminum with 120 equivalents of quaternary ammonium salt system that selectively produced cPC with a maximum TOF of 1.85×10^5 h^{-1}.[102] To achieve tunable selectivity between PPC and cPC, a temperature responsive flexible porphyrin aluminum catalyst was developed, allowing product distribution to be controlled by reaction temperature.[103] Further studies revealed that both

the electronic and steric properties of the porphyrin ligand critically affect selectivity. Strong electron-withdrawing substituents suppress PPC formation, whereas ligands with moderate electronic effects enhance PPC selectivity (**Fig. 2.20**).

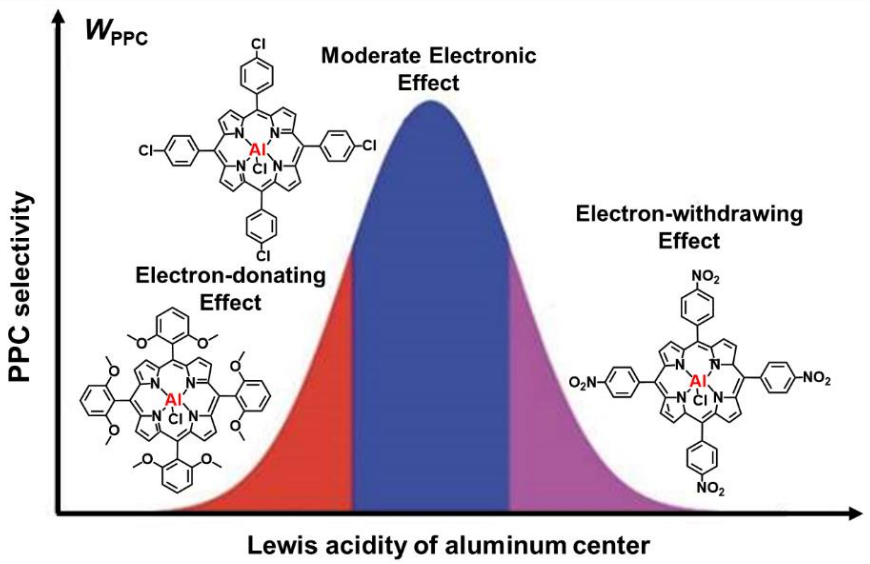

Fig. 2.20. Correlation between the Lewis acidity of the aluminum center in porphyrin complexes and the selectivity for PPC in the CO_2/PO copolymerization reaction.[103]

Building on prior work focused on PO and CHO, porphyrin aluminum catalysts were successfully extended to linear alkyl epoxides (C_3–C_{12}).[104] A series of catalysts (CAT-1 to CAT-5) were designed to investigate the influence of ligand sterics and electronics on CO_2/epoxide copolymerization (**Fig. 2.21**). The bulky ligand CAT-2 reduced selectivity due to steric hindrance, whereas less hindered analog CAT-1 improved monomer compatibility. CAT-3, with moderate electron-withdrawing groups, showed the best performance by balancing CO_2 insertion with side reaction suppression.

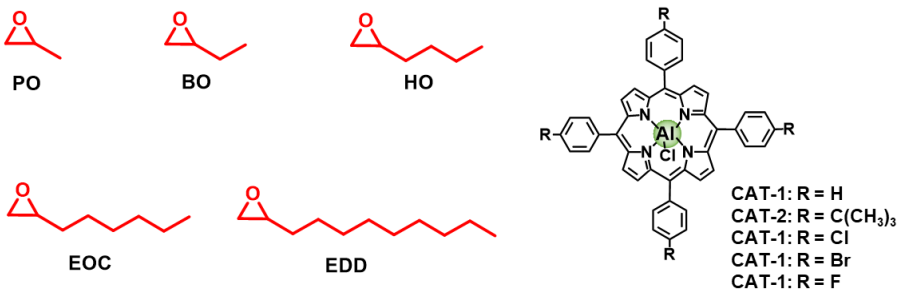

Fig. 2.21. Structures of linear alkyl epoxide monomers (C_3-C_{12}) and substituted porphyrin aluminum catalysts (CAT-1 to CAT-5).

To further elucidate the role of both metal center and ligand structure in catalytic performance, the Chisholm group systematically evaluated a series of nine binary metalloporphyrin catalysts derived from combinations of three porphyrin ligands (TPP, OEP, TFPP) and three metals (Co, Cr, Al) (**Fig. 2.22**).[101, 105, 106] Their study comprehensively addressed the influence of metal identity, ligand electronics, axial coordination, and cocatalyst selection on catalytic activity and selectivity.

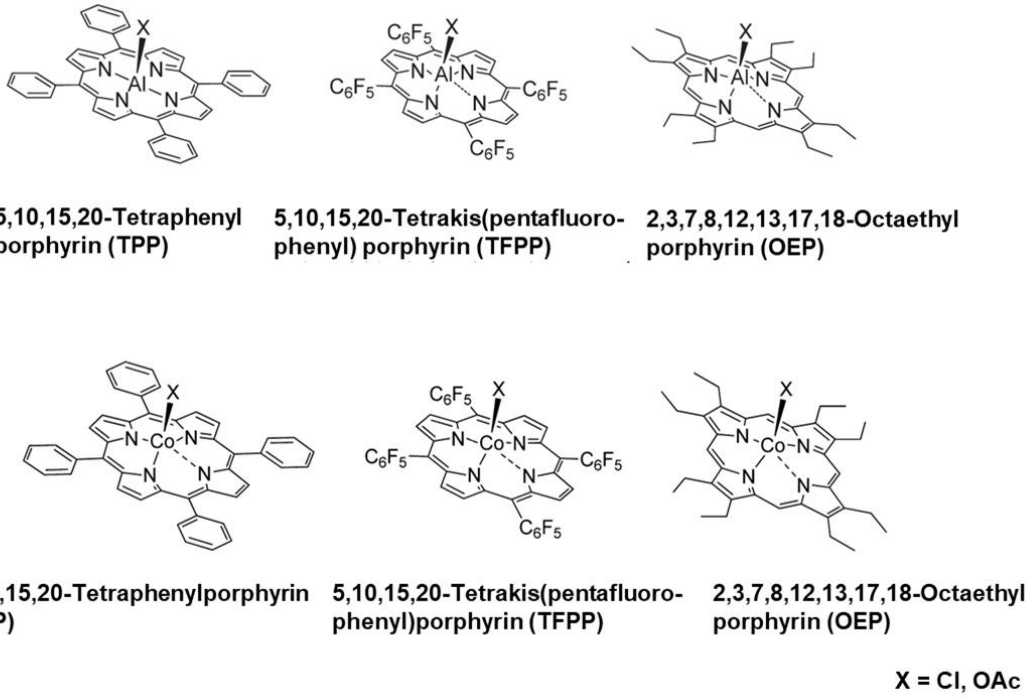

Fig. 2.22. Structures of the (porphyrin)AlX and (porphyrin)CoX catalysts used in the copolymerization reactions.

Among the metals evaluated, Cr(III) porphyrins exhibited the highest activity and carbonate selectivity, Co(III) porphyrins showed lower activity, partially due to in situ reduction to Co(II). In the presence of co-catalysts such as DMAP, both cobalt and chromium porphyrins tend to form six-coordinate complexes, potentially enabling bidirectional chain propagation. In contrast, aluminum porphyrins, with the smaller ionic radius of the Al^{3+} center, are more likely to favor single sided chain growth (**Fig. 2.23**). Ligand effects were equally important, as the electron-deficient TFPP decreased activity, whereas TPP offered an optimal balance between reactivity and selectivity. This facilitated efficient CO_2 insertion while minimizing the formation of ether and cyclic carbonate byproducts.

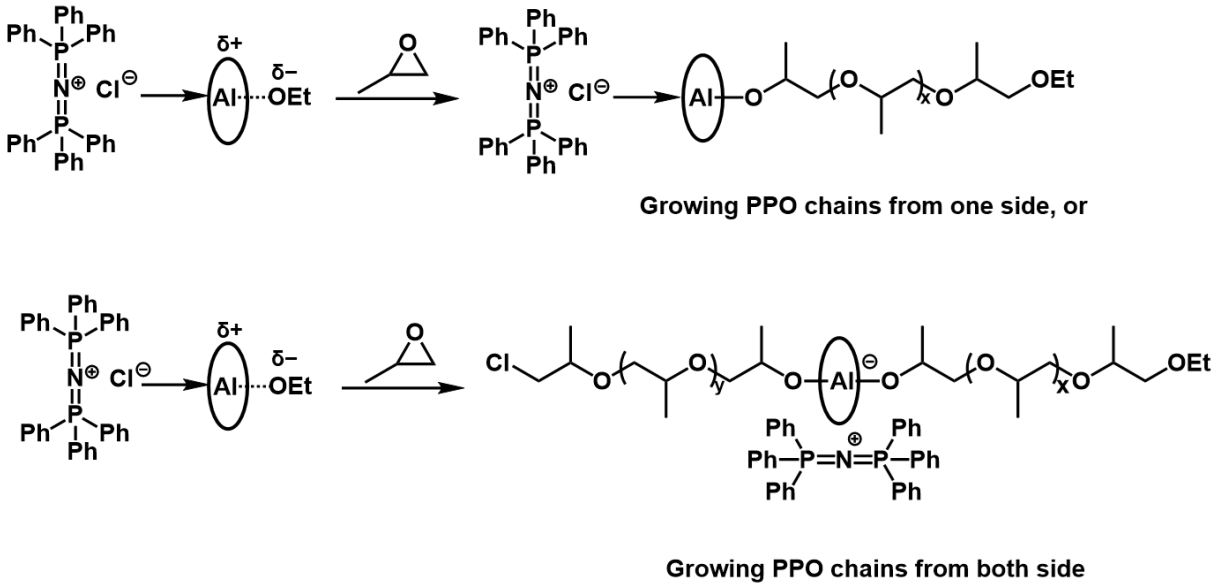

Fig. 2.23. Mechanistic possibilities for the growth of one or two polymer chains from a metal center.

2.3.2.3 Metal-salen complexes

The metal-salen complex is one of the most thoroughly investigated homogeneous catalysts for CO_2/epoxide copolymerization. First reported in 1995, (salen)CrCl complexes (**Fig. 2.24 a**) were shown to catalyze the formation of polycarbonates from CO_2 and epoxides.[107] Although these complexes are less active than β-diiminato zinc complexes (e.g., TOF = 160 h^{-1}, PPC = 71%),[47] they offer several advantages, including high polymer selectivity, excellent regioselectivity, and operation under mild conditions when combined with a cocatalyst.[60, 108, 109] Early research focused on Cr as the central metal, but interest shifted in 2003 when (Salen)Co(III) complexes were introduced (**Fig. 2.24 b**), delivering PPC with a TOF of 70 h^{-1}, 99% carbonate linkages, M_n of 6.9 kg/mol, and a narrow dispersity (PDI = 1.11).[110]

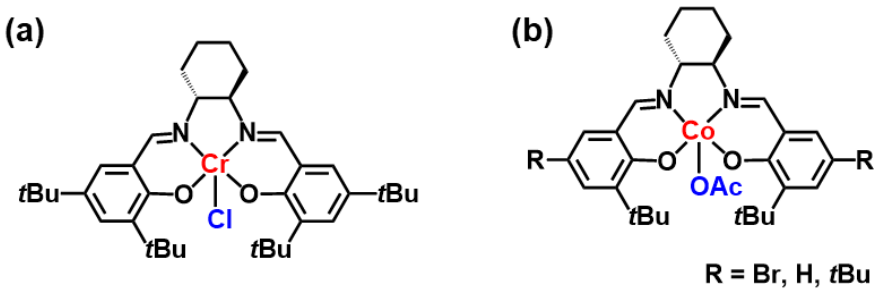

Fig. 2.24. Structures of the (salen)CrCl and (salen)CoOAc complexes.

The catalytic performance of (salen)MX complexes are highly dependent on the metal center, due to differences in Lewis acidity, ionic radius, and coordination geometry. Co(III) complexes exhibit excellent activity and selectivity in both PO/CO_2 and CHO/CO_2. In contrast, (salen)Cr(III) tends to generate small amounts of cyclic carbonate in PO/CO_2 reactions but performs well in CHO/CO_2 copolymerization. (salen)Al(III) complexes catalyze the formation of only cyclic carbonates from PO and CO_2, with no polymer observed. [19, 21, 28, 111, 112]. DFT calculations confirmed the catalytic mechanism for salen–Co, –Zn, and –Al systems proceeds via a single-site pathway.[113] In contrast, a bimetallic pathway involving Al(salen)-O-Al(salen) was found to be geometrically unfavorable, with CO_2 dissociates and an elongated Al–O bond observed during optimization (**Fig. 2.25**). The single-site pathway proceeds smoothly, with activation energies following the order Co < Zn < Al, consistent with the experimentally observed trend in catalytic performance.

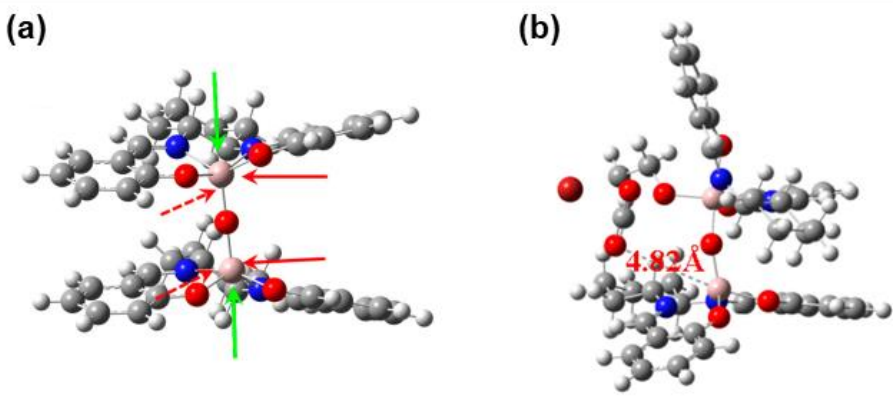

Fig. 2.25. (a) Structure of the Al(salen)-O-Al(salen) complex before optimization (intact μ-O bridge). (b) Optimized structure showing Al–O bond elongation and CO_2 dissociation, effectively yielding a single-site Al(salen) species.[113]

Following investigations on salen complexes incorporating various transition metals, titanium (salen) complexes have also been developed and evaluated for their copolymerization performance. Wang and co-workers introduced titanium based catalysts, including (salen)Ti(IV)Cl and (salen)Ti(III)Cl, as binary catalytic systems in combination with PPNCl for CHO/CO_2 copolymerization (**Fig. 2.26**). [114, 115] These catalysts produce highly alternating polycarbonates with >99% carbonate linkages. The Ti(IV) complex showed a relatively low TOF of 24 h^{-1}, attributed to the weak polarity of the Ti–O bond. In contrast, the

Ti(III) catalyst demonstrated excellent thermal stability and achieved a TOF as high as 577 h^{-1}, with no formation of cyclic carbonates.

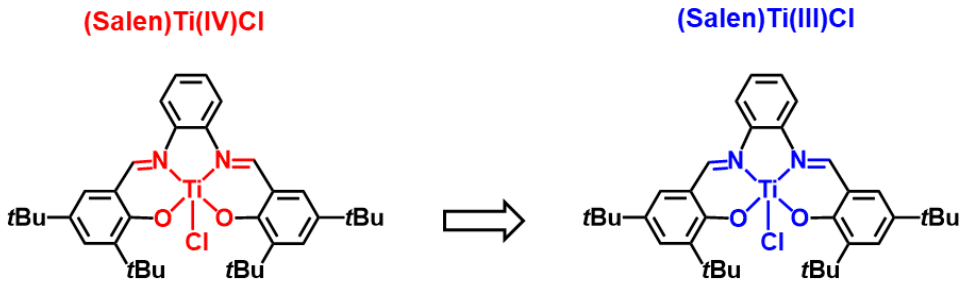

Fig. 2.26. Structure of (salen)Ti(IV)Cl and (salen)Ti(III)Cl complexes.

In addition to variations in the central metal, modifications to the axial ligand (X) in (salen)MX complexes can significantly the selectivity between poly(propylene carbonate) and cyclic carbonate. In 2004, a binary catalytic system consisting of Co(III)salenX complexes and quaternary ammonium salts (e.g., $nBu_4N^+Y^-$) was developed for the PO/CO_2 copolymerization.[116] A systematic structure–activity relationship study identified the influence of catalyst and cocatalyst structure on activity, selectivity, degree of alternation, and polymer microstructure (e.g., head-to-tail arrangement), thereby providing clear design guidelines. Optimal complexes combine sterically hindered salen backbones with weakly dissociating axial ligands. Effective cocatalysts include bulky, non-coordinating organic bases or large cations paired with poorly dissociating anions.[117] Cation effectiveness follows the trend $[PPN]^+ > [nHept_4N]^+ > [nBu_4N]^+ > [nEt_4N]^+$, while leaving group ability among anions decreases in the order $Cl^- > Br^- > I^- > ClO_4^-$. For neutral Lewis base cocatalysts, sterically hindered options like DMAP outperform coordinating bases such as N-methylimidazole (N-MeIm), which can deactivate the catalyst by occupying the metal coordination site.[60]

Cocatalyst concentration also plays a critical role in determining product outcome. Substoichiometric amounts of PPNCl significantly increase TOF in salen Co(III) catalysis, while the absence of co-catalyst results in no polymer formation.[37, 106, 118] However, excessive co-catalyst promotes polymer chain end dissociation, lowering the energy barrier for backbiting and increasing cyclic carbonate formation (**Fig. 2.27**).[119] Thus, co-catalysts

should be limited to one or two equivalents to maintain high polymer yields. Notably, similar co-catalyst concentration effects have also been observed in porphyrin based catalytic systems.

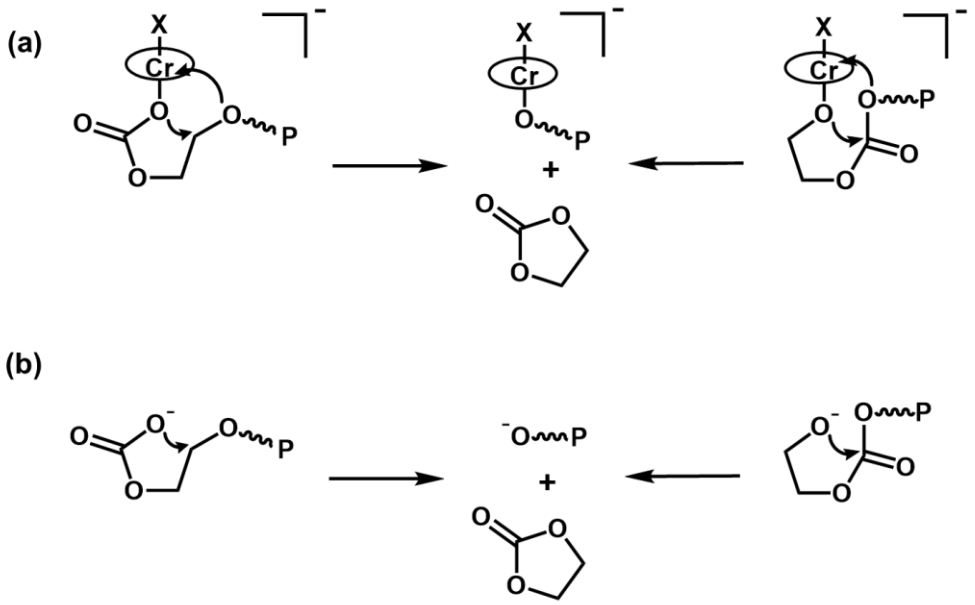

Fig. 2.27. Two possible backbiting routes leading to cyclic carbonate: (a) metal-mediated, (b) occurring on the unbound polymer anion.[119]

Although binary (salen)CoX complexes exhibit high catalytic activity and selectivity in the copolymerization of CO_2 with PO, elevated temperatures or prolonged reaction times promote backbiting reactions, resulting in the formation of significant amounts of cyclic carbonates.[120, 121] To suppress backbiting and improve polymer selectivity under demanding conditions, Nozaki and co-workers introduced a piperidine functionalized (salen)CoX complex, in which the piperidine group is covalently tethered to the ligand framework.[95] The mechanism begins with initiation by an acetate ligand (−OAc), generating a nucleophilic polymer chain end. A tethered piperidinium unit protonates this anionic site, suppressing its nucleophilicity and preventing intramolecular backbiting. Subsequent deprotonation by a neighboring piperidine restores nucleophilicity, allowing alternating copolymerization with PO to proceed (**Fig. 2.28**).

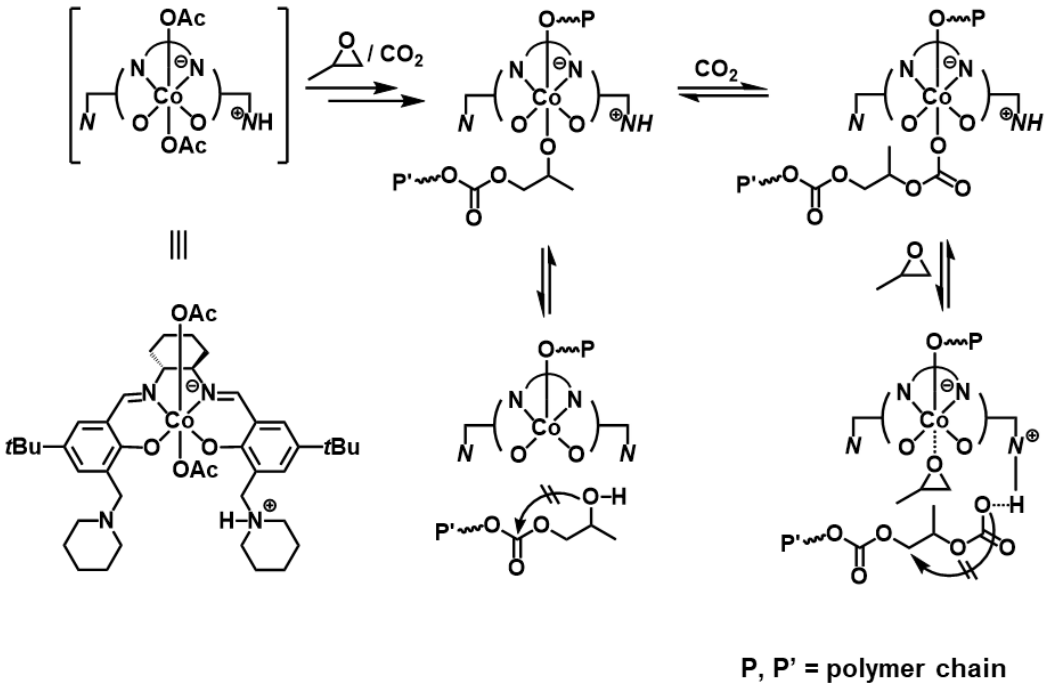

Fig. 2.28. Reaction mechanism for the suppression of cyclic carbonate formation by a salenCo(III)X complex bearing a piperidinium substituent.[95]

A more advanced system features a bifunctional Co(III)–salen catalyst bearing four tethered quaternary ammonium groups (**Fig. 2.29**). This catalyst achieves a TOF of 22,000 h^{-1}, M_n = 285 kg/mol, and PDI = 1.18 at 80 °C with a [PO]/[Co] ratio of 100,000:1.[122] Despite the eight steps synthetic procedure, the catalyst remains recyclable through silica gel chromatography, exhibiting minimal loss in catalytic activity. Mechanistic studies using NMR and DFT revealed an unusual bidentate coordination mode, where the counter anion replaces the typical Co–N bond and forms a planar structure with two oxygen atoms on the ligand. This deviation from the classic [NNOO] tetradentate coordination is considered the key to the catalyst's exceptional activity.

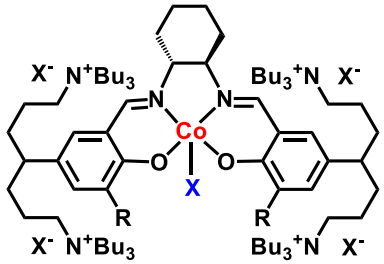

Fig. 2.29. The structure of the bifunctional cobalt(III) salen catalyst used in this study.[122]

Lv and co-workers developed catalyst by attaching a bulky organic base, TBD (1,5,7-triazabicyclo[4.4.0]dec-5-ene), to the phenyl ring of a (salen) cobalt(III) complex. This catalyst maintains high activity and selectivity over a broad temperature and pressure range in PO/CO_2 and CHO/CO_2 copolymerizations.[123] Mechanistic studies support a dual-chain growth model in which two polymer chains, initiated by the axial ligand and the TBD group respectively, reversibly coordinate to and dissociate from opposite sides of the cobalt center during propagation (**Fig. 2.30**). This alternating coordination stabilizes the Co(III) oxidation state and prevents its thermal reduction to inactive Co(II).

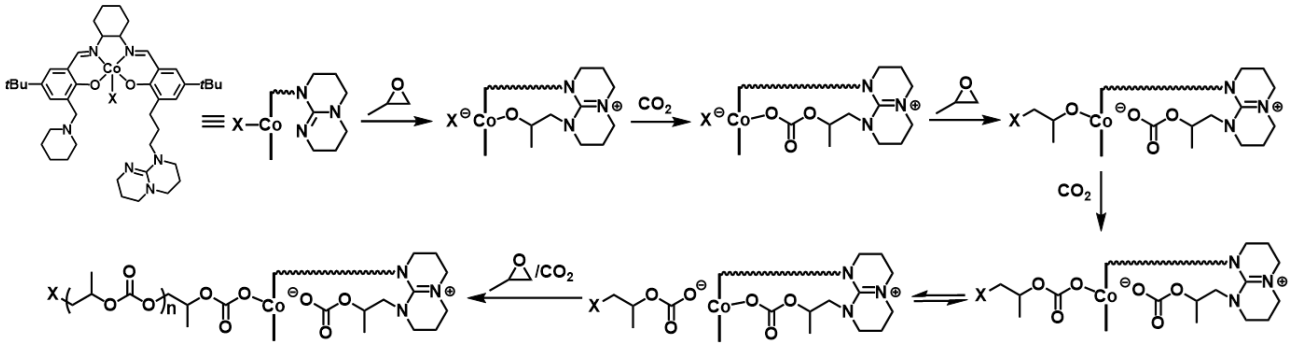

Fig. 2.30. Bidirectional chain propagation mechanism of CO_2/PO copolymerization catalyzed by a bifunctional SalenCo(III) complex.[123]

Salen-based complexes exhibit notable structural tunability and mechanistic versatility in the copolymerization of CO_2 and epoxides. Through strategic modifications of axial ligands, metal centers, and the surrounding electronic environment, catalyst performance can be precisely tuned in terms of activity, selectivity, and thermal stability. SalenCo(III) complexes remain among the most active homogeneous catalysts for this transformation. However, concerns over heavy metal toxicity and environmental sustainability have driven increasing interest toward the development of salen complexes incorporating environmentally benign metal centers. Future efforts should focus on designing catalysts based on earth-abundant, non-toxic metals while maintaining or enhancing catalytic efficiency. Such developments will be crucial for advancing the sustainable and industrial application of CO_2-based polymerization technologies.

2.3.2.4 Metal-free organocatalysts

Although metal complexes have shown great success in catalyzing the copolymerization of CO_2 and epoxides, increasing concerns over metal residues and environmental sustainability have motivated the development of metal-free catalytic systems. In this context, organocatalysts, especially those based on boron compounds, offer a greener and potentially more versatile alternative.

In 2016, a metal-free copolymerization of epoxides and CO_2 was first demonstrated using a Lewis acid–base pair comprising triethylborane (TEB) and a quaternary ammonium salt (**Fig. 2.31**).[124] The TEB/onium pair effectively catalyzed the copolymerization of PO and CO_2, with Bu_4NCl providing the highest activity (TON = 490 h^{-1}), though with moderate polymer selectivity (83%) and carbonate linkages (87%). In contrast, TEB/PPNCl delivered much higher polymer selectivity (99%). The same system also catalyzed the copolymerization of CHO and CO_2 efficiently, reaching a TON of 3600 h^{-1} with PPNCl.

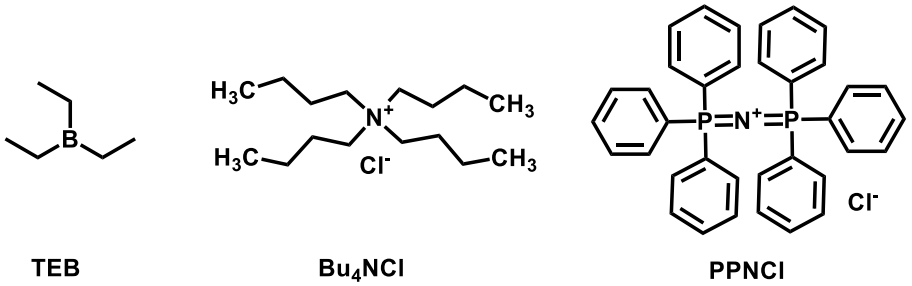

Fig. 2.31. Structures of the TEB catalyst and the co-catalysts Bu_4NCl and PPNCl used in copolymerization.

Mechanistic studies suggested that the Lewis base initiates the ring-opening of epoxides. TEB activates the epoxide through coordination and stabilizes the growing anionic chain end, which helps suppress backbiting and cyclic carbonate formation (**Fig. 2. 32**).[125] The catalytic performance was found to be highly sensitive to the molar ratio of TEB to the onium initiator.[126] In addition, the structure of the epoxide significantly influences the catalytic behavior.[40] For PO, CHO, and BO, a TEB to initiator ratio of 2 was sufficient to produce high selectivity polycarbonates with high CO_2 content. However, for allyl glycidyl ether (AGE), 3–4 equivalents of TEB were required, while for phenyl glycidyl ether (PGE) and styrene oxide

(SO), 4–8 equivalents were necessary. This is because the oxygen atom of the epoxide substituent competes with the ring oxygen for coordination with TEB, which reduces monomer reactivity and leads to increased cyclic carbonate formation.

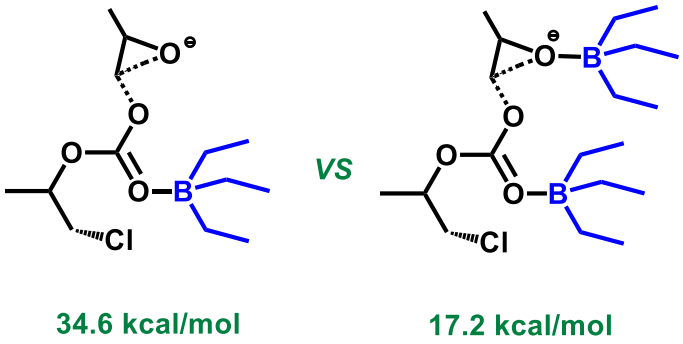

Fig. 2.32. Transition state comparison for epoxide insertion in CO_2/epoxide alternating copolymerization, highlighting the significantly reduced energy barrier (17.2 vs 34.6 kcal/mol) with TEB coordination.[125]

In 2020, Wu and co-workers designed a bifunctional organoborane catalyst containing a covalently tethered quaternary ammonium group.[127] Unlike conventional binary Lewis pair systems, this catalyst features a covalently linked boron center and onium site within a single molecule, enabling intramolecular Lewis acid–base cooperativity (**Fig. 2.33**). Despite its sensitivity to air and moisture, it is highly active and can be synthesized on a kilogram scale via a straightforward two-step route. The catalyst showed excellent activity in CHO/CO_2 copolymerization over a wide temperature range (25–150 °C), achieving up to 5,000 g polymer/g catalyst at [CHO]/[catalyst] = 20,000/1. Notably, the same catalyst was ineffective for PO/CO_2 copolymerization, primarily yielding cyclic carbonates rather than polycarbonates. The superior selectivity observed in CHO/CO_2 copolymerization is attributed to the thermodynamic instability of the cyclic carbonate byproduct derived from CHO. In contrast, the cyclic carbonates derived from aliphatic epoxides such as PO are thermodynamically stable, making their formation more favorable than polycarbonates under thermal conditions.

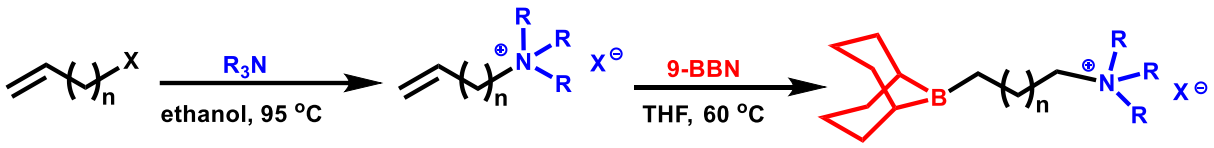

Fig. 2.33. Synthesis of bifunctional organoboron catalysts.[127]

Building upon this design, a tetranuclear "pinwheel" shaped bifunctional organoborane catalyst incorporating a central quaternary ammonium group was later introduced.[128] This catalyst efficiently catalyzed the copolymerization of epichlorohydrin (ECH) and CO_2 under mild conditions, achieving >99% selectivity for both polymer and carbonate linkages (**Fig. 2.34**). The resulting polymers had a high molecular weight (M_n = 36.5 kg/mol) and a T_g of 45.4 °C. Traditional metal-based catalysts require low temperatures (0 °C) to suppress cyclic carbonate formation and improve polymer selectivity, and their selectivity drops to ~72% at 25 °C.[129] In contrast, the organocatalyst exhibited a strong kinetic preference for polycarbonate formation, as evidenced by a large activation energy difference (ΔEa = 60.7 kJ/mol) between the polycarbonate and cyclic carbonate formation pathways. DFT calculations further revealed a unique chain-growth mechanism in which the polymer chain propagates cooperatively around the multimetallic "pinwheel" scaffold.

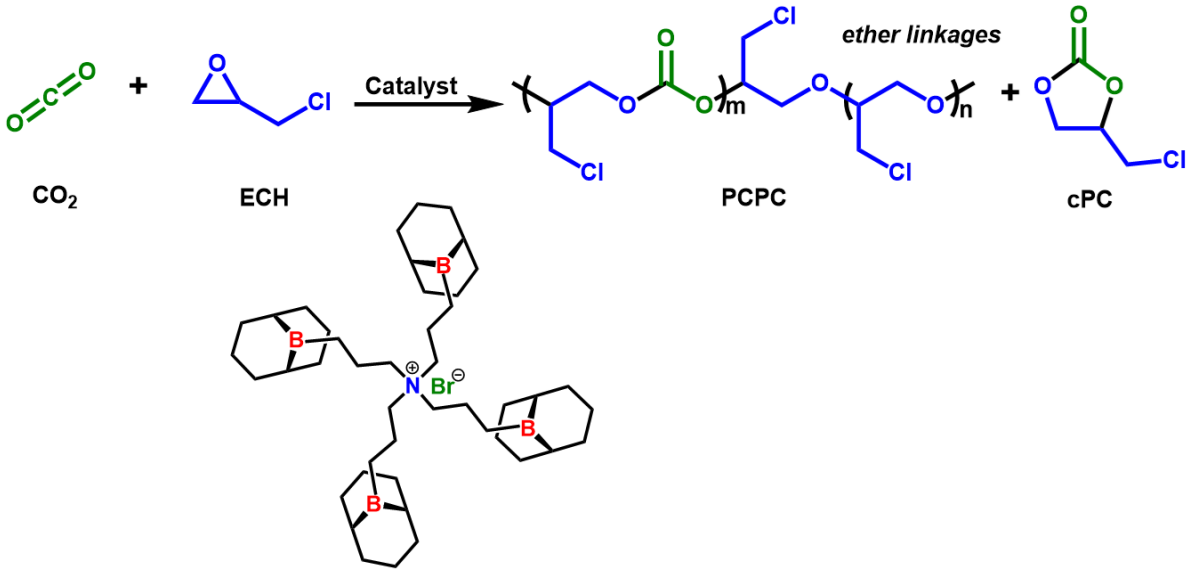

Fig. 2.34. TEB based catalysis for the copolymerization of CO_2 and ECH to poly(carbonate-co-ether)s.[128]

Across a broad catalyst loadings, bifunctional organoborane catalysts consistently outperform their binary counterparts, owing to intramolecular synergistic effects. A key feature is the cationic onium center, which stabilizes the growing anionic chain end and facilitates chain propagation. This stabilization occurs via electrostatic interactions, where the positive charge

is delocalized onto the α and β hydrogen atoms adjacent to the active site (**Fig. 2.35**).[127, 130] The structure of the Lewis base center plays a critical role in determining catalytic performance. Influential factors include the type of onium species (ammonium vs. phosphonium), the steric and electronic nature of the substituents, and the counterion identity. To investigate these effects, various organoborane catalysts with tailored onium centers have been synthesized. Notably, replacing nitrogen (**Fig. 2.35 A**) with phosphorus (**Fig. 2.35 B**) in the onium unit increased electrophilicity, enhanced initiating ion strength, and significantly boosted catalytic activity.[130]

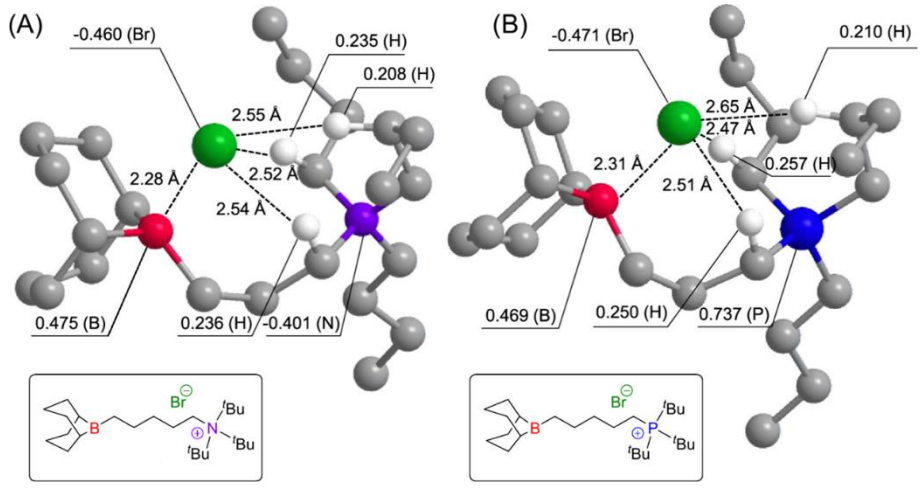

Fig. 2.35. Schematic diagram showing charge distribution and anion stabilization at the onium site in bifunctional organoborane catalysts. [130]

Beyond traditional CO_2/epoxide copolymers, the TEB/onium system has been extended to the synthesis of functional block copolymers. Feng and co-workers developed triblock copolymers consisting of a soft poly(octylene carbonate) (POC) middle block formed by 1-octene oxide/CO_2 copolymerization, flanked by two rigid poly(cyclohexene carbonate) (PCHC) blocks derived from CHO/CO_2 copolymerization (**Fig. 2.36**).[40] These materials exhibited rubber-like behavior, with high elongation at break and Young's moduli (1.4–2.5 MPa) falling within the mechanical range of soft biological tissues (0.3–10 MPa), indicating their promise for tissue engineering applications.

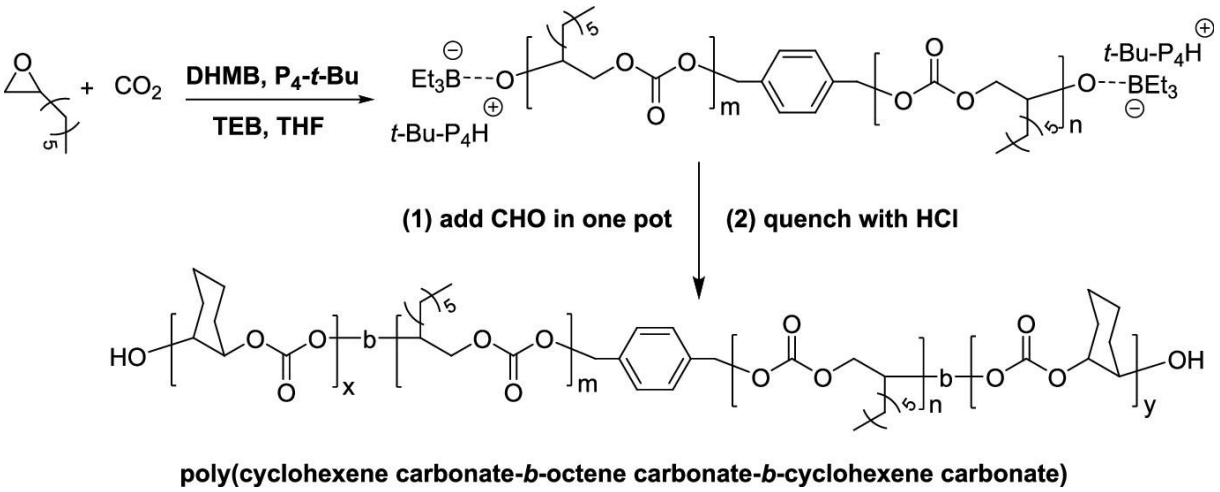

Fig. 2.36. Preparation of PCHC-*b*-POC-*b*-PCHC block copolymers.[40]

The TEB/onium system has also been used in one pot terpolymerization involving CO_2, epoxides, and cyclic anhydrides to yield poly(ester-carbonate)s with either random or block architectures (**Fig. 2.37**).[131] The influence of different anhydrides, such as succinic anhydride (SA) and phthalic anhydride (PA), on reactivity and polymer microstructure has been systematically investigated. SA, due to its stronger interaction with TEB, preferentially reacts with epoxides to generate well-defined block segments. In contrast, the lower reactivity of PA leads to the formation of random or tapered sequences.

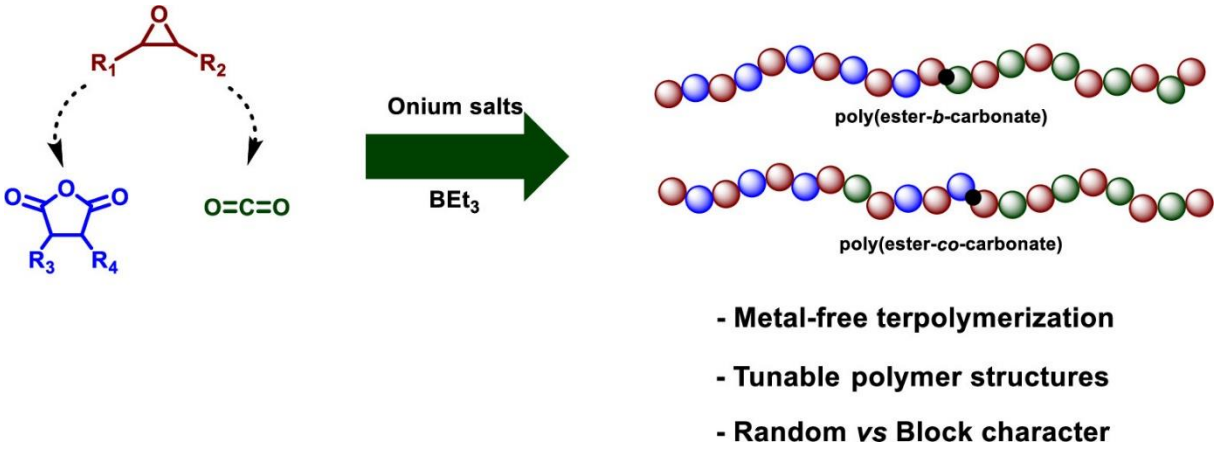

Fig. 2.37. Random and block poly(ester-carbonate)s formation via one pot copolymerization of CO_2, epoxides, and cyclic anhydrides using a TEB based catalytic system.[131]

In summary, organoborane catalysts have demonstrated significant progress in the copolymerization of CO_2 and epoxides, offering advantages such as structural diversity, high activity, tunable selectivity, and metal-free operation. Careful control over catalyst composition,

including the pairing of Lewis acid and base, the identity of the onium center, and the spatial arrangement of functional groups, has allowed for precise regulation of polymerization kinetics and the structure of the resulting materials. Nevertheless, important challenges remain, particularly in improving catalyst stability, expanding the range of applicable monomers, and achieving scalable production. These areas merit further investigation in future research.

2.4 Development of CO_2-based polymers

In recent years, catalytic systems for the copolymerization of CO_2 and epoxides have advanced significantly, with notable improvements in efficiency, selectivity, and suppressing side reactions. These advancements have enabled precise control over polymer structure and molecular weight, facilitating the scale-up from laboratory research to industrial application. CO_2-based polycarbonates offer tunable structures, thermal properties, biodegradability, and mechanical strength, making them attractive alternatives to traditional petrochemical derived polymers. As sustainable materials, they are increasingly viewed as essential building blocks for the next generation of environmentally friendly products.

Current research primarily targets three key application areas: the development of biodegradable plastics as alternatives to conventional polyolefins, the use of eco-friendly polyol precursors in polyurethane synthesis, and the design of molecular building blocks for high-performance elastomers. This section examines these applications in detail, with particular emphasis on structure–property relationships, recent technological progress, and the practical challenges associated with commercial implementation.

2.4.1 CO_2-based plastic

Among the various applications of CO_2-based polymers, plastics have attracted the most attention due to their broad relevance and commercial potential. The most thoroughly investigated CO_2-derived polycarbonates are poly(propylene carbonate) (PPC) and poly(cyclohexene carbonate) (PCHC) (**Fig. 2.38**). Unlike semi-crystalline polyesters such as

poly(ε-caprolactone) (PCL) and poly(lactic acid) (PLA), PPC and PCHC are fully amorphous and highly transparent.

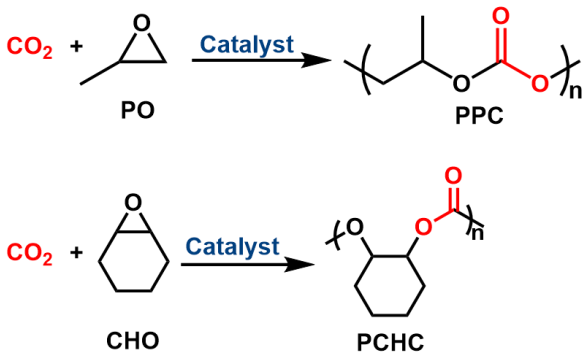

Fig. 2.38. CO_2 copolymerization with epoxides to produce PPC and PCHC.

PPC exhibits a T_g between 30−50 °C and is degradable under ambient conditions or through specific treatments into water, carbon dioxide, methane, and other compounds.[132] It combines good melt processability, gas barrier properties, and toughness with transparency and environmental compatibility. With a yield strength of around 30 MPa, which is comparable to that of polypropylene (PP, 27 MPa) and polyethylene (PE, 22 MPa),[133, 134] PPC shows promise for applications such as plastic films and bags.[135-137] However, its relatively low thermal stability and limited mechanical durability, especially under elevated temperatures or prolonged mechanical stress, remain major limitations that hinder broader industrial adoption. Compared to PPC, PCHC offers a higher T_g (110–120 °C), improved tensile modulus, and superior thermal resistance, making it as a potential green alternative to polystyrene. Nevertheless, its low elongation at break and inherent brittleness restrict its applicability in many practical scenarios.[104, 138]

To address these intrinsic limitations, researchers have developed several strategies, among which the incorporation of a third monomer into the polymer backbone has shown particular promise. This approach enables enhanced mechanical properties, improved thermal behavior, and opportunities for chemical modification.[31, 136] For example, Lee et al. employed (salen)cobalt(III) complexes with ligands bearing four quaternary ammonium groups to catalyze the terpolymerization of CO_2 with PO and epoxides such as CHO, 1,2-epoxyhexane (HO), and 1,2-epoxybutane (BO).[139] The resulting materials demonstrated increased thermal stability, with initial decomposition temperatures exceeding 200 °C.

Wang et al. further enhanced PPC performance by incorporating allyl glycidyl ether (AGE) into the polymer backbone through terpolymerization with CO_2 and PO, producing a UV-crosslinkable PPC.[140] The crosslinked polymer exhibited significantly improved thermal stability, mechanical strength, and reduced permanent deformation compared to neat PPC, thereby extending its applicability across a wider temperature range.

Williams and co-workers synthesized a series of poly(cyclohexene carbonate)-block-poly(ε-decalactone)-block-poly(cyclohexene carbonate) (PCHC–PDL–PCHC) triblock copolymers using a heterodinuclear Zn(II)/Mg(II) catalyst (**Fig. 2.39**).[141] At 50% PCHC content, the material functioned as a toughened plastic with a high modulus (up to 238 MPa) and an elongation at break of 900%, outperforming conventional CO_2-based polycarbonates. By adjusting the PCHC content to 28% and 20%, the resulting materials exhibited elastomeric and adhesive properties, respectively.

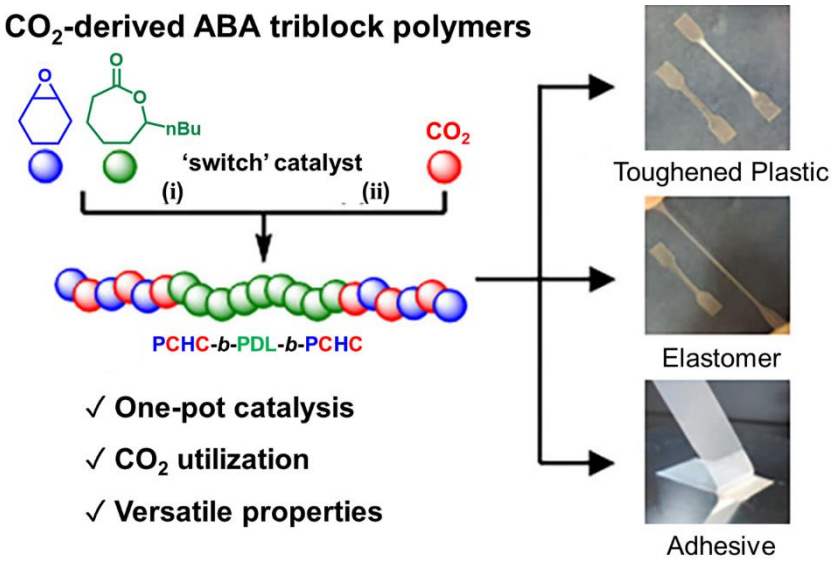

Fig. 2.39. A series of ABA-type PCHC–PDL–PCHC copolymers obtained via switchable catalysis, showing application potential as adhesives, elastomers, and toughened plastics.[141]

In summary, PPC and PCHC demonstrate considerable potential as CO_2-based plastics, but their limitations necessitate structural innovations. Advances such as terpolymerization, crosslinking, and block copolymer design are proving effective in overcoming these challenges and expanding the range of possible applications.

2.4.2 CO_2-based polyurethane

Polyurethanes (PUs) are synthesized through the reaction of isocyanate (–NCO) groups with polyol (–OH) groups, forming urethane linkages (–NH–COO–).[142] These linkages impart excellent mechanical strength, thermal stability, and chemical resistance. The performance of PUs can be tailored by selecting different types of diisocyanates and polyols. Among various polyols sources, CO_2-based polyols have emerged as a sustainable alternative.[143, 144] These polyols are typically produced via the copolymerizing CO_2 with epoxides, catalyzed in the presence of chain transfer agents. This approach incorporates carbonate groups directly into the polymer backbone, enabling the use of renewable carbon while preserving structural tunability. CO_2-based polyether polyols with over 40 wt% CO_2 content have been shown to reduce production costs by 20–30% compared to conventional polyether polyols.[145] Several of these materials have already been commercialized for PU synthesis.[144, 146] At the same time, ongoing innovation is crucial to further improve their production efficiency and material performance.

In one study, Wang et al. synthesized an amorphous CO_2-based triol by copolymerizing of CO_2 and PO using a Zn–Co DMC catalyst and 1,3,5-benzenetricarboxylic acid as the crosslinking agent (**Fig. 2.40**).[147] The resulting triol, containing both carbonate and ether linkages, was used to prepare a series of crosslinked thermoset PUs exhibiting shape memory behavior. Higher carbonate content accelerated the shape recovery process. The amorphous nature of the triol also imparted high elasticity to the PU network, allowing full shape recovery within three seconds when immersed in water at 70 °C.

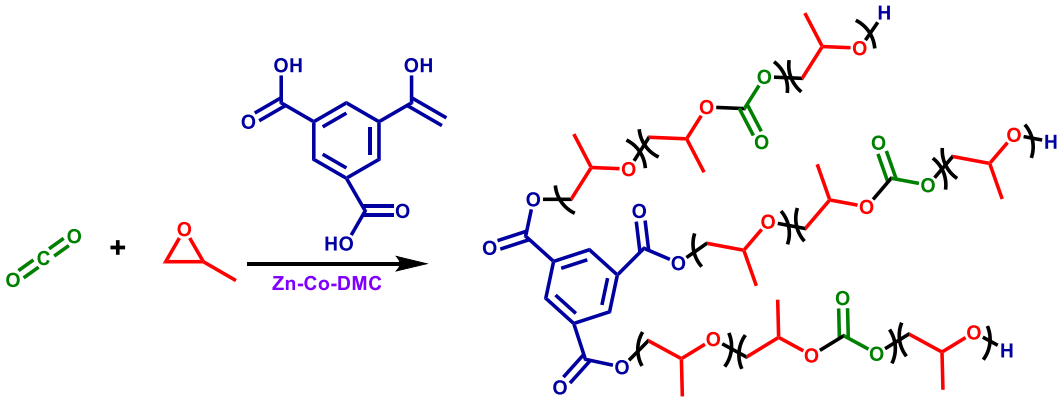

Fig. 2.40. Preparation of oligo(carbonate–ether) triol.[147]

Complementing this approach, Hong et al. explored the influence of polyol type and composition on the thermoplastic polyurethane (TPU) properties, comparing CO_2-based polyols with conventional polyether diol (PTMEG) (**Fig. 2.41**).[148] TPUs containing CO_2-based polyols showed greater rigidity, higher T_g, and increased tensile set. These changes were attributed to reduced chain flexibility resulting from the carbonate groups. In addition, the presence of carbonate linkages improved the corrosion resistance of the TPUs, due to their structural strength, low water affinity, and dense molecular packing.

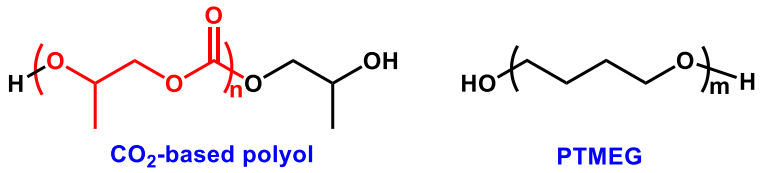

Fig. 2.41. Structure of CO_2-based polyol and petrochemical-derived polyether diol.[148]

To further explore the versatility of CO_2-based polyols, researchers have extended their application from conventional solvent-based PU systems to waterborne polyurethane (WPU), a more environmentally friendly platform that uses water as the primary dispersion medium.[143, 149] Wang et al. initiated systematic research by introducing CO_2-based polyols into UV-curable WPU formulations to create a crosslinkable CO_2-UV-WPU.[150] The material demonstrated excellent mechanical properties and outstanding hydrolytic resistance. After 15 hours in 1.5% NaOH solution, the CO_2-based WPU retained 88% of its tensile strength, while a polyester-based control sample lost all mechanical integrity, demonstrating the superior alkali resistance of the CO_2-derived material. This enhanced resistance is primarily attributed to the higher chemical stability of carbonate linkages compared to the ester bonds commonly present in polyester-based polyurethanes, which are more susceptible to base-catalyzed hydrolysis. In follow-up studies, the effect of carbonate linkages (CU%) on WPU performance was examined.[151] Increasing the CU% from 30% to 66% raised the T_g from −7.8 °C to 18.8 °C and improved tensile strength from 35.6 MPa to 52.2 MPa. Although the elongation at break decreased slightly, the overall mechanical properties was significantly enhanced.

2.4.3 CO_2-based elastomer

Beyond plastics and polyurethanes, CO_2-based polymers have also been actively investigated for elastomeric materials. Their structural tunability and compatibility with diverse copolymerization strategies offer a promising route to flexible, durable, and sustainable elastomer systems. One notable example is the CO_2-based thermoplastic elastomer (CO_2-TPE) developed by Wu and co-workers using a sequential polymerization approach.[152] They synthesized a triblock copolymer, PCHC-*b*-PAGEC-*b*-PCHC, from CO_2, allyl glycidyl ether (AGE), and cyclohexene oxide (CHO) using a salenCoTFA/PPNTFA catalyst. In this structure, PCHC acts as the hard segment and PAGEC as the soft segment. AGE derived functional groups enabled thiol–ene modification, while boronic ester crosslinks imparted the material with heat-triggered self-healing capabilities (**Fig. 2.42**).

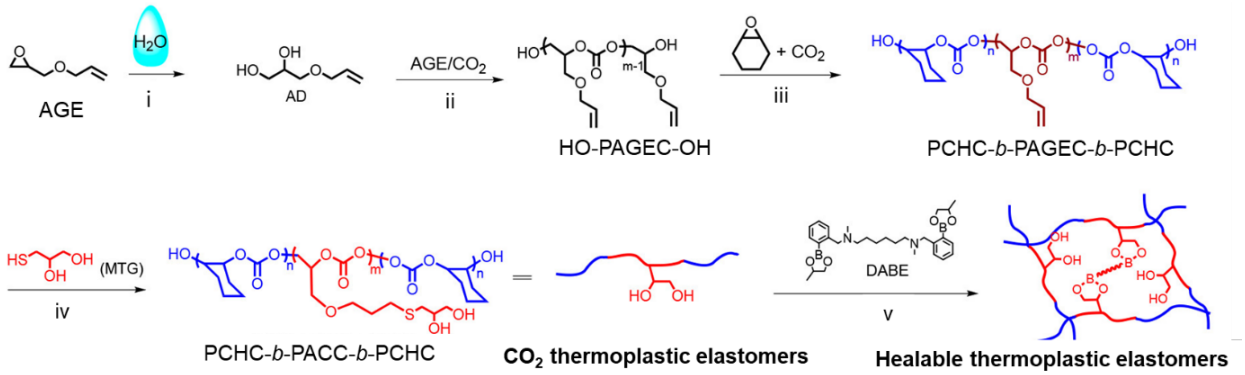

Fig. 2.42. Synthetic pathway toward CO_2-based self-healing thermoplastic elastomers. [152]

Other approaches introduced dynamic covalent interactions through reversible metal–ligand coordination. For instance, a terpolymer of CO_2, CHO, and vinyl-functionalized CHO (VCHO) was synthesized to produce PCHC based polymers with pendant vinyl groups.[153] These were subsequently modified with sulfur-containing ligands via thiol–ene chemistry, allowing coordination with Cu^+ ions to form reversible Cu–S crosslinks (**Fig. 2.43**). The resulting elastomer exhibited tunable T_g, tensile strength (up to 23 MPa), and high elongation at break (up to 1200%), with mechanical performance directly influenced by Cu^+ ion concentration.

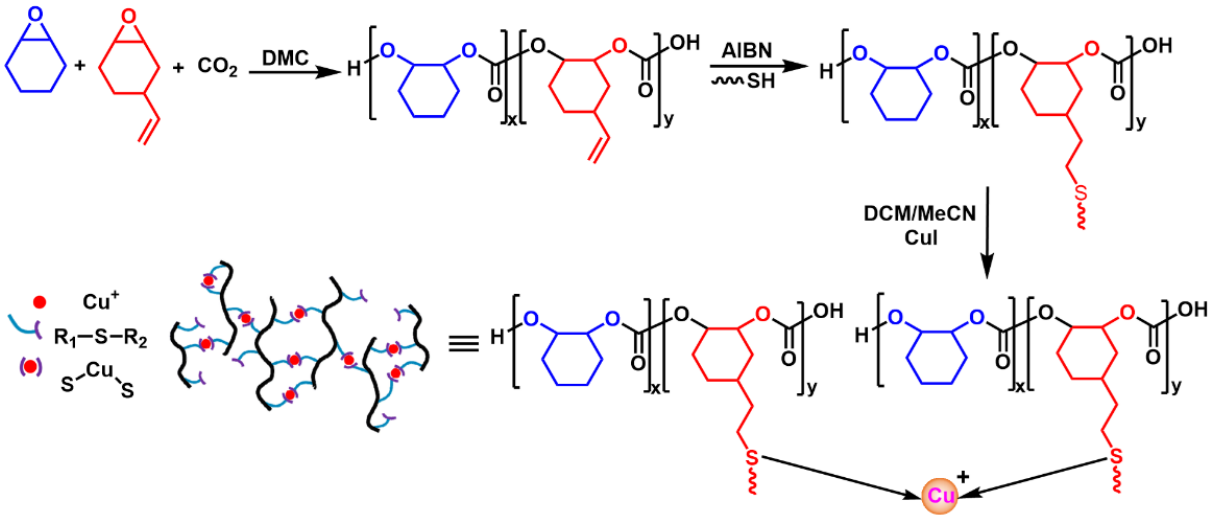

Fig. 2.43. Synthetic pathway toward CO_2-based thermoplastic elastomers.[153]

In addition to block copolymers, researchers have also developed amorphous CO_2-based elastomers by modulating polymer backbone flexibility and lowering the T_g. Rather than relying on hard/soft segment separation, these systems incorporate flexible linkages to achieve chain mobility at room temperature, resulting in stretchability and elastic recovery. Zhang and co-workers showed that using 1,2-epoxydodecane (EDD), an epoxide with significant steric hindrance, improved the molecular weight of CO_2/epoxide copolymers and suppressed the formation of cyclic by-products (**Fig. 2.44**).[27] The introduction of EDD also reduced the T_g, resulting in improved polymer flexibility suitable for elastomeric applications. Further studies explored the effect of different substituents, including linear alkyl chains, branched groups, and aromatic rings, on the T_g. The incorporation of alkyl chains showed a clear plasticizing effect, lowering T_g to −38 °C, while rigid aromatic rings raised it to 84 °C.[39] These findings highlight the potential of amorphous CO_2-based polymers for use in elastic materials.

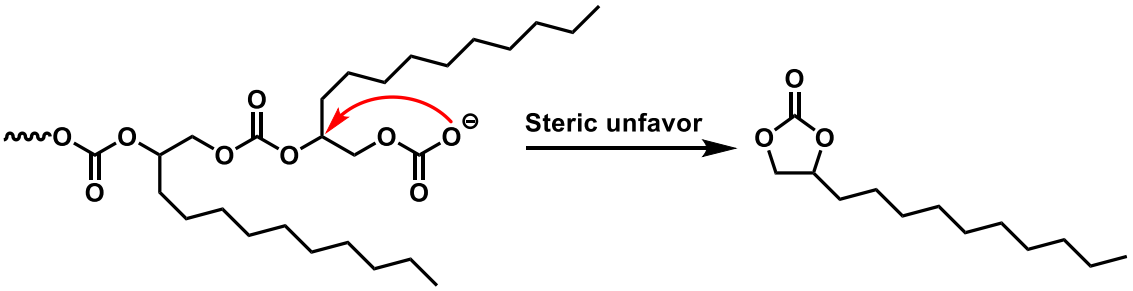

Fig. 2.44. The steric hindrance of EDD during CO_2 copolymerization suppresses the formation of cyclic carbonates.[27]

Recently, polycarbonates with T_g values below 0 °C were synthesized by copolymerizing CO_2, AGE, and long chain alkyl epoxides using an aluminum based binary catalyst system.[154] While these materials offer potential for elastomer applications and crosslinking, the limited catalytic activity led to low molecular weights (M_n < 10 kg/mol). As a result, the polymers remained liquid at room temperature (**Fig. 2.45)** and became brittle upon handling, significantly limiting their mechanical durability, ultimately restricting their suitability for elastomeric applications.



Fig. 2.45. Terpolymer polycarbonate synthesized via copolymerization reaction, exhibiting low viscosity in fluid state.[154]

In general, two major design strategies have emerged for CO_2-derived elastomers: (i) Phase-separated block copolymers, such as triblock structures (e.g., PCHC-*b*-PAGEC-*b*-PCHC), which combine thermoplasticity, self-healing, and reprocessability via dynamic covalent or supramolecular interactions; and (ii) Amorphous polymers with low T_g rely on flexible backbones or side chains to achieve chain mobility and stretchability at room temperature. To enhance mechanical strength in amorphous systems, post-crosslinking strategies are often employed by introducing epoxides with pendant groups. However, many of these monomers are structurally complex, and current catalysts show low activity toward such systems. Consequently, the resulting polymers often have limited molecular weight and suboptimal mechanical integrity, restricting their practical utility. Future work should focus on improving catalytic efficiency, optimizing polymerization conditions, and enhancing molecular design to achieve higher molecular weights and long-term durability. These developments are essential to unlock the full potential of CO_2-based polymers in advanced elastomer applications.

Chapter 3 Materials and characterization

A range of experimental resources and techniques was systematically employed throughout this study to support the investigation of polymer structures and properties. To streamline the discussion in the subsequent chapters, this chapter presents the core materials, processing techniques, and analytical methods used across Chapters 4 to 6. Section 3.1 outlines the chemicals, reagents, and preparation protocols used in this research. Section 3.2 outlines the characterization strategies employed to analyze polymer composition, conversion and selectivity, morphology, thermal and mechanical behavior, as well as viscoelastic properties, through various instrumental techniques.

3.1 Materials

All operations involving air-sensitive and water-sensitive chemicals were conducted in a glove box or using standard Schlenk techniques under dry nitrogen. Allyl glycidyl ether (AGE, 99%), 1,2-butylene oxide (BO, >99%), 1,2-hexene oxide (HO, >96%), and 1,2-octene oxide (OO, 97%) were obtained from Aladdin. All epoxides were dried over calcium hydride (CaH_2) with stirring for 24 hours and then distilled under reduced pressure. Tetrahydrofuran (THF, >99%), toluene (95%), and cyclohexane (>99%) were also dried similarly. Carbon dioxide gas (99.999%) was received and used without further purification. Zinc–cobalt(III) double metal cyanide complex (Zn–Co DMC) was synthesized according to the method reported in the literature.[155] The aluminum porphyrin complex was synthesized according to the literature method.[156, 157] Bis(triphenylphosphoranylidene)ammonium chloride (PPNCl, >96%) was recrystallized from dry dichloromethane and diethyl ether under nitrogen before use.

3.2 Characterizations

3.2.1 Product characterization and conversion/selectivity calculations

The compositions of product obtained from the terpolymerization were analyzed using ^1H NMR spectroscopy on a Bruker AV600 instrument. Deuterated chloroform ($CDCl_3$) served as

the solvent, and tetramethylsilane (TMS) was used as the internal standard. To further characterize the compositions, monomer conversion, polymer selectivity and carbonate moiety selectivity were defined as follows:

AGE Conversion (%) = [(moles of initial AGE) – (moles of unreacted AGE)] / (moles of initial AGE) × 100;

BO Conversion (%) = [(moles of initial BO) – (moles of unreacted BO)] / (moles of initial BO) × 100;

HO Conversion (%) = [(moles of initial HO) – (moles of unreacted HO)] / (moles of initial HO) × 100;

OO Conversion (%) = [(moles of initial OO) – (moles of unreacted OO)] / (moles of initial OO) × 100;

Polymer selectivity (%) = (moles of polymer in the product) / (total moles of polymer and cyclic carbonate in the product) × 100;

Carbonate linkage selectivity (%) = (moles of specific carbonate linkages in the polymer) / (total moles of carbonate and ether linkages in the polymer) × 100.

The calculation of each parameter was based on the integration of characteristic peaks in the ^{1}H NMR spectra. The chemical shifts and corresponding peak assignments are summarized in **Table 3.1** - **3.4**.

In **Chapter 4**, the products obtained from the Zn–Co DMC catalyzed polymerizations primarily consist of poly(carbonate-co-ether)s as the main products and cyclic carbonate byproducts as minor products. The ^{1}H NMR peak assignments for the copolymers derived from CO_2–BO–AGE, CO_2–HO–AGE, and CO_2–OO–AGE are listed in **Table 3.1**, **3.2**, and **3.3**, respectively. Using CO_2–HO–AGE as a representative system, the calculations of conversion, polymer selectivity, and carbonate linkages selectivity are provided.

In **Chapter 5**, the Al porphyrin/PPNCl catalytic system yields polycarbonates as the major products, along with cyclic carbonate byproducts. The corresponding ^{1}H NMR peak assignments for the CO_2–HO–AGE copolymer are shown in **Table 3.4**, and the associated calculation procedures are also described.

In **Chapter 6**, a dual catalyst system combining Zn–Co DMC and Al porphyrin/PPNCl was employed. The resulting products include both poly(carbonate-co-ether)s (main products) and cyclic carbonate byproducts (minor products). Since the monomer combination and product structure for CO_2–HO–AGE in this system are consistent with those in Chapter 4, the peak assignments remain the same (see **Table 3.2**), and the method for calculating conversion and selectivity is likewise applicable.

Table 3.1. ^{1}H NMR analysis of CO_2–AGE–BO terpolymerization products catalyzed by Zn–Co DMC.

Chemical Shift	Proton Assignment	Composition Type
5.81-5.94	b: -C**H**=CH_2	allyl group in AGE
5.10-5.34	a: -CH=C**H$_2$**	allyl group in AGE
5.00-5.08	e: -CH-	carbonate linkage of AGE
4.90-4.99	e': -CH-	ether linkage of AGE
4.80-4.90	g: -CH-	carbonate linkage of BO
4.69-4.75	p: -CH-	cyclic carbonate of AGE
4.69-4.80	g': -CH-	ether linkage of BO
4.63-4.69	q: -CH-	cyclic carbonate of BO
4.48-4.57	w: -CH-	cyclic carbonate of BO
4.48-4.50	n: -CH-	cyclic carbonate of AGE
4.38-4.44	m: -CH-	cyclic carbonate of AGE
4.14-4.50	f: -CH_2-	carbonate linkage of AGE
4.05-4.50	h: -CH_2-	carbonate linkage of BO
4.05-4.11	u: -CH-	cyclic carbonate of BO
3.94-4.05	c: -O-C**H$_2$**-	AGE
3.39-3.87	f': -CH_2-	ether linkage of AGE
3.54-3.74	d: -C**H$_2$**-O	AGE
3.26-3.79	h': -CH_2-	ether linkage of BO
1.38-1.89	i: -$(CH_2)_3$-	BO
0.77-1.14	j: -CH_3	BO

Table 3.2. ^{1}H NMR analysis of CO_2–AGE–HO terpolymerization products obtained using Zn-Co DMC or the dual catalyst system of Zn–Co DMC and Al porphyrin/PPNCl.

Chemical Shift	Proton Assignment	Composition Type
5.81-5.94	b: -**CH**=CH_2	allyl group in AGE
5.12-5.31	a: -CH=**CH_2**	allyl group in AGE
4.99-5.07	e: -CH-	carbonate linkage of AGE
4.88-4.99	e': -CH-	ether linkage of AGE
4.86-4.98	g: -CH-	carbonate linkage of HO
4.78-4.85	p: -CH-	cyclic carbonate of AGE
4.73-4.85	g': -CH-	ether linkage of HO
4.66-4.74	q: -CH-	cyclic carbonate of HO
4.48-4.59	w: -CH-	cyclic carbonate of HO
4.48-4.50	n: -CH-	cyclic carbonate of AGE
4.38-4.44	m: -CH-	cyclic carbonate of AGE
4.18-4.54	f: -CH_2-	carbonate linkage of AGE
3.91-4.50	h: -CH_2-	carbonate linkage of HO
4.05-4.11	u: -CH-	cyclic carbonate of HO
3.90-4.13	c: -O-**CH_2**-	AGE
3.39-3.87	f': -CH_2-	ether linkage of AGE
3.54-3.74	d: -**CH_2**-O	AGE
3.27-3.79	h': -CH_2-	ether linkage of HO
1.17-1.80	i, j, k: -$(CH_2)_3$-	HO
0.76-1.04	r: -CH_3	HO

Calculation procedures of conversion, polymer selectivity and carbonate linkages selectivity:

$$\text{AGE Conversion (\%)} = \frac{n_{\text{initial AGE}} - n_{\text{unreacted AGE}}}{n_{\text{initial AGE}}} = \frac{(A_{5.81\text{-}5.94} + A_{5.12\text{-}5.31}) - (A_{3.13\text{-}3.20} + A_{2.78\text{-}2.84} + A_{2.58\text{-}2.70})}{A_{5.81\text{-}5.94} + A_{5.12\text{-}5.31}} \times 100$$

$$\text{HO Conversion (\%)} = \frac{n_{\text{initial HO}} - n_{\text{unreacted HO}}}{n_{\text{initial HO}}} = \frac{A_{0.76\text{-}1.04} - (A_{2.87\text{-}2.97} + A_{2.70\text{-}2.78} + A_{2.41\text{-}2.53})}{A_{0.76\text{-}1.04}} \times 100$$

$$\text{Polymer selectivity} = \frac{n_{\text{carbonate linkage}} + n_{\text{ether linkage}}}{n_{\text{carbonate linkage}} + n_{\text{ether linkage}} + n_{\text{cyclic carbonate}}}$$

$$= \frac{A_{\text{carbonate linkage}} + A_{\text{ether linkage}}}{A_{\text{carbonate linkage}} + A_{\text{ether linkage}} + A_{\text{cyclic carbonate}}}$$

$$= \frac{A_{\text{e}} + A_{\text{f}} + A_{\text{g}} + A_{\text{h}} + A_{\text{e'}} + A_{\text{f'}} + A_{\text{g'}} + A_{\text{h'}}}{A_{\text{e}} + A_{\text{f}} + A_{\text{g}} + A_{\text{h}} + A_{\text{e'}} + A_{\text{f'}} + A_{\text{g'}} + A_{\text{h'}} + 3A_{\text{t, n}}}$$

$$= \frac{A_{\text{e}} + A_{\text{f, h}} + A_{\text{e', g}} + A_{\text{f', h'}} + (A_{\text{g', p}} - A_{\text{p}})}{A_{\text{e}} + A_{\text{f, h}} + A_{\text{e', g}} + A_{\text{f', h'}} + (A_{\text{g', p}} - A_{\text{p}}) + 3A_{\text{t, n}}}$$

$$= \frac{A_{\text{e}} + (A_{\text{m, f, h, u, c}} - A_{\text{w, n}} - A_{\text{a}}) + A_{\text{e', g}} + (A_{\text{f', d, h'}} - A_{\text{a}}) + [A_{\text{g', p}} - (A_{\text{w, n}} - A_{\text{q}})]}{A_{\text{e}} + (A_{\text{m, f, h, u, c}} - A_{\text{w, n}} - A_{\text{a}}) + A_{\text{e', g}} + (A_{\text{f', d, h'}} - A_{\text{a}}) + [A_{\text{g', p}} - (A_{\text{w, n}} - A_{\text{q}})] + 3A_{\text{w, n}}}$$

$$= \frac{A_{4.99\text{-}5.07} + (A_{3.90\text{-}4.54} - A_{4.48\text{-}4.59} - A_{5.10\text{-}5.34}) + A_{4.86\text{-}4.98} + (A_{3.27\text{-}3.87} - A_{5.10\text{-}5.34}) + [A_{4.73\text{-}4.85} - (A_{4.46\text{-}4.59} - A_{4.66\text{-}4.74})]}{A_{4.99\text{-}5.07} + (A_{3.90\text{-}4.54} - A_{4.48\text{-}4.59} - A_{5.10\text{-}5.34}) + A_{4.86\text{-}4.98} + (A_{3.27\text{-}3.87} - A_{5.10\text{-}5.34}) + [A_{4.73\text{-}4.85} - (A_{4.46\text{-}4.59} - A_{4.66\text{-}4.74})] + 3A_{4.48\text{-}4.59}}$$

$$\text{Carbonate linkage selectivity} = \frac{n_{\text{carbonate linkage}}}{n_{\text{carbonate linkage}} + n_{\text{ether linkage}}}$$

$$= \frac{A_{\text{carbonate linkage}}}{A_{\text{carbonate linkage}} + A_{\text{ether linkage}}}$$

$$= \frac{A_{\text{e}} + A_{\text{f}} + A_{\text{g}} + A_{\text{h}}}{A_{\text{e}} + A_{\text{f}} + A_{\text{g}} + A_{\text{h}} + A_{\text{e'}} + A_{\text{f'}} + A_{\text{g'}} + A_{\text{h'}}}$$

Since the peak of e' (-CH-, ether linkage of AGE) and the peak of g' (-CH-, carbonate linkage of HO) were unable to be separately integrated, the selectivity of carbonate is defined as: Carbonate linkages selectivity = the integral area of the -CH_2- peak in the carbonate linkages of the polymer / (the integral area of the -CH_2- peak in the carbonate linkages of the polymer + the integral area of the -CH_2- peak in the ether linkages of the polymer).

$$\text{Carbonate linkage selectivity} = \frac{A_{\text{f}} + A_{\text{h}}}{A_{\text{f}} + A_{\text{h}} + A_{\text{f'}} + A_{\text{h'}}}$$

$$= \frac{A_{\text{f, h, c}} - A_{\text{c}}}{(A_{\text{f, h, c}} - A_{\text{c}}) + (A_{\text{f', d, h'}} - A_{\text{d'}})}$$

$$= \frac{A_{\text{f, h, c}} - A_{\text{a}}}{(A_{\text{f, h, c}} - A_{\text{a}}) + (A_{\text{f', d, h'}} - A_{\text{a}})}$$

$$= \frac{A_{3.90\text{-}4.54} - A_{5.10\text{-}5.34}}{(A_{3.90\text{-}4.54} - A_{5.1\text{-}5.34}) + (A_{3.27\text{-}3.87} - A_{5.10\text{-}5.34})}$$

where n and A represent the molar number and ^{1}H NMR peak area, respectively, of carbonate and ether linkages in the copolymer, as well as cyclic carbonate in the product.

Table 3.3. ^{1}H NMR analysis of CO_2–AGE–OO terpolymerization products catalyzed by Zn–Co DMC.

Chemical Shift	Proton Assignment	Composition Type
5.81-5.94	b: -**CH**=CH_2	allyl group in AGE
5.12-5.31	a: -CH=**CH_2**	allyl group in AGE
4.99-5.07	e: -CH-	carbonate linkage of AGE
4.88-4.98	e': -CH-	ether linkage of AGE
4.85-4.98	g: -CH-	carbonate linkage of OO
4.78-4.85	p: -CH-	cyclic carbonate of AGE
4.73-4.85	g': -CH-	ether linkage of OO
4.66-4.74	q: -CH-	cyclic carbonate of OO
4.48-4.55	w: -CH-	cyclic carbonate of OO
4.48-4.50	n: -CH-	cyclic carbonate of AGE
4.38-4.44	m: -CH-	cyclic carbonate of AGE
4.18-4.52	f: -CH_2-	carbonate linkage of AGE
3.92-4.50	h: -CH_2-	carbonate linkage of OO
4.05-4.11	u: -CH-	cyclic carbonate of OO
3.90-4.13	c: -O-**CH_2**-	AGE
3.39-3.87	f': -CH_2-	ether linkage of AGE
3.54-3.74	d: -**CH_2**-O	AGE
3.27-3.79	h': -CH_2-	ether linkage of OO
1.13-1.76	i, j: -$(CH_2)_5$-	OO
0.74-1.01	r: -CH_3	OO

Table 3.4. ^{1}H NMR analysis of CO_2–AGE–HO terpolymerization products obtained using Al porphyrin/PPNCl.

Chemical Shift	Proton Assignment	Composition Type
5.81-5.97	b: -**CH**=CH_2	allyl group in AGE
5.14-5.35	a: -CH=**CH_2**	allyl group in AGE
4.99-5.08	e: -CH-	carbonate linkage of AGE
4.86-4.97	g: -CH-	carbonate linkage of HO
4.78-4.85	p: -CH-	cyclic carbonate of AGE
4.66-4.74	q: -CH-	cyclic carbonate of HO
4.48-4.55	w: -CH-	cyclic carbonate of HO
4.48-4.50	n: -CH-	cyclic carbonate of AGE
4.38-4.44	m: -CH-	cyclic carbonate of AGE
4.05-4.50	f: -CH_2-	carbonate linkage of AGE
4.01-4.50	h: -CH_2-	carbonate linkage of HO
4.05-4.11	u: -CH-	cyclic carbonate of HO
3.96-4.05	c: -O-**CH_2**-	AGE
3.57-3.67	d: -**CH_2**-O	AGE
3.13-3.20	o: -CH-	epoxy group of AGE
2.87-2.97	o': -CH-	epoxy group of HO
2.78-2.84	t: -CH-	epoxy group of AGE
2.70-2.78	t': -CH-	epoxy group of HO
2.58-2.70	s: -CH-	epoxy group of AGE
2.41-2.53	s': -CH-	epoxy group of HO
1.17-1.80	i, j, k: -$(CH_2)_3$-	HO
0.76-1.04	r: -CH_3	HO

Calculation procedures of polymer selectivity and carbonate moiety selectivity:

$$\text{AGE Conversion (\%)} = \frac{n_{\text{initial AGE}} - n_{\text{unreacted AGE}}}{n_{\text{initial AGE}}}$$

$$= \frac{(A_{5.81\text{-}5.97} + A_{5.14\text{-}5.35}) - (A_{3.13\text{-}3.20} + A_{2.78\text{-}2.84} + A_{2.58\text{-}2.70})}{A_{5.81\text{-}5.97} + A_{5.14\text{-}5.35}} \times 100$$

$$\text{HO Conversion (\%)} = \frac{n_{\text{initial HO}} - n_{\text{unreacted HO}}}{n_{\text{initial HO}}}$$

$$= \frac{A_{0.76\text{-}1.04} - (A_{2.87\text{-}2.97} + A_{2.70\text{-}2.78} + A_{2.41\text{-}2.53})}{A_{0.76\text{-}1.04}} \times 100$$

$$\text{Polycarbonate selectivity (\%)} = \frac{n_{\text{polycarbonate}}}{n_{\text{polycarbonate}} + n_{\text{cyclic carbonate}}}$$

$$= \frac{A_{\text{polycarbonate}}}{A_{\text{polycarbonate}} + A_{\text{cyclic carbonate}}}$$

$$= \frac{A_{\text{e}} + A_{\text{g}} + A_{\text{f, h}}}{A_{\text{e}} + A_{\text{g}} + A_{\text{f, h}} + 3A_{\text{w, n}}} \times 100$$

$$= \frac{A_{4.99\text{-}5.08} + A_{4.86\text{-}4.97} + (A_{3.96\text{-}4.44} - A_{4.48\text{-}4.55} - A_{5.14\text{-}5.35})}{A_{4.99\text{-}5.08} + A_{4.86\text{-}4.97} + (A_{3.96\text{-}4.44} - A_{4.48\text{-}4.55} - A_{5.14\text{-}5.35}) + 3A_{4.48\text{-}4.55}} \times 100$$

$$\text{Cyclic carbonate selectivity (\%)} = \frac{n_{\text{cyclic carbonate}}}{n_{\text{polycarbonate}} + n_{\text{cyclic carbonate}}}$$

$$= \frac{A_{\text{cyclic carbonate}}}{A_{\text{cyclic carbonate}} + A_{\text{polycarbonate}}}$$

$$= \frac{3A_{\text{w, n}}}{3A_{\text{w, n}} + A_{\text{e}} + A_{\text{g}} + A_{\text{f, h}}} \times 100$$

$$= \frac{3A_{4.48\text{-}4.55}}{3A_{4.48\text{-}4.55} + A_{4.99\text{-}5.08} + A_{4.86\text{-}4.97} + (A_{3.96\text{-}4.44} - A_{4.48\text{-}4.55} - A_{5.14\text{-}5.35})} \times 100$$

3.2.2 Characterization of molecular weights

Number-average molecular weight (M_n) and polydispersity index (PDI) were determined by gel permeation chromatography (GPC) on Waters 515 GPC instrument equiped with Waters Styragel HT3, HT5 and HT6 series columns using tetrahydrofuran as the eluent, where the flow rate was set at 1.0 mL min^{-1}. Calibration was performed using monodispersed polystyrene standards covering the molecular weight ranging from 1620 to 8500 kDa.

3.2.3 Glass transition temperature of polymers

Differential scanning calorimetry (DSC) measurements were performed under a nitrogen atmosphere using a Mettler Toledo DSC instrument. The sample was initially heated to 100 °C at a rate of 10 °C min^{-1} and held isothermally for 5 minutes. It was then cooled to −100 °C at 10 °C min^{-1} and subsequently reheated to 100 °C at the same rate.

3.2.4 Characterization of microstructure

The dispersions of silica in the CO_2-AGE-HO/silica composites were examined using a transmission electron microscope (TEM, FEI Tecnai G2 20 S Twin). To prepare TEM samples, ultrathin sections of the silica-filled CO_2–AGE–HO matrix were obtained through cryo-ultramicrotomy with a Reichert-Jung Ultracut instrument. These sections were then placed onto copper grids for further microscopic examination.

3.2.5 Characterization of rheological and viscoelastic properties

Dynamic mechanical analysis (DMA) in tensile mode was conducted using a TA Q800 instrument (TA Instruments Co., USA). The test was performed with a fixed initial strain of 0.1% and a constant frequency of 10 Hz. The temperature was progressively raised from −50 °C to 80 °C at a heating rate of 3 °C/min to generate the corresponding DMA curve.

3.2.6 Characterization of the dynamic viscoelastic properties and filler-rubber interactions

Rubber process analyzer (RPA) measurements were performed on an RPA 2000 instrument (Alpha Technologies Co., USA). For the unvulcanized compounds, the testing

conditions were set as follows: frequency (f) = 1 Hz, temperature (T) = 60 °C, and strain swept from 0.28% to 200%. Afterward, the same samples were in-situ vulcanized based on the vulcanization parameters previously obtained from a rheometer. The vulcanized compounds were then tested under the following conditions: f = 10 Hz, T = 60 °C, and strain swept from 0.28% to 42%.

3.2.7 Characterization of mechanical properties

Tensile strength and elongation at break were measured using a computer-controlled electronic universal testing machine (Zwick/Roell, Txet-port II, Germany) at a test speed of 50 mm/min and a temperature of 25 °C. The specimen size, with a narrow parallel-sided portion measuring 20 mm in length and 4 mm in width, was prepared according to ISO 37:2005 standards. Mechanical properties were evaluated based on three replicates for each sample.

Chapter 4 DMC catalyzed terpolymerization for CO_2-based elastomers

This chapter focuses on the synthesis and thermal–mechanical tuning of CO_2-based elastomers via bulk terpolymerization using a heterogeneous zinc–cobalt(III) double metal cyanide (Zn–Co DMC) catalyst. A series of elastomers was prepared by varying the content of allyl glycidyl ether (AGE) and the alkyl chain length of saturated epoxides. These structural modifications allow for precise control over the glass transition temperature (T_g) and mechanical properties of the resulting polymers. The impact of monomer composition on polymer selectivity, carbonate linkage selectivity, and tensile behavior was systematically evaluated. To establish a comprehensive understanding of structure–property relationships in these CO_2-derived elastomers, we investigate the effects of monomer feed ratio and side-chain structure on both the microscopic polymer network and the macroscopic material performance. Particular attention is paid to the role of AGE in introducing network flexibility and to the influence of epoxide chain length on thermal stability and mechanical strength. By integrating thermal analysis, spectroscopy, and mechanical testing, this chapter offers a detailed exploration of how molecular-level design parameters can be harnessed to tailor elastomer properties for targeted applications. The findings provide valuable insight into the rational design of functional elastomeric materials from renewable carbon sources, bridging polymer chemistry with material engineering.

Synthesis of CO_2-based elastomers with tunable glass transition temperatures via a Zinc−Cobalt (III) double metal cyanide catalyst

Abstract

Integrating carbon dioxide into polymeric materials aims to reduce dependence on fossil fuels in polymer development, while also helping to mitigate air pollution. In this study, we present a method for synthesizing CO_2-based polymers with tunable glass transition temperatures (T_g) ranging from −25 °C to +5 °C through the terpolymerization of CO_2, allyl glycidyl ether (AGE, an unsaturated epoxide), and a saturated epoxide containing a long alkyl chain. By varying the AGE content and the alkyl chain length, we produced a series of elastomers with diverse mechanical properties. AGE incorporation provides effective cross-linking sites, resulting in higher cross-linking density, increased tensile strength, and reduced elongation at break as AGE content rises. Additionally, the introduction of saturated epoxides modulates the cross-linking density, with the T_g decreasing linearly as the alkyl chain length of the saturated epoxides increases.

Keywords: CO_2-based polymers, Glass transition temperature (T_g), Terpolymerization, Cross-linking density, Mechanical properties

1. Introduction

The reduction of fossil fuel dependence necessitates the development of alternative carbon feedstocks.[158, 159] In this context, carbon dioxide (CO_2) has emerged as a promising raw material for synthesizing novel molecules and materials, contributing to the sustainable advancement of the chemical industry.[153, 160-163] Significant progress has been made in recent years in the coupling reaction of CO_2 with epoxides to produce polycarbonates.[127, 134, 146, 164-167] However, industrial applications of this transformation have been primarily limited to propylene oxide (PO), cyclohexene oxide (CHO), and their derivatives, which yield poly(propylene carbonate) (PPC), poly(cyclohexene carbonate) (PCHC), and related plastics.[17, 49, 104, 138, 168] These limitations have driven efforts to expand CO_2-based polymers to include elastomers.

Unlike plastics, elastomers possess lower glass transition temperatures (T_g) and feature cross-linking sites (e.g., double bonds) that impart desirable mechanical properties. Zhang and co-workers investigated the effect of epoxide substituents on the CO_2/epoxide copolymerization catalyzed by a nanosized zinc–cobalt(III) double metal cyanide complex denoted as Zn–Co DMC. They found that when the length of linear alkyl substituents exceeded four carbon atoms, the resulting copolymer exhibited a T_g below −18 °C.[39] Epoxides containing double bonds, such as limonene oxide (LO), glycidyl methacrylate (GMA), and allyl glycidyl ether (AGE), have been identified as promising monomers for CO_2-based polymers.[31, 165, 169, 170] For instance, Greiner and co-workers synthesized poly(limonene carbonate) (PLC) through the copolymerization of LO and CO_2. However, PLC's high T_g (~130 °C) renders it suitable only for plastic applications, precluding its use in CO_2-based elastomers.[171] Zhang et al. synthesized a poly(carbonate-*co*-ether) containing pendant acrylate groups from the copolymerization of GMA with CO_2.[26] By adjusting the polymerization conditions, they obtained polymers with molecular weights (M_n) ranging from 2.2 kg/mol to 12.7 kg/mol. However, the relatively low M_n values limited their practical applications.

Glycidyl esters, which feature electron-withdrawing ester groups, exhibit lower reactivity than glycidyl ethers, leading to a larger body of research on the copolymerization of glycidyl

ethers with CO_2.[30, 140, 162, 172-174] To enhance the thermal and mechanical properties of PPC, Wang and co-workers synthesized UV-crosslinkable PPC by terpolymerizing CO_2, AGE and PO.[140] Darensbourg et al. prepared an ABA-type copolymer of CO_2, AGE and PO.[175] However, the presence of the methyl group in PO hindered segmental mobility, resulting in a T_g above 0 °C. Meng et al. employed zinc glutarate (ZnGA) to catalyze the ternary copolymerization of CO_2, AGE and PO, yielding poly(propylene carbonate-allyl glycidyl ether) with varying alkenyl content.[176] They observed that increasing AGE content reduced the T_g of the terpolymer due to the flexiblility of AGE's pendant groups. When the PO-to-AGE molar ratio was 2:8, the terpolymer exhibited a T_g of −13.5 °C. However, excessive cross-linking density negatively impacted tensile strength and elongation at break.[177]

Pescarmona and co-workers developed a binary catalytic system comprising an aluminum amino-tris(phenolate) complex and bis(triphenylphosphine)iminium chloride (PPNCl) for the copolymerization of CO_2, AGE, and various long-chain alkyl epoxides.[154] The resulting polycarbonates exhibited T_gs below 0 °C and were liquids at room temperature (RT). However, due to low catalytic activity, the resulting polymers had low molecular weights (M_ns < 10 kg/mol) and became breakable after repeated handling, restricting their potential as elastomers. To overcome these limitations, optimizing both the catalyst and the composition of cross-linking functional groups is crucial. Achieving high molecular weight polymers and an optimal balance of cross-linking density is essential for enhancing mechanical properties.

To develop elastomers with low T_g and appropriate cross-linking density, it is necessary to incorporate epoxides containing flexible alkyl chains. This study proposes a strategy for synthesizing CO_2-based elastomers through the one-pot terpolymerization of CO_2, AGE, and long-chain alkyl epoxides (**Fig. 1**). The steric hindrance of substituents influences monomer reactivity,[40] which is why Zn–Co DMC, a single-component heterogeneous catalyst, was selected for its high selectivity toward epoxides with long side groups [19, 27, 178, 179]. AGE was chosen for its ether segments, which lower T_g, and its double bonds, which provide cross-linking sites. Long chain alkyl epoxides (e.g., 1,2-butene oxide (BO), 1,2-hexene oxide (HO), and 1,2-octene oxide (OO)) were incorporated to modulate cross-linking density while maintaining a low T_g. Using this approach, we synthesized CO_2-based terpolymers with varying

double bond densities and alkyl chain lengths. These materials were systematically characterized, and differential scanning calorimetry (DSC) and uniaxial tensile tests demonstrated that the CO_2-based polymers exhibited a wide range of T_gs (−25 °C to +5 °C) and tunable mechanical properties, depending on the AGE content and alkyl chain length.

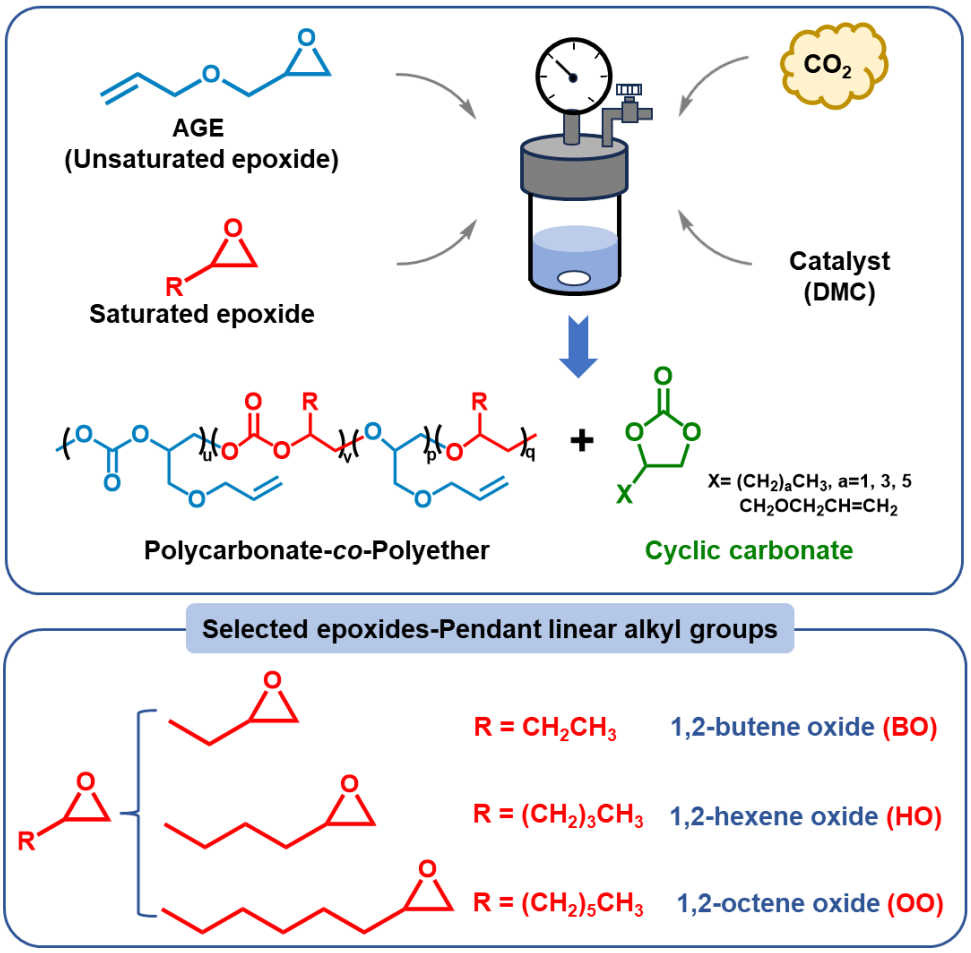

Fig. 1. Schematic diagram of the terpolymerization of CO_2, AGE and epoxides containing long alkyl chains using Zn–Co DMC catalyst.

2. Experimental section

2.1 Materials

All operations involving air-sensitive and water-sensitive chemicals were conducted in a glove box or using standard Schlenk techniques under dry nitrogen. Allyl glycidyl ether (AGE, 99%), 1,2-butylene oxide (BO, >99%), 1,2-hexene oxide (HO, >96%), and 1,2-octene oxide (OO, 97%) were obtained from Aladdin. All epoxides were dried by stirring over CaH_2 for 24 hours and then distilled under reduced pressure. Carbon dioxide gas (99.999%) was received

and used without further purification. Zinc-cobalt(III) double metal cyanide complex (Zn–Co DMC) was synthesized according to the method reported in the literature.[155]

2.2 Terpolymerization of CO_2 with epoxides

Epoxides and the catalyst were transferred to a pre-dried high-pressure reactor (10 mL) inside a glove box to prevent moisture from reacting with the catalyst. The reactor was then heated and pressurized to the desired temperature and CO_2 pressure. After the prescribed reaction time, the reactor was cooled in an ice-water bath, and the CO_2 pressure was released slowly. A small aliquot of the crude product was taken to deteimine monomer conversion and polymer selectivity using ^{1}H NMR spectroscopy. The remaining product was dissolved in dichloromethane, then precipitated by adding excess methanol to remove unreacted monomers and cyclic carbonat by-products. The precipitated polymer was collected and dried at 40 °C under vacuum for 48 hours. A small amount of the purified polymer was used to determine its carbonate linkage selectivity by ^{1}H NMR and molecular weight by gel permeation chromatography (GPC).

2.3 Preparation of cross-linked CO_2-based elastomers

Initially, CO_2-based polymer (3.0 g, 100 phr) and dicumyl peroxide (DCP, 0.003 g, 0.1 phr) were dissolved in tetrahydrofuran (10 mL) and stirred for 12 hours at room temperature (RT). The solvent was then removed by evaporation at RT over a 24-hour period. The resulting mixture was crosslinked at 160 °C under a pressure of 15 MPa for 30 minutes. Following the crosslinking, the specimens were allowed to rest at RT for 12 hours before tensile testing.

2.4 Characterization

2.4.1 Compositions of the product obtained from the terpolymerization

As shown in **Fig. 1**, the terpolymerization of CO_2, AGE and saturated epoxide yields a crude product which is composed of a polymer containing carbonate linkage and ether linkage, cyclic carbonate by-products, and unreacted monomer. Their compositions were determined using ^{1}H NMR spectroscopy on a Bruker AV600 instrument, with deuterated chloroform ($CDCl_3$) as the solvent and tetramethylsilane (TMS) as the internal standard. To provide a more detailed characterization of the compositions, polymer selectivity and carbonate linkage

selectivity were defined as follows:

Polymer selectivity (%) = (moles of carbonate and ether linkage of the polymer in the crude product) / (total moles of carbonate and ether linkage of the polymer in the crude product + cyclic carbonate in the crude product) × 100;

Carbonate linkage selectivity (%) = (moles of carbonate linkage of the polymer) / (total moles of carbonate and ether linkage of the polymer) × 100.

The detailed calculation procedures are provided in the **Chapter 3**.

2.4.2 Molecular weights of polymers

Number-average molecular weight (M_n) and polydispersity index (PDI) were determined by gel permeation chromatography (GPC) on Waters 515 GPC instrument equiped with Waters Styragel HT3, HT5 and HT6 series columns using tetrahydrofuran as the eluent, where the flow rate was set at 1.0 mL min^{-1}. Calibration was performed using monodispersed polystyrene standards covering the molecular weight ranging from 1620 to 8500 kDa.

2.4.3 Glass transition temperature of polymers

Differential scanning calorimetry (DSC) measurements were performed under a nitrogen atmosphere using a Mettler Toledo DSC instrument. The sample was initially heated to 100 °C at a rate of 10 °C min^{-1} and held isothermally for 5 minutes. It was then cooled to −100 °C at 10 °C min^{-1} and subsequently reheated to 100 °C at the same rate.

2.4.4 Tensile properties of polymers

Tensile strength and elongation at break were measured using a computer-controlled electronic universal testing machine (Zwick/Roell, Txet-port II, Germany) at a test speed of 50 mm/min and a temperature of 25 °C. The specimen size, with a narrow parallel-sided portion measuring 20 mm in length and 4 mm in width, was prepared according to ISO 37:2005 standards. Mechanical properties were evaluated based on three replicates for each sample.

3. Results

3.1 Effects of temperature and CO_2 pressure on the product of terpolymerization

Terpolymerization of CO_2–AGE–HO was conducted at various temperatures and CO_2 pressures to evaluate their effects on the properties of the resulting product (see **Table** for

details). The resulting product contained carbonate linkage, ether linkage, and cyclic carbonate (**Fig. 2**). After purification, the cyclic carbonate was removed, yielding a copolymer of carbonate and ether linkage (**Fig. 3**). As shown in **Table** (entries 1-5), at a given CO_2 pressure (4 MPa), increasing polymerization temperature reduced polymer selectivity, carbonate linkage selectivity and M_n of the polymer. Specifically, when the temperature was raised from 50 °C to 90 °C, the polymer selectivity decreased from 98 to 94%, the carbonate linkage selectivity from 77 to 37%, and the M_n of the terpolymer from 61 to 28 kg/mol. This suggests that increasing temperature promotes the formation of cyclic carbonate by facilitating the backbiting mechanism that terminates chain propagation.[27, 168, 180] The higher energy barrier for consecutive AGE-HO insertion compared to CO_2 addition after AGE-HO moieties promotes epoxide incorporation at elevated temperatures, thereby reducing carbonate linkage selectivity.[155] Consequently, the lowest carbonate linkage selectivity (37%) was observed at the highest reaction temperature (90 °C).

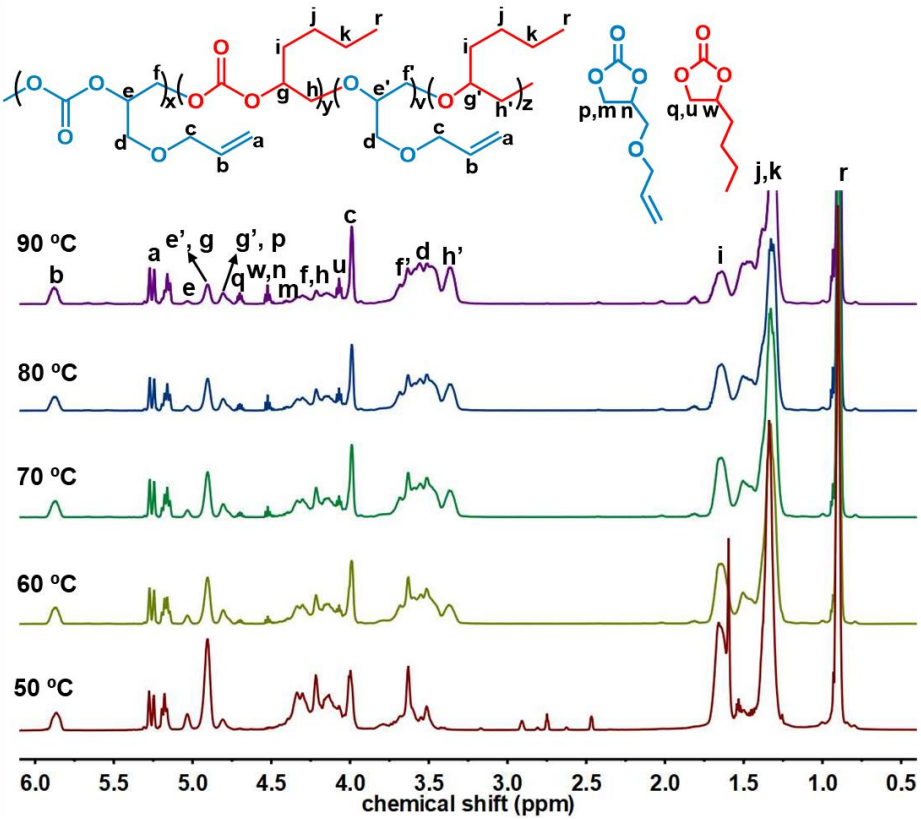

Fig. 2. ^{1}H NMR spectra of crude product obtained from the terpolymerization of CO_2–AGE–HO conducted at 50-90 °C and under a CO_2 pressure of 4 MPa (Table 1, entries 1-5).

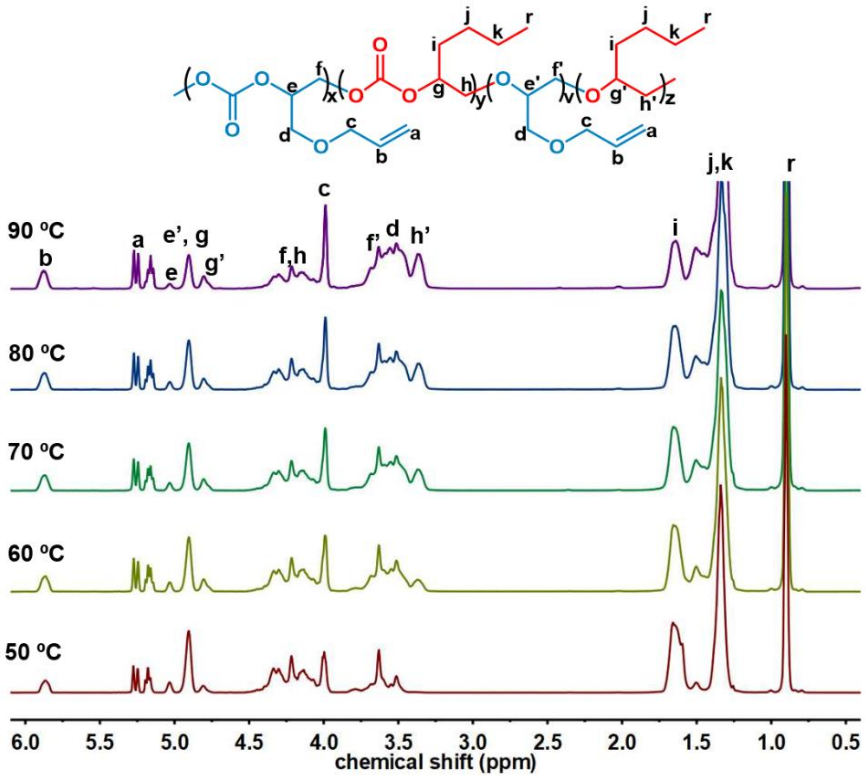

Fig. 3. ^{1}H NMR spectra of purified product obtained from the terpolymerization of CO_2–AGE–HO conducted at 50-90 °C and under a CO_2 pressure of 4 MPa.

Additionally, as temperature increased, the M_n decreased, and PDI broadened (**Fig. 4**). This was attributed to chain transfer to epoxide monomers or trace impurities (e.g., water, alcohols), which could cause premature chain termination and reinitiation. These processes not only shorten the polymer chain length, leading to a decrease in M_n, but also generated polymer chains of varying lengths, resulting in broader PDI.

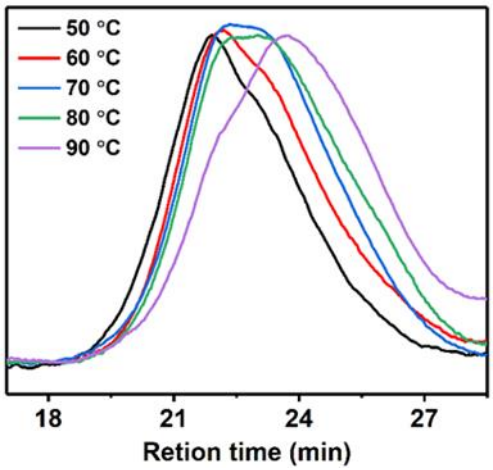

Fig. 4. GPC curves of the copolymers obtained from the terpolymerization of CO_2–AGE–HO at various reaction temperatures.

Table 1. Effects of temperature and CO_2 pressure on the properties of the terpolymer produced from terpolymerization of CO_2–AGE–HO[a].

Entry	Temp. [°C]	CO_2 [MPa]	Conversion[b] [%] AGE	HO	Polymer[c] [%]	Carbonate linkage[d] [%]	M_n[e] [kg/mol]	PDI[e]	T_g[f] [°C]
1	50	4	93	95	98	77	61	2.42	−11
2	60	4	>99	>99	97	54	45	2.65	−17
3	70	4	>99	>99	97	45	39	2.78	−19
4	80	4	>99	>99	96	43	34	2.85	−21
5	90	4	>99	>99	94	37	28	2.83	−23
6	60	3	>99	>99	98	43	40	2.62	−18
7	60	5	>99	>99	96	72	55	2.53	−15

[a]Reaction conditions: DMC (5.0 mg); epoxides (5.0 mL with AGE/HO molar ratio = 20/80), polymerization time (4h, except for 50 °C at which the reaction lasted for 12 h); CO_2 pressure (3, 4 or 5 MPa). [b]Calculated by ^{1}H NMR of the crude products. [c]Polymer selectivity defined as the molar percentage of the polymer in the crude product determined by ^{1}H NMR. [d]Carbonate linkage selectivity defined as the molar percentage of carbonate linkage in the polymer determined by ^{1}H NMR. [e]Determined by gel permeation chromatography (GPC) in THF using polystyrene as the standard. [f]Determined by DSC.

Each polymer displayed a single T_g (**Fig. 5**), indicating that the segments of consecutive carbonate linkage and those of ether linkage of the poly(carbonate-*co*-ether) are short. As the reaction temperature increased from 50 to 90 °C, the T_g values decreased from −11 to −23 °C, corresponding to a reduced carbonate linkage selectivity or an increased ether linkage selectivity. Increasing CO_2 pressure from 3 to 5 MPa (**Table**, entries 6, 2 and 7) further contributed to the incorporation of carbonate linkage in the poly(carbonate-co-ether) and higher M_n, with carbonate linkage selectivity reaching 72% and M_n attaining 55 kg/mol at the highest CO_2 pressure.

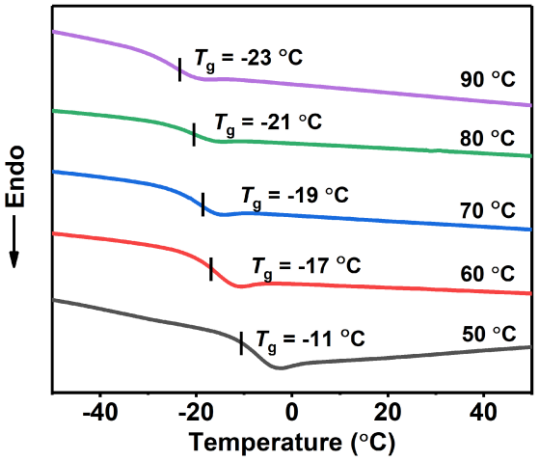

Fig. 5. DSC curves of the terpolymers obtained from the terpolymerization of CO_2–AGE–HO at various reaction temperatures under 4MPa CO_2.

3.2 Kinetics of the terpolymerization of CO_2-AGE-HO

To gain a deeper understanding of the terpolymerization process, we monitored the evolution of several properties (monomer conversion, polymer selectivity, carbonate linkage selectivity, and polymer molecular weight) as a function of polymerization time. Over the first 120 minutes, the CO_2 pressure remained constant at the initial value (4 MPa). After this period, the pressure began to decrease (**Fig. 6a**), indicating that the terpolymerization did not proceed during this time. This delay in polymerization during the first 120 minutes was attributed to the induction period of the DMC catalyst, a phenomenon previously observed in other studies,[67, 181, 182] as will be discussed later. As a result, the polymerization initiation was delayed. Once polymerization began, HO exhibited higher reactivity compared to AGE between 130 and 160 minutes (**Fig. 6b**). As the reaction continued, the reactivity of AGE increased and eventually

slightly surpassed that of HO. At 160 minutes, the conversions of AGE and HO were 49% and 51%, respectively. In the following 5 minutes, the terpolymerization accelerated significantly, causing a rapid increase in monomer conversions (with AGE and HO reaching 79%) and a swift release of heat, which led to a rise in temperature and a temporary increase in CO_2 pressure inside the reactor (**Fig. 6a**). The sudden acceleration of the terpolymerization was linked to the reaction's exothermic nature. Since the polymerization was conducted in bulk, the generated heat could not be efficiently removed from the reactor, causing the temperature of the reaction medium to rise continuously and further accelerating the reaction rate.

The polymer selectivity remained high throughout the polymerization, decreasing slightly from 100% to 97% as the reaction progressed (**Fig. 6c**). Meanwhile, the carbonate linkage selectivity increased slightly from 72% to 76% between 130 and 160 minutes, followed by a sharp decline to 58% due to the sudden temperature increase mentioned above, and then gradually decreased to 54% after 190 minutes. The M_n continuously increased with polymerization time, while its PDI remained nearly constant at approximately 2.76.

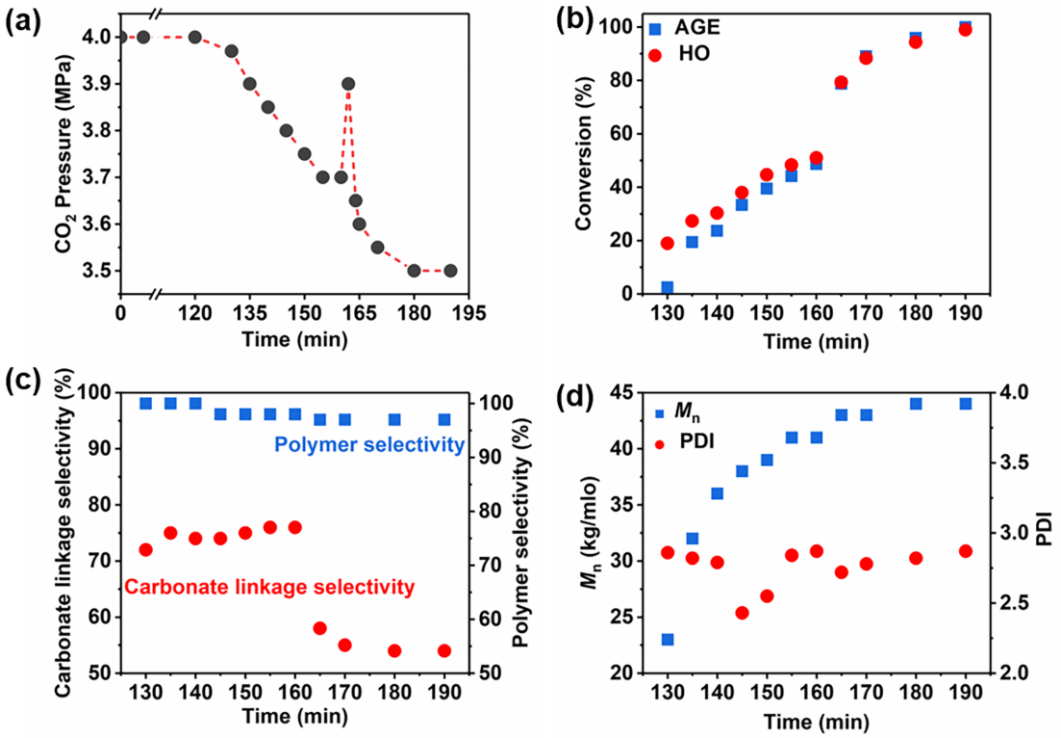

Fig. 6. Kinetics of the terpolymerization of CO_2, AGE, and HO in terms of the evolution of the CO_2 pressure (a), monomer conversions (b), polymer selectivity and carbonate linkage selectivity (c), and polymer molecular weight as a function of polymerization time (d).

3.3 Mechanism of terpolymerization of CO_2, AGE, and HO

The Zn–Co DMC catalyzed copolymerization of CO_2 and epoxides proceeded through three fundamental stages (coordination, activation, and initiation) before entering the chain propagation step (**Fig. 7**). Initially, the Zn–OH moiety on the catalyst surface coordinated with the oxygen atom of the epoxide, forming a pre-complex. Subsequently, ring-opening of the epoxide generates a Zn–alkoxide intermediate. This intermediate then facilitated the insertion of either CO_2 or another epoxide, producing a Zn–carbonate or Zn–alkoxide species, respectively, and completing the initiation step.

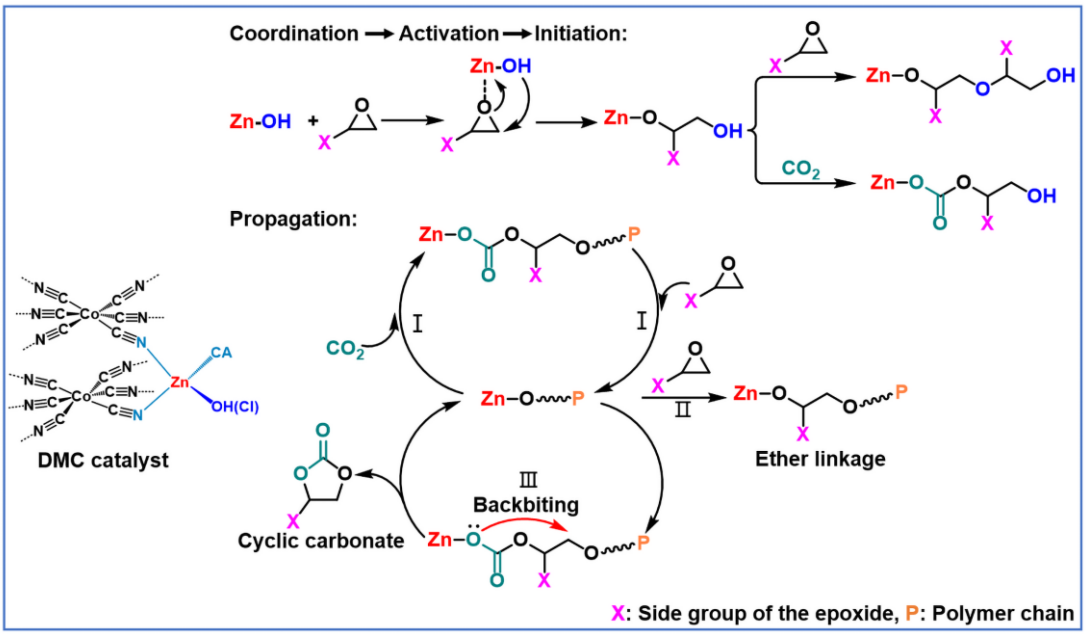

Fig. 7. Proposed ground-state structure of the active site in the DMC catalyst (left) and the corresponding reaction mechanism (right). The complexing agent (CA) is typically H_2O or t-BuOH. Path I depicts the alternating insertion of epoxide and CO_2 leading to carbonate linkage; Path II shows the successive insertion of epoxide resulting in ether linkage; and Path III illustrates intramolecular backbiting, which forms cyclic carbonate.

The induction period observed experimentally was primarily attributed to the slow activation of the catalyst. Strongly coordinating polar ligands, such as H_2O (from residual moisture) and t-BuOH (from DMC synthesis), competed with the epoxide for coordination at the Zn center.[39, 80] This competition effectively blocked the active sites, hindered epoxide insertion, and extended the induction period. During the chain propagation stage, carbonate

linkage formation competed with ether linkage formation and cyclic carbonate generation [48]. As the reaction temperature increased, the system favored the formation of thermodynamically more stable products: cyclic carbonate and ether linkage.[26, 183] Consequently, a slight decrease in polymer selectivity and a significant reduction in carbonate linkage selectivity were observed (**Fig. 6c**).

3.4 Tailoring T_g and mechanical properties of the poly(carbonate-co-ether) elastomer

To tailor the T_g and mechanical properties of the resulting elastomer, a series of terpolymerizations were conducted by adjusting the feed ratio of AGE to HO to achieve targeted double bond contents of 5-25 mol% in the resulting terpolymers (**Fig. 8**). As summarized in **Table**, variations in the AGE to HO feed ratio had minimal impact on polymer selectivity, carbonate linkage selectivity, and the M_n. In contrast, the T_g was strongly affected by the AGE content. The lowest T_g of −18 °C was obtained at the highest AGE content (25 mol%), whereas the highest T_g of –11 °C corresponded to the lowest AGE content (5 mol%). A linear decrease in T_g was observed with increasing AGE content (**Fig. 9**), which is attributed to the enhanced flexibility of the polymer arising from the ether linkages in the AGE side groups.[152, 176]

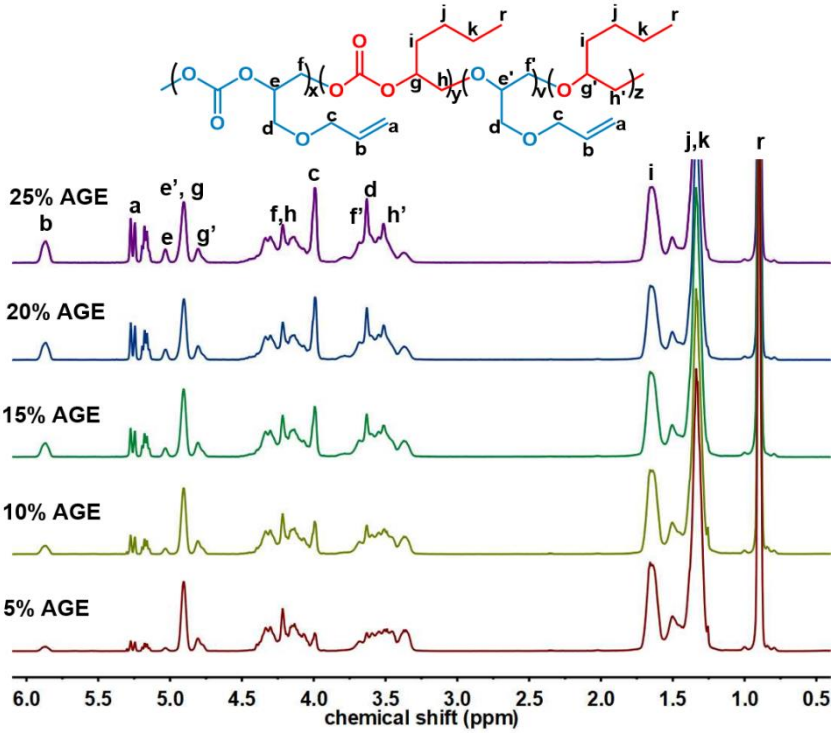

Fig. 8. ^{1}H NMR spectra of purified polymer obtained from the terpolymerization of CO_2-AGE-HO with varying AGE contents at 60 °C and 4 MPa CO_2 pressure

Table 2. Effect of AGE/HO mole ratio on the product properties of the CO_2-AGE-HO terpolymerization[a].

Entry	AGE[b] [mol%]	Conversion [%] AGE	HO	Polymer [%]	Carbonate linkage [%]	M_n [kg/mol]	PDI	T_g [°C]	σ[c] [MPa]	ε[d] [%]
1	5	>99	>99	97	54	42	2.93	−11	0.5 ± 0.1	467 ± 37
2	10	>99	>99	97	55	41	2.93	−13	0.6 ± 0.0	295 ± 21
3	15	>99	>99	98	55	45	2.55	−14	0.7 ± 0.1	284 ± 5
4	20	>99	>99	98	54	45	2.65	−17	0.8 ± 0.1	171 ± 9
5	25	99	99	98	56	41	2.55	−18	0.8 ± 0.1	136 ± 6

[a]Reaction conditions: DMC (5.0 mg); CO_2 (4 MPa); polymerization temperature (60 °C); time (4 h). [b]The mole percentage of AGE monomer in the total monomer mixture. [c]Maximum stress of a stress-strain curve. [d]Strain at break. Strain rate = 50 mm/min, testing temperature = 25 °C. All mechanical properties were determined from three replicates for each sample.

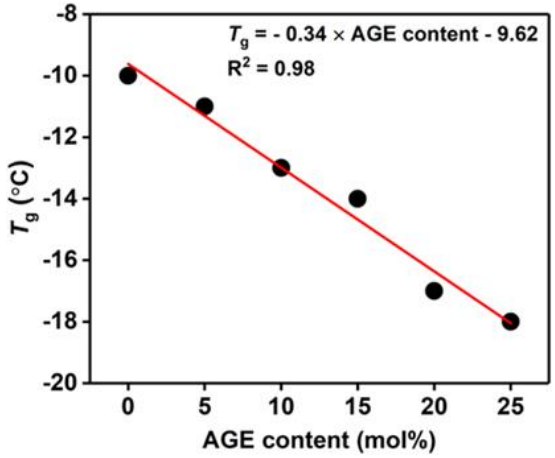

Fig. 9. Plot of T_g of CO_2-AGE-HO terpolymer versus the AGE content, showing a linear decrease in T_g with increasing AGE content.

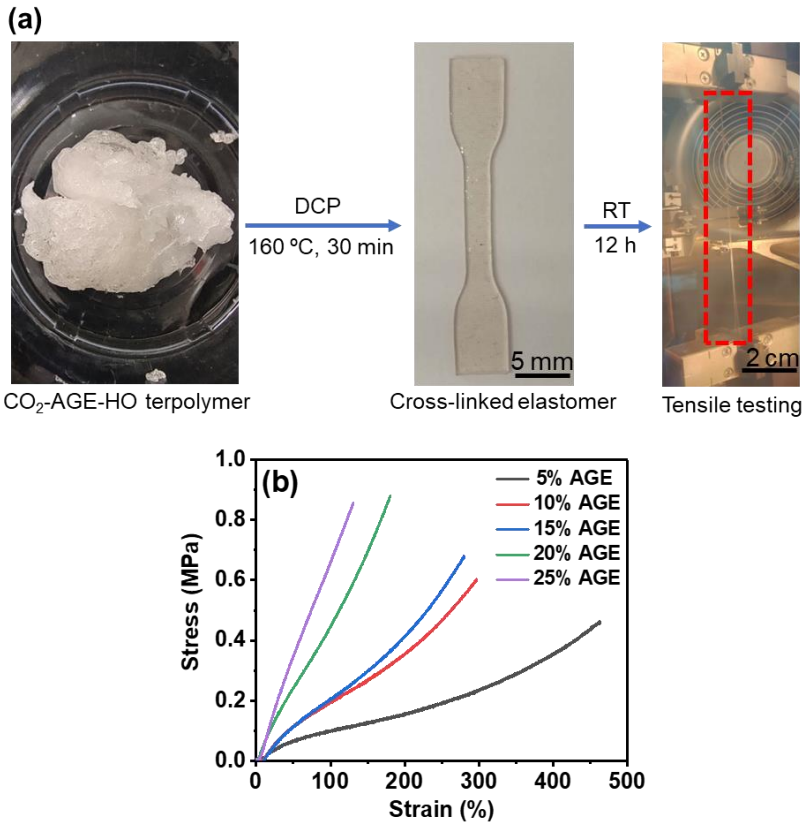

Fig. 10. (a) Crosslinking and tensile testing of CO_2–AGE–HO terpolymers. The terpolymers were crosslinked in a mold using dicumyl peroxide (DCP) at 160 °C for 30 min. The specimens were then rested at room temperature (RT) for 12 h before undergoing tensile testing. (b) Tensile stress-strain curves of the crosslinked CO_2–AGE–HO terpolymers.

The mechanical properties of the five terpolymers were evaluated after crosslinking. The crosslinking procedure was illustrated in **Fig. 10a**. Each terpolymer was uniformly mixed with 0.1 phr DCP and melt-pressed using a plate vulcanizing machine at 160 °C for 30 minutes. The resulting plate was cooled to room temperature and rested for 12 hours before being cut into dumbbell-shaped specimens for tensile testing. **Fig. 10b** presents mechanical properties of the crosslinked terpolymers. As expected, varying the AGE to HO ratio significantly influenced their mechanical performances. Specifically, the tensile strength at break increased, while the elongation at break decreased with higher AGE content. This trend is attributed to the increased crosslinking density resulting from the greater number of double bonds introduced by the AGE units. The terpolymer with 5 mol% AGE (**Table**, Entry 1) exhibited the softest behavior, with the lowest tensile strength at break (0.5 ± 0.1 MPa) and the highest elongation at break (467 ±

37%). In contrast, the terpolymer containing 25 mol% AGE (**Table**, Entry 5) showed the most rigid behavior, with the highest tensile strength at break (0.8 ± 0.1 MPa) and the lowest elongation at break (136 ± 6%).

3.5 Effect of epoxide alkyl chain length and crosslinking

Epoxide substituents play a crucial role in determining the T_g of copolymers.[30, 184, 185] To develop CO_2-based elastomers suitable for various applications at ambient temperatures, terpolymerizations of CO_2, AGE, and epoxides with different side chain lengths were carried out (**Table 3, Figs.11-12**). When the AGE content in the feed was fixed, for example, at 5 mol% (**Table 3**, entries. 1, 4,7), a clear linear decrease in T_g was observed with increasing alkyl chain length of epoxide (**Fig. 13**). This trend is attributed to the plasticizing effect of the longer alkyl chains, which enhances chain flexibility. Similar behavior was observed in terpolymers with 10 and 15 mol% AGE content. When the alkyl chain length of the saturated epoxide was fixed, as in the CO_2–AGE–BO terpolymer series, T_g decreased from 5 °C to −1 °C with increasing AGE from 5 to 15 mol%. Substituting BO with longer alkyl chain epoxides such as HO or OO further lowered T_g, and this reduction became more pronounced with increasing AGE content. These tunable thermal properties make the materials highly adaptable for diverse applications at ambient conditions.

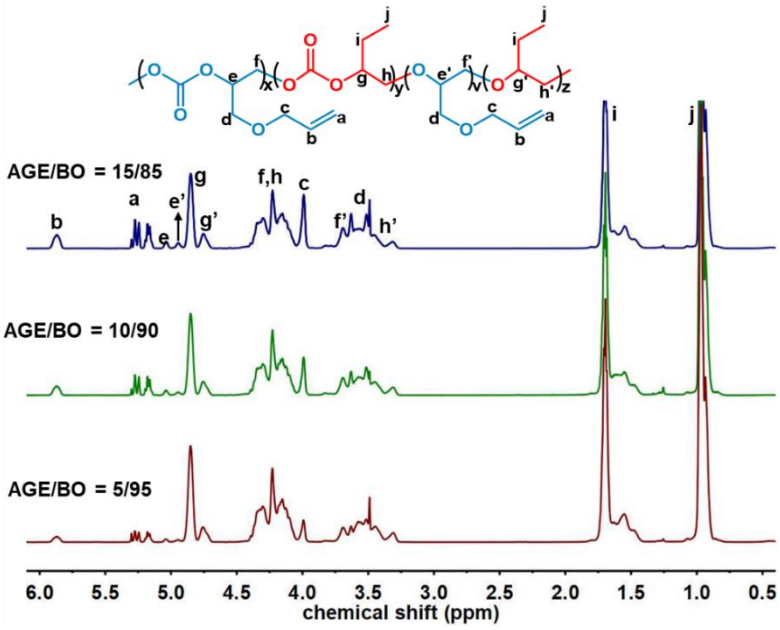

Fig. 11. ^{1}H NMR spectra of purified polymer obtained from the terpolymerization of CO_2-AGE-BO with varying AGE contents at 60 °C and 4 MPa CO_2 pressure (Table 3, entries 1-3).

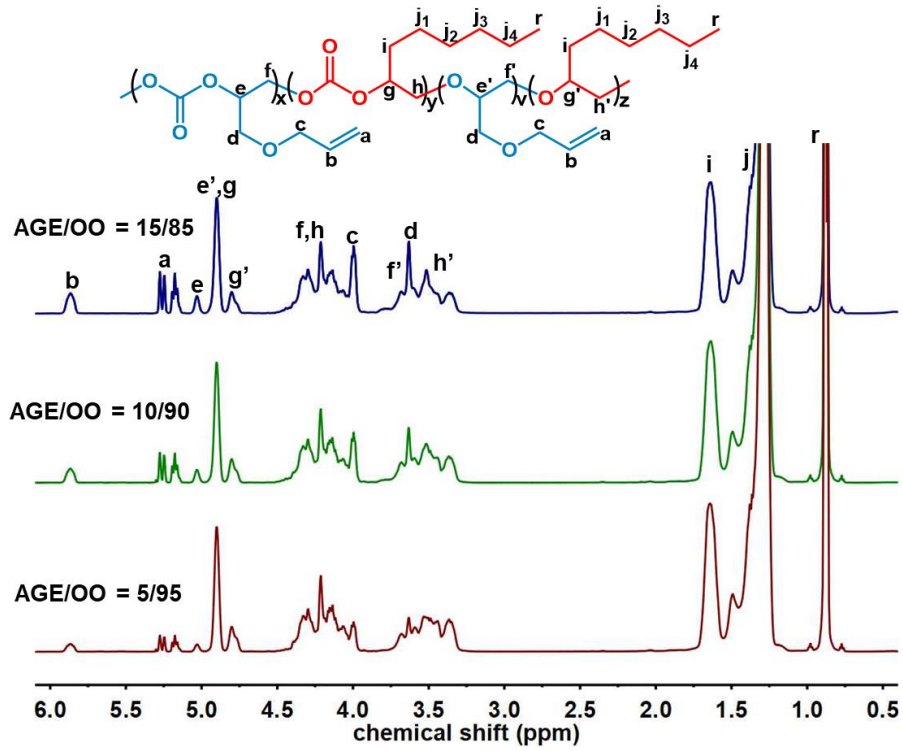

Fig. 12. ^{1}H NMR spectra of purified polymer obtained from the terpolymerization of CO_2–AGE–OO with varying AGE contents at 60 °C and 4 MPa CO_2 pressure (Table 3, entries 7-9).

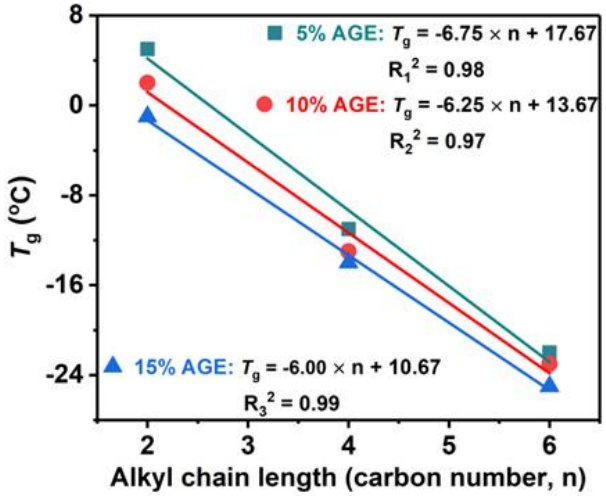

Fig. 13. Effect of the alkyl chain length in saturated epoxides (BO, HO and OO) and AGE content on the T_g of the terpolymer.

Table 3. Terpolymerization of CO_2 with AGE and epoxide containing long alkyl chain by DMC[a]

Entry	Epoxide	Feed[b]	Conversion [%]		Polymer [%]	Carbonate linkage [%]	M_n [kg/mol]	PDI	T_g [°C]	σ [MPa]	ε [%]
			AGE	RnO							
1	AGE/BO	5/95	>99	>99	96	67	38	3.41	5	2.2 ± 0.3	654 ± 68
2	AGE/BO	10/90	>99	>99	96	66	39	2.99	2	1.6 ± 0.0	272 ± 9
3	AGE/BO	15/85	>99	99	97	62	35	2.97	−1	2.0 ± 0.1	201 ± 12
4	AGE/HO	5/95	>99	>99	97	54	42	2.93	−11	0.5 ± 0.1	467 ± 37
5	AGE/HO	10/90	>99	>99	97	55	41	2.93	−13	0.6 ± 0.0	295 ± 21
6	AGE/HO	15/85	>99	>99	97	55	45	2.55	−14	0.7 ± 0.1	284 ± 5
7	AGE/OO	5/95	>99	>99	97	56	44	2.83	−22	0.3 ± 0.0	373 ± 28
8	AGE/OO	10/90	>99	>99	97	58	40	3.05	−23	0.3 ± 0.0	126 ± 19
9	AGE/OO	15/85	>99	>99	98	60	45	2.65	−25	0.5 ± 0.1	106 ± 13

[a]DMC (5.0 mg); CO_2 (4 MPa); polymerization temperature (60 °C). [b]AGE/saturated epoxide molar ratio.

The mechanical behavior of these terpolymers was shown in the stress–strain curves in **Fig. 14a–c**, which highlighted the influence of alkyl chain length at a fixed AGE content. At any given AGE content, both tensile strength and elongation at break decreased in the order BO > HO > OO. Furthermore, as the AGE content increased (**Fig. 14d–f**), the crosslinking density rose, leading to enhanced tensile strength but reduced elongation at break.

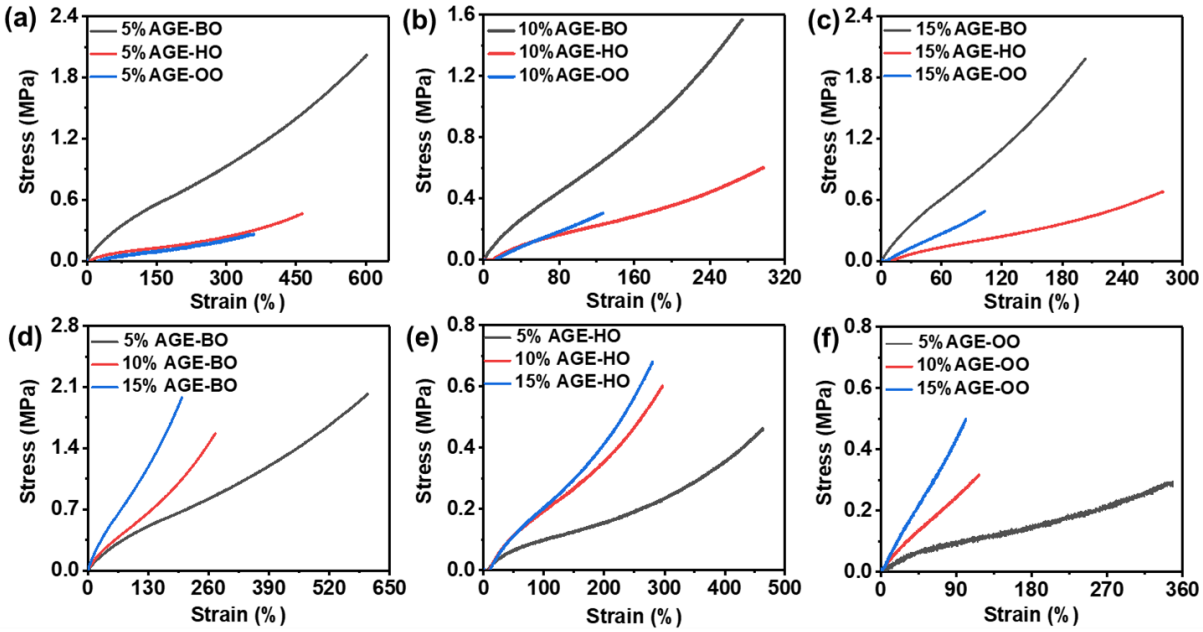

Fig. 14. Effect of the alkyl chain length of the saturated epoxide on the tensile stress-strain curve of the terpolymer of CO_2-AGE-saturated epoxide. (a), (b) and (c): given AGE/saturated epoxide molar ratios and different alkyl chain lengths of the saturated epoxide; (d), (e) and (f): various AGE/saturated epoxide molar ratios for given alkyl chain lengths of the saturated epoxides.

4. Conclusion

The integration of CO_2 into polymeric materials offers a sustainable pathway to reducing fossil fuel dependence while addressing environmental challenges. In this study, we developed crosslinkable CO_2-based elastomers through the terpolymerization of CO_2, allyl glycidyl ether (AGE, an unsaturated epoxide), and a saturated epoxides containing long alkyl chain. By adjusting the epoxide composition, we achieved tunable glass transition temperatures (T_gs) ranging from −25 °C to +5 °C, along with controlled mechanical properties. Key findings include the high efficiency of the Zn−Co(III) double metal cyanide (Zn–Co DMC) catalyst,

which facilitated the synthesis of high-molecular-weight terpolymers with minimal cyclic carbonate byproducts. The T_g of the terpolymer was found to decrease linearly with increasing AGE content or alkyl chain length, enabling the design of elastomers suited for diverse conditions. Additionally, the incorporation of AGE introduced crosslinking sites, enhancing tensile strength while reducing elongation at break as crosslinking density increased. By optimizing the balance between double bond content and alkyl chain length, we produced elastomers with tailored mechanical performance. This study highlights CO_2-based terpolymerization as a versatile strategy for designing sustainable elastomers with tunable thermal and mechanical properties, making them promising candidates for environmentally friendly and high-performance polymer applications.

Chapter 5 Solution vs. Bulk terpolymerization via Al porphyrin/PPNCl catalysis

To address the exothermic risk and potential safety hazards observed in bulk polymerization systems, this chapter investigates the use of a homogeneous aluminum porphyrin catalyst for the terpolymerization of CO_2, allyl glycidyl ether (AGE), and 1,2-hexene oxide (HO). By leveraging a well-defined molecular catalyst, the study seeks to achieve controlled reactivity while minimizing thermal runaway potential and improving catalytic precision under mild conditions. Both bulk and solution polymerization strategies were explored to assess their impact on reaction kinetics, product distribution, and molecular weight development. Special emphasis is placed on the mechanistic understanding of the terpolymerization process, particularly the interplay between backbiting reactions and carbonate linkage formation. Kinetic parameters related to initiation, propagation, and side reactions were systematically examined to elucidate the factors governing chain growth and sequence control. The effect of solvent polarity and coordination environment on the competition between cyclic carbonate formation and linear polycarbonate propagation was also analyzed, providing deeper insight into the dynamic behavior of homogeneous CO_2/epoxide polymerization systems. This mechanistic investigation forms the basis for optimizing reaction pathways toward selective and high-performance CO_2-based polymers.

Kinetic insights into CO_2/epoxides terpolymerization using an aluminum porphyrin/PPNCl system: solution and bulk polymerization

Abstract

This study investigates the kinetics of CO_2 terpolymerization with allyl glycidyl ether (AGE) and 1,2-hexene oxide (HO) using an aluminum porphyrin/PPNCl co-catalytic system. The effects of solvent polarity and reaction conditions on polymer selectivity, molecular weight, and cyclic carbonate formation were systematically analyzed. Kinetic studies revealed that the copolymerization follows first-order dependence on monomer concentration in both solution and bulk polymerization. High polarity solvents, such as THF, promote backbiting reactions, leading to increased cyclic carbonate formation and lower molecular weight polymers. In contrast, non-polar solvents like cyclohexane stabilize the catalytic complex, enhancing polycarbonate selectivity and molecular weight. Bulk polymerization, free of solvent effects, exhibited higher polymerization rate constants, higher molecular weights, and greater polycarbonate selectivity, but was limited by increased viscosity at higher conversions. Temperature significantly influenced reaction selectivity, with higher temperatures favoring backbiting and reducing molecular weight. These findings provide valuable insights into optimizing polymerization conditions for selective polycarbonate production using the aluminum porphyrin/PPNCl catalytic system.

Key words: Polycarbonate, Cyclic carbonate, Kinetics, Solvent polarity, Molecular weight (M_n)

1. Introduction

The utilization of carbon dioxide (CO_2) as a feedstock for polymer synthesis represents a significant advancement in sustainable chemistry, offering an alternative to petroleum-based materials while contributing to carbon capture efforts.[162, 186] Among the various strategies for CO_2-based polymerization, the copolymerization of CO_2 with epoxides has emerged as a promising approach for producing polycarbonates with high thermal stability, transparency, and biodegradability.[1, 17, 141]

Despite these advantages, a key challenge in CO_2/epoxide copolymerization is the formation of cyclic carbonates as by-products, which reduces polycarbonate selectivity and limits molecular weight growth.[23] To address these issues, the development of highly selective catalysts with precise control over polymer structure is essential. Homogeneous aluminum porphyrin (Al porphyrin) complex has gained attention due to their well-defined active sites and low toxicity.[104, 187] When combined with a co-catalyst such as bis(triphenylphosphine)iminium chloride (PPNCl), these systems exhibit reversible chain transfer behavior, facilitating immortal polymerization and enabling precise control over polymer architecture.[188, 189] Compared to heterogeneous catalysts such as zinc-cobalt(III) double metal cyanide complex (DMC)[39, 80] and rare-earth ternary complex[140], Al porphyrin/PPNCl systems provide superior regulation of molecular weight (M_n) and polydispersity index (PDI).

Additionally, in the copolymerization of CO_2 with epoxides, the presence of solvent plays a critical role in determining polymerization performance.[83, 190, 191] For example, solvents reduce system viscosity and enhance mass transfer,[192-195] preventing heat accumulation and helping to suppress backbiting, a side reaction that leads to cyclic carbonate formation. Solvents also mitigate uncontrolled epoxide insertion that results in undesired ether linkages.[146, 196] Therefore, understanding solvent effects on catalytic activity and selectivity is essential for improving polymer quality and guiding the rational design of copolymerization systems.

Numerous studies have explored solvent effects in systems employing simple epoxides such as propylene oxide (PO) or cyclohexene oxide (CHO).[17, 30] For example, Darensbourg et al. reported that toluene increases activation parameters and promotes the formation of cyclic

carbonates catalyzed by (salen)-metal complexes.[191] Zhang et al. demonstrated that the introduction of THF into DMC catalyzed systems effectively suppresses the formation of ether linkages, thereby affording high carbonate linkage selectivity (>95%).[80] In metal-free catalytic systems, such as those employing onium or phosphazene cations paired with a Lewis acidic activator like triethylborane (TEB), THF enhance anionic reactivity and accelerate polymerization, while less polar solvents like toluene result in markedly slower reactions.[124] Under bulk conditions, the reaction exhibits slightly higher activity, but at the expense of reduced selectivity of linear polycarbonates over cyclic by-products.

Studies employing model monomers like PO and CHO have elucidated general solvent effects, but these monomers do not adequately reflect the complexity and selectivity issues encountered with functionalized epoxides, particularly those bearing pendent vinyl groups. Recent research has thus shifted towards more representative monomers, such as vinylcyclohexene dioxide (VCD), which contains a pendant vinyl group and significant steric bulk. Copolymerizations of VCD with CO_2 have been carried out using the aminotriphenolate iron/PPNBz binary catalyst (PPN = bis(triphenylphosphine)iminium, Bz = benzoate). In such systems, solvents like THF can both reduce viscosity and increase cyclic carbonate formation compared to bulk systems.[197] These findings highlight that solvent coordination can strongly influence propagation versus backbiting, yet systematic kinetic investigations in such systems remain limited.

In this work, we investigate the terpolymerization of allyl glycidyl ether (AGE) and 1,2-hexene oxide (HO) with CO_2 using an Al porphyrin/PPNCl catalyst. AGE provides a pendant vinyl group for post-polymerization modification,[167, 176] while HO contributes to chain flexibility through its long alkyl side chain, together enabling the design of CO_2-based elastomeric materials.[40, 198] Whereas most previous studies on solvent effects have only reported product-level outcomes, systematic kinetic investigations remain scarce. This lack of insight is particularly critical for functionalized epoxides, which present more complex selectivity issues and require clarification of the influence of solvent polarity and coordination on the balance between chain propagation and backbiting. By addressing this gap, our work establishes the mechanistic basis of solvent-mediated selectivity in functionalized epoxide

systems and offers guidance for the development of selective and scalable routes to elastic CO_2-based polycarbonates.

2. Experimental section

2.1 Materials

All water-sensitive and oxygen-sensitive operations were performed in a glove box under an argon atmosphere or using the Schlenk technique under nitrogen protection. Allyl glycidyl ether (AGE, 99%) and 1,2-hexene oxide (HO, >96%) were purchased from Aladdin and dried over CaH_2 under nitrogen for 24 hours, followed by distillation under reduced pressure. Tetrahydrofuran (THF, >99%), toluene (95%), and cyclohexane (>99%) were also dried similarly. Carbon dioxide gas (99.999%) was used as received. The aluminum porphyrin complex was synthesized according to the literature method.[156, 157] Bis(triphenylphosphoranylidene)ammonium chloride (PPNCl, >96%) was recrystallized from dry dichloromethane and diethyl ether under nitrogen before use.

2.2 Terpolymerion of CO_2, AGE and HO

In the glove box, the pre-dried autoclave was charged with the desired amounts of Al porphyrin, PPNCl, AGE, HO, and solvent (THF, toluene, cyclohexane, or solvent-free). Next, the autocalve was taken out of the glove box, placed in a water bath at the specified temperature with magnetic stirring, and then charged with CO_2 to the predetermined pressure and maintained constant throughout the reaction. The mixture was stirred continuously for the designated reaction time under these controlled conditions. After a selected duration of time, the autoclave was cooled to room temperature. The unreacted CO_2 in the autoclave was then slowly released, and the autoclave was opened to take a small portion of the crude product for ^{1}H NMR and GPC testing. The remaining crude product was dissolved in dichloromethane and precipitated in methanol three times to remove residual epoxides and cyclic carbonates. The purified product was collected and dried at 40 °C under vacuum for 48 h.

2.3 Characterization

2.3.1 Characterization of the product structure

The structure and composition of the crude product were analyzed using ^{1}H NMR

spectroscopy. The monomer conversion and the composition of polycarbonate and cyclic carbonate in the crude product were determined by integrating the peaks in the ^{1}HNMR spectrum, recorded on a Bruker AV-600 spectrometer using $CDCl_3$ as the solvent. The compositions of the crude product were quantified by polycarbonate selectivity and cyclic carbonate selectivity which are defined as follows:

Polycarbonate selectivity (%) = (moles of carbonate linkage in the crude product) / (total moles of carbonate linkage and cyclic carbonate by-products in the crude product) × 100;

Cyclic carbonate selectivity (%) = (moles of cyclic carbonate by-products in the crude product) / (total moles of carbonate linkage and cyclic carbonate by-products in the crude product) × 100.

The detailed calculation procedures, along with the ^{1}H NMR peak assignments used in the analysis, are provided in the **Chapter 3**.

2.3.2 Molecular weights of polymers

The number-average molecular weight (M_n) and polydispersity index (PDI) of the polymers were measured by gel permeation chromatography (GPC) using a Waters 515 GPC system equipped with Styragel HT3, HT5, and HT6 columns. THF was used as the mobile phase with a flow rate maintained at 1.0 mL min^{-1}.

3. Results

3.1 Solution terpolymerization kinetics of CO_2-AGE-HO

To evaluate the effect of the polymerization environment, solution polymerization was conducted in a solvent under the same conditions, except that the nature of solvent was varied: THF, toluene, and cyclohexane whose polarity decreases from high to low.[199] With 30 vol% of solvent, the polymerization in all three solvents exhibited a similar overall trend, with monomer conversion (p) increasing steadily over time and reaching ~90% within 36 hours (**Fig. 1**). These results suggest that solvent polarity had minimal impact on overall reaction completion and monomer reactivity under the given conditions. The ^{1}H NMR spectra of the products obtained from terpolymerization (**Fig. 2**) showed no characteristic peaks of ether linkages, indicating that during the terpolymerization of CO_2, AGE, and HO, both AGE and HO

reacted with CO_2 instead of polymerizing with each other. Based on this observation, we proposed an Al porphyrin catalyzed reaction mechanism, detailing the chain initiation and propagation steps, as illustrated in **Fig. 3**.

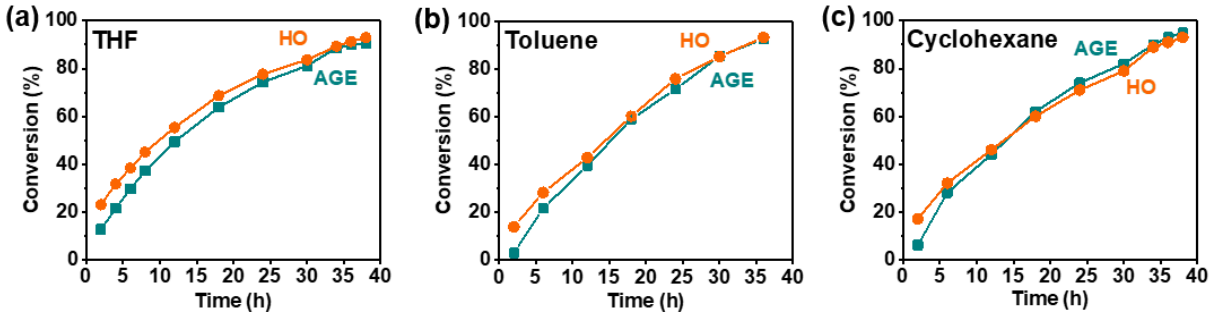

Fig. 1. Conversions (*p*) of AGE and HO over time during the terpolymerization of CO_2–AGE–HO in three different solvents: (a) THF, (b) toluene, and (c) cyclohexane. Reaction conditions: Al porphyrin/PPNCl/epoxide molar ratio = 1/1/2000; AGE/HO molar ratio = 20/80; epoxide volume = 3.5 mL; solvent volume = 1.5 mL (solvent volume fraction = 30%); CO_2 pressure = 4 MPa (maintained throughout); reaction temperature = 70 °C.

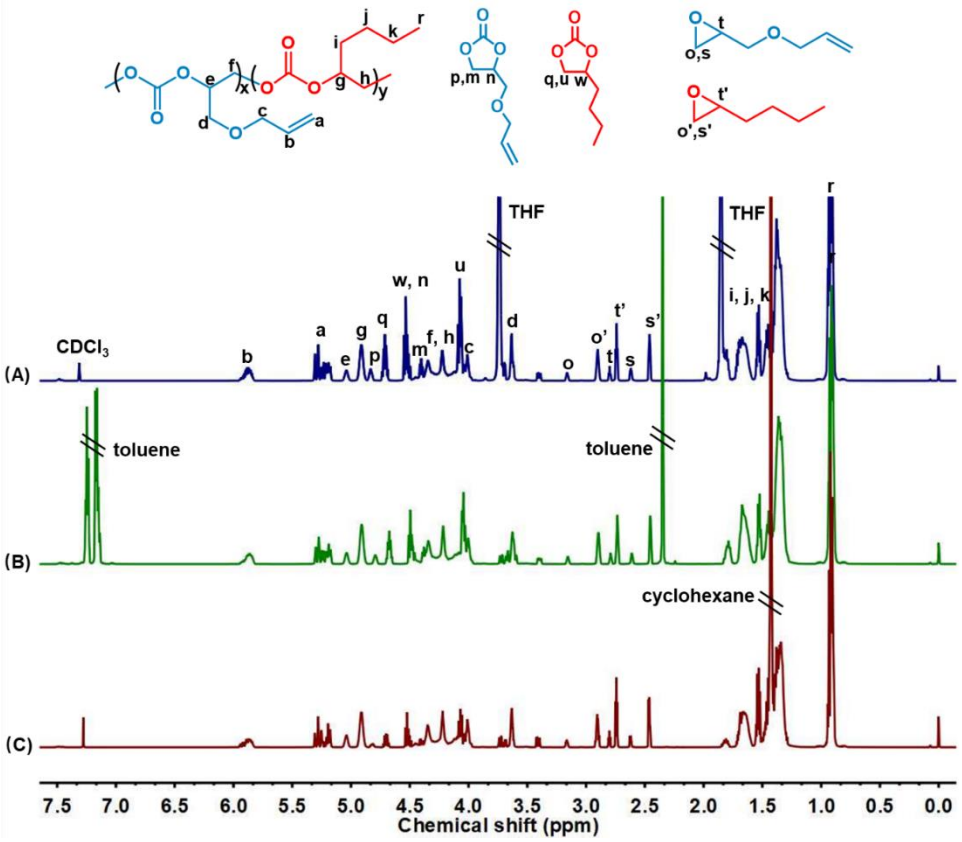

Fig. 2. ^{1}H NMR spectra of crude product obtained from the terpolymerization of CO_2–AGE–HO in three different solvents: (A) THF, (B) toluene, and (C) cyclohexane.

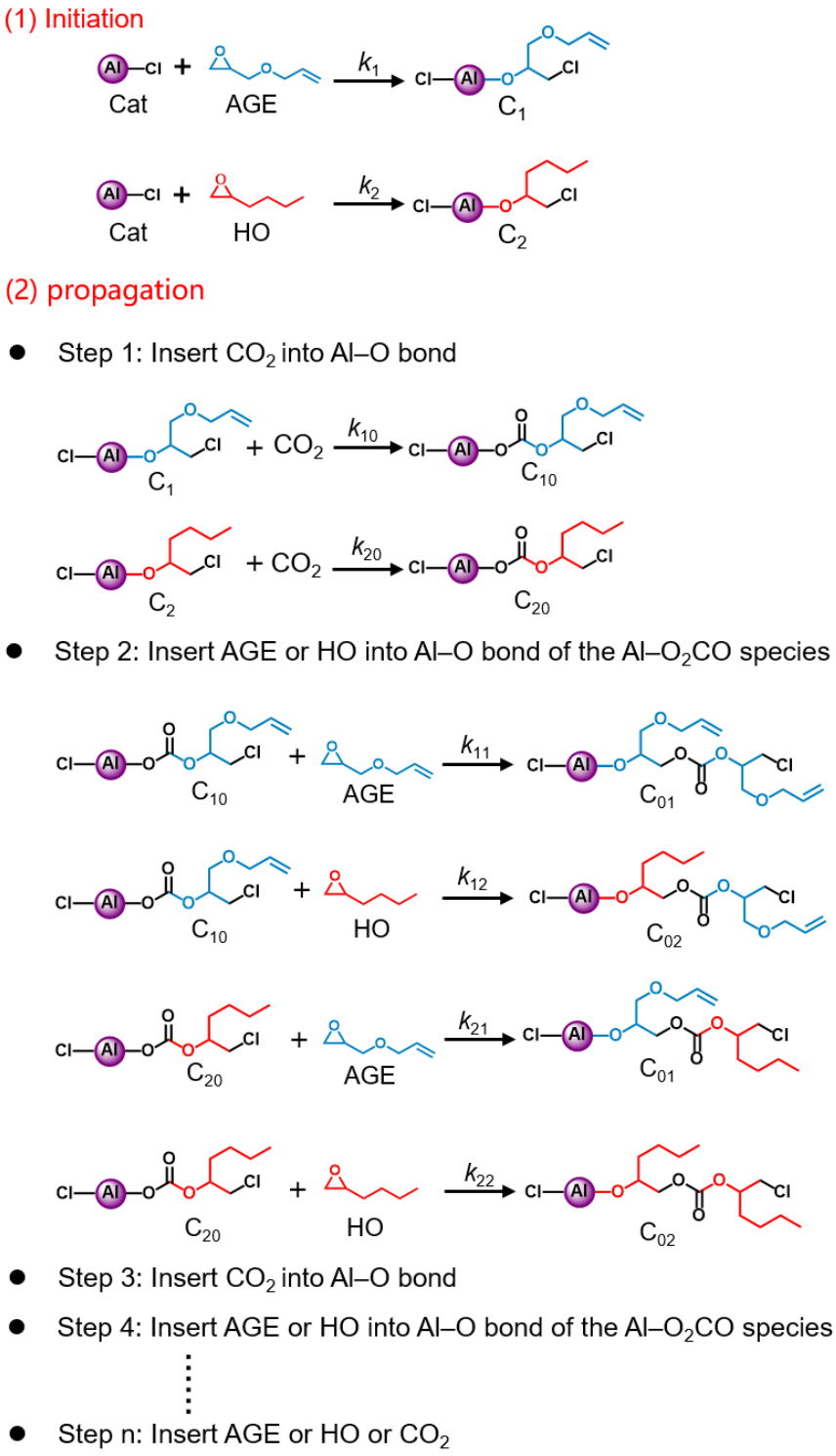

Fig. 3. Mechanism of aluminum porphyrin catalyzed polymerization: initiation and propagation. Cat represents the catalyst.

Consumption rate of AGE monomer:

$$-\frac{d[AGE]}{dt} = k_1[Cat][AGE] + k_{11}[C_{10}][AGE] + k_{21}[C_{20}][AGE]$$

$$= (k_1[Cat] + k_{11}[C_{10}] + k_{21}[C_{20}])\,[AGE] \quad (1)$$

Consumption rate of HO monomer:

$$-\frac{d[HO]}{dt} = k_2[Cat][HO] + k_{12}[C_{10}][HO] + k_{22}[C_{20}][HO]$$

$$= (k_2[Cat] + k_{12}[C_{10}] + k_{22}[C_{20}])\,[HO] \quad (2)$$

Assuming that the terms $k_1[Cat] + k_{11}[C_{10}] + k_{21}[C_{20}]$ in Eq.1 and $k_2[Cat] + k_{12}[C_{10}] + k_{22}[C_{20}]$ in Eq.2 remain constant throughout the reaction, these equations can be simplified as follows:

Eq.1 can be simplified to:

$$-\frac{d[AGE]}{dt} = k_{AGE}\,[AGE]$$

$$\text{or } -\ln(1 - p_{\mathrm{AGE}}) = k_{\mathrm{AGE}}\,t \quad (3)$$

Here, $k_{AGE} = k_1[Cat] + k_{11}[C_{10}] + k_{21}[C_{20}]$, and p_{AGE} is the conversion of AGE defined as $([AGE]_0 - [AGE]) / [AGE]_0$.

Eq.2 can be reduced to:

$$-\frac{d[HO]}{dt} = k_{HO}\,[HO]$$

$$\text{or } -\ln(1 - p_{\mathrm{HO}}) = k_{\mathrm{HO}}\,t \quad (4)$$

Here, $k_{HO} = k_2[Cat] + k_{12}[C_{10}] + k_{22}[C_{20}]$, and p_{HO} is the conversion of HO defined as $([HO]_0 - [HO]) / [HO]_0$.

The validity of this assumption can be partially justified by the following considerations: The catalyst concentration ($[Cat]$) is expected to remain constant throughout the reaction due to its non-reactive nature; CO_2 is maintained at a constant concentration because it is present in excess and kept at a fixed pressure of 4 MPa during the reaction.

Under these conditions, the polymerization kinetics can be meaningfully analyzed. **Figs. 4a** and **4b** depict the plots of $-\ln(1 - p_{AGE})$ and $-\ln(1 - p_{HO})$ as functions of polymerization time for three solvents: THF, toluene, and cyclohexane. Two key observations can be made

from these plots, as discussed below.

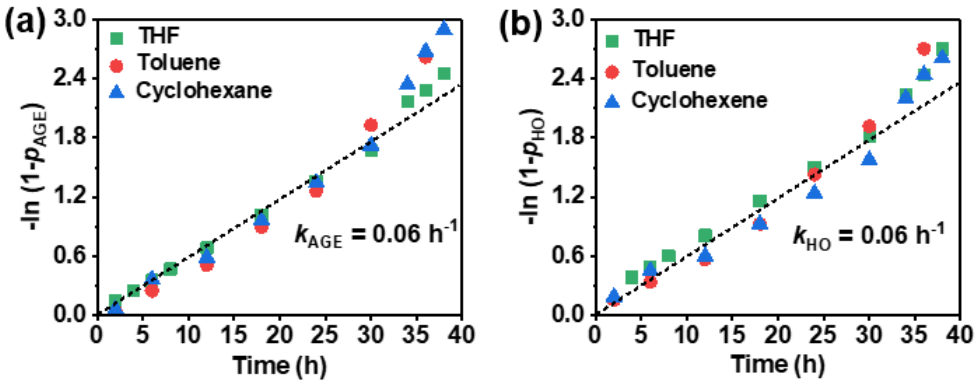

Fig. 4. Plots of $-\ln(1-p_{AGE})$ and $-\ln(1-p_{HO})$ as functions of polymerization time for three solvents: THF, toluene, and cyclohexane.

First, for all three solvents, the plots of $-\ln(1-p_{AGE})$ versus polymerization time are nearly identical, as are the plots of $-\ln(1-p_{HO})$ versus polymerization time. This suggests that the polarity of the solvent does not significantly affect the overall polymerization kinetics under the given conditions. This observation suggests that both monomers are incorporated into the copolymer at similar rates, which is beneficial for achieving a random copolymer. The similar apparent rate constants ($k_{AGE} \approx k_{HO} = 0.06\ h^{-1}$) may be attributed to the comparable ring strain and electronic nature of the two linear aliphatic epoxides, as well as the catalyst's non-selective and effective control over both monomers.

Second, both $-\ln(1-p_{AGE})$ and $-\ln(1-p_{HO})$ exhibit linear relationships with polymerization time up to approximately 30 hours, corresponding to about 80% monomer conversion, indicating that the apparent rate constants k_{AGE} and k_{HO} remain constant during this stage. Beyond 80% conversion, a consistent upward deviation from linearity is observed across all three solvent systems (THF, toluene, and cyclohexane). This common behavior suggests that the deviation is not caused by experimental errors. At high conversion, the calculation of $-\ln(1-p)$ becomes increasingly sensitive to small variations in p. Minor delays during sampling, during which polymerization may still proceed, as well as a reduced signal-to-noise ratio in NMR at low residual monomer concentrations, can lead to a slight overestimation of conversion. Consequently, the observed deviations are more likely attributed to limitations in sampling and analytical precision.

Although solvent polarity has only a minor effect on polymerization kinetics, it significantly influences product composition and M_n. **Fig. 5**a_1–c_1 and **Fig. 5**a_2–c_2 illustrate the evolution of polycarbonate selectivity, cyclic carbonate selectivity, M_n, and PDI over time in different solvents. The results demonstrate that solvent polarity directly impacts the formation of polycarbonate and cyclic carbonate. In cyclohexane, polycarbonate selectivity remains consistently high (>75%), while the formation of cyclic carbonate byproducts is relatively suppressed. In contrast, THF and toluene lead to lower polycarbonate selectivity and a higher proportion of cyclic carbonate, indicating that increased solvent polarity promotes side reactions leading to cyclic carbonate formation.

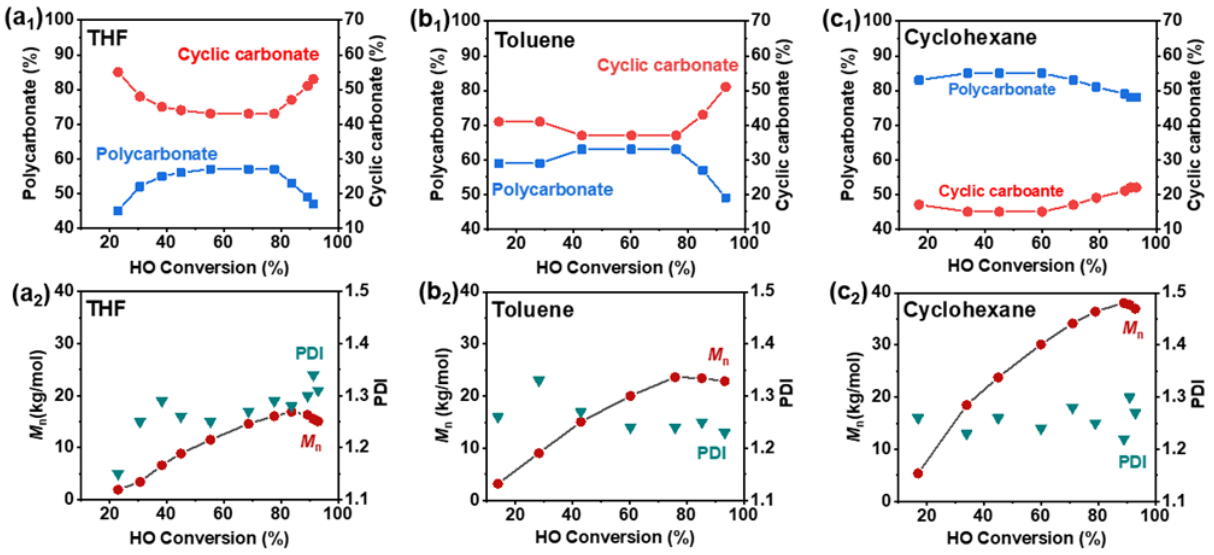

Fig. 5. Evolution of polycarbonate selectivity, cyclic carbonate selectivity, M_n, and PDI over HO conversion during the terpolymerization of CO_2–AGE–HO in different solvents: (a) THF, (b) toluene, and (c) cyclohexane.

The choice of solvent also has a significant impact on M_n. Cyclohexane facilitates the formation of higher molecular weight polymers compared to THF and toluene, suggesting that it promotes chain propagation while suppressing chain degrading side reactions such as backbiting. Regardless of solvent, a common trend is observed in which M_n initially increases but declines at higher conversion. This decrease is attributed to chain unzipping and intramolecular backbiting.[101, 200] As a result, polymer selectivity and M_n diminish in the later stages of the reaction. Among the tested solvents, THF yields the lowest M_n (~16 kg/mol)

and the highest cyclic carbonate content (~40–60%), whereas cyclohexane favors polycarbonate formation (~80%) and produces the highest M_n (~34 kg/mol).

3.2 Mechanistic elucidation of backbiting pathways and solvent effects

To better clarify the mechanistic origins of cyclic carbonate formation during CO2-based terpolymerization, this section is divided into two parts: (1) the fundamental depolymerization pathways involving backbiting reactions, and (2) solvent–catalyst interactions that modulate the stability of active species and influence polymer selectivity.

3.2.1 Depolymerization pathways via backbiting

A key factor governing polymer chain growth versus backbiting is the coordination–dissociation equilibrium between the growing polymer chain and the catalytic metal center.[21, 43] As shown in **Fig. 6**, when the anionic chain is insufficiently stabilized by the metal center Al^{3+}, it tends to undergo backbiting leading to the formation of cyclic carbonate by-products. Previous studies have demonstrated that free anionic chains backbite much more readily than metal-coordinated anionic polymers.[22, 201] This highlights the critical role of metal coordination in suppressing undesired side reactions. Two backbiting pathways were proposed. Path A involves backbiting initiated from the alkoxide-terminated polymer chain (Al–alkoxide species), leading to the interruption of chain propagation and the release of one monomer unit and one molecule of CO_2. Path B proceeds through backbiting from the carbonate-terminated polymer chain (Al–carbonate species), similarly resulting in cyclic carbonate formation. Each backbiting event cleaves the polymer chain by one monomer unit and one molecule of CO_2, cumulatively leading to stepwise depolymerization. As polymerization progresses and the epoxide concentration decreases, the probability of backbiting increases, accelerating cyclic carbonate production over time.[48, 200]

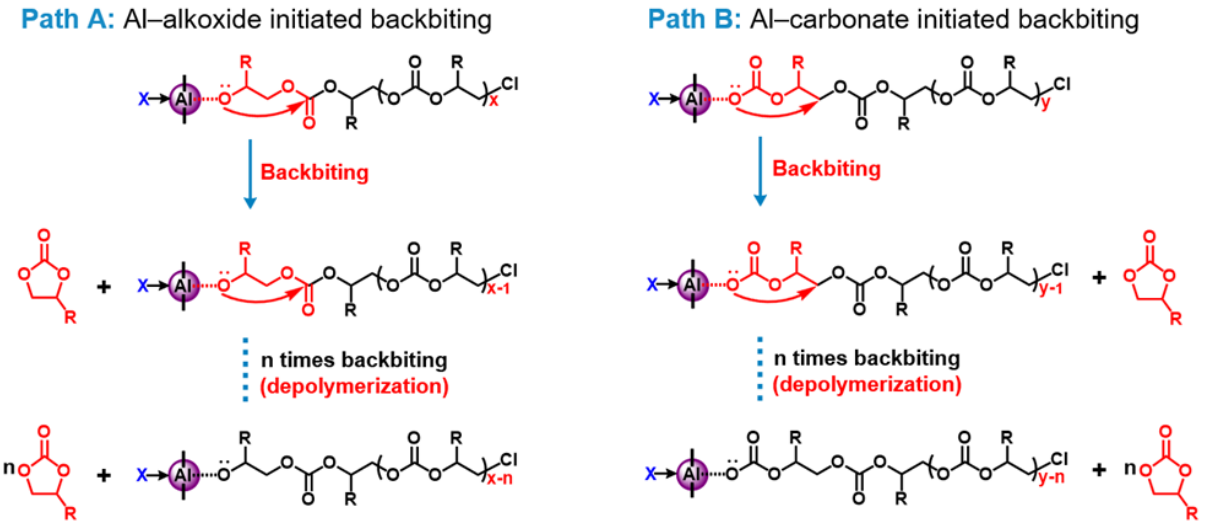

Fig. 6. Mechanisms for polymer chain depolymerization via backbiting. Path (A) proceeds through backbiting from the Al–alkoxide chain end, while Path (B) involves backbiting from the Al–carbonate chain end. Each backbiting event releases one monomer unit and one molecule of CO_2, cumulatively driving stepwise depolymerization. X denotes a coordinating species bound to the Al^{3+}, including solvent (THF, Toluene) and anionic species (Cl^- derived from the co-catalyst PPNCl).

3.2.2 Solvent–catalyst interactions and their effect on selectivity

Examination of solvent–catalyst interactions rationalize the differences in cyclic carbonate formation observed under various solvents. Among the three solvents used, THF exhibits the strongest coordination to the metal center through its lone pairs.[34, 124, 197] This coordination weakens the Al–O bond, facilitates its dissociation, and increases the concentration of free anionic chains, thereby promoting backbiting and enhancing cyclic carbonate formation.[202, 203] By contrast, toluene interacts more weakly with the Al^{3+} center through π-electron donation. This weaker coordination results in a more stable Al–O bond compared to THF, which helps stabilize the growing polymer chain and suppress backbiting. However, the interaction is still stronger than that of cyclohexane, leading to a moderate degree of Al–O bond weakening and thus a slightly higher level of cyclic carbonate formation than in cyclohexane. Cyclohexane, as a nonpolar solvent, exhibits minimal interaction with the Al^{3+} center. This results in the most stable Al–O bond among the three solvents, leading to the highest polycarbonate selectivity and the lowest cyclic carbonate content. Regardless of the nature of the solvent, extended reaction

times (over 30 hours) and high conversion levels (above 80%) inevitably favor depolymerization. This process predominantly proceeds through successive backbiting reactions, which cumulatively generate significant amounts of cyclic carbonates over time.

3.3 Bulk terpolymerization of CO_2-AGE-HO

To eliminate solvent effects and investigate the intrinsic polymerization behavior, the reaction is conducted under solvent-free conditions. The conversions of both AGE and HO are monitored over time, as shown in **Fig. 7a**. Conversions steadily increase throughout the polymerization, reaching approximately 70% after 10 hours. Beyond this point, the polymerization proceeds at a noticeably slower rate. This deceleration is attributed to a decrease in monomer concentration, especially to a rise in viscosity, which hinder monomer diffusion and lower the reaction rate.[60, 204] As a result, the conversion curves gradually level off, exhibiting a relatively steady trend. The bulk polymerization kinetics for AGE and HO follow Eqs.3 and 4, respectively (**Figs. 7b** and **7c**), like the solution polymerization described above. Moreover, the apparent rate constants k_{AGE} and k_{HO} for AGE and HO are higher in bulk polymerization (0.09 h^{-1}) than in solution polymerization (0.06 h^{-1}).

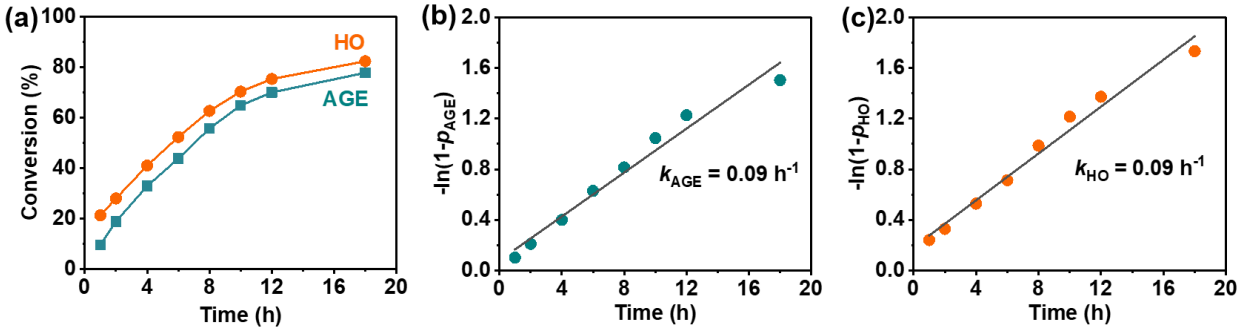

Fig. 7. Kinetics of the bulk polymerization of CO_2–AGE–HO. (a) Plots of AGE and HO conversions versus time; (b) $-\ln(1-p_{AGE})$ versus time; (c) $-\ln(1-p_{HO})$ versus time. Reaction conditions: Al porphyrin/PPNCl/epoxide molar ratio = 1/1/2000; epoxides, 5.0 mL (AGE/HO molar ratio = 20/80); CO_2 pressure = 4 MPa (maintained throughout); reaction temperature = 70 °C.

In addition to the bulk polymerization kinetics, the evolution of product composition over polymerization time is investigated. As shown in **Fig. 8a**, while the polycarbonate selectivity is

initially as high as 85%, it decreases as monomer conversion increases. In parallel, the cyclic carbonate selectivity increases, indicating that backbiting becomes more and more important as the polymerization proceeds, as expected. Overall, the level of cyclic carbonate formation follows the order: polymerization without solvent ≈ polymerization in cyclohexane < polymerization in toluene < polymerization in THF. **Fig. 8b** shows a linear relationship between M_n and monomer conversion, indicating an immortal polymerization mechanism.[205]

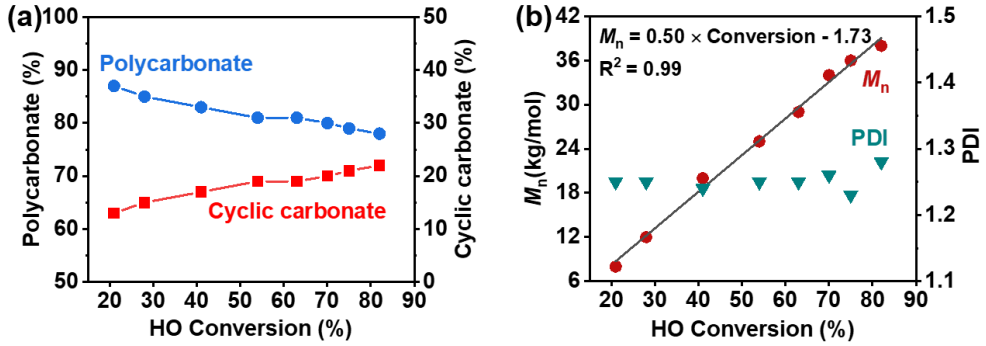

Fig. 8. (a) Evolution of polycarbonate selectivity and cyclic carbonate selectivity and (b) M_n and PDI as a function of HO conversion.

Having identified solvent-dependent trends in polycarbonate selectivity and molecular weight, we next focused on additional reaction parameters, particularly temperature, which modulates catalyst activity and governs the relative rates of chain propagation and side reactions. These factors collectively determine both molecular weight and polycarbonate selectivity. Therefore, a series of polymerizations of CO_2–AGE–HO were conducted in the bulk at varying temperatures to determine optimal conditions for maximizing molecular weight and polycarbonate selectivity. As shown in **Table 1**, raising the reaction temperature from 60 °C to 70 °C significantly enhances both monomer conversion and control over molecular weight, as evidenced by an increase in M_n from 29 to 36 kg/mol and a quasi-constant PDI (1.27 versus 1.23). This suggests that at 70 °C, chain propagation is more efficient and the rate of chain exchange between active and dormant species is optimal, consistent with a living polymerization process. However, further increasing the temperature to 80 °C leads to detrimental effects, as M_n decreases to 22 kg/mol and PDI increases to 1.46, indicating less well controlled polymer growth. Additionally, the polycarbonate selectivity decreases sharply from

86% to 45%, while the cyclic carbonate selectivity increases from 14% to 55%. These results imply that at elevated temperatures, side reactions, especially intramolecular backbiting, become more favorable.[23, 42, 158] A higher temperature not only favors chain exchange, but also irreversible chain transfer and termination, ultimately compromising polymer uniformity.Therefore, an adequate temperature is essential to balance chain propagation, reversible chain exchange, and suppression of side reactions during aluminum porphyrin catalyzed CO_2/epoxide copolymerization.

Table 1. Effect of reaction temperature on the CO_2–AGE–HO terpolymerization[a].



Entry	Temp. [°C]	Conversion [%] AGE	HO	Polycarbonate [%]	Cyclic carbonate [%]	M_n [kg/mol]	PDI
1	60	45	52	97	3	29	1.27
2	70	70	75	86	14	36	1.23
3	80	86	87	45	55	22	1.46

[a]Reaction conditions: Al porphyrin/PPNCl/epoxide molar ratio = 1/1/2000; epoxides, 5.0 mL (AGE/HO molar ratio = 20/80); CO_2 pressure = 4 MPa (maintained throughout); reaction time = 12 h.

4. Conclusions

This study systematically examined the kinetics of CO_2 terpolymerization with allyl glycidyl ether (AGE) and 1,2-hexene oxide (HO) using an aluminum porphyrin/PPNCl catalytic system. Solvent polarity was found to play a critical role in determining polymerization outcomes. High polarity solvents, such as THF, coordinate with the Al^{3+} center, weakening the Al–O bond and promoting backbiting, which leads to increased cyclic carbonate formation and lower molecular weight polymers. In contrast, low-polarity solvents, such as cyclohexane, stabilize the catalytic complex, enhancing polycarbonate selectivity. Bulk polymerization, by eliminating solvent effects, produced higher molecular weight polymers with greater polycarbonate selectivity, though increased viscosity at high conversions restricted

monomer diffusion and slowed the reaction. Kinetic studies confirmed that copolymerization follows first-order dependence on monomer concentration in both solution and bulk polymerization, with bulk polymerization exhibiting higher rate constants. Temperature significantly influenced reaction selectivity, with higher temperatures favoring backbiting and reducing molecular weight. These findings provide a deeper understanding of CO_2-based polymerization and highlight strategies for optimizing reaction conditions to enhance polycarbonate yield while minimizing cyclic carbonate formation. Future studies could explore catalyst modifications to further suppress backbiting and improve reaction efficiency.

Chapter 6 Dual catalyst strategy and composite reinforcement

Building upon the strengths and limitations of the previous catalytic systems, this chapter introduces a dual-catalyst approach that combines a heterogeneous Zn–Co double metal cyanide (Zn–Co DMC) catalyst with a homogeneous aluminum porphyrin/PPNCl system for the synthesis of high molecular weight CO_2-based elastomers. This integrated strategy leverages the high polymerization activity of the Zn–Co DMC catalyst, while simultaneously exploiting the high polycarbonate selectivity, and living polymerization characteristics enabled by the aluminum porphyrin complex. The complementary reactivity of the two catalysts enables a more controlled competition between backbiting and chain propagation, thereby affording precise modulation of polymer sequence distribution and carbonate linkage content. To further enhance the mechanical performance of the resulting elastomers, silica nanoparticles were incorporated as reinforcing agents. Their uniform dispersion within the polymer matrix was designed to maximize interfacial adhesion through hydrogen bonding and physical entanglement, promoting efficient stress transfer across phases while minimizing phase separation. This not only improves elasticity and toughness, but also contributes to the thermal and dimensional stability of the nanocomposite materials. This chapter systematically investigates the influence of catalyst composition on polymerization kinetics, polymer selectivity, and microstructural evolution, as well as the mechanistic role of nanoparticle–matrix interactions in dictating viscoelastic behavior and tensile response. Together, these studies provide a mechanistic and materials-level framework for the rational design of high-performance, sustainable CO_2-derived elastomeric materials.

Dual catalysis for high molecular weight CO_2-based poly(carbonate-co-ether)s toward enhanced elastomeric nanocomposites

Abstract

The utilization of carbon dioxide (CO_2) as a sustainable carbon feedstock for polymer synthesis presents a promising strategy to mitigate environmental concerns while developing high-performance materials. In this work, we report a hybrid catalytic system combining a Zn–Co DMC complex with an Al porphyrin/PPNCl cocatalyst system for the efficient terpolymerization of CO_2, 1,2-epoxyhexane (HO), and allyl glycidyl ether (AGE). This dual catalyst system leverages the high activity of heterogeneous catalysis and the molecular control of homogeneous catalysis, affording poly(carbonate-*co*-ether)s with a high molecular weight (M_n up to 141 kg/mol). Mechanistic studies reveal a synergistic interplay between Al and Zn active centers, enabling controlled chain propagation and reducing undesired chain termination and side reactions. The resulting terpolymers, containing pendant vinyl groups from AGE, were crosslinked via peroxide curing and reinforced with silica nanoparticles to yield elastomeric nanocomposites. Mechanical testing showed a significant enhancement in tensile strength and elongation at break, particularly at 30 phr silica loading and 10 mol% AGE incorporation. These findings offer a versatile and scalable approach for producing high performance CO_2-based elastomers with potential applications in sustainable materials and carbon capture utilization.

Keywords: CO_2-based polymers, Dual catalysis, High molecular weight, Elastomeric nanocomposites, Silica reinforcement

1. Introduction

With the rapid industrialization and extensive reliance on fossil fuels, atmospheric carbon dioxide (CO_2) levels have continued to rise, becoming a major driver of global warming and ecological imbalance.[31, 158, 206] As a low-cost, nontoxic, and abundant carbon feedstock, CO_2 has gained significant attention in green chemistry and sustainable materials science.[207] In particular, its incorporation into polymerization reactions offers a promising route to high performance functional materials.[167, 208] Among various approaches to prepare CO_2-based polymers, the ring-opening copolymerization of CO_2 with epoxides stands out for its high atom economy and tunable properties.[16, 209] The resulting polymers have potential applications in plastics, thermosets, thermoplastic elastomers, and as polyols for polyurethane production.[17, 26, 152] Importantly, the structure and performance of these CO_2-derived polymers are highly sensitive to the molecular design of the epoxide monomers, which directly influences their thermal, mechanical, and rheological properties.[136]

To develop CO_2-based polymers with elastomeric properties, two key design criteria must be addressed: (i) achieving a glass transition temperature (T_g) below room temperature to ensure flexibility, and (ii) incorporating reactive functionalities to enable crosslinking, which is critical for enhancing mechanical strength and thermal stability.[39, 154, 198] In this study, we employed 1,2-epoxyhexane (HO), which contains a long alkyl side chain that imparts a low T_g and amorphous rubbery behavior. Concurrently, allyl glycidyl ether (AGE) was chosen for its terminal vinyl group, enabling network formation via peroxide induced crosslinking (**Fig. 1a**). The resulting CO_2–AGE–HO terpolymer is thus expected to combine flexibility with crosslinking capability.

A major challenge in synthesizing such functional polycarbonates lies in the catalytic system. Homogeneous catalysts such as salen Co(III) complexes are widely used in AGE/CO_2 copolymerization and show excellent carbonate linkages selectivity (>99%) and living polymerization behavior (PDI < 1.1).[152, 167, 175] They typically produce polymers with low molecular weights (M_n < 35 kg/mol) and show reduced catalytic efficiency when incorporating longer chain monomers like HO, in contrast to shorter chain epoxides such as propylene oxide (PO).[139] Similarly, Al porphyrin complexes demonstrate high selectivity and a turnover

frequency (TOF) of 206 h^{-1} for the copolymerization of CO_2 and HO.[104] In comparison, shorter chain epoxides such as PO and 1,2-butylene oxide (BO) exhibit higher TOFs of 425 and 651 h^{-1}, respectively. These results suggest that increasing the alkyl chain length slightly decreases catalytic activity, although the resulting polymer structure remains well-controlled. Metal free systems such as triethylborane (TEB) can effectively catalyze the copolymerization of CO_2 with various epoxides, including HO and AGE, yielding polymers with M_n of ~40 kg/mol and narrow PDI of ~1.2.[40] Nevertheless, ether containing monomers such as AGE require a high catalyst loading (4 equivalents) and exhibit reduced selectivity, with a polycarbonate content of approximately 81%. This suggests that the steric and electronic effects of bulky or polar side groups may hinder catalytic performance.

These homogeneous systems often require long reaction times (> 12 h) and exhibit limited monomer conversions (< 80%). These systems follow a living polymerization mechanism, and prolonged reaction times could theoretically result in higher molecular weight. Nevertheless, chain degradation often occurs, resulting in the formation of cyclic carbonates and a decrease in molecular weight.[101, 200] These limitations motivate the exploration of alternative catalytic systems. Heterogeneous catalysts, particularly Zn–Co double metal cyanide (Zn–Co DMC) complexes, are attractive for their high activity, stability, and industrial applicability. However, they typically yield poly(carbonate-*co*-ether)s rather than perfectly alternating polycarbonates, and due to multiple active sites,[80] often show broad PDI and long induction periods.[39, 67, 181] In our prior work, we used the Zn–Co DMC catalyst to terpolymerize CO_2 with HO and AGE, confirming these limitations.[198]

Given the strengths and weaknesses of both systems, we developed a hybrid homogeneous–heterogeneous catalytic system by combining Zn–Co DMC complex, Al porphyrin and bis(triphenylphosphine)iminium chloride (PPNCl) serving as co-catalyst (**Fig. 1b**). This multicomponent system leverages the high activity of heterogeneous catalysis along with the precise molecular weight control and carbonate linkage selectivity enabled by homogeneous catalysts. It enables the efficient terpolymerization of CO_2, HO, and AGE under mild conditions, achieving a balance of activity, selectivity, and polymer structure control. After obtaining high molecular weight CO_2-based materials, we turned to enhancing their

mechanical properties for elastomer applications. Pendant ethenyl groups from AGE enable crosslinking through peroxide initiation, forming robust three-dimensional network structures. To further reinforce the resulting elastomers, silica nanoparticles were incorporated as inorganic fillers (**Fig. 1c**), which significantly enhanced their mechanical strength, modulus, and durability, as confirmed by mechanical testing.

In summary, we present a hybrid catalytic strategy for efficient CO_2-based terpolymerization, yielding high molecular weight elastomeric materials. The dual system of Zn–Co DMC and Al porphyrin/PPNCl overcomes limitations of conventional catalysts. Subsequent crosslinking and nanofiller reinforcement produce high performance elastomers, advancing sustainable polymer design and CO_2 utilization.

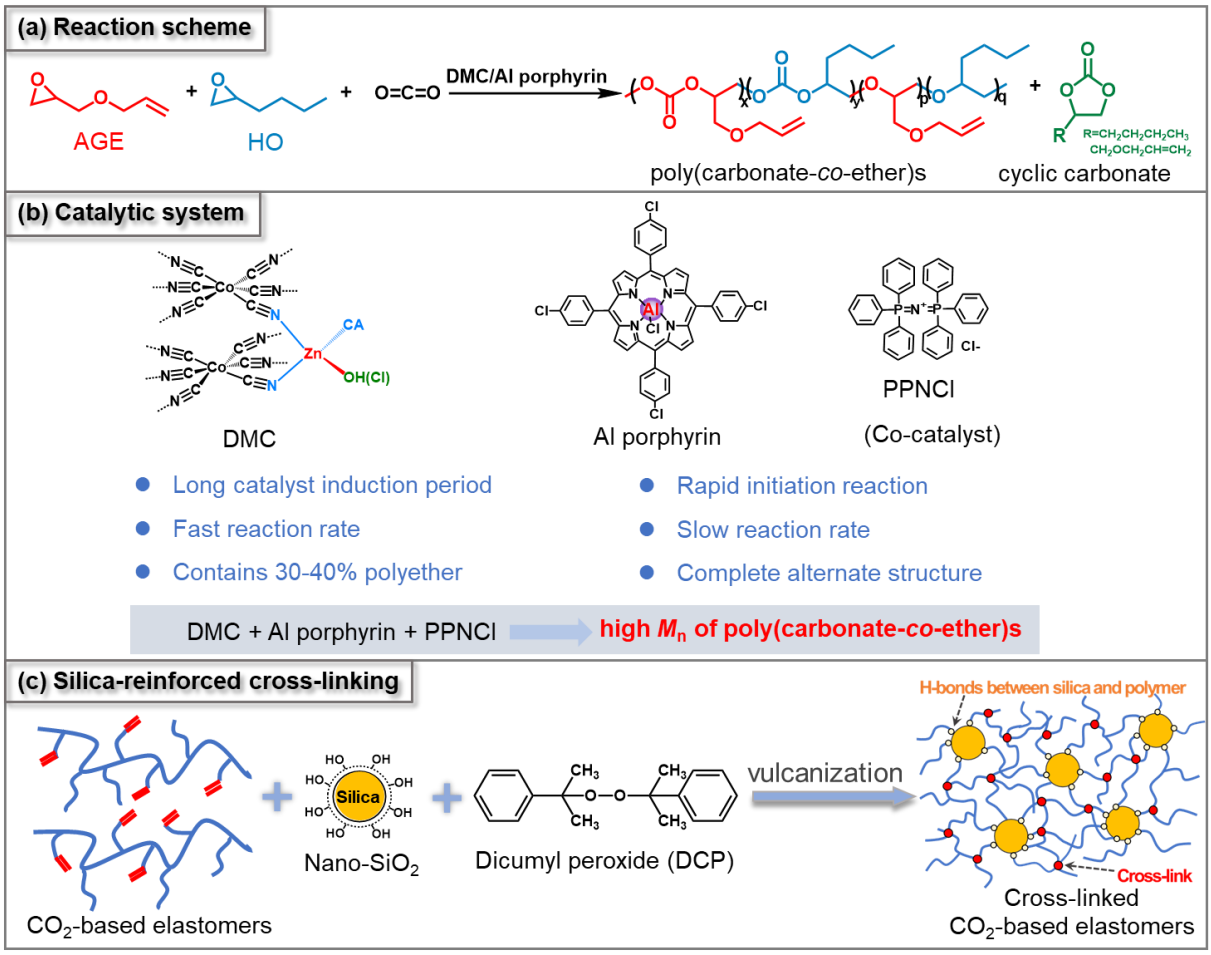

Fig. 1. (a) Terpolymerization of allyl glycidyl ether (AGE), 1,2-hexene oxide (HO), and CO_2 to prepare poly(carbonate-*co*-ether)s. (b) The dual catalytic system employed in this study incorporates Zn–Co DMC and Al porphyrin/PPNCl. (c) Peroxide cross-linking poly(carbonate-*co*-ether)s and nano-silica reinforcement to form Nanocomposites.

2. Experimental section

2.1 Materials

All operations involving air-sensitive and water-sensitive chemicals were conducted in a glove box or using standard Schlenk techniques under dry nitrogen. Allyl glycidyl ether (AGE, 99%), and 1,2-hexene oxide (HO, >96%) were obtained from Aladdin. Dicumyl peroxide (DCP, 98%) was purchased from Alfa Aesar. Silicon dioxide (SiO_2, specific surface area = 200 m^2/g, primary particle size = 12 nm) was obtained from Degussa AG, Germany. All epoxides were dried by stirring over calcium hydride (CaH_2) for 24 hours and then distilled under reduced pressure. Carbon dioxide gas (99.999%) was received and used without further purification. Zinc-cobalt(III) double metal cyanide complex (Zn–Co DMC) was synthesized according to the method reported in the literature.[80] Aluminum porphyrin complex was synthesized according to the method reported in the literature.[156, 157] Bis(triphenylphosphoranylidene)ammonium chloride (PPNCl, >96%, Aladdin) was recrystallized from dry dichloromethane and diethyl ether under a nitrogen atmosphere before use.

2.2 Terpolymerization of CO_2 with epoxides

To prevent moisture from affecting the catalyst, epoxides and the catalyst were placed into a pre-dried 10 mL high-pressure reactor inside a glove box. The reactor was subsequently heated and brought to the desired temperature and CO_2 pressure. After the specified reaction duration, it was cooled using an ice water bath, followed by a slow release of CO_2 pressure. A portion of the crude product was collected for monomer conversion, carbonate moiety , and cyclic carbonate quantification via ^1H NMR spectroscopy. Another portion was taken for molecular weight (M_n) and polydispersity index (PDI) analysis using gel permeation chromatography (GPC). The remaining product was dissolved in dichloromethane, then precipitated using excess methanol to eliminate residual monomers and small molecule by-products. The resulting polymer was collected and dried under vacuum at 40 °C for 48 hours. A small fraction of the purified polymer was analyzed for glass transition temperature (T_g) and using differential scanning calorimeter (DSC).

2.3 Preparation of cross-linked CO_2-AGE-HO/silica composites

First, CO_2–AGE–HO elastomer (100 phr), dicumyl peroxide (DCP, 0.05 phr), and an appropriate amount of silica were sequentially added into a Haake internal mixer at room temperature and 60 rpm for 10 min to obtain a well mixed rubber compound. The obtained compound was then left to rest for 12 h before being transferred to a plate vulcanizer, where it was cured at 160 °C and 15 MPa for 30 min. The vulcanized sample was then aged for an additional 12 h before being subjected to tensile testing and dynamic mechanical analysis (DMA).

2.4 Characterization

2.4.1 Characterization of product structure

The compositions of product obtained from the terpolymerization were analyzed using ^{1}H NMR spectroscopy on a Bruker AV600 instrument. Deuterated chloroform ($CDCl_3$) served as the solvent, and tetramethylsilane (TMS) was used as the internal standard. To further characterize the compositions, polymer selectivity and carbonate moiety selectivity were defined as follows:

Polymer selectivity (%) = (moles of polymer in the product) / (total moles of polymer and cyclic carbonate in the product) × 100;

Carbonate linkage selectivity (%) = (moles of specific carbonate linkage in the copolymer) / (total moles of carbonate and ether linkage in the copolymer) × 100.

The detailed calculation procedures are provided in the section of **Chapter 3**.

2.4.2 Characterization of molecular weights

The number-average molecular weight (M_n) and polydispersity index (PDI) were measured using gel permeation chromatography (GPC) on a Waters 515 system. The instrument was equipped with a set of Waters Styragel columns, specifically HT3, HT5, and HT6 series, while tetrahydrofuran (THF) served as the eluent. The eluent was pumped at a constant flow rate of 1.0 mL min^{-1}. Calibration was carried out with monodisperse polystyrene standards covering a molecular weight range from 1620 to 8500 kDa.

2.4.3 Characterization of glass transition temperature

Glass transition temperatures were determined using differential scanning calorimetry (DSC). The DSC analysis was conducted in a nitrogen environment with a Mettler Toledo DSC instrument. Initially, the sample was heated at a rate of 10 °C min^{-1} to 100 °C and maintained at this temperature for 5 min. Following this, it was cooled to –100 °C at the same rate before being reheated to 100 °C under identical conditions.

2.4.4 Characterization of microstructure

The dispersions of silica in the CO_2–AGE–HO/silica composites were examined using a transmission electron microscope (TEM, FEI Tecnai G2 20 S Twin). To prepare TEM samples, ultrathin sections of the silica-filled CO_2–AGE–HO matrix were obtained through cryo-ultramicrotomy with a Reichert-Jung Ultracut instrument. These sections were then placed onto copper grids for further microscopic examination.

2.4.5 Characterization of rheological and viscoelastic properties

Dynamic mechanical analysis (DMA) in tensile mode was conducted using a TA Q800 instrument (TA Instruments Co., USA). The test was performed with a fixed initial strain of 0.1% and a constant frequency of 10 Hz. The temperature was progressively raised from –50 °C to 80 °C at a heating rate of 3 °C/min to generate the corresponding DMA curve.

2.4.6 Characterization of viscoelasticity and filler-rubber interactions

Rubber process analyzer (RPA) measurements were performed on an RPA 2000 instrument (Alpha Technologies Co., USA). For the unvulcanized compounds, the testing conditions were set as follows: frequency (f) = 1 Hz, temperature (T) = 60 °C, and strain swept from 0.28% to 200%. Afterward, the same samples were in-situ vulcanized based on the vulcanization parameters previously obtained from a rheometer. The vulcanized compounds were then tested under the following conditions: f = 10 Hz, T = 60 °C, and strain swept from 0.28% to 42%.

2.4.7 Characterization of mechanical properties

Tensile strength and elongation at break were assessed using a computer-controlled universal testing machine (Zwick/Roell, Txet-port II, Germany) under a test speed of 50 mm/min at 25 °C. The specimens, prepared following ISO 37:2005 guidelines, featured a

narrow, parallel-sided section measuring 20 mm in length and 4 mm in width. Each sample's mechanical properties were analyzed based on three replicate measurements.

3. Results

3.1 Effect of catalyst composition on polymerization performance

To evaluate the impact of the combinatory approach, the terpolymerization of CO_2, AGE, and HO was carried out using both single and dual catalysts under the same conditions (**Table 1**). The ^{1}H NMR spectra of product were shown in **Fig. 2**. The product structure depends significantly on the catalyst used DMC catalysis yielded 97% poly(carbonate-*co*-ether) copolymer and 3% cyclic carbonates, with carbonate linkages constituting 54% of the copolymer backbone. The Al porphyrin/PPNCl catalytic system produced a mixture of 95% polycarbonate and 5% cyclic carbonate. The polymer backbone consisted exclusively of carbonate linkages, indicating the complete absence of ether segments. The combination of Zn–Co DMC and Al porphyrin/PPNCl catalysts yielded 92% poly(carbonate-co-ether) and 8% cyclic carbonate, with 79% carbonate linkages in the copolymer backbone.

Table 1. Catalytic performance and polymerization data for CO_2/AGE/HO terpolymerization[a].

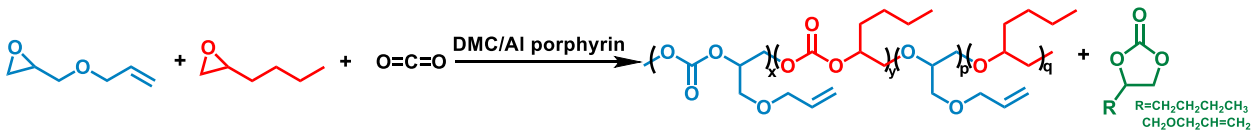

Entry	DMC [mg]	Al porphyrin [mg]	PPNCl [mg]	Conv.[b] [%] AGE	HO	Polymer[c] [%]	Carbonate linkage[d] [%]	M_n[e] [kg/mol]	PDI[e]	T_g[f] [°C]
1	5.0	0	0	99	99	97	54	45	2.65	-17
2	0	16.9	11.9	27	37	95	100	20	1.24	-6
3	2.5	8.4	6.0	95	93	92	79	113	2.42	-14
4	2.5	8.4	0	-	-	-	-	-	-	-
5	2.5	0	6.0	-	-	-	-	-	-	-

[a]Reaction conditions: epoxides, 5.0 mL (AGE/HO molar ratio = 20/80), 60 °C, 4 MPa CO_2. [b]Calculated by ^{1}H NMR of the crude products. [c]Polymer selectivity defined as the molar percentage of the polymer in the crude product determined by ^{1}H NMR. [d]Carbonate linkage selectivity defined as the molar percentage of carbonate linkage in the polymer determined by ^{1}H NMR. [e]Determined by gel permeation chromatography (GPC) in THF using polystyrene as the standard. [f]Determined by DSC. "-" meant "no product was obtained".

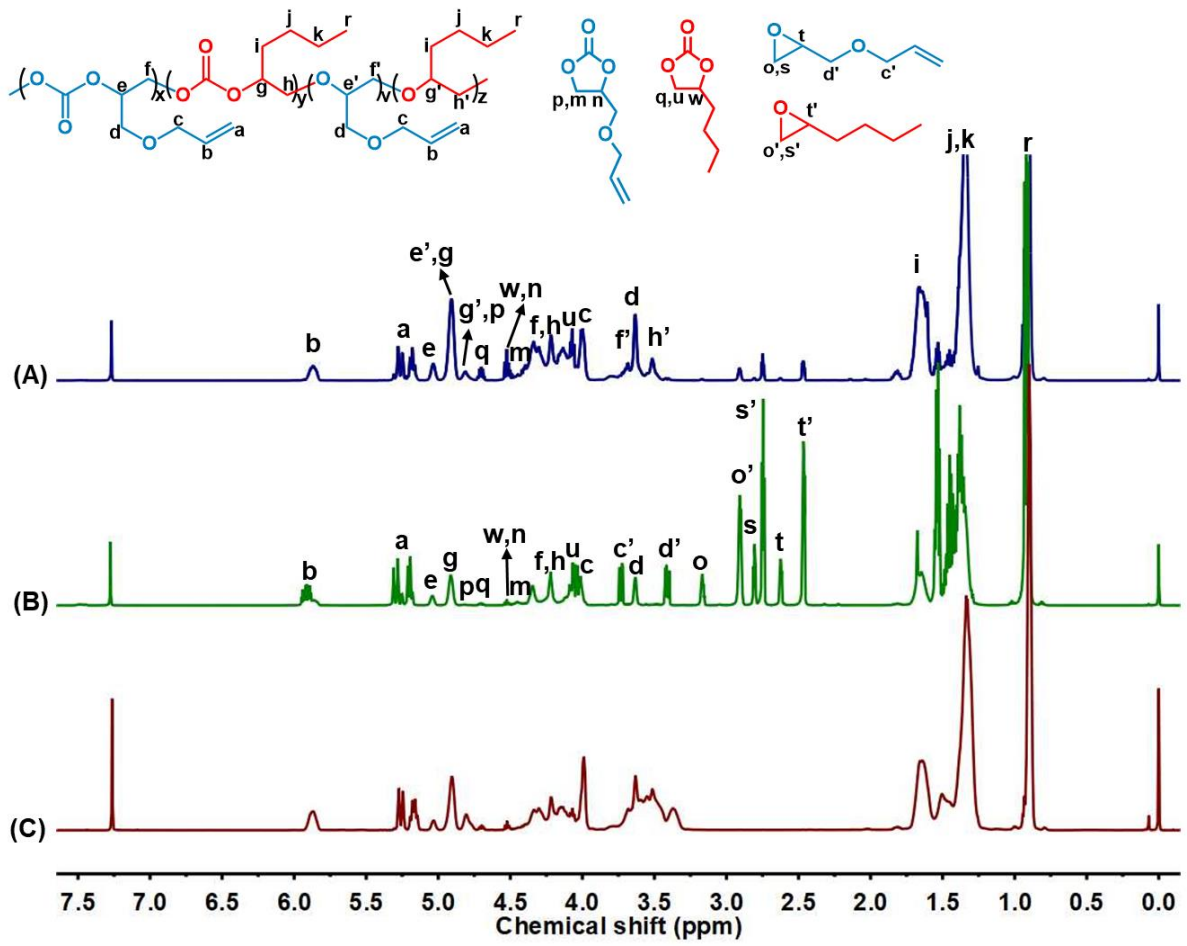

Fig. 2. ^{1}H NMR spectra of crude product obtained from the terpolymerization of CO_2–AGE–HO in three different catalytic systems: (A) a dual-catalyst system combining Zn–Co DMC and Al porphyrin/PPNCl, (B) Al porphyrin/PPNCl, and (C) Zn–Co DMC.

As shown in **Fig. 3**, the M_n and PDI also varied with the catalyst. The polymer catalyzed by Zn–Co DMC exhibited a relatively low M_n with a broader PDI. The polymer obtained using Al porphyrin/PPNCl as the catalyst had an even lower M_n, and its GPC curve displayed a bimodal distribution. This bimodal molecular weight distribution likely resulted from chain transfer to trace water, leading to the formation of polymer chains with two distinct M_ns.[157, 210] When Zn–Co DMC and Al/PPNCl were used together, the resulting polymer had the highest M_n, and its GPC curve showed a trimodal distribution. This suggested that the synergistic effect of the two catalysts may have contributed to the increased M_n. As summarized in **Table 1**, the dual catalyst (Zn–Co DMC + Al porphyrin/PPNCl) produced CO_2–AGE–HO with a M_n of 113 kg/mol, significantly higher than when using a single catalyst. Specifically,

the resulting poly(carbonate-*co*-ether) exhibited a M_n increase of 151% and 465% compared to polymerization catalyzed individually by Zn–Co DMC (45 kg/mol) and Al porphyrin/PPNCl (20 kg/mol), respectively. Furthermore, in Entries 4 and 5, which either Al porphyrin or PPNCl was omitted, no product was formed. This indicated that both components were essential for catalytic activity. These results highlight the strong synergistic effect between Zn–Co DMC and the Al porphyrin/PPNCl catalyst, both of which are indispensable for polymer formation.

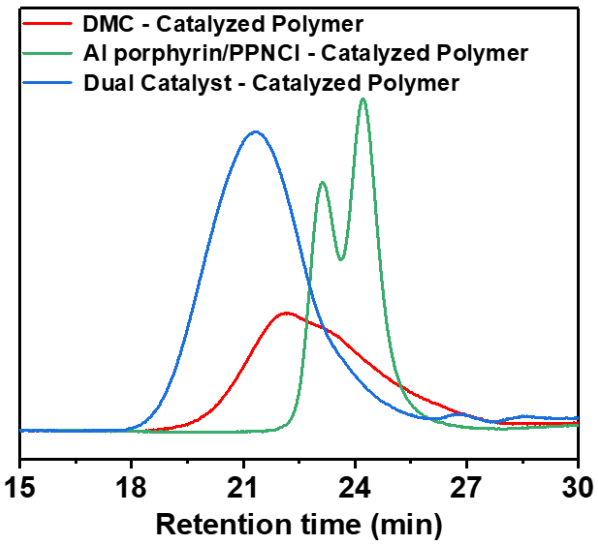

Fig. 3. GPC curves of the copolymers obtained from the terpolymerization of CO_2–AGE–HO using various catalysts.

3.2 Kinetics of CO_2-based terpolymerization under dual catalysis

To elucidate the reaction mechanism of the dual catalyst, the apparent reaction kinetics were studied (**Fig. 4**). At the early stage of the reaction (1.5 h), polymer selectivity was relatively low at 57%, with nearly half of the product consisting of cyclic carbonates (**Table 2**, entry 1). As a result, the polymer had a low M_n (2 kg/mol) and a narrow PDI (1.34). The polymer contained 100% carbonate linkages without ether linkages, and the GPC curve exhibited a bimodal distribution. These observations suggested that polymerization was initiated and propagated solely by Al porphyrin/PPNCl, while Zn–Co DMC had not yet participated in chain propagation.

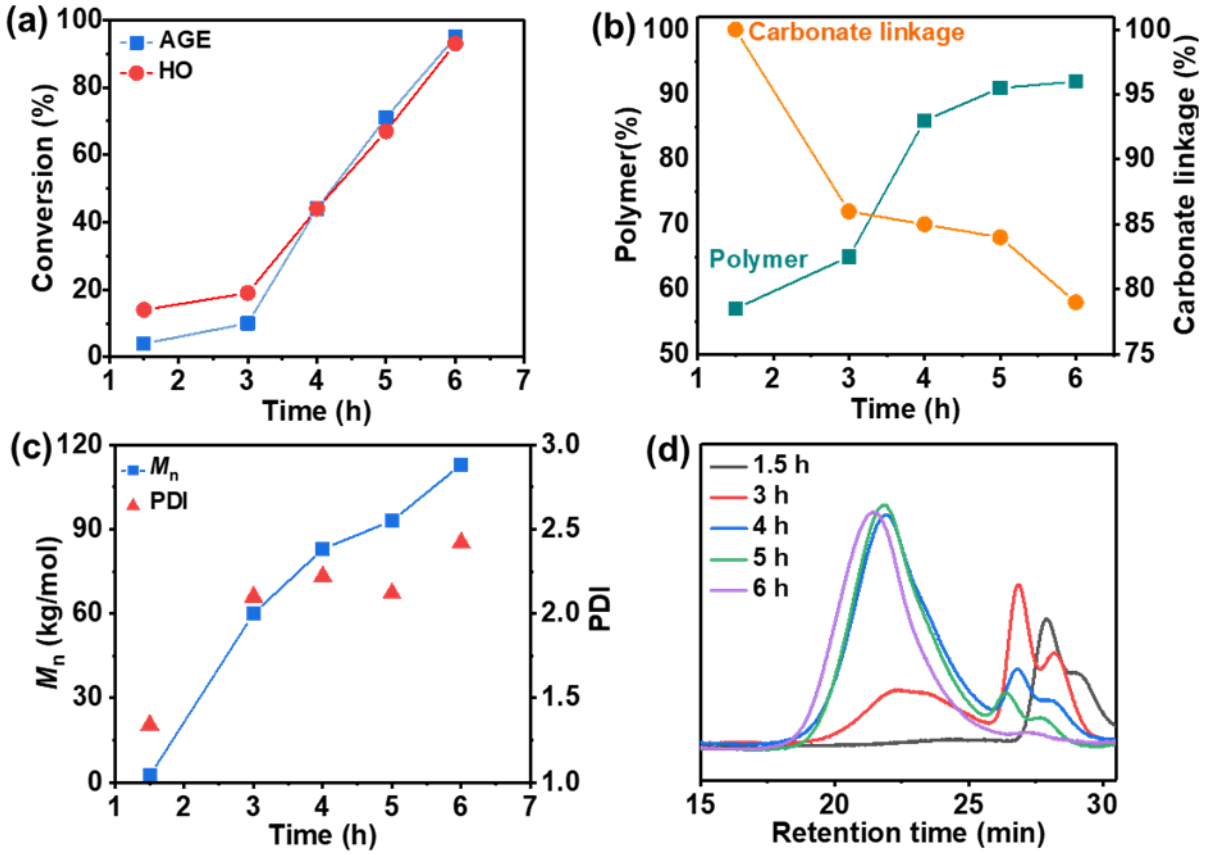

Fig. 4. Monitoring terpolymerizations of CO_2, AGE, and HO. (a) Plots of conversions of AGE and HO versus time. (b) Plots of polymer and carbonate linkage selectivity versus time. (c) Plots of M_n and PDI versus time. (d) GPC traces of terpolymers with different reaction time.

Table 2. Kinetics of the terpolymerization of CO_2, AGE and HO catalyzed by the dual catalyst system[a].

Entry	Time [h]	Conversion[b] [%] AGE	HO	Polymer[c] [%]	Carbonate linkages[d] [%]	M_{n1}[e] [kg/mol]	PDI_1[e]	$Area_1$ [%]	M_{n2}[e] [kg/mol]	PDI_2[e]	$Area_2$ [%]
1	1.5	4	14	57	100	2	1.34	100	-	-	-
2	3	10	19	65	86	60	2.10	43	5.3	1.33	57
3	4	44	44	86	85	83	2.22	85	5.2	1.32	15
4	5	71	67	91	84	92	2.12	89	6.6	1.29	11
5	6	95	93	92	79	113	2.42	98	4.8	1.18	2

[a]Reaction conditions: Zn–Co DMC, 2.5 mg; Al porphyrin, 8.4 mg; PPNCl, 6.0mg; epoxides, 5.0 mL (AGE/HO molar ratio = 20/80); 60 °C; 4 MPa CO_2. [b]Calculated by ^{1}H NMR of the crude products. [c]Polymer selectivity defined as the molar percentage of the polymer in the crude product determined by ^{1}H NMR. [d]Carbonate linkage selectivity defined as the molar percentage of carbonate linkage in the polymer determined by ^{1}H NMR. [e]Determined by gel permeation chromatography (GPC) in THF using polystyrene as the standard.

When the reaction time reached 3 h, polymer selectivity had increased to 65%, with carbonate and ether linkages at 86% and 14%, respectively (**Table 2**, entry 2). The polymer consisted of both high and low molecular weight fractions. The high molecular weight (M_{n1}) fraction reached 60 kg/mol, with a broader PDI of 2.10, accounting for 43% of the total area in the GPC curve. The GPC curve shifted from a bimodal to a trimodal distribution, indicating that at this stage, DMC had started cooperating with Al porphyrin/PPNCl in chain propagation. As the reaction progressed, monomer conversion increased, polymer selectivity improved, carbonate content decreased, and M_n steadily increased.

After 6 h, monomer conversion had exceeded 90%, and polymer selectivity had reached 92%, with 79% carbonate linkages (**Table 2**, entry 5). The high M_n fraction accounted for 98%, and the M_{n1} had increased to 113 kg/mol, a value significantly exceeding the 45 kg/mol achieved with DMC alone and the 20 kg/mol obtained using Al porphyrin /PPNCl alone. (**Table 1**, entry 1 and entry 2). These results indicated that the cooperative catalysis of Zn–Co DMC, Al porphyrin, and PPNCl facilitated the formation of high molecular weight polymers.

3.3 Proposed mechanism of the terpolymerization catalyzed by the dual catalysis

Although the exact nature of the active species in the heterogeneous Zn–Co DMC catalyst remains elusive, we propose a plausible dual metal cooperative mechanism involving both an aluminum complex and a zinc species to account for the observed polymerization behavior (**Fig. 5**). Due to the long induction period of DMC (> 3 h), polymerization is initially dominated by the Al porphyrin/PPNCl complex. In the proposed mechanism, Al porphyrin/PPNCl complex first induces epoxide ring opening and promotes alternating insertion of epoxide and CO_2, resulting in chain propagation and the formation of Al-coordinated carbonate anion chain ends (**Fig. 5**, Chain initiation, Step 1). Those anionic species may subsequently nucleophilically attack epoxide coordinated to Zn–OH, thereby activating the DMC catalyst and transferring the growing polymer chain from the Al center to the Zn center (**Fig. 5**, Chain initiation, Step 2).[155, 211] As a result, Zn-alkoxide chains are formed, and the Al porphyrin/PPNCl complexes are regenerated, enabling them to continue alternating insertion of epoxide and CO_2.

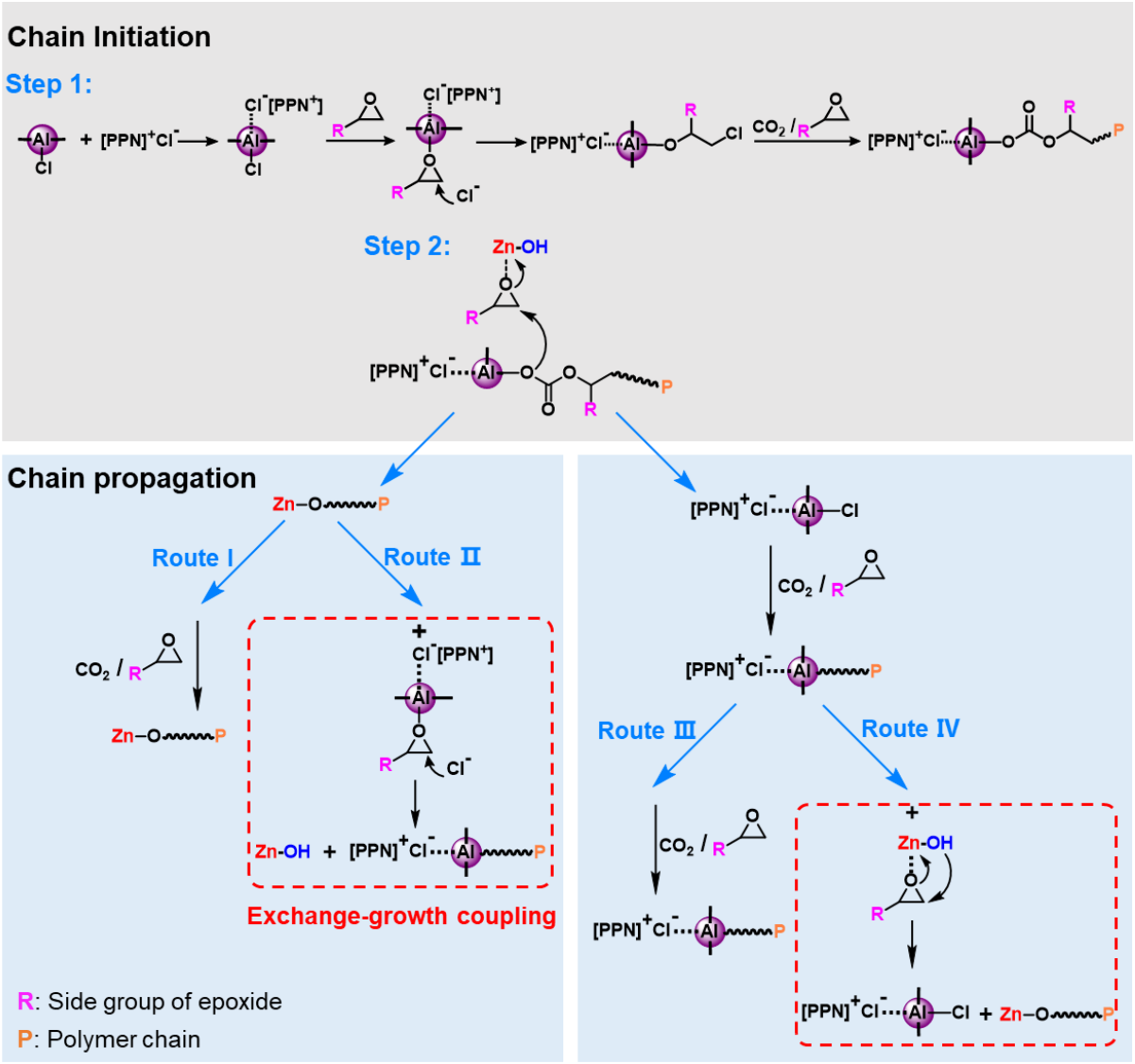

Fig. 5. Proposed mechanistic pathways for the terpolymerization of CO_2 and epoxides catalyzed cooperatively by Al porphyrin/PPNCl and Zn–Co DMC.

Once the Zn–alkoxide active chain is formed, the polymerization may proceed through four distinct pathways, illustrating the dynamic interplay between the Zn center and the Al porphyrin/PPNCl complex (**Fig. 5**). In Route I, the Zn–alkoxide species directly promote chain propagation via the random insertion of epoxide and CO_2, consistent with classical Zn–Co DMC-type catalysis. In Route II, the Zn–alkoxide chain nucleophilically attacks an epoxide that is pre-coordinated to the Al porphyrin/PPNCl complex, resulting in chain transfer back to the Al center where propagation continues.[182, 212] This pathway highlights the dual catalytic

character of the system and demonstrates an exchange-growth coupling process between the two metal centers.

Route III involves continued chain propagation from the regenerated Al porphyrin/PPNCl complex following the second step of chain initiation, suggesting that the Al catalyst can continue participation in the propagation cycle after initial chain formation. Route IV is similar to Route II in involving the chain transfer, but is characterized by initial chain formation at the Al center, followed by transfer to the Zn center for continued propagation. This bidirectional transfer mechanism forms the foundation of a highly coordinated and synergistic catalytic system involving both Al and Zn centers. This mechanistic foundation directly translates into key advantages in chain propagation control and polymer performance.

The ability of the polymer chain to reversibly migrate between two distinct catalytic centers effectively reduces undesired chain termination and minimizes backbiting reactions, thereby enabling prolonged chain propagation.[213] Furthermore, the synergistic effect between Zn–Co DMC and Al porphyrin, aided by the presence of PPNCl, enhances epoxide activation and promotes efficient chain transfer. These factors collectively contribute to the formation of high molecular weight poly(carbonate-co-ether)s and highlight the superior performance of the dual catalyst system.

3.4 Preparation of CO_2–AGE–HO/Si nanocomposites

To investigate the potential of poly(carbonate-*co*-ether) in elastomer applications, silica was employed as a nanofiller to enhance its mechanical strength and dimensional stability, aiming to develop sustainable and high performance elastomeric composites. As shown in **Fig. 6**, the CO_2–AGE–HO terpolymer serves as the elastomeric matrix, while silica nanoparticles act as reinforcing agents. Dicumyl peroxide (DCP) facilitates the crosslinking of polymer chains during vulcanization, forming a robust network reinforced by hydrogen bonding interactions with silica. Accordingly, varying amounts of silica (10 phr, 20 phr, 30 phr, 40 phr, 50 phr, respectively) were incorporated into the polymer matrix to systematically investigate the effect of filler content on the composite's mechanical and thermal properties.

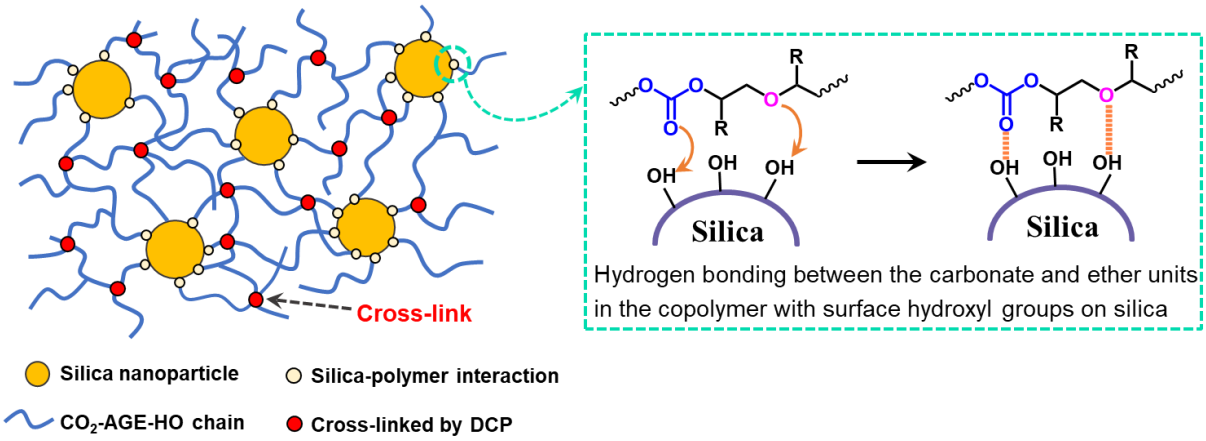

Fig. 6. Microstructure of the cross-linked, silica-reinforced poly(carbonate-*co*-ether) elastomer

3.4.1 Effect of SiO_2 content on the temperature-dependent viscoelastic properties of CO_2–AGE–HO/Si nanocomposites

The viscoelastic behavior of the CO_2–AGE–HO/Si nanocomposites were evaluated by dynamic mechanical analysis (DMA). With increasing SiO_2 content, G' increased significantly (**Fig. 7a**), indicating the formation of a stronger filler–rubber network that improved the composites' resistance to deformation. This behavior was further supported by the enhanced dispersion of SiO_2 and stronger filler–polymer interfacial interactions, which restricted the mobility of CO_2–AGE–HO chains.[214, 215] As a result, energy dissipation decreased while energy storage capability increased, leading to an overall reduction in the tanδ with increasing SiO_2 loading.

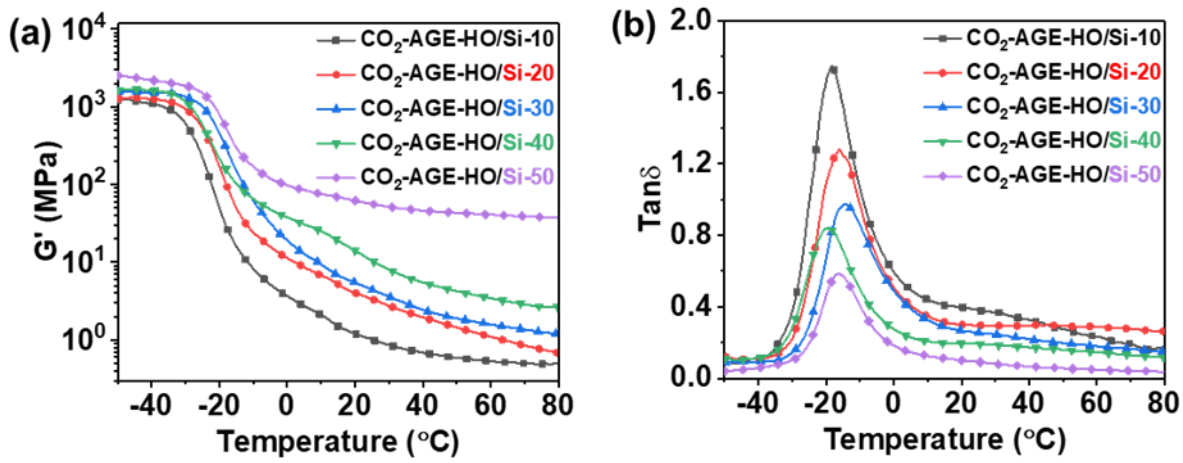

Fig. 7. (a) storage modulus (G') and (b) loss tangent (tanδ) versus temperature of vulcanized CO_2–AGE–HO/Si nanocomposites with varying silica contents.

As for the T_g corresponding to the tanδ peak, it exhibited a trend of first increasing and then decreasing with increasing SiO_2 content (**Fig. 7b**). Specifically, when the SiO_2 loading was below 30 phr, enhanced interfacial interactions restricted segmental motion of polymer chains, resulting in T_g elevation. However, at loadings above 30 phr, filler aggregation (**Fig. 8**) reduced the effective interfacial area and weakened the constraining effect, thereby facilitating chain mobility and leading to a decrease in T_g.

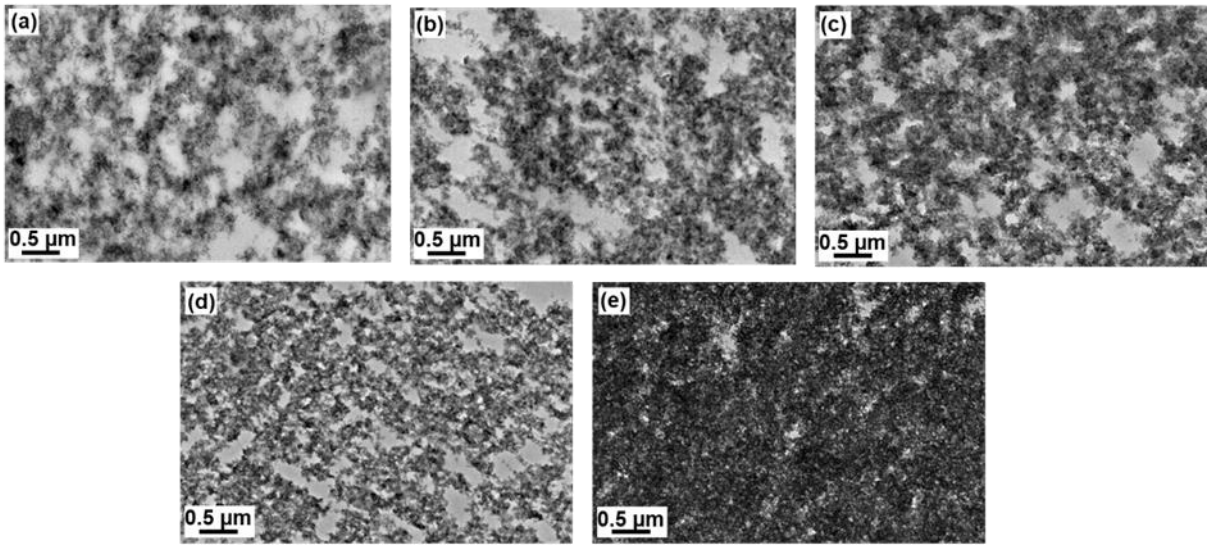

Fig. 8. TEM images of AGE-HO-CO_2/Si nanocomposites with varying silica contents. (a) CO_2–AGE–HO/Si–10, (b) CO_2–AGE–HO/Si–20, (c) CO_2–AGE–HO/Si–30, (d) CO_2–AGE–HO/Si–40, (e) CO_2–AGE–HO/Si–50.

3.4.2 Effect of SiO_2 content on the strain-dependent filler network behavior of CO_2–AGE–HO/Si nanocomposites

The evolution of the filler network strength and filler–polymer interactions in the SiO_2-filled elastomer was investigated using a Rubber Process Analyzer (RPA). In the small strain region, the storage modulus (G') increased significantly with higher SiO_2 content (**Fig. 9a**), indicating the formation of a stronger filler network structure.[216, 217] While as the strain increased, particularly in in high filler content (e.g., CO_2–AGE–HO/Si–50), G' dropped sharply due to the breakdown of weak filler–filler interactions, demonstrating a typical Payne effect.[218]

After vulcanization (**Fig. 9b**), the variation of tanδ with strain changed significantly. At low strains, samples with higher filler loadings showed lower tan δ values, indicating reduced energy dissipation due to restricted chain mobility in the denser filler network.[219] As the strain increased, tan δ rose sharply, particularly in highly filled samples. This was attributed to filler network disruption and increased polymer chain mobility.

These results suggested that while increasing filler content enhances the initial stiffness of the nanocomposites, it also makes them more sensitive to large deformations. Under high strain, the filler–filler network breaks down, leading to slippage and friction between particles. Additionally, relatively weak filler–matrix interfacial interactions promote interfacial slippage, further intensifying energy dissipation. Consequently, nanocomposites with high filler contents exhibit elevated tan δ values in the high strain region.

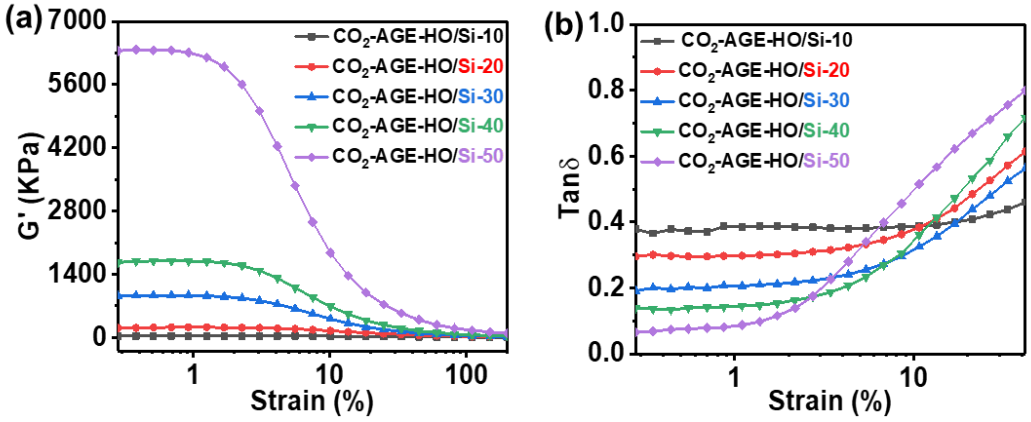

Fig. 9. Strain amplitude dependence of (a) storage modulus (G') of unvulcanized CO_2–AGE–HO/Si nanocomposites, (b) loss tangent (tanδ) of vulcanized CO_2–AGE–HO/Si nanocomposites with varying silica contents.

3.4.3 Effect of SiO_2 content on the stress–strain behavior of CO_2–AGE–HO/Si nanocomposites

The stress–strain curves of the CO_2–AGE–HO/Si nanocomposites with varing SiO_2 contents were presented in **Fig. 10**. The incorporation of SiO_2 significantly enhanced the mechanical properties of the CO_2–AGE–HO matrix. For instance, the tensile strength of the CO_2–AGE–HO/Si–30 nanocomposite reached 5.5 MPa, which is 7.9 times higher than that of the unfilled sample. As the SiO_2 content increased, the tensile strength and elongation at break

of the nanocomposites first increased and then decreased, with optimal values observed at 30 phr. This behavior is attributed to the formation of a well-developed filler network that enhanced stress transfer efficiency and crack resistance by restricting rubber chain mobility. However, when the SiO_2 content exceeded 30 phr, filler aggregation and matrix discontinuities led to stress concentration, which diminished both the load-bearing capacity and deformability of the composites. Yielding behavior became more evident under strain, further compromising mechanical performance. Therefore, a SiO_2 loading of 30 phr is identified as the optimal filler content for achieving balanced strength and flexibility in the nanocomposite system.

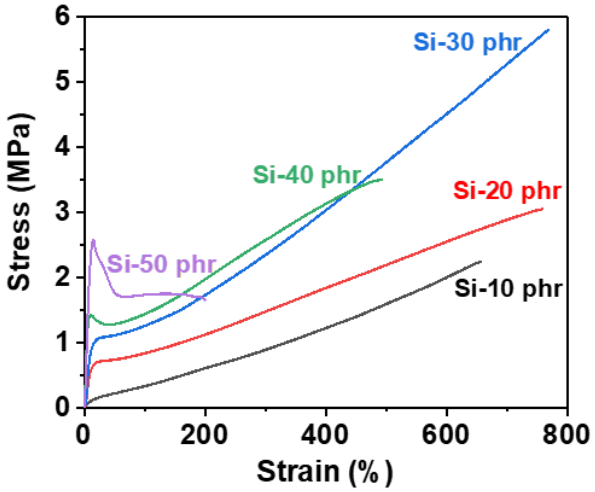

Fig. 10. Mechanical properties of CO_2–AGE–HO/Si nanocomposites with varying silica contents.

3.4.4 Effect of AGE/HO molar ratios on the mechanical properties of CO_2–AGE–HO/Si–30 nanocomposites

In order to regulate the mechanical behavior of the elastomer, a series of terpolymerizations was carried out by tuning the molar ratio of AGE to HO, aiming to introduce 5, 10, and 15 mol% of double bonds into the resulting polymers. As shown in **Table 3**, varying the AGE to HO ratio had negligible effects on both the carbonate linkage selectivity and the M_n. Moreover, the T_g was significantly influenced by the incorporation of AGE. The reduction in T_g with higher AGE content is likely attributed to the enhanced chain mobility introduced by the flexible ether functionalities in the AGE side chains. Based on the synthesized polymers, 30 phr of SiO_2 was incorporated as a reinforcing filler, and DCP was added to initiate crosslinking. The resulting

nanocomposites were then subjected to mechanical property testing. As shown in **Fig. 11**, the nanocomposites containing 10 mol% AGE exhibited the highest tensile strength (5.5 ± 0.3 MPa) and elongation at break (748 ± 19%). Compared with the CO_2-AGE-HO terpolymer of the same AGE content but without silica, these values were improved by 686% and 298%, respectively.

Table 3. Molecular characteristics and mechanical properties of CO_2-AGE-HO terpolymers and mechanical properties of CO_2–AGE–HO/Si–30 nanocomposites[a].

Entry	AGE[b] [mol%l]	Carbonate linkage[c] [%]	M_n[d] [kg/mol]	PDI[d]	T_g[e] [°C]	σ[f] [MPa]	ε[g] [%]
1	5	90	141	2.26	-11	2.4 ± 0.4	650 ± 42
2	10	87	134	2.24	-14	5.5 ± 0.3	748 ± 19
3	15	84	127	2.40	-15	5.0 ± 0.3	568 ± 38
4*	10	87	134	2.24	-14	0.7 ± 0	188 ± 5

[a]Reaction conditions: DMC (3.1 mg); Al porphyrin (10.5 mg); PPNCl (7.5 mg); total monomer (25 mL); 60 °C; 4 MPa CO_2. [b]The mole percentage of AGE monomer in the total monomer mixture. [c]Carbonate linkage selectivity defined as the molar percentage of carbonate linkage in the polymer determined by ^{1}H NMR. [d]Determined by gel permeation chromatography (GPC) in THF using polystyrene as the standard. [e]Determined by DSC. [f]Maximum stress of a stress-strain curve. [g]Strain at break. Strain rate = 50 mm/min, testing temperature = 25 °C. All mechanical properties were determined from three replicates for each sample. *Unfilled silica.

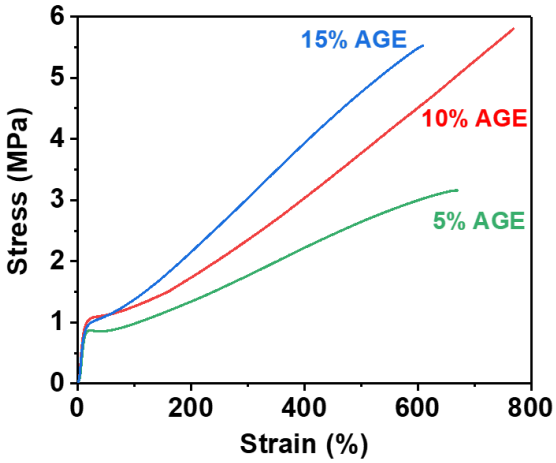

Fig. 11. Tensile stress-strain curves of the CO_2–AGE–HO/Si–30 nanocomposites with various AGE.

4. Conclusion

In this study, we developed a hybrid homogeneous–heterogeneous catalytic system by integrating Zn–Co DMC and Al porphyrin/PPNCl complexes to achieve the efficient terpolymerization of CO_2, HO, and AGE. This dual catalytic strategy successfully overcomes the limitations of traditional systems by enabling high monomer conversion, improved polymer selectivity, and significantly increased molecular weights. Detailed mechanistic investigations demonstrated a cooperative interaction between the Al and Zn catalytic centers, facilitating dynamic chain transfer and promoting sustained chain propagation. The incorporation of pendant allyl groups enabled peroxide induced crosslinking, and the addition of silica nanofillers further enhanced mechanical performance. Notably, the nanocomposites containing 30 phr silica and 10 mol% AGE exhibited the best balance of tensile strength and flexibility. This work provides a robust framework for the design of CO_2-based elastomers with tunable properties and demonstrates the feasibility of using a hybrid catalytic system to tailor polymer structure and function. The results provide a foundation for future advances in sustainable polymer chemistry and the utilization of carbon dioxide into functional, high performance materials.

Chapter 7 General conclusions and perspectives

7.1 General conclusions

This thesis presents a systematic investigation into the design, synthesis, and performance tuning of CO_2-based elastomers through the terpolymerization of CO_2 with functional and aliphatic epoxides. Three distinct catalytic strategies were developed and compared, aiming to improve polymer selectivity, molecular weight, and elastomeric properties, as well as to provide insights into the catalytic mechanisms and structure–property relationships. From these studies, the following conclusions emerge:

(1) A zinc–cobalt(III) double metal cyanide (Zn–Co DMC) catalyst was employed to develop a one-pot strategy for preparing poly(carbonate-co-ether)s via terpolymerization of CO_2, allyl glycidyl ether (AGE), and long-chain saturated epoxides. By varying the monomer composition, especially the content of AGE and the length of the alkyl chain, the T_g of the resulting polymers was tuned over a broad range (−25 °C to +5 °C). The presence of allyl groups allowed for post-crosslinking, which enhanced tensile strength but reduced elongation at break, depending on crosslinking density. These findings demonstrate a versatile approach to preparing CO_2-based elastomers with controllable physical properties through molecular level design.

(2) Solvent polarity was shown to have a decisive impact: polar solvents such as THF promoted Al–O bond cleavage and backbiting reactions, leading to lower molecular weights and more cyclic byproducts. In contrast, low polarity solvents like cyclohexane enhanced catalyst stability and polycarbonate selectivity. Bulk polymerization, which eliminates solvent effects, further improved molecular weight and selectivity, although high viscosity at high conversion slowed reaction rates. The reaction followed first-order kinetics with respect to monomer concentration, and temperature was found to be a critical variable in balancing conversion, selectivity, and side reactions. These insights offer valuable guidance for optimizing reaction conditions in CO_2 polymerization systems.

(3) A dual catalytic system was developed by combining Zn-Co DMC with Al porphyrin/PPNCl. This hybrid approach successfully integrated the advantages of both heterogeneous and homogeneous catalysis, resulting in poly(carbonate-co-ether)s with high molecular weights (M_n up to 141 kg/mol). Mechanistic analysis revealed a synergistic cooperation between the Zn and Al centers, facilitating dynamic chain transfer and sustained propagation. The terpolymers containing pendant allyl groups were successfully crosslinked via peroxide treatment. Moreover, the incorporation of silica nanoparticles yielded nanocomposites with significantly enhanced mechanical performance. The formulation containing 30 phr silica and 10 mol% AGE achieved the best balance of tensile strength and flexibility, demonstrating the potential of this system in advanced elastomeric materials.

In summary, this work establishes a scalable and tunable strategy for the synthesis of high performance CO_2-based elastomers through rational catalyst design, kinetic control, and composite engineering. It provides both theoretical understanding and practical guidance for developing sustainable polymeric materials from carbon dioxide

7.2 Innovations

This thesis contributes several significant innovations to the field of sustainable polymer chemistry. A one-pot terpolymerization method was developed to efficiently synthesize crosslinkable, high-molecular-weight CO_2-based poly(carbonate-co-ether)s. The effects of catalyst type and polymerization method were systematically investigated, with particular emphasis on the role of solvent polarity in solution polymerization. These studies provided mechanistic insights into catalyst behavior and reaction pathways, enabling the rational optimization of reaction conditions. A synergistic dual catalytic system was designed by integrating homogeneous and heterogeneous catalysts, which successfully overcame the limitations of each individual system and allowed for the selective synthesis of ultrahigh-molecular-weight polymers. Finally, the resulting copolymers were used to fabricate elastomeric nanocomposites with enhanced mechanical performance. Together, these

innovations collectively establish a scalable and practical method for producing high performance elastomers from CO_2, and emphasize the critical role of catalytic design and process engineering in advancing sustainable polymer chemistry.

7.3 Perspectives

Building on the foundation established in this thesis, several promising directions can be envisioned for future research in the field of CO_2-based elastomers and their nanocomposites:

(1) Catalyst development and mechanistic elucidation. Although the Zn-Co DMC and aluminum porphyrin systems exhibited high activity and selectivity, further improvement in catalyst efficiency, monomer compatibility, and process robustness are still desirable. The design of multinuclear catalysts with switchable coordination environments may enable better control over chain architecture and copolymer sequence. In-depth mechanistic investigations using in situ spectroscopy, kinetic modeling, and computational simulations could provide valuable insights into propagation, backbiting, and deactivation pathways. These insights could inform the rational design of more selective and durable catalytic platforms tailored for a wider range of monomer structures.

(2) Monomer scope expansion and functional diversification. Future work should focus on expanding the accessible monomer library to enhance both the functionality and sustainability of CO_2-derived polymers. In particular, renewable functional monomers derived from bio-based feedstocks such as terpenes, lignocellulosic biomass, and fatty acid derivatives offer opportunities to introduce structural diversity while advancing the principles of green chemistry. These monomers can contribute to the development of fully sustainable polymer systems with tunable mechanical, thermal, and degradability profiles. However, challenges remain in achieving efficient and selective polymerization with such complex structures, and in ensuring their compatibility with existing or newly developed catalysts. Addressing these issues will require a deeper understanding of catalyst–monomer interactions and polymerization kinetics to enable precise control over macromolecular architecture.

(3) Interface engineering of nanocomposites. While silica served as a reinforcing filler in this study, its limited interfacial compatibility with the polymer matrix led to suboptimal dispersion and mechanical performance. Future work could focus on surface functionalization strategies to improve filler–matrix interactions, thereby enhancing dispersion and interfacial adhesion.

Nomenclature

CO_2	Carbon dioxide
AGE	Allyl glycidyl ether
T_g	Glass transition temperature
Zn-Co DMC	Zinc–cobalt(III) double metal cyanide
Al porphyrin	Aluminum porphyrin
PPNCl	Bis(triphenylphosphine)ammonium chloride
M_n	Number average molecular weight
PDI	Polydispersity index
THF	Tetrahydrofuran
PO	Propylene oxide
CHO	Cyclohexene oxide
PPC	Poly(propylene carbonate)
PCHC	Poly(cyclohexene carbonate)
LO	Limonene oxide
SO	Styrene oxide
ECH	Epichlorohydrin
$ZnEt_2$	Diethylzinc
DMAP	4-(dimethylamino)pyridine
NMeIm	N-methylimidazole
$PPNN_3$	Bis(triphenylphosphine)ammonium azide
EOH	Proton compounds
DP	Degree of polymerization
k_i	Initiation rate
k_p	Propagation rate
k_{tr}	Chain transfer rate
ZnGA	Zinc glutarate

TOF	Turnover frequency
ZnAA	Zinc adipate
ZnPA	Zinc pimelate
ZnSA	Zinc succinate
REM	Rare earth metal complex
CA	Complexing agent
TPPAl	Tetraphenylporphyrin aluminum
cPC	Cyclic carbonate
CAT	Catalyst
TEB	Triethylborane
POC	Poly(octylene carbonate)
SA	Succinic anhydride
PA	Phthalic anhydride
PCL	Poly(ε-caprolactone)
PLA	Poly(lactic acid)
BO	1,2-butylene oxide
HO	1,2-hexene oxide
OO	1,2-octene oxide
PU	Polyurethane
TPU	Thermoplastic polyurethane
PTMEG	Polyether diol
TPE	Thermoplastic elastomer
EDD	1,2-epoxydodecane
$CDCl_3$	Deuterated chloroform
TMS	Tetramethylsilane
^1H NMR	Proton nuclear magnetic resonance
GPC	Gel permeation chromatography
DSC	Differential scanning calorimetry
DMA	Dynamic mechanical analysis

RPA	Rubber process analyzer
TEM	Transmission electron microscope
DFT	Density functional theory
RT	Room temperature
DCP	Dicumyl peroxide
p	Conversion
SiO_2	Silicon dioxide
G'	Storage modulus
tanδ	Loss factor

Publications

[1] **Shuo Zeng**, Qinghai Zhou, Xianhong Wang, Guo-Hua Hu, Zhao Wang, Liqun Zhang. Synthesis of CO_2-based elastomers with tunable glass transition temperatures via a Zinc–Cobalt (III) double metal cyanide catalyst. *Polymer*, 2025, 332, 128562.

[2] **Shuo Zeng**, Qinghai Zhou, Xianhong Wang, Guo-Hua Hu, Zhao Wang, Liqun Zhang. Kinetic insights into CO_2/epoxides terpolymerization using an aluminum porphyrin/PPNCl system: solution and bulk polymerization [J]. *European Polymer Journal*, 2025, 241, 114360.

[3] Zhao Wang, **Shuo Zeng**, Liqun Zhang, Qinghai Zhou, Xianhong Wang. High molecular weight CO_2-based elastomer, crosslinked CO_2-based elastomer, and preparation method thereof. Chinese patent application CN202510276210.1, Mar. 10, 2025.

[4] **Shuo Zeng**, Qinghai Zhou, Xianhong Wang, Guo-Hua Hu, Zhao Wang, Liqun Zhang. Dual catalysis for high molecular weight CO_2-based poly(carbonate-co-ether)s toward enhanced elastomeric nanocomposites. In preparation.

References

[1] Y. Liu, X.-B. Lu, Current challenges and perspectives in CO_2-based polymers, Macromolecules 56(5) (2023) 1759-1777.

[2] S. Cui, J. Borgemenke, Z. Liu, Y. Li, Recent advances of "soft" bio-polycarbonate plastics from carbon dioxide and renewable bio-feedstocks via straightforward and innovative routes, Journal of CO_2 Utilization 34 (2019) 40-52.

[3] J. Godin, W. Liu, S. Ren, C.C. Xu, Advances in recovery and utilization of carbon dioxide: A brief review, Journal of Environmental Chemical Engineering 9(4) (2021) 105644.

[4] L. Fu, Z. Ren, W. Si, Q. Ma, W. Huang, et al., Research progress on CO_2 capture and utilization technology, Journal of CO_2 Utilization 66 (2022) 102260.

[5] P. Friedlingstein, M. O'Sullivan, M.W. Jones, R.M. Andrew, L. Gregor, et al., Global Carbon Budget 2022, Earth System Science Data 14(11) (2022) 4811-4900.

[6] G.B. Bonan, Forests and climate change: Forcings, feedbacks, and the climate benefits of forests, Science 320(5882) (2008) 1444-1449.

[7] N. Gruber, D. Clement, B.R. Carter, R.A. Feely, S. van Heuven, et al., The oceanic sink for anthropogenic CO_2 from 1994 to 2007, Science 363(6432) (2019) 1193-1199.

[8] A. Saravanan, P. Senthil kumar, D.-V.N. Vo, S. Jeevanantham, V. Bhuvaneswari, V. Anantha Narayanan, P.R. Yaashikaa, S. Swetha, B. Reshma, A comprehensive review on different approaches for CO_2 utilization and conversion pathways, Chemical Engineering Science 236 (2021) 116515.

[9] P. Challa, G. Paleti, V.R. Madduluri, S.B. Gadamani, R. Pothu, D.R. Burri, R. Boddula, V. Perugopu, S.R.R. Kamaraju, Trends in emission and utilization of CO_2: Sustainable feedstock in the synthesis of value-added fine chemicals, catalysis surveys from Asia 26(2) (2022) 80-91.

[10] H. Wang, F. Xu, Z. Zhang, M. Feng, M. Jiang, S. Zhang, Bio-based polycarbonates: progress and prospects, RSC Sustainability 1(9) (2023) 2162-2179.

[11] C.-H. Huang, C.-S. Tan, A Review: CO_2 utilization, aerosol and air quality research 14(2) (2014) 480-499.

[12] S. Valluri, V. Claremboux, S. Kawatra, Opportunities and challenges in CO_2 utilization,

Journal of Environmental Sciences 113 (2022) 322-344.

[13] K. Armstrong, P. Styring, Assessing the potential of utilization and storage strategies for post-combustion CO_2 emissions reduction, Frontiers in Energy Research 3 (2015).

[14] N. Mac Dowell, P.S. Fennell, N. Shah, G.C. Maitland, The role of CO_2 capture and utilization in mitigating climate change, Nature Climate Change 7(4) (2017) 243-249.

[15] Q.-W. Song, Z.-H. Zhou, L.-N. He, Efficient, selective and sustainable catalysis of carbon dioxide, Green Chemistry 19(16) (2017) 3707-3728.

[16] J. Artz, T.E. Müller, K. Thenert, J. Kleinekorte, R. Meys, A. Sternberg, A. Bardow, W. Leitner, Sustainable conversion of carbon dioxide: An integrated review of catalysis and life cycle assessment, Chemical Reviews 118(2) (2017) 434-504.

[17] H. Cao, X. Wang, Carbon dioxide copolymers: Emerging sustainable materials for versatile applications, SusMat 1(1) (2021) 88-104.

[18] D. Adhikari, A.W. Miller, M.H. Baik, S.T. Nguyen, Intramolecular ring-opening from a CO_2-derived nucleophile as the origin of selectivity for 5-substituted oxazolidinone from the (salen)Cr-catalyzed [aziridine + CO_2] coupling, Chemical Science 6(2) (2015) 1293-1300.

[19] J. Huang, J.C. Worch, A.P. Dove, O. Coulembier, Update and challenges in carbon dioxide‐based polycarbonate synthesis, ChemSusChem 13(3) (2020) 469-487.

[20] G. Trott, P.K. Saini, C.K. Williams, Catalysts for CO_2/epoxide ring-opening copolymerization, Philosophical Transactions of the Royal Society A 374(2061) (2016) 20150085.

[21] X.B. Lu, D.J. Darensbourg, Cobalt catalysts for the coupling of CO_2 and epoxides to provide polycarbonates and cyclic carbonates, Chemical Society Reviews 41(4) (2012) 1462-1484.

[22] D.J. Darensbourg, A.D. Yeung, Thermodynamics of the carbon dioxide–epoxide copolymerization and kinetics of the metal-free degradation: A computational study, Macromolecules 46(1) (2012) 83-95.

[23] A.J. Kamphuis, F. Picchioni, P.P. Pescarmona, CO_2-fixation into cyclic and polymeric carbonates: principles and applications, Green Chemistry 21(3) (2019) 406-448.

[24] F. Della Monica, C. Capacchione, Recent advancements in metal‐catalysts design for

CO_2/epoxide reactions, Asian Journal of Organic Chemistry, Asian Journal of Organic Chemistry 11(8) (2022) e202200300.

[25] I. Kim, M.J. Yi, K.J. Lee, D.-W. Park, B.U. Kim, C.-S. Ha, Aliphatic polycarbonate synthesis by copolymerization of carbon dioxide with epoxides over double metal cyanide catalysts prepared by using ZnX_2 (X=F, Cl, Br, I), Catalysis Today 111(3-4) (2006) 292-296.

[26] R.-J. Wei, X.-H. Zhang, Y.-Y. Zhang, B.-Y. Du, Z.-Q. Fan, G.-R. Qi, Functional poly(carbonate-co-ether) synthesis from glycidyl methacrylate/CO_2 copolymerization catalyzed by Zn–Co(iii) double metal cyanide complex catalyst, RSC Advances. 4(7) (2014) 3188-3194.

[27] Y.Y. Zhang, R.J. Wei, X.H. Zhang, B.Y. Du, Z.Q. Fan, Efficient solvent-free alternating copolymerization of CO_2 with 1, 2-epoxydodecane and terpolymerization with styrene oxide via heterogeneous catalysis, Journal of Polymer Science Part A: Polymer Chemistry 53(6) (2014) 737-744.

[28] G.A. Luinstra, G.R. Haas, F. Molnar, V. Bernhart, R. Eberhardt, B. Rieger, On the formation of aliphatic polycarbonates from epoxides with chromium(III) and aluminum(III) metal-salen complexes, Chemistry 11(21) (2005) 6298-6314.

[29] B. Li, G.P. Wu, W.M. Ren, Y.M. Wang, D.Y. Rao, X.B. Lu, Asymmetric, regio- and stereo-selective alternating copolymerization of CO_2 and propylene oxide catalyzed by chiral chromium Salan complexes, Journal of Polymer Science Part A: Polymer Chemistry 46(18) (2008) 6102-6113.

[30] Y. Xu, L. Lin, M. Xiao, S. Wang, A.T. Smith, L. Sun, Y. Meng, Synthesis and properties of CO_2-based plastics: Environmentally-friendly, energy-saving and biomedical polymeric materials, Progress in Polymer Science 80 (2018) 163-182.

[31] G.W. Yang, R. Xie, Y.Y. Zhang, C.K. Xu, G.P. Wu, Evolution of copolymers of epoxides and CO_2: Catalysts, monomers, architectures, and applications, Chemical Reviews 124(21) (2024) 12305-12380.

[32] X.B. Lu, W.M. Ren, G.P. Wu, CO_2 copolymers from epoxides: Catalyst activity, product selectivity, and stereochemistry control, Accounts of Chemical Research 45 (10) (2012) 1721–1735.

[33] X. Xie, Z. Huo, E. Jang, R. Tong, Recent advances in enantioselective ring-opening polymerization and copolymerization, Communications Chemistry 6(1) (2023) 202.

[34] M.R. Kember, A. Buchard, C.K. Williams, Catalysts for CO_2/epoxide copolymerisation, Chemical Communications 47(1) (2011) 141-163.

[35] G.-P. Wu, S.-H. Wei, X.-B. Lu, W.-M. Ren, D.J. Darensbourg, Highly selective synthesis of CO_2 copolymer from styrene oxide, Macromolecules 43(21) (2010) 9202-9204.

[36] Z. Hua, G. Qi, S. Chen, Ring-opening copolymerization of maleic anhydride with propylene oxide by double-metal cyanide, Journal of Applied Polymer Science 93(4) (2004) 1788-1792.

[37] R. Eberhardt, M. Allmendinger, B. Rieger, DMAP/Cr(III) catalyst ratio: The decisive factor for poly(propylene carbonate) formation in the coupling of CO_2 and propylene oxide, Macromolecular Rapid Communications 24(2) (2003) 194-196.

[38] R.-J. Wei, X.-H. Zhang, B.-Y. Du, Z.-Q. Fan, G.-R. Qi, Selective production of poly(carbonate–co–ether) over cyclic carbonate for epichlorohydrin and CO_2 copolymerization via heterogeneous catalysis of Zn–Co (III) double metal cyanide complex, Polymer 54(23) (2013) 6357-6362.

[39] X.-H. Zhang, R.-J. Wei, Y.Y. Zhang, B.-Y. Du, Z.-Q. Fan, Carbon dioxide/epoxide copolymerization via a nanosized Zinc–Cobalt(III) double metal cyanide complex: Substituent effects of epoxides on polycarbonate selectivity, regioselectivity and glass transition temperatures, Macromolecules 48(3) (2015) 536-544.

[40] M. Jia, D. Zhang, G.W. de Kort, C.H.R.M. Wilsens, S. Rastogi, N. Hadjichristidis, Y. Gnanou, X. Feng, All-polycarbonate thermoplastic elastomers based on triblock copolymers derived from triethylborane-mediated sequential copolymerization of CO_2 with various epoxides, Macromolecules 53(13) (2020) 5297-5307.

[41] Y. Inoue, H. Koinuma, T. Tsuruta, Copolymerization of carbon dioxide and epoxide, Polymer Letters 7 (1969) 287–292.

[42] C.M. Kozak, K. Ambrose, T.S. Anderson, Copolymerization of carbon dioxide and epoxides by metal coordination complexes, Coordination Chemistry Reviews 376 (2018) 565–587.

[43] D.J. Darensbourg, A.D. Yeung, A concise review of computational studies of the carbon dioxide–epoxide copolymerization reactions, Polymer Chemistry 5(13) (2014) 3949-3962.

[44] F. Jutz, A. Buchard, M.R. Kember, S.B. Fredriksen, C.K. Williams, Mechanistic investigation and reaction kinetics of the low-pressure copolymerization of cyclohexene oxide and carbon dioxide catalyzed by a dizinc complex, Journal of the American Chemical Society 133(43) (2011) 17395-17405.

[45] F. Della Monica, B. Maity, T. Pehl, A. Buonerba, A. De Nisi, et al., [OSSO]-type iron(III) complexes for the low-pressure reaction of carbon dioxide with epoxides: Catalytic activity, reaction kinetics, and computational study, ACS Catalysis 8(8) (2018) 6882-6893.

[46] D.J. Darensbourg, P. Bottarelli, J.R. Andreatta, Inquiry into the formation of cyclic carbonates during the (salen)CrX catalyzed CO_2/cyclohexene oxide copolymerization process in the presence of ionic initiators, Macromolecules 40 (2007) 7727–7729.

[47] G.W. Coates, D.R. Moore, Discrete metal-based catalysts for the copolymerization of CO_2 and epoxides: discovery, reactivity, optimization, and mechanism, Angewandte Chemie International Edition 43(48) (2004) 6618-6639.

[48] D.J. Darensbourg, A.D. Yeung, Kinetics of the (salen)Cr(iii)- and (salen)Co(iii)-catalyzed copolymerization of epoxides with CO_2, and of the accompanying degradation reactions, Polymer Chemistry 6(7) (2015) 1103-1117.

[49] G.-W. Yang, C.-K. Xu, R. Xie, Y.-Y. Zhang, C. Lu, H. Qi, L. Yang, Y. Wang, G.-P. Wu, Precision copolymerization of CO_2 and epoxides enabled by organoboron catalysts, Nature Synthesis 1(11) (2022) 892-901.

[50] G.A. Bhat, D.J. Darensbourg, Coordination complexes as catalysts for the coupling reactions of oxiranes and carbon dioxide, Coordination Chemistry Reviews 492 (2023) 215277.

[51] M. Ree, J.Y. Bae, J.H. Jung, T.J. Shin, A new copolymerization process leading to poly(propylene carbonate) with a highly enhanced yield from carbon dioxide and propylene oxide, Journal of Polymer Science Part A: Polymer Chemistry 37(12) (1999) 1863-1876.

[52] J.-S. Kim, H. Kim, M. Ree, Hydrothermal synthesis of single-crystalline zinc glutarate and its structural determination, Chemistry of Materials 16 (2004) 2981–2983.

[53] M. Ree, Y. Hwang, J.-S. Kim, H. Kim, G. Kim, H. Kim, New findings in the catalytic

activity of zinc glutarate and its application in the chemical fixation of CO_2 into polycarbonates and their derivatives, Catalysis Today 115(1-4) (2006) 134-145.

[54] Y.Z. Meng, L.C. Du, S.C. Tiong, Q. Zhu, A.S. Hay, Effects of the structure and morphology of zinc glutarate on the fixation of carbon dioxide into polymer, Journal of Polymer Science Part A: Polymer Chemistry 40(21) (2002) 3579-3591.

[55] S. Klaus, M.W. Lehenmeier, E. Herdtweck, P. Deglmann, A.K. Ott, B. Rieger, Mechanistic insights into heterogeneous zinc dicarboxylates and theoretical considerations for CO_2-epoxide copolymerization, Journal of the American Chemical Society 133(33) (2011) 13151-13161.

[56] R. Eberhardt, M. Allmendinger, M. Zintl, C. Troll, G.A. Luinstra, B. Rieger, New zinc dicarboxylate catalysts for the CO_2/propylene oxide copolymerization reaction: Activity enhancement through Zn(II)-ethylsulfinate initiating groups, Macromolecular Chemistry and Physics 205(1) (2004) 42-47.

[57] Y. Hwang, H. Kim, M. Ree, Zinc glutarate catalyzed synthesis and biodegradability of poly(carbonate-co-ester)s from CO_2, propylene oxide, and ε-caprolactone, Macromolecular Symposia 224(1) (2005) 227-238.

[58] J.T. Wang, D. Shu, M. Xiao, Y.Z. Meng, Copolymerization of carbon dioxide and propylene oxide using zinc adipate as catalyst, Journal of Applied Polymer Science 99(1) (2005) 200-206.

[59] Q. Zhu, Y.Z. Meng, S.C. Tjong, Y.M. Zhang, W. Wan, Catalytic synthesis and characterization of an alternating copolymer from carbon dioxide and propylene oxide using zinc pimelate, Polymer 52(5) (2003) 799-804.

[60] S. Klaus, M.W. Lehenmeier, C.E. Anderson, B. Rieger, Recent advances in CO_2/epoxide copolymerization—New strategies and cooperative mechanisms, Coordination Chemistry Reviews 255(13-14) (2011) 1460-1479.

[61] X. Chen, Z. Shen, Y. Zhang, New catalytic systems for the fixation of carbon dioxide. 1. Copolymerization of CO_2 and propylene oxide with new rare-earth catalysts—RE(P2O4)3–Al(i-Bu)3–R(OH)n, Macromolecules 24 (1991) 5305–5308.

[62] C.-S. Tan, T.-J. Hsu, Alternating copolymerization of carbon dioxide and propylene oxide with a rare-earth-metal coordination catalyst, Macromolecules 30 (1997) 3147–3150.

[63] T.-J. Hsu, C.-S. Tan, Synthesis of polyethercarbonate from carbon dioxide and cyclohexene oxide by yttrium–metal coordination catalyst, Polymer 42 (2001) 5143–5150.

[64] H. Lu, Y. Qin, X. Wang, X. Yang, S. Zhang, F. Wang, Copolymerization of carbon dioxide and propylene oxide under inorganic oxide supported rare earth ternary catalyst, Journal of Polymer Science Part A: Polymer Chemistry 49(17) (2011) 3797-3804.

[65] Z. Quan, X. Wang, X. Zhao, F. Wang, Copolymerization of CO_2 and propylene oxide under rare earth ternary catalyst: design of ligand in yttrium complex, Polymer 44(19) (2003) 5605-5610.

[66] B. Liu, X. Zhao, X. Wang, F. Wang, Copolymerization of carbon dioxide and propylene oxide with $Ln(CCl_3COO)_3$-based catalyst: The role of rare-earth compound in the catalytic system, Journal of Polymer Science Part A: Polymer Chemistry 39(16) (2001) 2751-2754.

[67] S.H. Lee, I.K. Lee, J.Y. Ha, J.K. Jo, I. Park, C.-S. Ha, H. Suh, I. Kim, Tuning of the activity and induction period of the polymerization of propylene oxide catalyzed by double metal cyanide complexes bearing β-alkoxy alcohols as complexing agents, Industrial & Engineering Chemistry Research 49 (2010) 4107–4116.

[68] R. Cheng, Y. Zhou, Q. Hou, B. Liu, ZnO/SiO_2-modified rare-earth-metal ternary catalyst bearing quaternary ammonium salts for synthesis of high molecular weight poly(propylene carbonate), Chinese Journal of Catalysis 39(8) (2018) 1303-1310.

[69] J. Milgrom, Method of making a polyether using a double metal cyanide complex compound, U.S. Patent 3,278,457, Oct. 11, 1966.

[70] I.E. Nifant'ev, P.V. Ivchenko, Synthesis, structure, and actual applications of double metal cyanide catalysts, International Journal of Molecular Sciences 25(19) (2024).

[71] C.H. Tran, S. Kim, H.-K. Choi, B.-R. Moon, W. Song, J. Yeong Heo, I. Kim, Multi-role heterogeneous Zn–Co double metal cyanide catalysts valid for ring-opening polymerizations and hydrofunctionalizations, Journal of Industrial and Engineering Chemistry 137 (2024) 524-535.

[72] C.H. Tran, H.B. Jang, B.-r. Moon, E.-g. Lee, H.-k. Choi, I. Kim, Organic carbonates as green and sustainable complexing agents for double metal cyanide catalysts for the synthesis of polyether and poly(ether-carbonate) polyols, Catalysis Today 425 (2024) 114319.

[73] C.H. Tran, L.T.T. Pham, Y. Lee, H.B. Jang, S. Kim, I. Kim, Mechanistic insights on Zn(II)−Co(III) double metal cyanide-catalyzed ring-opening polymerization of epoxides, Journal of Catalysis 372 (2019) 86-102.

[74] W.J. Kruper Jr., D.J. Swart, Carbon dioxide oxirane copolymers prepared using double metal cyanide complexes, U.S. Patent 4,500,704, Feb. 19, 1985.

[75] S. Chen, Z. Hua, Z. Fang, G. Qi, Copolymerization of carbon dioxide and propylene oxide with highly effective zinc hexacyanocobaltate(III)-based coordination catalyst, Polymer 45(19) (2004) 6519-6524.

[76] N.J. Robertson, Z. Qin, G.C. Dallinger, E.B. Lobkovsky, S. Lee, G.W. Coates, Two-dimensional double metal cyanide complexes: highly active catalysts for the homopolymerization of propylene oxide and copolymerization of propylene oxide and carbon dioxide, Dalton Trans (45) (2006) 5390-5395.

[77] Z. Li, Y. Qin, X. Zhao, F. Wang, S. Zhang, X. Wang, Synthesis and stabilization of high-molecular-weight poly(propylene carbonate) from ZnCo-based double metal cyanide catalyst, European Polymer Journal 47(11) (2011) 2152-2157.

[78] D.J. Darensbourg, M.J. Adams, J.C. Yarbrough, Toward the design of double metal cyanides for the copolymerization of CO_2 and epoxides, Inorganic Chemistry 40 (2001) 6543–6544.

[79] X.K. Sun, X.H. Zhang, R.J. Wei, B.Y. Du, Q. Wang, Z.Q. Fan, G.R. Qi, Mechanistic insight into initiation and chain transfer reaction of CO_2/cyclohexene oxide copolymerization catalyzed by zinc-cobalt double metal cyanide complex catalysts, Journal of Polymer Science Part A: Polymer Chemistry 50(14) (2012) 2924-2934.

[80] R.-J. Wei, X.-H. Zhang, B.-Y. Du, X.-K. Sun, Z.-Q. Fan, G.-R. Qi, Highly regioselective and alternating copolymerization of racemic styrene oxide and carbon dioxide via heterogeneous double metal cyanide complex catalyst, Macromolecules 46(9) (2013) 3693-3697.

[81] X.-H. Zhang, R.-J. Wei, X.-K. Sun, J.-F. Zhang, B.-Y. Du, Z.-Q. Fan, G.-R. Qi, Selective copolymerization of carbon dioxide with propylene oxide catalyzed by a nanolamellar double metal cyanide complex catalyst at low polymerization temperatures, Polymer 52(24) (2011)

5494-5502.

[82] J.K. Varghese, D.S. Park, J.Y. Jeon, B.Y. Lee, Double metal cyanide catalyst prepared using $H_3Co(CN)_6$ for high carbonate fraction and molecular weight control in carbon dioxide/propylene oxide copolymerization, Journal of Polymer Science Part A: Polymer Chemistry 51(22) (2013) 4811-4818.

[83] X.-K. Sun, X.-H. Zhang, S. Chen, B.-Y. Du, Q. Wang, Z.-Q. Fan, G.-R. Qi, One-pot terpolymerization of CO_2, cyclohexene oxide and maleic anhydride using a highly active heterogeneous double metal cyanide complex catalyst, Polymer 51(24) (2010) 5719-5725.

[84] S.H. Lee, I.K. Lee, J.Y. Ha, J.K. Jo, I. Park, C.-S. Ha, H. Suh, I. Kim, Tuning of the activity and induction period of the polymerization of propylene oxide catalyzed by double metal cyanide complexes bearing β-alkoxy alcohols as complexing agents, Industrial & Engineering Chemistry Research 49 (2010) 4107–4116.

[85] J. Sebastian, D. Srinivas, Factors influencing catalytic activity of Co–Zn double-metal cyanide complexes for alternating polymerization of epoxides and CO_2, Applied Catalysis A: General 506 (2015) 163-172.

[86] M.M. Dharman, J.-Y. Ahn, M.-K. Lee, H.-L. Shim, K.-H. Kim, I. Kim, D.-W. Park, Moderate route for the utilization of CO_2-microwave induced copolymerization with cyclohexene oxide using highly efficient double metal cyanide complex catalysts based on $Zn_3[Co(CN)_6]$, Green Chemistry 10(6) (2008) 678–684.

[87] L.K. Johnson, C.M. Killian, M. Brookhart, New Pd(II)- and Ni(II)-based catalysts for polymerization of ethylene and α-olefins, Journal of the American Chemical Society 117 (1995) 6414–6415.

[88] M. Cheng, D.R. Moore, J.J. Reczek, B.M. Chamberlain, E.B. Lobkovsky, G.W. Coates, Single-site β-diiminate zinc catalysts for the alternating copolymerization of CO_2 and epoxides: Catalyst synthesis and unprecedented polymerization activity, Journal of the American Chemical Society 123 (2001) 8738–8749.

[89] S.D. Allen, D.R. Moore, E.B. Lobkovsky, G.W. Coates, High-activity, single-site catalysts for the alternating copolymerization of CO_2 and propylene oxide, Journal of the American Chemical Society 124 (2002) 14284–14285.

[90] L.R. Rieth, D.R. Moore, E.B. Lobkovsky, G.W. Coates, Single-site beta-diiminate zinc catalysts for the ring-opening polymerization of beta-butyrolactone and beta-valerolactone to poly(3-hydroxyalkanoates), Journal of the American Chemical Society 124(51) (2002) 15239-15248.

[91] D.R. Moore, M. Cheng, E.B. Lobkovsky, G.W. Coates, Mechanism of the alternating copolymerization of epoxides and CO_2 using β-diiminate zinc catalysts: Evidence for a bimetallic epoxide enchainment, Journal of the American Chemical Society 125 (2003) 11911–11924.

[92] R. Eberhardt, M. Allmendinger, G.A. Luinstra, B. Rieger, The ethylsulfinate ligand: A highly efficient initiating group for the zinc β-diiminate catalyzed copolymerization reaction of CO_2 and epoxides, Organometallics 22 (2003) 211–214.

[93] B. Liu, C. Tian, L. Zhang, W. Yan, W. Zhang, Copolymerization of carbon dioxide and cyclohexene oxide with zinc/β-ketoiminato complexes: Investigating the influence of the electron structure of zinc/β-ketoiminato complexes on the catalytic activity and resultant copolymer properties, Journal of Polymer Science Part A: Polymer Chemistry 44(21) (2006) 6243-6251.

[94] M. Reiter, S. Vagin, A. Kronast, C. Jandl, B. Rieger, A Lewis acid beta-diiminato-zinc-complex as all-rounder for co- and terpolymerisation of various epoxides with carbon dioxide, Chemical Science 8(3) (2017) 1876-1882.

[95] N. Takeda, S. Inoue, Polymerization of 1,2-epoxypropane and copolymerization with carbon dioxide catalyzed by metalloporphyrins, Die Makromolekulare Chemie 179(5) (2003) 1377-1381.

[96] Z.Q. Ren, X.H. Qian, Y.F. Zhang, New catalytic systems for the fixation of carbon dioxide. 2. Synthesis of high-molecular-weight epichlorohydrin–carbon dioxide copolymer with rare-earth phosphonates triisobutylaluminum systems, Macromolecular Chemistry and Physics 1956 (1994) 2003–2011.

[97] M.H. Chisholm, Z. Zhou, Concerning the mechanism of the ring opening of propylene oxide in the copolymerization of propylene oxide and carbon dioxide to give poly(propylene carbonate), Macromolecules 38 (2005) 8121–8123.

[98] S. Mang, A.I. Cooper, M.E. Colclough, N. Chauhan, A.B. Holmes, Copolymerization of CO_2 and 1,2-cyclohexene oxide using a CO_2-soluble chromium porphyrin catalyst, Macromolecules 33 (2000) 303–308.

[99] H. Sugimoto, H. Ohshima, S. Inoue, Alternating copolymerization of carbon dioxide and epoxide by manganese porphyrin: The first example of polycarbonate synthesis from 1-atm carbon dioxide, Journal of Polymer Science Part A: Polymer Chemistry 41(22) (2003) 3549-3555.

[100] H. Sugimoto, K. Kuroda, The cobalt porphyrin–Lewis base system: A highly selective catalyst for alternating copolymerization of CO_2 and epoxide under mild conditions, Macromolecules 41 (2008) 312–317.

[101] C. Chatterjee, M.H. Chisholm, The influence of the metal (Al, Cr, and Co) and the substituents of the porphyrin in controlling the reactions involved in the copolymerization of propylene oxide and carbon dioxide by porphyrin metal(III) complexes. 1. Aluminum chemistry, Inorganic Chemistry 50(10) (2011) 4481-4492.

[102] Y. Qin, H. Guo, X. Sheng, X. Wang, F. Wang, An aluminum porphyrin complex with high activity and selectivity for cyclic carbonate synthesis, Green Chemistry 17 (2015) 2853–2858.

[103] C. Zhuo, Y. Qin, X. Wang, F. Wang, Temperature-responsive catalyst for the coupling reaction of carbon dioxide and propylene oxide, Chinese Journal of Chemistry 36(4) (2018) 299-305.

[104] W. Mo, C. Zhuo, H. Cao, S. Liu, X. Wang, F. Wang, Facile aluminum porphyrin complexes enable flexible terminal epoxides to boost properties of CO_2-polycarbonate, Macromolecular Chemistry and Physics 223(13) (2021).

[105] C. Chatterjee, M.H. Chisholm, Influence of the metal (Al, Cr, and Co) and the substituents of the porphyrin in controlling the reactions involved in the copolymerization of propylene oxide and carbon dioxide by porphyrin metal(III) complexes. 2. Chromium chemistry, Inorg Chem 51(21) (2012) 12041-12052.

[106] C. Chatterjee, M.H. Chisholm, A. El-Khaldy, R.D. McIntosh, J.T. Miller, T. Wu, Influence of the metal (Al, Cr, and Co) and substituents of the porphyrin in controlling reactions

involved in copolymerization of propylene oxide and carbon dioxide by porphyrin metal(III) complexes. 3. Cobalt chemistry, Inorganic Chemistry 52(8) (2013) 4547-4553.

[107] L.E. Martínez, J.L. Leighton, D.H. Carsten, E.N. Jacobsen, Highly enantioselective ring opening of epoxides catalyzed by (salen)Cr(III) complexes, Journal of the American Chemical Society 117 (1995) 5897–5898.

[108] D.J. Darensbourg, R.M. Mackiewicz, J.L. Rodgers, A.L. Phelps, (Salen)Cr(III)X catalysts for the copolymerization of carbon dioxide and epoxides: Role of the initiator and cocatalyst, Inorganic Chemistry 43 (2004) 1831–1833.

[109] D.J. Darensbourg, Making plastics from carbon dioxide: Salen metal complexes as catalysts for the production of polycarbonates from epoxides and CO_2, Chemical Reviews 107 (2007) 2388–2410.

[110] Z. Qin, C.M. Thomas, S. Lee, G.W. Coates, Cobalt-based complexes for the copolymerization of propylene oxide and CO_2: active and selective catalysts for polycarbonate synthesis, Angew Chem Int Ed Engl 42(44) (2003) 5484-5487.

[111] C.T. Cohen, C.M. Thomas, K.L. Peretti, E.B. Lobkovsky, G.W. Coates, Copolymerization of cyclohexene oxide and carbon dioxide using (salen)Co(III) complexes: synthesis and characterization of syndiotactic poly(cyclohexene carbonate), Dalton Trans (1) (2006) 237-249.

[112] R.L. Paddock, S.T. Nguyen, Chemical CO_2 fixation: Cr(III) salen complexes as highly efficient catalysts for the coupling of CO_2 and epoxides, Journal of the American Chemical Society 123 (2001) 11498–11499.

[113] T.T. Wang, Y. Xie, W.Q. Deng, Reaction mechanism of epoxide cycloaddition to CO_2 catalyzed by salen-M (M = Co, Al, Zn), Journal of Physical Chemistry A 118(39) (2014) 9239-9243.

[114] Y. Wang, Y. Qin, X. Wang, F. Wang, Coupling reaction between CO_2 and cyclohexene oxide: selective control from cyclic carbonate to polycarbonate by ligand design of salen/salalen titanium complexes, Catalysis Science & Technology 4(11) (2014) 3964-3972.

[115] Y. Wang, Y. Qin, X. Wang, F. Wang, Trivalent titanium salen complex: Thermally robust and highly active catalyst for copolymerization of CO_2 and cyclohexene oxide, ACS Catalysis

5(1) (2014) 393-396.

[116] X.B. Lu, Y. Wang, Highly active, binary catalyst systems for the alternating copolymerization of CO_2 and epoxides under mild conditions, Angewandte Chemie International Edition 43(27) (2004) 3574-3577.

[117] X.-B. Lu, L. Shi, Y.-M. Wang, R. Zhang, Y.-J. Zhang, X.-J. Peng, Z.-C. Zhang, B. Li, Design of highly active binary catalyst systems for CO_2/epoxide copolymerization: Polymer selectivity, enantioselectivity, and stereochemistry control, Journal of the American Chemical Society 128 (2006) 1664–1674.

[118] C.T. Cohen, T. Chu, G.W. Coates, Cobalt catalysts for the alternating copolymerization of propylene oxide and carbon dioxide: Combining high activity and selectivity, Journal of the American Chemical Society 127 (2005) 10869–10878.

[119] D.J. Darensbourg, P. Bottarelli, J.R. Andreatta, Inquiry into the formation of cyclic carbonates during the (salen)CrX catalyzed CO_2/cyclohexene oxide copolymerization process in the presence of ionic initiators, Macromolecules 40 (2007) 7727–7729.

[120] D.J. Darensbourg, J.C. Yarbrough, Mechanistic aspects of the copolymerization reaction of carbon dioxide and epoxides, using a chiral salen chromium chloride catalyst, Journal of the American Chemical Society 124 (2002) 6335–6342.

[121] D.J. Darensbourg, J.C. Yarbrough, C. Ortiz, C.C. Fang, Comparative kinetic studies of the copolymerization of cyclohexene oxide and propylene oxide with carbon dioxide in the presence of chromium salen derivatives. In situ FTIR measurements of copolymer vs cyclic carbonate production, Journal of the American Chemical Society 125 (2003) 7586–7591.

[122] S. Sujith, J.K. Min, J.E. Seong, S.J. Na, B.Y. Lee, A highly active and recyclable catalytic system for CO_2/propylene oxide copolymerization, Angewandte Chemie International Edition 47(38) (2008) 7306-7309.

[123] W.-M. Ren, Z.-W. Liu, Y.-Q. Wen, R. Zhang, X.-B. Lu, Mechanistic aspects of the copolymerization of CO_2 with epoxides using a thermally stable single-site cobalt(III) catalyst, Journal of the American Chemical Society 131 (2009) 11509–11518.

[124] D. Zhang, S.K. Boopathi, N. Hadjichristidis, Y. Gnanou, X. Feng, Metal-free alternating copolymerization of CO_2 with epoxides: Fulfilling "green" synthesis and activity, Journal of

the American Chemical Society 138(35) (2016) 11117-11120.

[125] D.-D. Zhang, X. Feng, Y. Gnanou, K.-W. Huang, Theoretical mechanistic investigation into metal-free alternating copolymerization of CO_2 and epoxides: The key role of triethylborane, Macromolecules 51(15) (2018) 5600-5607.

[126] Z. Chen, J.-L. Yang, X.-Y. Lu, L.-F. Hu, X.-H. Cao, G.-P. Wu, X.-H. Zhang, Triethyl borane-regulated selective production of polycarbonates and cyclic carbonates for the coupling reaction of CO_2 with epoxides, Polymer Chemistry 10(26) (2019) 3621-3628.

[127] G.W. Yang, Y.Y. Zhang, R. Xie, G.P. Wu, Scalable bifunctional organoboron catalysts for copolymerization of CO_2 and epoxides with unprecedented efficiency, Journal of the American Chemical Society 142(28) (2020) 12245-12255.

[128] G.W. Yang, C.K. Xu, R. Xie, Y.Y. Zhang, X.F. Zhu, G.P. Wu, Pinwheel-shaped tetranuclear organoboron catalysts for perfectly alternating copolymerization of CO_2 and epichlorohydrin, Journal of the American Chemical Society 143(9) (2021) 3455-3465.

[129] G.P. Wu, S.H. Wei, W.M. Ren, X.B. Lu, T.Q. Xu, D.J. Darensbourg, Perfectly alternating copolymerization of CO_2 and epichlorohydrin using cobalt(III)-based catalyst systems, Journal of the American Chemical Society 133(38) (2011) 15191-15199.

[130] Y.-Y. Zhang, C. Lu, G.-W. Yang, R. Xie, Y.-B. Fang, Y. Wang, G.-P. Wu, Mechanism-inspired upgradation of phosphonium-containing organoboron catalysts for epoxide-involved copolymerization and homopolymerization, Macromolecules 55(15) (2022) 6443-6452.

[131] V.K. Chidara, S.K. Boopathi, N. Hadjichristidis, Y. Gnanou, X. Feng, Triethylborane-assisted synthesis of random and block poly(ester-carbonate)s through one-pot terpolymerization of epoxides, CO_2, and cyclic anhydrides, Macromolecules 54(6) (2021) 2711-2719.

[132] X. Li, L. Meng, Y. Zhang, Z. Qin, L. Meng, C. Li, M. Liu, Research and application of polypropylene carbonate composite materials, Polymers 14(11) (2022) 2159.

[133] Y. Meng, J. Wu, M. Xiao, S. Wang, H. He, D. Han, Progress and application of biodegradable plastic derived from copolymerization of carbon dioxide with epoxides, Shiyou Huagong/Petrochemical Technology 39 (2010) 241-248.

[134] M. Taherimehr, P.P. Pescarmona, Green polycarbonates prepared by the

copolymerization of CO_2 with epoxides, Journal of Applied Polymer Science 131(21) (2014) 41141.

[135] R. Muthuraj, T. Mekonnen, Carbon dioxide–derived poly(propylene carbonate) as a matrix for composites and nanocomposites: Performances and applications, Macromolecular Materials and Engineering 303(11) (2018) 1800366.

[136] H. Li, W. Wang, S. Liu, D. Xue, J. Wang, Y. Liu, Q. Huang, Design and syntheses of functional carbon dioxide-based polycarbonates via ternary copolymerization, Journal of CO_2 Utilization 80 (2024) 102689.

[137] Y. Qin, X. Sheng, S. Liu, G. Ren, X. Wang, F. Wang, Recent advances in carbon dioxide based copolymers, Journal of CO_2 Utilization 11 (2015) 3-9.

[138] S. Kernbichl, B. Rieger, Aliphatic polycarbonates derived from epoxides and CO_2: A comparative study of poly(cyclohexene carbonate) and poly(limonene carbonate), Polymer 205 (2020) 122667.

[139] J.E. Seong, S.J. Na, A. Cyriac, B.-W. Kim, B.Y. Lee, Terpolymerizations of CO_2, propylene oxide, and various epoxides using a cobalt(III) complex of salen-type ligand tethered by four quaternary ammonium salts, Macromolecules 43(2) (2009) 903-908.

[140] Y. Tao, X. Wang, X. Zhao, J. Li, F. Wang, Crosslinkable poly(propylene carbonate): High-yield synthesis and performance improvement, Journal of Polymer Science Part A: Polymer Chemistry 44(18) (2006) 5329-5336.

[141] G.S. Sulley, G.L. Gregory, T.T.D. Chen, L. Pena Carrodeguas, G. Trott, A. Santmarti, K.Y. Lee, N.J. Terrill, C.K. Williams, Switchable catalysis improves the properties of CO_2-derived polymers: Poly(cyclohexene carbonate-b-ε-decalactone-b-cyclohexene carbonate) adhesives, elastomers, and toughened plastics, Journal of the American Chemical Society 142(9) (2020) 4367-4378.

[142] J.O. Akindoyo, M.D.H. Beg, S. Ghazali, M.R. Islam, N. Jeyaratnam, A.R. Yuvaraj, Polyurethane types, synthesis and applications – a review, RSC Advances 6(115) (2016) 114453-114482.

[143] X. Ou, Y. Niu, Q. Liu, L. Li, F. Wei, Y. Cui, Y. Zhou, F. Yan, Recent progress in CO_2-based polyurethanes and polyureas, Progress in Polymer Science 149 (2024) 101780.

[144] E. Orgilés-Calpena, F. Arán-Aís, A.M. Torró-Palau, E. Montiel-Parreño, C. Orgilés-barceló, synthesis of polyurethanes from CO_2-based polyols: A challenge for sustainable adhesives, International Journal of Adhesion and Adhesives 67 (2016) 63-68.

[145] N. von der Assen, A. Bardow, Life cycle assessment of polyols for polyurethane production using CO_2 as feedstock: insights from an industrial case study, Green Chemistry 16(6) (2014) 3272-3280.

[146] D.J. Darensbourg, S.J. Wilson, What's new with CO_2? Recent advances in its copolymerization with oxiranes, Green Chemistry 14(10) (2012).

[147] S. Liu, Y. Qin, X. Wang, F. Wang, Bulk CO_2-based amorphous triols used for designing biocompatible shape-memory polyurethanes, Journal of Renewable Materials 3(2) (2015) 101-112.

[148] P. Alagi, R. Ghorpade, Y.J. Choi, U. Patil, I. Kim, J.H. Baik, S.C. Hong, Carbon dioxide-based polyols as sustainable feedstock of thermoplastic polyurethane for corrosion-resistant metal coating, ACS Sustainable Chemistry & Engineering 5(5) (2017) 3871-3881.

[149] J. Wang, H. Zhang, Y. Miao, L. Qiao, X. Wang, A whole-procedure solvent-free route to CO_2-based waterborne polyurethane by an elevated-temperature dispersing strategy, Green Chemistry 19(9) (2017) 2194-2200.

[150] J. Wang, H. Zhang, Y. Miao, L. Qiao, X. Wang, F. Wang, UV-curable waterborne polyurethane from CO_2-polyol with high hydrolysis resistance, Polymer 100 (2016) 219-226.

[151] J. Wang, H. Zhang, Y. Miao, L. Qiao, X. Wang, F. Wang, Waterborne polyurethanes from CO_2 based polyols with comprehensive hydrolysis/oxidation resistance, Green Chemistry 18(2) (2016) 524-530.

[152] G.-W. Yang, G.-P. Wu, High-efficiency construction of CO_2-based healable thermoplastic elastomers via a tandem synthetic strategy, ACS Sustainable Chemistry & Engineering 7(1) (2018) 1372-1380.

[153] W. Mo, C. Zhuo, S. Liu, X. Wang, F. Wang, From plastic to elastomers: introducing reversible copper–thioether coordination in CO_2-based polycarbonate, Polymer Chemistry 14(2) (2023) 152-160.

[154] G. Chiarioni, M. van Duin, P.P. Pescarmona, Novel elastic rubbers from CO_2-based

polycarbonates, Green Chemistry 25 (2023) 7612.

[155] Y. Dong, X. Wang, X. Zhao, F. Wang, Facile synthesis of poly(ether carbonate)s via copolymerization of CO_2 and propylene oxide under combinatorial catalyst of rare earth ternary complex and double metal cyanide complex, Journal of Polymer Science Part A: Polymer Chemistry 50(2) (2011) 362-370.

[156] C. W. Zhuo, Y. S. Qin, X. H. Wang, F. S. Wang, Mechanistic insights into CO_2/epoxide copolymerization catalyzed by metal complexes, Chinese Journal of Chemistry 36 (2018) 299–305.

[157] W. Wu, X. Sheng, Y. Qin, L. Qiao, Y. Miao, X. Wang, F. Wang, Bifunctional aluminum porphyrin complex: Soil tolerant catalyst for copolymerization of CO_2 and propylene oxide, Journal of Polymer Science Part A: Polymer Chemistry 52(16) (2014) 2346-2355.

[158] G.A. Bhat, D.J. Darensbourg, Progress in the catalytic reactions of CO_2 and epoxides to selectively provide cyclic or polymeric carbonates, Green Chemistry 24(13) (2022) 5007-5034.

[159] R. Muthuraj, T. Mekonnen, Recent progress in carbon dioxide (CO_2) as feedstock for sustainable materials development: Co-polymers and polymer blends, Polymer 145 (2018) 348-373.

[160] R. Meys, A. Kätelhön, A. Bardow, Towards sustainable elastomers from CO_2: life cycle assessment of carbon capture and utilization for rubbers, Green Chemstry 21(12) (2019) 3334-3342.

[161] P. Holzmüller, C. Gardiner, J. Preis, H. Frey, CO_2-based polycarbonates with low glass transition temperatures sourced from long-chain terpenes, Macromolecules 57(11) (2024) 5358-5367.

[162] B. Grignard, S. Gennen, C. Jérôme, A.W. Kleij, C. Detrembleur, Advances in the use of CO_2 as a renewable feedstock for the synthesis of polymers, Chemical Society Reviews 48(16) (2019) 4466-4514.

[163] Y. Liu, W.-M. Ren, K.-K. He, X.-B. Lu, Crystalline-gradient polycarbonates prepared from enantioselective terpolymerization of meso-epoxides with CO_2, Nature Communications 5(1) (2014).

[164] S. Naumann, Borane catalysis for epoxide (co)polymerization, Polymer Chemistry 14(16)

(2023) 1834-1862.

[165] Y. Wang, D.J. Darensbourg, Carbon dioxide-based functional polycarbonates: Metal catalyzed copolymerization of CO_2 and epoxides, Coordination Chemistry Reviews 372 (2018) 85-100.

[166] G.A. Bhat, A.Z. Rashad, D.J. Darensbourg, Synthesis of terpyridine-containing polycarbonates with post polymerization providing water-soluble and micellar polymers and their metal complexes, Polymer Chemistry 11(29) (2020) 4699-4705.

[167] G.-W. Yang, Y.-Y. Zhang, Y. Wang, G.-P. Wu, Z.-K. Xu, D.J. Darensbourg, Construction of autonomic self-healing CO_2-based polycarbonates via one-pot tandem synthetic strategy, Macromolecules 51(4) (2018) 1308-1313.

[168] S.-F. Stahl, G. Luinstra, DMC-mediated copolymerization of CO_2 and PO—mechanistic aspects derived from feed and polymer composition, Catalysts 10(9) (2020).

[169] M. Luo, Y. Li, Y.-Y. Zhang, X.-H. Zhang, Using carbon dioxide and its sulfur analogues as monomers in polymer synthesis, Polymer 82 (2016) 406-431.

[170] M.A. Subhani, B. Köhler, C. Gürtler, W. Leitner, T.E. Müller, Transparent films from CO_2-based polyunsaturated poly(ether carbonate)s: A novel synthesis strategy and fast curing, Angewandte Chemie International Edition 55(18) (2016) 5591-5596.

[171] O. Hauenstein, M. Reiter, S. Agarwal, B. Rieger, A. Greiner, Bio-based polycarbonate from limonene oxide and CO_2 with high molecular weight, excellent thermal resistance, hardness and transparency, Green Chemistry 18(3) (2016) 760-770.

[172] Y. Li, Y.-Y. Zhang, L.-F. Hu, X.-H. Zhang, B.-Y. Du, J.-T. Xu, Carbon dioxide-based copolymers with various architectures, Progress in Polymer Science 82 (2018) 120-157.

[173] M. Scharfenberg, J. Hilf, H. Frey, Functional polycarbonates from carbon dioxide and tailored epoxide monomers: Degradable materials and their application potential, Advanced Functional Materials 28(10) (2018).

[174] D.J. Darensbourg, Y. Wang, Terpolymerization of propylene oxide and vinyl oxides with CO_2: copolymer cross-linking and surface modification via thiol–ene click chemistry, Polymer Chemistry 6(10) (2015) 1768-1776.

[175] Y. Wang, J. Fan, D.J. Darensbourg, Construction of versatile and functional

nanostructures derived from CO_2-based polycarbonates, Angewandte Chemie International Edition 54(35) (2015) 10206-10210.

[176] K. Deng, S. Wang, S. Ren, D. Han, M. Xiao, Y. Meng, A novel single-ion-conducting polymer electrolyte derived from CO_2-based multifunctional polycarbonate, ACS Applied Materials & Interfaces 8(49) (2016) 33642-33648.

[177] J. Huang, P. Fu, W. Li, L. Xiao, J. Chen, X. Nie, Influence of crosslinking density on the mechanical and thermal properties of plant oil-based epoxy resin, RSC Advances 12(36) (2022) 23048-23056.

[178] Y. Li, Y.-Y. Zhang, B. Liu, X.-H. Zhang, HCAII-inspired catalysts for making carbon dioxide-based copolymers: The role of metal-hydroxide bond, Chinese Journal of Polymer Science 36(2) (2017) 139-148.

[179] I. Kim, M.J. Yi, S.H. Byun, D.W. Park, B.U. Kim, C.S. Ha, Biodegradable polycarbonate synthesis by copolymerization of carbon dioxide with epoxides using a heterogeneous zinc complex, Macromolecular Symposia 224 (2005) 181-191.

[180] X.B. Lu, L. Shi, Y.M. Wang, R. Zhang, Y.J. Zhang, X.J. Peng, Z.C. Zhang, B. Li, Design of highly active binary catalyst systems for CO_2/epoxide copolymerization: Polymer selectivity, enantioselectivity, and stereochemistry control, Journal of the American Chemical Society 128(5) (2006) 1664-1674.

[181] Y.J. Huang, G.R. Qi, Y.H. Wang, Controlled ring-opening polymerization of propylene oxide catalyzed by double metal-cyanide complex, Journal of Polymer Science Part A: Polymer Chemistry 40(8) (2002) 1142-1150.

[182] J.K. Varghese, A. Cyriac, B.Y. Lee, Incorporation of ether linkage in CO_2/propylene oxide copolymerization by dual catalysis, Polyhedron 32(1) (2012) 90-95.

[183] D.J. Darensbourg, J.C. Yarbrough, C. Ortiz, C.C. Fang, Comparative kinetic studies of the copolymerization of cyclohexene oxide and propylene oxide with carbon dioxide in the presence of chromium salen derivatives. In situ FTIR measurements of copolymer vs cyclic carbonate production, Journal of the American Chemical Society 125(25) (2003) 7586-7591.

[184] Y.-Y. Zhang, X.-H. Zhang, R.-J. Wei, B.-Y. Du, Z.-Q. Fan, G.-R. Qi, Synthesis of fully alternating polycarbonate with low T_g from carbon dioxide and bio-based fatty acid, RSC

Advances 4(68) (2014) 36183-36188.

[185] Y. Yu, L.-M. Fang, Y. Liu, X.-B. Lu, Chemical synthesis of CO_2-based polymers with enhanced thermal stability and unexpected recyclability from biosourced monomers, ACS Catalysis 11(13) (2021) 8349-8357.

[186] F. Siragusa, C. Detrembleur, B. Grignard, The advent of recyclable CO_2-based polycarbonates, Polymer Chemistry 14(11) (2023) 1164-1183.

[187] C. Maeda, K. Kawabata, K. Niki, Y. Sako, T. Okihara, T. Ema, Catalytic synthesis and physical properties of CO_2-based cross-linked poly(cyclohexene carbonate)s, Polymer Chemistry 14(37) (2023) 4338-4343.

[188] X. Sheng, Y. Wang, Y. Qin, X. Wang, F. Wang, Aluminum porphyrin complexes via delicate ligand design: emerging efficient catalysts for high molecular weight poly(propylene carbonate), RSC Advances 4(96) (2014) 54043-54050.

[189] H.F. Hsu, G.L. Liu, Y.C. Su, B.T. Ko, Bimetallic nickel complexes containing imidazole-based phenolate ligands as efficient catalysts for the copolymerization of carbon dioxide with epoxides, Dalton Trans 53(1) (2023) 299-314.

[190] P.J. Dyson, P.G. Jessop, Solvent effects in catalysis: rational improvements of catalysts via manipulation of solvent interactions, Catalysis Science & Technology 6(10) (2016) 3302-3316.

[191] D.J. Darensbourg, R.R. Poland, A.L. Strickland, (Salan)CrCl, an effective catalyst for the copolymerization and terpolymerization of epoxides and carbon dioxide, Journal of Polymer Science Part A: Polymer Chemistry 50(1) (2011) 127-133.

[192] H. You, E. Wang, H. Cao, C. Zhuo, S. Liu, X. Wang, F. Wang, From impossible to possible: Atom-economic polymerization of low strain five-membered carbonates, Angewandte Chemie International Edition 61(5) (2022) e202113152.

[193] G.P. Wu, W.M. Ren, Y. Luo, B. Li, W.Z. Zhang, X.B. Lu, Enhanced asymmetric induction for the copolymerization of CO_2 and cyclohexene oxide with unsymmetric enantiopure salenCo(III) complexes: synthesis of crystalline CO_2-based polycarbonate, Journal of the American Chemical Society 134(12) (2012) 5682-5688.

[194] K. Nakano, T. Kamada, K. Nozaki, Selective formation of polycarbonate over cyclic

carbonate: copolymerization of epoxides with carbon dioxide catalyzed by a cobalt(III) complex with a piperidinium end-capping arm, Angewandte Chemie International Edition 45(43) (2006) 7274-7277.

[195] S. Huijser, E. HosseiniNejad, R. Sablong, C. de Jong, C.E. Koning, R. Duchateau, Ring-opening co- and terpolymerization of an alicyclic oxirane with carboxylic acid anhydrides and CO_2 in the presence of chromium porphyrinato and salen catalysts, Macromolecules 44(5) (2011) 1132-1139.

[196] L.-F. Hu, C.-J. Zhang, D.-J. Chen, X.-H. Cao, J.-L. Yang, X.-H. Zhang, Synthesis of high-molecular-weight maleic anhydride-based polyesters with enhanced properties, ACS Applied Polymer Materials 2(12) (2020) 5817-5823.

[197] X. Wu, W. Zhang, H. Ding, Y. Wen, K. Guo, Z. Duan, B. Liu, Construction of polycarbonates with pendant multifunctional groups via a one-step CO_2/diepoxide copolymerization approach, Biomacromolecules 25(5) (2024) 2925-2933.

[198] S. Zeng, Q. Zhou, X. Wang, G.-H. Hu, Z. Wang, L. Zhang, Synthesis of CO_2-based elastomers with tunable glass transition temperatures via a Zinc–Cobalt (III) double metal cyanide catalyst, Polymer 332 (2025) 128562.

[199] S. Li, Z.X. Liu, Y.N. Zhou, Z.H. Luo, Determining the kinetic and thermodynamic parameters of anionic polymerization of styrene using linear free-energy relationship, Macromolecular Reaction Engineering 18(6) (2024) 2400021.

[200] S. Tang, H. Suo, R. Qu, H. Tang, M. Sun, Y. Qin, Copolymerization of carbon dioxide with 1,2-butylene oxide and terpolymerization with various epoxides for tailorable properties, Polymers 15(3) (2023) 748.

[201] E.V. Chernikova, I.P. Beletskaya, From epoxides and carbon dioxide to polycarbonates: synthesis, properties and applications, Russian Chemical Reviews 93(2) (2024) RCR5112.

[202] M. Taherimehr, S.M. Al-Amsyar, C.J. Whiteoak, A.W. Kleij, P.P. Pescarmona, High activity and switchable selectivity in the synthesis of cyclic and polymeric cyclohexene carbonates with iron amino triphenolate catalysts, Green Chemistry 15(11) (2013) 3083.

[203] E. Hernández, P. Navarro, P.P. Pescarmona, J. Palomar, Dissociation role on the catalytic activity of organic halides in CO_2 conversion to cyclic carbonates: Experimental and

computational study, Journal of CO_2 Utilization 88 (2024) 102929.

[204] B. Y. Lee, H. Y. Kwon, S. Y. Lee, S. J. Na, S. Han, H. Yun, H. Lee, Y.-W. Park, Bimetallic anilido-aldimine zinc complexes for epoxide/CO_2 copolymerization, Journal of the American Chemical Society 2005, 127, 3031–3037.

[205] H. Zhang, M.W. Grinstaff, Synthesis of atactic and isotactic poly(1,2-glycerol carbonate)s: degradable polymers for biomedical and pharmaceutical applications, Journal of the American Chemical Society 135(18) (2013) 6806-6809.

[206] L. Karulf, B. Singh, R. Singh, T. Repo, Carbon dioxide utilization: CO_2-based polyurethane foam, Journal of CO_2 Utilization 91 (2025) 103000.

[207] Q. Wang, Y. Zhang, X. Li, Q. Chen, M. Kang, Q. Li, J. Wang, Modification of the Zn–Co double metal cyanide complex for the synthesis of carbon dioxide–derived poly(ether–carbonate) polyols, Journal of CO_2 Utilization 82 (2024) 102768.

[208] C. Chen, Y. Gnanou, X. Feng, Ultra-productive upcycling CO_2 into polycarbonate polyols via borinane-based bifunctional organocatalysts, Macromolecules 56(3) (2023) 892-898.

[209] K. Nakaoka, T. Ema, Terpolymerization reactions of epoxides, CO_2, and the third monomers toward sustainable CO_2-based polymers with controllable chemical and physical properties, Chemical Communications 61(1) (2024) 46-60.

[210] T. Aida, M. Ishikawa, S. Inoue, Alternating copolymerization of carbon dioxide and epoxide catalyzed by the aluminum porphyrin–quaternary organic salt or –triphenylphosphine system. Synthesis of polycarbonate with well-controlled molecular weight, Macromolecules 1986, 19, 8–13.

[211] G.A. Luinstra, F. Molnar, Poly(propylene carbonate), old CO_2 copolymer with new attractiveness, Macromolecular Symposia 259(1) (2007) 203-209.

[212] K. Nakano, S. Hashimoto, K. Nozaki, Bimetallic mechanism operating in the copolymerization of propylene oxide with carbon dioxide catalyzed by cobalt–salen complexes, Chemical Science 1(3) (2010) 369–373.

[213] X. Li, R.-l. Duan, C.-y. Hu, X. Pang, M.-x. Deng, Copolymerization of lactide, epoxides and carbon dioxide: a highly efficient heterogeneous ternary catalyst system, Polymer

Chemistry 12(11) (2021) 1700-1706.

[214] C. Gauthier, E. Reynaud, R. Vassoille, L. Ladouce-Stelandre, Analysis of the non-linear viscoelastic behaviour of silica filled styrene butadiene rubber, Polymer 45(8) (2004) 2761-2771.

[215] X. Zhou, L. Cai, W. Lei, H. Qiao, C. Liu, X. Zhao, J. Chen, R. Wang, L. Zhang, Preparation and intermolecular interaction of bio-based elastomer/hindered phenol hybrid with tunable damping properties, Pure and Applied Chemistry 87(8) (2015) 767-777.

[216] H. Zhu, Z. Wang, X. Huang, F. Wang, L. Kong, B. Guo, T. Ding, Enhanced comprehensive performance of SSBR/BR with self-assembly reduced graphene oxide/silica nanocomposites, Composites Part B: Engineering 175 (2019) 107027.

[217] N. Ye, J. Zheng, X. Ye, J. Xue, D. Han, H. Xu, Z. Wang, L. Zhang, Performance enhancement of rubber composites using VOC-Free interfacial silica coupling agent, Composites Part B: Engineering 202 (2020) 108301 .

[218] A.R. Payne, The dynamic properties of carbon black-loaded natural rubber vulcanizates. Part I, Journal of Applied Polymer Science 6(19) (2003) 57-63.

[219] H. Qiao, M. Chao, D. Hui, J. Liu, J. Zheng, W. Lei, X. Zhou, R. Wang, L. Zhang, Enhanced interfacial interaction and excellent performance of silica/epoxy group-functionalized styrene-butadiene rubber (SBR) nanocomposites without any coupling agent, Composites Part B: Engineering 114 (2017) 356-364.